Understanding the complexity of the corneal endothelium for regenerative medicine

Understanding the complexity of the corneal endothelium for regenerative medicine

Pere Català Quilis

The work described in this thesis was carried out at the Department of Cell Biology–Inspired Tissue Engineering (cBITE), MERLN Institute for Technology-Inspired Regenerative Medicine, Maastricht University, and the Universit Eye Clinic Maastricht, University Medical Center Maastricht+, the Netherlands

ISBN: 978-94-6469-447-5
Printed by: Proefschrift Maken
Cover design by: Elisabet Català Quilis

Understanding the complexity of the corneal endothelium for regenerative medicine

Dissertation

To obtain the degree of Doctor at Maastricht University,
on the authority of the Rector Magnificus,
Prof. Dr. Pamela Habibovic
in accordance with the decision of the Board of Deans,
to be defended in public
on Wednesday the 13th of September 2023, at 16:00 hours

by

Pere Català Quilis
born on 13 January 1994 in Sant Cugat del Vallès,
Barcelona, Spain

Promotor:

Prof. Dr. Rudy Nuijts

Co-promotor:

Dr. Vanessa LaPointe
Dr. Mor Dickman

Assessment committee:

Prof. Dr. (Chair) Judith Sluimer (Maastricht UMC+)
Prof. Dr. Björn Bachman (University Clinic of Cologne)
Prof. Dr. Han Brunner (Maastricht UMC+)
Dr. Aurelie Carlier (MERLN Institute)
Prof. Dr. Berthold Seitz (Saarland University Medical Center)

Paranymphs
Winant van Os
Daniel Carvalho

CONTENTS

1

Introduction

General introduction

The cornea is an avascular and transparent tissue that allows light to enter the front of the eye. It measures 10–12 mm in diameter and 500–600 μm in thickness, and accounts for most of the eye's refractive power.[1] The cornea is composed of five layers (Figure 1), with the top layer comprising a stratified sheet of corneal epithelial cells covering the outer surface.[2,3] Epithelial cells act as a biological barrier to block the passage of foreign material and provide a smooth surface that absorbs nutrients. The next layer, named the Bowman's layer, is a collagen-based acellular membrane synthesized by the stromal keratocytes; it separates the epithelium from the stroma.[2,3] The middle layer of the cornea is the stroma and accounts for 80%– 90% of the tissue thickness, conferring most of its biomechanical strength and optical properties.[2,3] The stroma is composed of highly structured extracellular matrix proteins such as collagen and is populated by keratocytes that maintain its homeostasis. The next layer is the Descemet's membrane composed of collagen types IV and VIII, laminin, and nidogen among other proteins[4] which are produced by the corneal endothelial cells (CECs)[2,3] of the innermost layer of the cornea. In adults, the Descemet's membrane is 3–10 μm thick.[5] Due to its avascular nature, the cells populating the cornea obtain nutrients and oxygen through diffusion from the eye's anterior chamber and from the limbal vasculature.

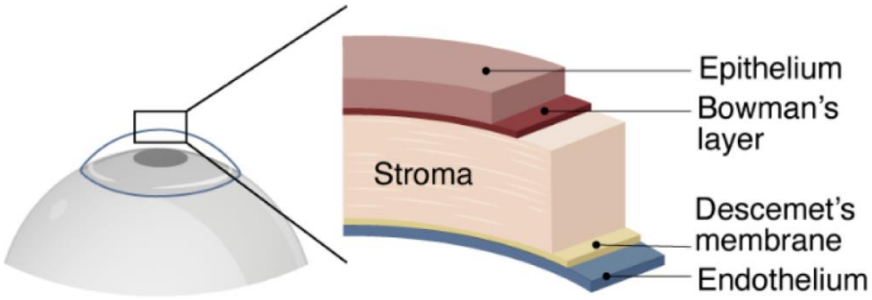

Figure 1. The human cornea is composed of five layers: the corneal epithelium, Bowman's layer, corneal stroma, Descemet's membrane and corneal endothelium.

CECs are an important cell population in the cornea because of their structure and function and their loss is implicated in corneal disease. CECs originate from the neural crest of the neuroectoderm,[6] which is different from other cell populations found in the ocular surface such as corneal or conjunctival epithelial cells that originate from the cranial ectoderm. After embryonic development, human CECs are arrested at the G1 phase, and are unable to proliferate. Consequently, the corneal endothelium lacks regenerative capacity through cell division. Nevertheless, there is ongoing discussion whether a peripheral population of CECs retains some proliferative capacity.[7–10] On the contrary, CEC of other species such as rodents and rabbits, retain a high proliferative capacity and can repopulate the endothelium in response to damage.[11]

Regarding their function, CECs act as an active metabolic pump transporting ions (such as Na^+, K^+, Cl^-, and HCO_3^-) and metabolites (such as glucose and lactic acid), leading to a net stromal to aqueous humor solute flux. Moreover, the tight junctions present in CECs act as a barrier to prevent the imbibition of water to the corneal stroma.[12,13] This process maintains the slight dehydration of the cornea and is fundamental to its transparency (Figure 2).

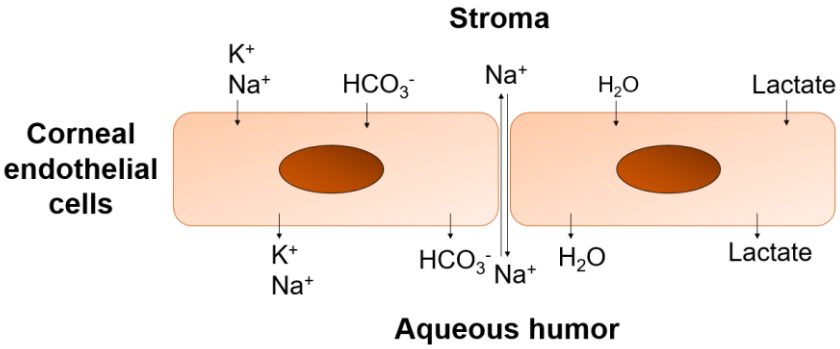

Figure 2. CECs act as an active metabolic pump, transporting ions and metabolic remnants from the stroma to the aqueous humor, thus maintaining the cornea in a slightly dehydrated state.

The average CEC density in healthy adults aged 20 to 39 years is 3000 cells/mm^2. CEC density decreases by 0.6% each year, reaching an average CEC count of 2600 cells/mm^2 in adults aged 60 to 79 years.[14] Iatrogenic damage after surgery, infection or genetic diseases such as Fuchs' endothelial corneal dystrophy (FECD) can cause dysfunction and accelerated loss of CECs, resulting in corneal endothelial disease, characterized by corneal edema and opacity. Corneal opacity is one of the leading causes of blindness worldwide, and an estimated 12.7 million people worldwide are awaiting treatment.[15]

The state-of-the-art therapy for treating corneal endothelial disease is the selective replacement of the dysfunctional monolayer of CECs with that of a donor, namely Descemet's membrane endothelial keratoplasty (DMEK).[16] Therefore, novel regenerative medicine therapies will be measured in comparison to DMEK. DMEK has set the bar high with a relatively low cost and a graft survival measured 85% twelve months after intervention.[17] Nevertheless, this therapy has shortcomings: First, the global availability of donor tissue cannot fit the demand. Advances in corneal transplantation are improving its reproducibility and accessibility, decreasing the threshold for intervention at earlier disease stages and increasing the donor tissue demand aggravating the donor shortage. It has been estimated that there is only one donor cornea available for every 70 patients in need.[15] Furthermore, DMEK grafts have a limited lifespan, and graft survival is reduced to 77% two years after surgery.[17] Re-grafting is already the second indication for corneal transplantation with 16% of the cases in Europe.[18] Secondly, graft delivery is challenging and the stripping of endothelial tissue by novice surgeons in the operation room can result in iatrogenic damage of the donor graft. Finally, there is the need to develop novel therapies to treat patients groups that cannot benefit from DMEK such as patients with complex eyes where the operation is technically challenging, patients with glaucoma drainage devices, and patients with a failed penetrating keratoplasty due to endothelial decompensation

Over the years, several strategies have been pursued to improve therapeutic options for corneal endothelial disease. Approaches to regenerate the corneal endothelium offer a solution to the current donor cornea scarcity. The pharmacological modulation of the endothelium using rho-associated kinase inhibitors offers the possibility to regenerate this tissue through an increased cell migration and proliferation without the need of donor tissue.[19–21] Nevertheless, it has only shown success in a few cases of relatively young patients with intact peripheral endothelium.[19–21] Protocols for generating CECs into quantities that could address the current tissue shortage and the possible strategies to deliver them, whether using a cell injection or a scaffold, have now become a therapeutic reality with several clinical trials taking place worldwide.[22] One of the most promising strategies is the isolation and primary culture of human CECs,[23–27] which led to a successful clinical trial in 2018.[25] Despite this landmark clinical trial, this therapy has limitations preventing its adoption.

The primary culture of CEC is a challenging technique, culture success is limited to young donors, and major cell alterations appear after the second passage with the current culture protocols, limiting the amount of cells suitable for therapy.[22] More recently, the development of the first protocols to derive human CECs from induced pluripotent and human embryonic stem cells has opened the possibility to obtain CEC without the need of donors.[28–30] In addition to cell-based therapies, acellular corneal endothelial graft equivalents could provide a treatment option for specific disease conditions without the need of donor tissue or cells, though it is not yet well understood for how long these constructs could keep corneal deturgescence.[31,32] Finally, gene modulation therapies to treat corneal endothelial disease may be used to treat pre symptomatic patients or those presenting early symptoms, drastically reducing the need for donor tissue.[33–35] Nevertheless, we have no tools to predict the progression of the disease to know if treatment would be actually required and gene modulation therapies would address the existing guttae in patients with FECD.

A central technology used in this thesis to gain knowledge on CECs and improve regenerative medicine therapies is single cell RNA sequencing (scRNAseq). The corneal layers have been traditionally regarded as bulk units and analyzed with conventional transcriptomics, missing on information of cellular subtypes. scRNAseq offers the possibility to gain transcriptomic knowledge of single cells, accounting for the cellular heterogeneity within corneal layers, providing the basis to improve current primary cell expansion protocols, for future profiling of corneal disease states, to help guide pluripotent stem cells into different corneal lineages, and to understand how engineered substrates affect corneal cells to improve regenerative therapies.

Outline of this thesis

In **Chapter 2,** the approaches currently studied for regenerating the human corneal endothelium are introduced. This chapter summarizes possible sources for cell therapy and their delivery methods, novel drugs and materials for the regeneration of the corneal endothelium, and gene therapy approaches to treat corneal endothelial disease. Moreover, this chapter gives an overview of the current clinical trials worldwide using regenerative medicine approaches and describes the regulatory framework in the European Union, with the aim to help scientists and clinicians to bring therapies from bench to bedside.

Chapter 2 further proposes how the field is likely to develop and how each patient could be treated in order to take most advantage of the new therapeutic arsenal. Namely, lamellar corneal transplantation is currently the default procedure to treat corneal endothelial disease. In the coming years, research will reveal a deeper understanding of what spectrums and types of corneal endothelial disease could be successfully treated with each approach. It is possible that young patients with early corneal endothelial disease could be candidates for genetic modulation. On the other hand, patients with a relatively intact peripheral corneal endothelium could be treated

with pharmacological approaches, and severe or advanced cases of corneal endothelial disease could be treated with lamellar keratoplasty or cell therapy delivered by injection or using a carrier. A personalized medicine approach will allow greater access to therapy for more people and tackle the global donor shortage. Finally, this chapter gives a perspective on the ethics and societal challenges these therapies face.

Chapter 3 outlines an example of the symbiosis between our laboratory and the clinic. This chapter reports a translational study to determine if a novel device for the transport of preloaded and ready-to-transplant corneal endothelial donor tissue can deliver the tissue to the operating theater as successfully as the conventional pre-stripped whole cornea transport. These types of devices have the potential to reduce costly operating theater time and the risk of iatrogenic tissue damage. Moreover, they will allow eye banks to send only the tissue necessary for Descemet's membrane endothelial keratoplasty (DMEK), optimizing availability of donor tissue for other surgical procedures.[15,36]

As previously introduced, the cornea is a complex tissue composed of five layers that are populated by different cell types and subtypes. To develop regenerative medicine therapies for the cornea, it is crucial to understand the complexity of all the cells populating this tissue. In **Chapter 4**, we report a single cell RNA sequencing (scRNAseq) analysis to elucidate the heterogeneity of the cells present in the healthy human cornea. To do so, we isolated and sequenced 19,472 corneal cells from eight healthy donors. The transcriptomic cell census that we created identified subpopulations with different roles in the maintenance of corneal homeostasis and provided a baseline to improve primary cell expansion protocols, for future profiling of corneal disease states, and to understand how engineered substrates affect corneal cells to improve regenerative therapies. Furthermore, our study identified markers exclusively expressed in cells comprising the epithelial limbal stem cell niche, highly

proliferating epithelial cells, and stromal keratocytes, which could be used as reference to improve current corneal cell replacement therapies.

In **Chapter 5,** we focus on CECs. The primary culture of human CECs can generate an adequate number of cells from one donor to graft multiple recipients,[24,25] an approach successfully demonstrated in a landmark clinical trial in Japan in 2018.[17] This approach could offer a solution to the current donor tissue shortage breaking the established paradigm of one donor cornea–one recipient eye. The 5-year outcomes of this clinical trial are promising,[37] but various limitations have prevented the approach from being adopted worldwide. First, the CEC cultures are only successful if derived from donors younger than 45 years. Second, forcing CECs to enter a proliferative state can cause an undesired endothelial-to-mesenchymal transition resulting in loss of function. Third, a lack of cellular markers prevents sorting clinical-grade CECs. We hypothesize that primary cultured human CECs are highly heterogeneous and instead of evaluating the cultures as bulk entities, we analyzed them at the single-cell level. To do so we isolated, cultured, and sequenced the transcriptome of 42,220 CEC from three different donors, at five different time points over three different passages. Our scRNAseq analysis revealed clusters of high-quality therapy-grade CECs, and other clusters of cells entering a senescent and fibrotic state, confirming the heterogeneity of primary cultured CECs. Our study also revealed crucial transcriptomic differences across the therapy-grade and senescent/fibrotic CEC clusters, which were further validated at the protein level. This chapter portrays the heterogeneity at the single cell level of primary cultured CECs, providing a baseline for the deep understanding necessary to overcome the limitations of using cultivated CECs for regenerative medicine.

To further understand the regenerative capacity of CECs, we studied how *in vivo* proliferation differs between species. In humans, sheep and other higher-order mammals, CECs are arrested at the G1 phase of the cell cycle.[11] However, CECs of rodents and rabbits retain a high proliferative capacity, and can repopulate the

endothelium in response to damage.[11] In **Chapter 6,** we describe a transcriptome comparison between human, sheep, rabbit, and mouse CECs to unravel the mechanisms governing corneal endothelial regeneration and proliferation. Our dataset provides a comprehensive transcriptome comparison of species with proliferating and quiescent CECs that can be used to improve current cell expansion protocols and identify novel drug targets to promote corneal endothelial proliferation and regeneration.

Chapter 7 highlights and discusses the major findings of this thesis and concludes with recommendations for future research. Finally, in **Chapter 8**, we provide a perspective on how this thesis could impact the field of corneal endothelium regenerative medicine.

References

1. Patel, S., Alió, J. L. & Pérez-Santonja, J. J. Refractive index change in bovine and human corneal stroma before and after LASIK: A study of untreated and re-treated corneas implicating stromal hydration. *Investig. Ophthalmol. Vis. Sci.* **45**, 3523–3530 (2004).

2. DelMonte, D. W. & Kim, T. Anatomy and physiology of the cornea. *J. Cataract Refract. Surg.* **37**, 588–598 (2011).

3. Eghrari, A. O., Riazuddin, S. A. & Gottsch, J. D. Overview of the Cornea: Structure, Function, and Development. *Prog. Mol. Biol. Transl. Sci.* **134**, 7-23 (2015).

4. Kabosova, A. *et al.* Compositional differences between infant and adult human corneal basement membranes. *Investig. Ophthalmol. Vis. Sci.* **48**, 4989–4999 (2007).

5. Johnson, D. H., Bourne, W. M. & Campbell, R. J. The Ultrastructure of Descemet's Membrane: I. Changes with age in Normal Corneas. *Arch. Ophthalmol.* **100**, 1942–1947 (1982).

6. Lwigale, P. Y. Corneal Development: Different Cells from a Common Progenitor. *Prog. Mol. Biol. Transl. Sci.* **134**, 43–59 (2015).

7. Yam, G. H. *et al.* Characterization of Human Transition Zone Reveals a Putative Progenitor-Enriched Niche of Corneal Endothelium. *Cells* **8**, 1244 (2019).

8. Amano, S., Yamagami, S., Mimura, T., Uchida, S. & Yokoo, S. Corneal Stromal and Endothelial Cell Precursors. *Cornea* **25**, S73–S77 (2006).

9. He, Z. *et al.* Revisited microanatomy of the corneal endothelial periphery: New evidence for continuous centripetal migration of endothelial cells in humans. *Stem Cells* **30**, 2523–2534 (2012).

10. Whikehart, D. R., Parikh, C. H., Vaughn, A. V., Mishler, K. & Edelhauser, H. F. Evidence suggesting the existence of stem cells for the human corneal endothelium. *Mol. Vis.* **11**, 816–824 (2005).

11. Park, S. *et al.* Animal models of corneal endothelial dysfunction to facilitate development of novel therapies. *Ann. Transl. Med.* **9**, 1271–1271 (2021).

12. Bonanno, J. A. Molecular mechanisms underlying the corneal endothelial pump. *Exp. Eye Res.* **95**, 2–7 (2012).

13. Bonanno, J. A. Identity and regulation of ion transport mechanisms in the corneal endothelium. *Prog. Retin. Eye Res.* **22**, 69–94 (2003).

14. Zheng, T., Le, Q., Hong, J. & Xu, J. Comparison of human corneal cell density by age and corneal location: An in vivo confocal microscopy study. *BMC Ophthalmol.* **16**, 109 (2016).

15. Gain, P. *et al.* Global survey of corneal transplantation and eye banking. *JAMA Ophthalmol* **134**, 167–173 (2016).

16. Price, M. O., Mehta, J. S., Jurkunas, U. V. & Price, F. W. Corneal endothelial dysfunction: Evolving understanding and treatment options. *Prog. Retin. Eye Res.* **82**, 100904 (2021).

17. Dunker, S. L. *et al.* Real-World Outcomes of DMEK: A Prospective Dutch registry study. *Am. J. Ophthalmol.* **222**, 218–225 (2021).

18. Dunker, S. L. *et al.* Practice patterns of corneal transplantation in Europe. *J. Cataract Refract. Surg.* **47**, 865–869 (2021).

19. Okumura, N. *et al.* The ROCK inhibitor eye drop accelerates corneal endothelium wound healing. *Investig. Ophthalmol. Vis. Sci.* **54**, 2439–2502 (2013).

20. Moloney, G. *et al.* Descemetorhexis without grafting for fuchs endothelial dystrophy-supplementation with topical ripasudil. *Cornea* **36**, 642–648 (2017).

21. Koizumi, N., Okumura, N., Ueno, M. & Kinoshita, S. New therapeutic modality for corneal endothelial disease using Rho-associated kinase inhibitor eye drops. *Cornea* **33**, S25–S31 (2014).

22. Català, P. *et al.* Approaches for corneal endothelium regenerative medicine. *Prog. Retin. Eye Res.* **87**, 100987 (2022).

23. Peh, G. S. L., Toh, K.-P., Wu, F.-Y., Tan, D. T. & Mehta, J. S. Cultivation of human corneal endothelial cells isolated from paired donor corneas. *PLoS One* **6**, e28310 (2011).

24. Peh, G. S. L. *et al.* Propagation of human corneal endothelial cells: A novel dual media approach. *Cell Transpl.* **24**, 287–304 (2015).

25. Kinoshita, S. *et al.* Injection of cultured cells with a ROCK inhibitor for bullous keratopathy. *N. Engl. J. Med.* **378**, 995–1003 (2018).

26. Koizumi, N. *et al.* Cultivated Corneal Endothelial Cell Sheet Transplantation in a Primate Model. *Investig. Ophthalmol. Vis. Sci.* **48**, 4519–4526 (2007).

27. Ueno, M. *et al.* Superiority of mature differentiated cultured human corneal endothelial cell injection therapy for corneal endothelial failure. *Am. J. Ophthalmol.* **237**, 267–277 (2022).

28. Zhao, J. J. & Afshari, N. A. Generation of human corneal endothelial cells via in vitro ocular lineage restriction of pluripotent stem cells. *Invest Ophthalmol Vis Sci* **57**, 6878–6884 (2016).

29. Grönroos, P., Ilmarinen, T. & Skottman, H. Directed differentiation of human pluripotent stem cells towards corneal endothelial-like cells under defined conditions. *Cells* **10**, 331 (2021).

30. Wagoner, M. D. *et al.* Feeder-free differentiation of cells exhibiting characteristics of corneal endothelium from human induced pluripotent stem cells. *Biol. Open* **7**, 1–10 (2018).

31. Daphna, O. & Marcovich, A. L. EndoArt: Multi center ongoing study of innovative artificial implant designed to treat corneal edema. in *38th Congress of the European Society of Chataract and Refractive Surgeons* **2-4 October**, (2020).

32. Bhogal, M., Lwin, C. N., Seah, X. Y., Peh, G. & Mehta, J. S. Allogeneic descemet's membrane transplantation enhances corneal endothelial monolayer formation and restores functional integrity following descemet's stripping. *Investig. Ophthalmol. Vis. Sci.* **58**, 4249–4260 (2017).

33. Zarouchlioti, C. *et al.* Antisense Therapy for a Common Corneal Dystrophy Ameliorates TCF4 Repeat Expansion-Mediated Toxicity. *Am. J. Hum. Genet.* **102**, 528–539 (2018).

34. Rong, Z., Gong, X., Hulleman, J. D., Corey, D. R. & Mootha, V. V. Trinucleotide repeat-targeting dCas9 as a therapeutic strategy for fuchs' endothelial corneal dystrophy. *Transl. Vis. Sci. Technol.* **9**, 47 (2020).

35. Hu, J. *et al.* Oligonucleotides targeting TCF4 triplet repeat expansion inhibit RNA foci and mis-splicing in Fuchs' dystrophy. *Hum. Mol. Genet.* **27**, 1015–1026 (2018).

36. Tan, D. T. H., Dart, J. K. G., Holland, E. J. & Kinoshita, S. Corneal transplantation. *Lancet* **379**, 1749–1761 (2012).

37. Numa, K. *et al.* Five-year follow-up of first eleven cases undergoing injection of cultured corneal endothelial cells for corneal endothelial failure. *Ophthalmology* **128**, 504–514 (2021).

2

Approaches for corneal endothelium regenerative medicine

This chapter has been published as:

Català, P., Thuret, G., Skottman, H., Mehta, J.S., Parekh, M., Ni Dhubhghaill, S., Collin, R.W.J., Nuijts, R.M.M.A., Ferrari, S., LaPointe, V.L.S., Dickman, M.M. Approaches for corneal endothelium regenerative medicine. *Prog. Retin. Eye Res.* 2022; 87: 100987

Abstract

The state of the art therapy for treating corneal endothelial disease is transplantation. Advances in the reproducibility and accessibility of surgical techniques are increasing the number of corneal transplants, thereby causing a global deficit of donor corneas and leaving 12.7 million patients with addressable visual impairment. Approaches to regenerate the corneal endothelium offer a solution to the current tissue scarcity and a treatment to those in need. Methods for generating corneal endothelial cells into numbers that could address the current tissue shortage and the possible strategies used to deliver them have now become a therapeutic reality with clinical trials taking place in Japan, Singapore and Mexico. Nevertheless, there is still a long way before such therapies are approved by regulatory bodies and become clinical practice. Moreover, acellular corneal endothelial graft equivalents and certain drugs could provide a treatment option for specific disease conditions without the need of donor tissue or cells. Finally, with the emergence of gene modulation therapies to treat corneal endothelial disease, it would be possible to treat presymptomatic patients or those presenting early symptoms, drastically reducing the need for donor tissue. It is necessary to understand the most recent developments in this rapidly evolving field to know which conditions could be treated with which approach. This article provides an overview of the current and developing regenerative medicine therapies to treat corneal endothelial disease and provides the necessary guidance and understanding towards the treatment of corneal endothelial disease.

Introduction

The cornea is the clear window that lets light into the eye. This avascular tissue measures 10–12 mm in diameter and 500–600 μm in thickness in adults, and has a light refractive index of 1.38.[1] The outer surface of the cornea is composed of a stratified sheet of corneal epithelial cells. The Bowman's layer, a collagen-based acellular membrane synthesized by the stromal keratocytes, separates the epithelium from the stroma. The corneal stroma accounts for 80–90% of the corneal thickness, conferring most of the tissue mechanical strength. It is mainly composed of highly structured collagen fibers and extracellular matrix proteins and populated by a scattered population of keratocytes, which maintain stromal homeostasis. The inner part of the cornea is lined by a monolayer of tightly packed hexagonal corneal endothelial cells (CECs) which reside in contact with the stroma on the Descemet's membrane. The adult Descemet's membrane is a 3–10 μm thick[2] basement membrane primarily composed of collagen type IV and VIII [3] generated by the CECs.

CECs are thought to originate from the embryonic neural crest cells in the periocular mesenchyme. After embryonic development, human CECs are arrested at G1 phase, thus are unable to divide and lack regenerative capacity of this layer through cell division. Nevertheless, there is ongoing discussion whether a peripheral population of CECs retains some proliferative potential.[4–7] Functionally, CECs act as an active metabolic pump transporting ions, namely Na^+, K^+ and Cl^-, bicarbonate, glucose, and lactic acid leading to a net basolateral/stromal to apical/aqueous humor solute flux acting as a barrier preventing the imbibition of water from the anterior chamber of the eye to the corneal stroma.[8,9] This maintains the slightly dehydrated state of the cornea, a process called deturgescence that is fundamental to its transparency.

The average CEC density in healthy adults aged 20 to 39 years is 3000 cells/mm^2. This density decreases 0.3% yearly, reaching an average of 2600 cells/mm^2 in the

endothelium of healthy adults aged 60 to 79 years.[10] Iatrogenic damage after surgery, infection or genetic diseases such as Fuchs' endothelial corneal dystrophy (FECD) can cause dysfunction and accelerated loss of CECs. Corneal endothelial disease is characterized by a loss of barrier function causing corneal edema and opacity impairing sight. Corneal opacity is one of the leading causes of blindness worldwide, and an estimated 12.7 million people worldwide are awaiting treatment.[11]

State-of-the art: cornea transplantation

Corneal transplantation is the state-of the-art therapy for corneal endothelial disease. Since the first transplantation performed by Eduard Zirm in 1905, the cornea has become the most transplanted tissue worldwide. In 2012, 184,576 corneal transplantations were performed in 116 countries.[11]

Penetrating keratoplasty effectively restores vision, but ten-year graft survival rates vary from 36–90%.[12,13] The major limitations of this technique are high rates of allograft rejection and complications related to the use of sutures: astigmatism, infection, and wound dehiscence.[14]

Endothelial keratoplasty enables selective replacement of diseased corneal endothelium with that of a donor. Descemet stripping automated endothelial keratoplasty (DSAEK) remains the most widely used technique,[15] but Descemet's membrane endothelial keratoplasty (DMEK) is on the rise.[16] DMEK was first described in 2006, and allows selective replacement of the recipient's dysfunctional endothelium and Descemet's membrane.[17] DMEK offers excellent and rapid recovery of vision[18] with a low risk of allograft rejection.[19,20] However, it is technically challenging and graft detachment requiring intervention complicates about one fourth of cases.[15]

Current research is focused on pre-loaded DMEK grafts (Figure 1) which could be directly transported from the eye bank to the operation theatre making the procedure available for novice surgeons worldwide, reducing surgery time[21–26] and improving cost-effectiveness.[27] In an effort to overcome tissue shortage, the use of hemi[28] and even quarter DMEK[29] grafts has been reported. Nevertheless, given the low CEC densities reported after these procedures, increased graft detachment compared to conventional DMEK, cases of persistent peripheral corneal edema and bullae, and narrow indication for use (i.e. FECD), these techniques remain controversial and have not gained popularity. Other strategies explored to overcome tissue shortage have been the use of one donor cornea to treat two patients with different corneal pathologies, a technique also known as a split-cornea approach. The split-cornea approach optimizes the donor tissue use allowing a DMEK and a deep anterior lamellar keratoplasty to be performed with grafts originating from the same cornea.[30,31]

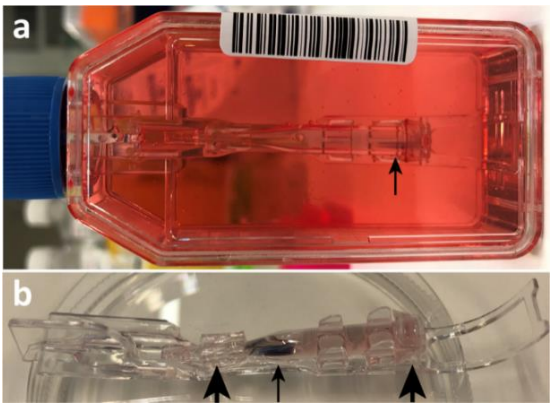

Figure 1. Image of a DMEK graft in the preloaded DMEK cartridge system (DMEK RAPID Geuder system) in a flask containing organ culture media (A). The cartridge with transport support for the preloaded DMEK graft has two liquid permeable plugs that allow gentle washing steps and staining of the graft within the transport cartridge indicated by the arrow heads (B). Full arrows indicate the stained DMEK graft. This figure was obtained from Català et al. 2020.[22] Licensed under a Creative Commons Attribution-NonCommercial-NoDerivatives 4.0 International License (CC BY-NC-ND 4.0) https://creativecommons.org/licenses/by-nc-nd/4.0/.

Surgical removal of 4–5 mm of Descemet's membrane without subsequent endothelial transplantation has been described in selected cases of relatively young patients with FECD with central guttae and relatively healthy peripheral endothelium.[32–34] This technique known as Descemet's stripping only (DSO) or Descemetorhexis without endothelial keratoplasty (DWEK) is still in an early stage of development (Figure 2). Current limitations are its unpredictable outcomes and a long recovery period during which the cornea remains swollen. To improve its success, this technique may require the use of pharmacological modulation with Rho-associated protein kinase (ROCK) inhibitors or the use of acellular corneal endothelial graft equivalents to promote corneal endothelial regeneration, which are further discussed in Sections *5. Acellular corneal endothelial graft substitutes* and *6. Pharmacological modulation of the corneal endothelium*.

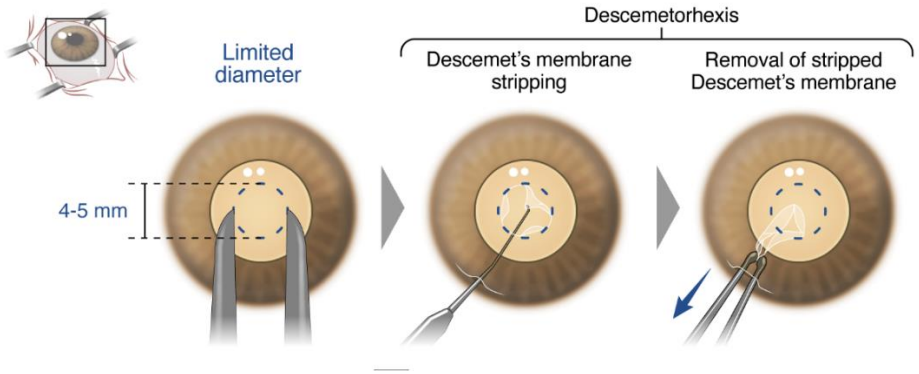

Figure 2: Schematic representation of Descemet's stripping only (DSO). First the pupil is pharmacologically dilated for a better red reflex. Then a caliper is used to mark the central 4-5 mm diameter of the cornea. A cleavage hook is then used to fashion a small Descemet's membrane tag at the edge of the 4–5 mm mark. The tag is then grasped by forceps and Descemet's membrane is stripped.

Advances in corneal transplantation are improving its reproducibility and accessibility, leading to increasing numbers of transplantations worldwide and decreasing the threshold for intervention at earlier disease stages. Unfortunately, the increase in transplantation activity aggravates the global donor tissue shortage. It has

been estimated that there is only one donor cornea available for every seventy patients in need and 12.7 million people require a corneal transplantation worldwide.[11] Moreover, considering the COVID-19 pandemic, tissue requisites to be deemed acceptable for transplant have become more stringent, affecting the global corneal tissue supply.[35] While improving donor cornea logistics and attitudes to donation in different societies could partially improve the current donor shortage, in our view, one of the most appealing ways to tackle the current tissue shortage problem and to make the treatment available to those in need is to develop novel and improve ongoing approaches for corneal endothelial regeneration (Figure 3).

Cell sources for corneal endothelial regenerative medicine

In order to tackle the current tissue scarcity and make therapy available for more patients the *in vitro* expansion or the *de novo* generation of CECs from pluripotent stem cells or other cell sources is needed. However, challenges remain that must be overcome. The main barriers for the in vitro culture of CECs, are the difficulties of forcing quiescent cells to proliferate while avoiding endothelial to mesenchymal transition (EndMT), which would lead to a cellular transdifferentiation towards a myofibroblastic phenotype causing a cellular loss of function. But also the strict selection parameters for the donor tissue suitable for primary expansion. The alternative of differentiating CECs from pluripotent stem cells or other cell sources requires the development of protocols and strict end-point parameters to assure that the final cell source resembles CECs.

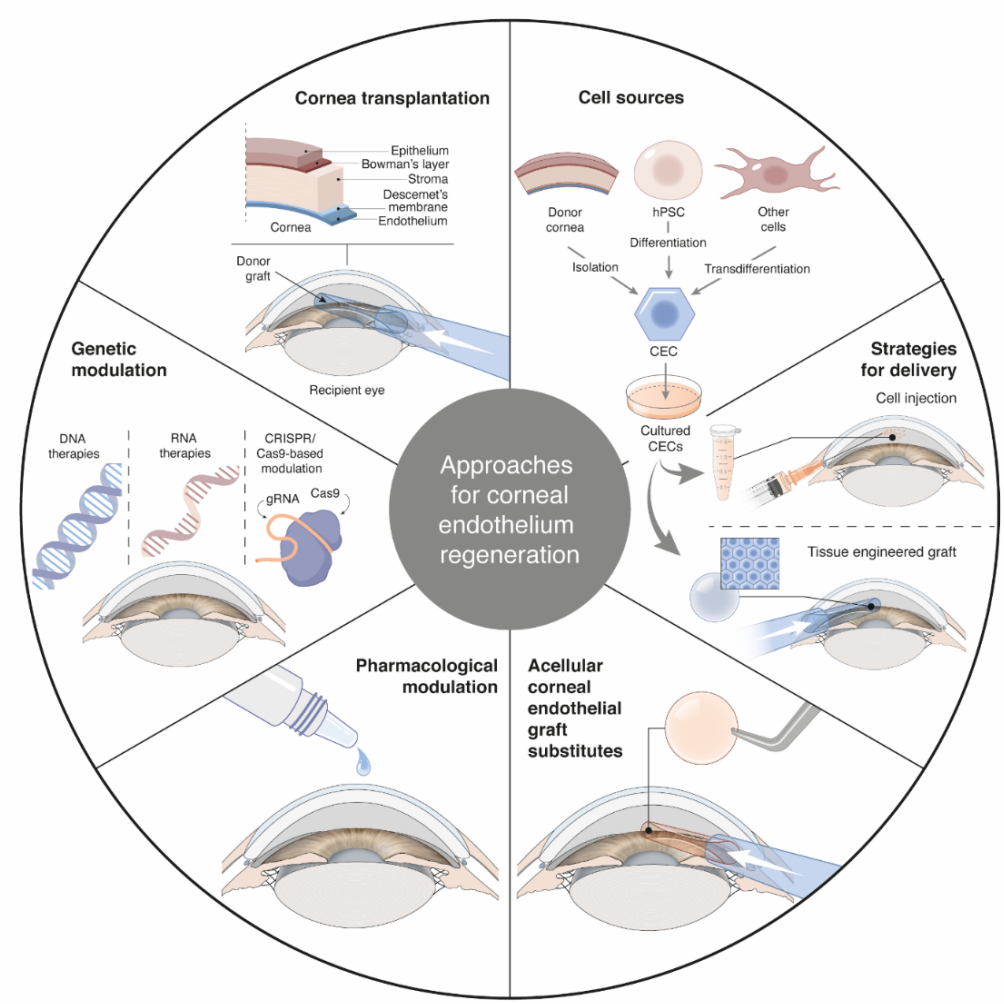

Figure 3. There are multiple approaches for corneal endothelial regeneration that have been studied or are under development. These include cornea transplantation, cell therapies, acellular graft substitutes, pharmacological and genetic modulation of the corneal endothelium.

Primary culture of corneal endothelial cells

Attempts to culture human CECs date back to the early 1980s. At the time, published protocols significantly differed in the method used for isolating the corneal endothelium and the culture media composition for *in vitro* expansion. The selection of the culture media focused on increasing the *in vitro* proliferation capacity of CECs with different preparations of basal media (Ham's F12, Medium 199, Dulbecco's

Modified Eagle Medium or OPTI-MEM-I), growth factors (nerve growth factor, basic fibroblast growth factor or epidermal growth factor), and additives (pituitary extract, calcium chloride, ascorbic acid, insulin and sodium selenite among others). The isolation techniques varied from dissecting pieces of corneal endothelium and culturing the cells via explants,[36–38] generating a single-cell suspension by scraping the endothelial surface with a curved scalpel,[38,39] or treating the corneal endothelium *in situ* with a collagenase-based enzymatic cocktail to generate single-cell suspensions.[40–42] Explant isolation was time-consuming and difficult to reproduce because of the manual variations in the technique, drawbacks which made it difficult to implement in a therapeutic setting. Moreover, the previous isolation methods were prone to contamination with stromal fibroblasts, which were undesired as the fibroblastic population would outgrow the CEC population due to its faster rate of proliferation. Furthermore, the significant donor-to-donor variability in cause of death, age, use of drugs or ethnicity made the first steps for the validation and generation of protocols to culture primary CECs more difficult.

In 2004, research performed by Amano and colleagues paved the way for the use of primary cultured human CECs in regenerative medicine. In these experiments, it was demonstrated that primary cultured CECs isolated from corneal explants could reconstruct the corneal endothelium of *ex vivo* human corneas[43] and could reverse corneal edema in rabbits and rats.[44–46]

After the introduction of Descemet's stripping in the early 2000s, primary culture protocols evolved to adopt the peel and digest approach. In this method the corneal endothelium was first mechanically stripped from the cornea and then digested into a single-cell suspension using a collagenase-based enzymatic digestion. This approach both increased reproducibility and drastically reduced the risk of contamination by other corneal cell types,[47–51] a necessary improvement to protocols for generating cells for clinical use.

Forcing CECs to exit their G1 phase quiescence, and enter a proliferative state, may unwittingly induce an undesired EndMT resulting in a loss of cellular function.[52] EndMT is typified by a number of cellular events such as loss of cell–cell junctional proteins, loss of cellular polarity, reorganization of the actin cytoskeleton, increased cell mobility, abnormal extracellular matrix production, and changes to gene expression.[52] EndMT is therefore one of the greatest threats in primary endothelial culture as it can render a cell product useless at best, and dangerous at worst. To date, a wide range of media and supplements have been used to culture CECs, with the main focus on promoting proliferation while maintaining the phenotype and avoiding a transition towards a mesenchymal state. By combining different basal media, fetal bovine serum and either epithelial growth factor[48–51] or basic fibroblast growth factor,[42,44,45,51] protocols have efficiently promoted *in vitro* proliferation while maintaining the cell phenotype.

Comparative studies performed in Mehta's[51] and Engelmann's[53] groups have shown how different media compositions affect the primary cultured CECs. In 2015, Peh and colleagues developed a unique protocol using a dual media approach to expand the corneal endothelial cells and then maintain their phenotype *in vitro*.[54] The dual media approach allowed first the expansion of the cells and then the maintenance of a confluent monolayer of corneal endothelial cells for a week using a low proliferation media and has since been widely adopted in the field[55–58] (Figure 4).

Different supplements and additives, such as pituitary extract, transferrin, ascorbic acid, calcium chloride or sodium selenite have also been studied. One of most successful approaches to increase cell proliferation and survival has been the addition of Y-27632 ROCK inhibitor, a small molecule blocker of apoptotic pathways.[54,59–61] Other approaches have been the use of human serum,[62] conditioned media which increases protocol variability due to human serum inconsistency[63,64] and a serum-free approach,[53] to study possible alternatives to the use of fetal bovine serum. The addition of L-ascorbate 2-phosphate,[65] an antioxidant to reduce oxidative

stress, and TGF-β inhibitors to avoid EndMT,[66] have also been assessed for the primary expansion of CECs.

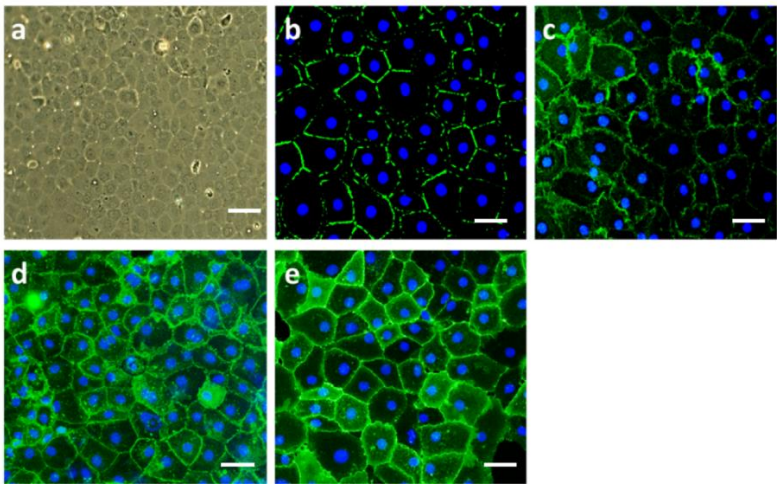

Figure 4. Human corneal endothelial cell culture from donor tissue. Phase contrast light microscope image showing typical hexagonal cell morphology (A). Immunofluorescence analysis shows the presence of zonula occludens-1 (ZO-1) (B), Na^+/K^+ ATPase (C), CD166 (D) and Prdx6 (E) expressed by primary corneal endothelial cells. Scale bar is 100 µm (A) and 50 µm (B-E). This Figure was kindly provided by Dr Mohit Parekh.

The improvements in the design of protocols for CEC *in vitro* expansion led to a first-in-human clinical trial. In 2018, Kinoshita and colleagues reported using primary cultured CECs to successfully restore the vision of patients with bullous keratopathy and FECD.[59] This landmark clinical trial succeeded in translating basic research into the clinical setting, demonstrating the therapeutic potential of primary cultured CECs.

Despite the current advances in primary culture of CECs, many questions remain unresolved. While cell seeding density[67] and young donor age[68,69] have been directly correlated to the proliferative potential and maintenance of the CEC phenotype, these do not necessarily translate to a successful primary culture. Donor-related factors, namely the use of drugs[70] or oxidative stress due to high cell metabolic activity or

high exposure to ultraviolet light,[71,72] could affect proliferation and phenotype maintenance. Sorting donors based on specific characteristics such as cause of death, age, previous pathologies, use of drugs, and other relevant factors, could be crucial to explain the varying success of *in vitro* expansion, though this requires further research and considerable numbers of research cornea. Nevertheless, developing a comprehensive and specific donor analysis could help to predict if a certain donor cornea would lead to successful *in vitro* CEC expansion and ultimately reduce waste tissue.

Another complicating factor is the method of donor tissue preservation. Most research performed to date has been done using corneas preserved in cold storage for up to 14 days. In Europe however, a warm organ culture media is usually the preferred preservation method. Most European countries cannot directly adapt the data obtained with cold storage preserved corneas to organ culture–preserved corneas. To date, there are few reports using donor corneas preserved in organ culture media.[73,74] The question that remains unresolved is how different storage conditions affect the expansion of primary human CECs.

Another problem to overcome is that forcing cells to exit their natural quiescence could so fundamentally change them and result in genetic and phenotypic alterations (Figure 5). *In vitro* expansion can potentially introduce alterations in the genomic signature, affecting their phenotype with functional implications. Primary CECs can only be passaged two times before presenting genetic and functional alterations, limiting the number of cells that can be generated from a single donor cornea.[56,75,76] Furthermore, it is possible that during the *in vitro* expansion of CECs, different cell populations arise. Identifying the sub-populations that best resemble the native CECs based on specific markers is of utmost importance for their therapeutic application. Nevertheless, such specific markers have not been identified yet, representing another urgent area of attention.

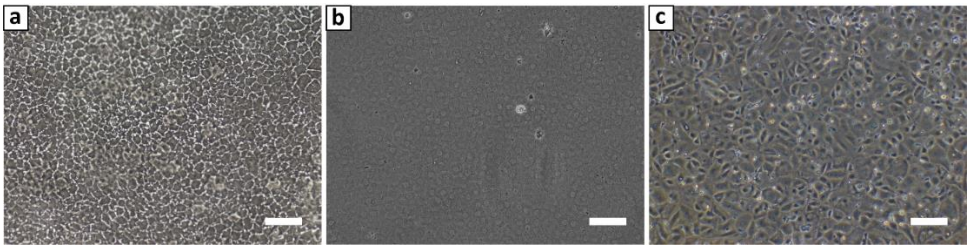

Figure 5. Phase contrast light microscope images of human CECs in a corneal endothelium biopsy (A), primary cultured human CECs (B) and primary cultured CECs showing a characteristic morphological change experienced during primary expansion correlated with a cell loss of function and possible endothelial to mesenchymal transition (C). Scale bar is 100 μm.

Finally, mostly high quality corneas in terms of cell density, i.e. more than 2500 cells/mm^2, and a young age (less than 40 years) that have been used for the primary expansion of CECs. This considerably limits the number of suitable corneas, a challenge given the shortage of donors. The use of older corneas[57,58,74] or discarded endothelial peripheral rims of corneas used for surgery, where cells are thought to be more proliferative,[4,73,77] would increase the availability of primary cultured cells to be used in therapy. Mehta and colleagues have recently isolated primary cells from corneas deemed unsuitable for transplantation for reasons related to connective tissue disorders, diabetes mellitus or low CEC density, to directly treat corneal bullous keratopathy in a rabbit model. This approach has the potential to increase the pool of cells available for therapy since this procedure uses non-cultured cells, and the corneas would be used for either lamellar surgery or discarded from the donor pool.[78] Using alternative cell sources for CEC primary culture and regenerative medicine could drastically increase the availability of cells for therapeutic use. Nevertheless solutions for the low proliferation and rapid loss of phenotype seen with the current protocols need to be found.

Pluripotent stem cells

A new source of CECs for use in regenerative medicine could be generated from pluripotent stem cells (Figure 6). Since Yamanaka and colleagues first introduced the concept of induced pluripotent stem cells (iPSCs) in 2006,[79] stem cell–based personalized regenerative medicine has become a reality. CECs differentiated from pluripotent stem cells could be used for disease modelling and *in vitro* drug testing. Due to the low rejection index of donor tissue experienced during cornea transplantation, therapy-grade CECs could be successfully generated from both embryonic pluripotent stem cells and iPSCs. Nevertheless, such hypothesis still needs confirmation. When generating CECs from iPSCs from the patient, this risk of rejection could be further reduced. Moreover, current international initiatives to establish homozygous HLA iPSC banks will allow to overcome the logistical and financial difficulties of derivating iPSC from every single donor.[80] Overall, differentiating human pluripotent stem cells to CECs presents several advantages, such as the faster *in vitro* expansion of pluripotent stem cells compared to primary cultured CECs and independence from donor corneas. However, protocols for deriving CECs from pluripotent stem cells are still at an early developmental stage.

An intuitive way of designing a protocol for differentiating pluripotent stem cells, whether embryonic or iPSC, into CECs is to follow an approach inspired by developmental biology. CECs derive from neural crest during embryonic development[81] and most protocols published to date differentiate pluripotent stem cells into CEC–like cells following initial neural crest induction.[82–92] The approaches used to generate a neural crest–like population from human pluripotent stem cells focus on the inhibition of the SMAD signaling pathway using the ALK5/TGF-β type I receptor kinase inhibitor SB431542 combined with either the bone morphogenetic protein antagonist Noggin,[82,83,86] or the Wnt pathway regulators IWP2 and CHIR99021.[84,90–92] Interestingly, the use of dual SMAD inhibition with SB431542 and Noggin does not seem an intuitive method to induce a neural crest–like state as it is generally considered to be a neuroectoderm induction method.[93–95]

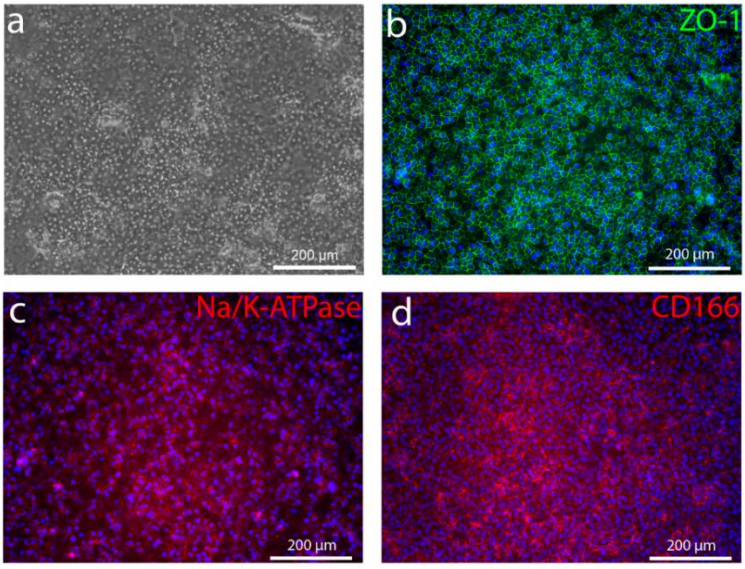

Figure 6. Characterization of human pluripotent stem cell derived CECs. Phase contrast light microscope image shows typical hexagonal cell morphology (A). Immunofluorescence analysis shows the presence of commonly used CEC markers ZO-1 (B), Na^+/K^+ ATPase (C) and CD166 (D) expressed by human embryonic stem cell derived CECs. Representative data conducted with Regea08/017 human embryonic stem cell line. Scale bar is 200 µm. This Figure was kindly provided by Pyry Grönroos from Professor Heli Skottman's Lab.

Once the neural crest–like stage has been achieved, several approaches have been followed to induce the CEC fate. First, exposing the cells to platelet-derived growth factor-B (PDGF-B), Dickkopf-related protein 2 (DKK2) and basic fibroblast growth factor results in the generation of confluent hexagonal cells with a CEC–like phenotype.[82,83,86,92] A combination of SB431542 with the ROCK inhibitor H-1125 can also generate CEC–like cells.[85] Moreover, a study from Skottman and colleagues portrayed the importance of retinoic acid for further differentiating neural crest like cells to CEC–like cells.[84] In addition, the use of a recombinant laminin coating, instead of the animal–derived matrigel, could reduce the undesired batch-to-batch variability and allow a xenogeneic–free culture.[84]

The use of primary cell conditioned media has also shown success in differentiating neural–crest like cells to CEC–like cells.[86,90] A similar differentiation approach has been used for differentiating rodent pluripotent stem cells into CECs through the neural crest–like stage.[87–89]

Although the developmental biology approach seems intuitive, competing approaches for inducing a direct differentiation without passing through the neural crest precursor stage are also being studied.[96–99] Direct differentiation of pluripotent stem cells into CEC–like cells has been reported by either using primary cell culture–conditioned media,[96,99] triggering spontaneous differentiation by cell seeding in corneoscleral disks,[97] or the use of a defined media containing cholera toxin, epithelial growth factor and the ROCK inhibitor Y-27632.[98]

In recent years, significant progress has been made thanks to dedicated efforts to develop protocols for differentiating human pluripotent stem cells into CECs; nevertheless, there remain unsettled challenges. One of the biggest challenges is cell purity. Given the potential of these cells, undesired side populations may arise during differentiation, and these often vary between differentiation batches because of the low efficacy of current protocols. Since differentiation protocols are highly complex, characterization should be performed using an array of markers for every stage of differentiation. For early neural crest or periocular mesenchyme identification p75[100] or Pitx2[101] should be detected. Finally, the recent identification of CEC markers such as CD166 and sPrdx6,[102] comparable to ΔNp63α or keratin 12 in corneal epithelial cells, could open the possibility to enrich for cell populations expressing these markers and improve current differentiation protocols.

In addition to purity, there are a number of other challenges to overcome. It is crucial to demonstrate that the differentiated cells are functional and safe, and therefore suitable for therapeutic use. Functional characterization is needed to confirm the active metabolic pump activity. It is also not fully understood how the differentiation

protocols affect the (epi)genomic signature of the cells and whether they induce DNA alterations in the cells such as epigenetic modifications and karyotype abnormalities. Finally, it is crucial to prove that differentiation is complete and the generated cells do not maintain any stem cell–associated pluripotency, which might lead to tumorigenic potential. Scientists aiming to bring pluripotent stem cell–derived CECs to therapy should put special focus on investigating and resolving the aforementioned matters.

Other cell sources

The differentiation of pluripotent stem cells into CECs is considered a promising method for generating a therapeutic cell source for regenerative medicine. There is growing and encouraging evidence that tumor generation will not present a prohibitive risk for therapy, but this concern still requires careful consideration. Moreover, difficulties to generate pure populations of pluripotent stem cell–derived CECs makes it difficult to implement them in a therapeutic setting. Together, these are reasons to consider other cell sources.

Transdifferentiation is a method for rapidly and reproducibly generating CECs with therapeutic potential without the associated risk and difficulties of pluripotent stem cell differentiation. It involves the reprogramming of mature somatic cells into cells of a different mature somatic lineage. Various cell types have been transdifferentiated to CEC–like cells capable of reverting corneal edema in rabbit animal models. These include bone marrow derived endothelial precursors,[103] neural crest cells,[88] and corneal stromal stem cells.[89] Interestingly, skin derived precursors[104,105] and mesenchymal stem cells[106] have also been transdifferentiated to CECs in a process resembling a reversed endothelial to mesenchymal transition. In order to implement such approaches in a therapeutic setting it is crucial to demonstrate the stability of transdifferentiation to assure a safe therapy and avoid a

return of the cells to their somatic origin improve the transidfferentiation efficiency and purity of the existing protocols.

Taking a different approach, Joyce and colleagues used human mesenchymal stem cells to heal the damaged endothelium in human corneas *ex vivo*.[107] They showed that human mesenchymal stem cells have the capacity to adhere and repopulate denuded areas in the corneal endothelium, and possibly providing paracrine support to surrounding CECs, recovering the corneal endothelial barrier. Despite the successful preliminary results, further studies will be required in order to identify the interactions of these cells with their environment and how their genetic and phenotypic signature correlates with the native corneal endothelium.

Need for standardization of endpoint parameters

Whatever the approach for generating cells for regenerative medicine, whether primary expansion from donor cells, derivation from pluripotent stem cells, or the use of other cell sources, it is crucial to reach a consensus on endpoint parameters to assess their quality. In this section we present a perspective on the assessment criteria that generated CECs should fulfill to be used for therapeutic purposes.

Morphology

A parameter that can be readily assessed is the morphology of the generated CECs. A cellular hexagonal morphology upon reaching confluence in culture could be assessed to preclude the presence of spindle-shaped fibroblastic morphologies associated with a mesenchymal transition. Rating the circularity index of the generated cells confirming the hexagonality and a low polymorphism is a quality check that should be performed.[54,67,74,108] In addition to that, Yamamoto and colleagues have been able to correlate the physical intercellular interactions in a bi-dimensional *in vitro* system with a better regeneration of the corneal endothelium after cell injection.[109] This could be used as a tool to correlate a physical marker with the suitability of the generated cells for therapeutic use.

Genotype and phenotype

For their use in regenerative medicine CECs should possess a gene and protein expression comparable to native human CECs. As previously reviewed by Ni Dhubhghaill and colleagues, the most frequently used markers to characterize the generated CECs are Na^+/K^+ ATPase (*ATP1A1*), ZO-1 (*TJP1*) and collagen type VIII (*COL8*).[110] While each are important markers to establish the presence of metabolically active transporters, extracellular matrix production and tight junctions, respectively, these markers are not specifically expressed in the corneal endothelium but also in many other cell types such as lung[111] or intestinal epithelium,[112] and even in corneal epithelial cells.[113] The hexagonal phenotype is not even exclusive to the CECs in the eye; it is also prominent in the retinal pigment epithelium. Therefore, for better characterization of the generated cells, it is of utmost necessity to prove the expression of specific markers for corneal endothelium. CD166[102,114,115] and sPrdx6[102] (Figure 4) have been recently identified as CEC markers within the cornea that correlate to therapeutic success. Moreover, a recent study by Thuret and colleagues suggested that the hexagonal shape of the CEC apical surface and the interdigitated shape of the CEC basal site together with the expression of functional and structural proteins such as CD56, CD166, Vimentin, N-cadherin and integrin a3b1 is an important hallmark of human CECs.[113]

It is also important to show the absence of fibroblastic markers associated with an EndMT or contamination by stromal fibroblasts, namely CD44 or CD73.[114] To conclude that the generated CECs are of sufficient quality to use in regenerative medicine, the characterization should thus be done by assessing a panel of diverse markers. An example of this is the panel developed and used by Kinoshita and colleagues[59,116,117] They reported that $CD166^+CD24^-CD26^-CD44^-CD105^-CD133^-$ cells have the correct gene expression and phenotype to be used in therapy. In this panel, CD166 was used as a marker for CECs and the negative makers were analyzed to exclude the fibroblastic-like phenotype.[59,116,117]

Karyotype

During the expansion of primary CECs, they are stimulated to exit their arrested phase to proliferate. This has the potential to induce karyotype abnormalities in their genome.[118,119] Likewise, the generation and culture of iPSCs can also cause karyotype abnormalities[120] and less commonly aneuploidy.[121,122] To prove that the cells are safe to use in regenerative medicine, it is crucial to confirm that they retain a normal and safe karyotype after their manipulation.

Kinoshita and colleagues set the basis for a clinical trial using primary expanded CECs and monitored the cell karyotype during primary expansion, nevertheless no endpoint parameter was established on what would be a suitable karyotype for therapeutic use.[59] In Singapore, a batch of cultured CECs is deemed unsuitable for therapy if there is a clonal chromosomal addition or deletion, such as more than two metaphase cells showing the same chromosomal trisomy, or more than three cells showing the same monosomic abnormality, or there is the presence of more than 20 cells in the metaphasic phase.[123]

Functionality

In order to maintain corneal deturgescence and transparency, it is necessary to demonstrate that the generated cells possess their active metabolic pump activity. The expression of transporters, namely Na^+/K^+ ATPase or the electrogenic sodium bicarbonate cotransporter 1 *(SLC4A4)*, is insufficient proof of functionality alone, as protein expression could not necessarily correlate to an active metabolic pump activity in the cells. To date, *in vitro*, *ex vivo* and *in vivo* methods have been developed to test the functionality of CECs.

A rapid way of demonstrating functionality is an *in vitro* test designed to show active metabolic substance transport, namely ion transport, across a monolayer of CECs. The most commonly used methods are transepithelial electrical resistance (TEER) measurements[56] and Ussing's chamber measurements.[43,44,89,96] While the first does

not strictly measure transport, the sensitivity to external factors (electrode distance to measurement membrane, cell monolayer sensitivity to temperature, pH changes and cell shedding plus sensitivity of the instrumentation to vibration oscillations) of the latter makes it a difficult technique to implement.

Another possibility to assess the functionality of the CECs is to assess their active repair in *ex vivo* corneas. Maintaining the *ex vivo* corneas in a setting that mimics physiological conditions allows the measurement of corneal thickness and its correlation to cell functionality.[124,125] To fully mimic the human physiological conditions in an *ex vivo* cornea, Thuret and colleagues developed a bioreactor that opens the possibility to use *ex vivo* corneas for functionality testing (Figure 7).[126]

Finally, animal models of corneal edema have also been used to test cellular functionality by measuring the decrease in the induced corneal edema.[127–130] Depending on the selected model and due to interspecies physiological differences, it is crucial to perform the required controls. For instance, while rabbits are one of the most frequently used animal models, they possess a self-healing corneal endothelium. Animal models represent a valuable method to check safety and efficacy during research and development of cellular therapies.[130] Nevertheless, animal models used are only representative for bullous keratopathy and there is a lack of accurate FECD models. Finally, it is not ethically justifiable to routinely use animal models as quality control to test each single batch of generated cells before clinical use.

Demonstrating CEC functionality is arguably the most important prerequisite for a successful regenerative medicinal product. Although there is no perfect test, it can be accurately assessed using a combination of methods. Nevertheless, there remains a need to develop straightforward functional testing platforms to be used in quality control before the use of each CEC batch for therapy. Organ-on-a-chip technology[131] consists of microfluidic cell culture chips that can successfully mimic physiological

responses of organs. Such a system is an interesting candidate to develop a high-throughput functional model of the corneal endothelial barrier to be systematically used as a quality control check for every batch of generated CECs.

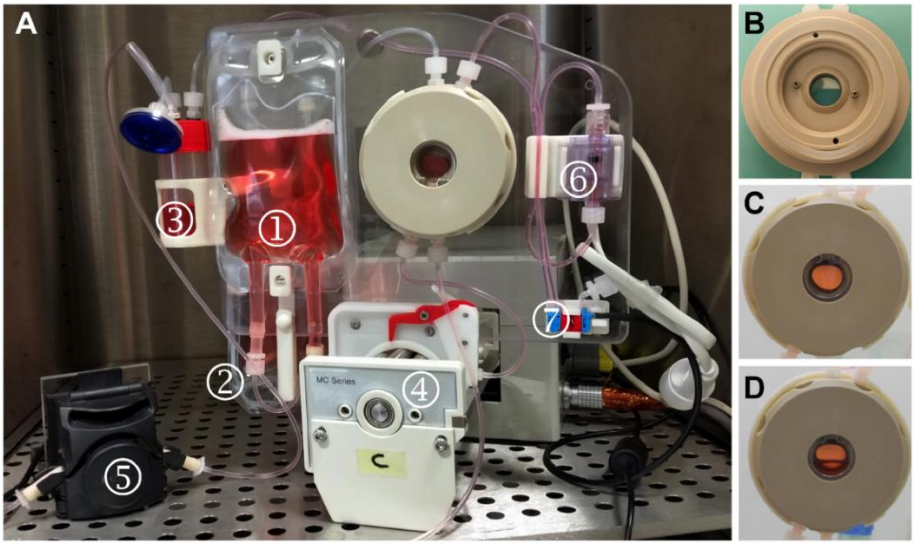

Figure 7. Bioreactor used for the preservation of corneas in physiological-like conditions. The general set up of the bioreactor system inside a CO_2 culture incubator (A) includes a bag with fresh media for the corneal endothelial side (1), a medium waste bag (2), a flask with fresh media for the corneal epithelial side (3), two peristaltic pumps (4 and 5), a pressure sensor (6), and a miniature solenoid valve (7). (B) Empty inside of the bioreactor chamber. Bioreactor corneal chamber containing a porcine cornea after sealing the chamber (C) and during corneal medium immersion phase during operation (D). This Figure was obtained from Guindolet et al., 2017.[126] Licensed under a Creative Commons Attribution-NonCommercial-NoDerivatives 4.0 International License (CC BY-NC-ND 4.0) https://creativecommons.org/licenses/by-nc-nd/4.0/.

Strategies for delivery of corneal endothelial cells

Advances in primary culture of CECs, pluripotent stem cell differentiation and generation of CECs from other cell sources are highly promising approaches for developing a cellular therapy to treat corneal endothelial disease. However, their success hinges on a suitable method to deliver them into the cornea (Figure 8). Cells must be delivered alive and with sufficient potential to adhere to the posterior part

of the cornea. The main two methods currently studied for delivery of CECs are cell injection into the anterior chamber of the eye and the use of different substrates in the effort of bioengineering corneal endothelial grafts.[130]

Cell injection

Cell injection is the delivery of CECs in a simple and minimally invasive manner via injection in the anterior chamber of the eye (Figure 9). In the early 2000s, Mimura and colleagues set the basis for the delivery of primary cultured CECs via intracameral injection in a rabbit bullous keratopathy model.[46,132] After this proof-of-concept work, research proceeded in optimizing the technique of CEC delivery via cell injection.

Gravity, for example, has been shown to increase CEC adherence to the posterior part of the cornea. After cell injection, subjects must stay in prone position for two to three hours to enable the attachment of CECs.[133,134] Co-delivery of the cells with the ROCK inhibitor Y-27632 combined with prone position of the recipient significantly improved cell adhesion [134–136]. Another strategy explored the enhancement of CEC attachment by the use of magnetic force using cells laden with ferromagnetic beads.[132,137,138]

In the pioneering first-in-human clinical trial using primary cultured CECs, Kinoshita and colleagues reversed corneal edema in cataract surgery–derived bullous keratopathy patients and FECD patients with an injection of primary cultured CECs together with Y-27632.[59] The landmark clinical trial from Kinoshita and colleagues has been a major milestone in the development of a cell therapy for treating corneal endothelial disease, and has promoted the identification of the aspects that need to be addressed to ensure an efficient and safe therapy. In the recent 5-year follow up study, the clinical reversal in the endothelial disease was retained in 10 of the 11 patients.[139] This landmark clinical trial raised several questions.

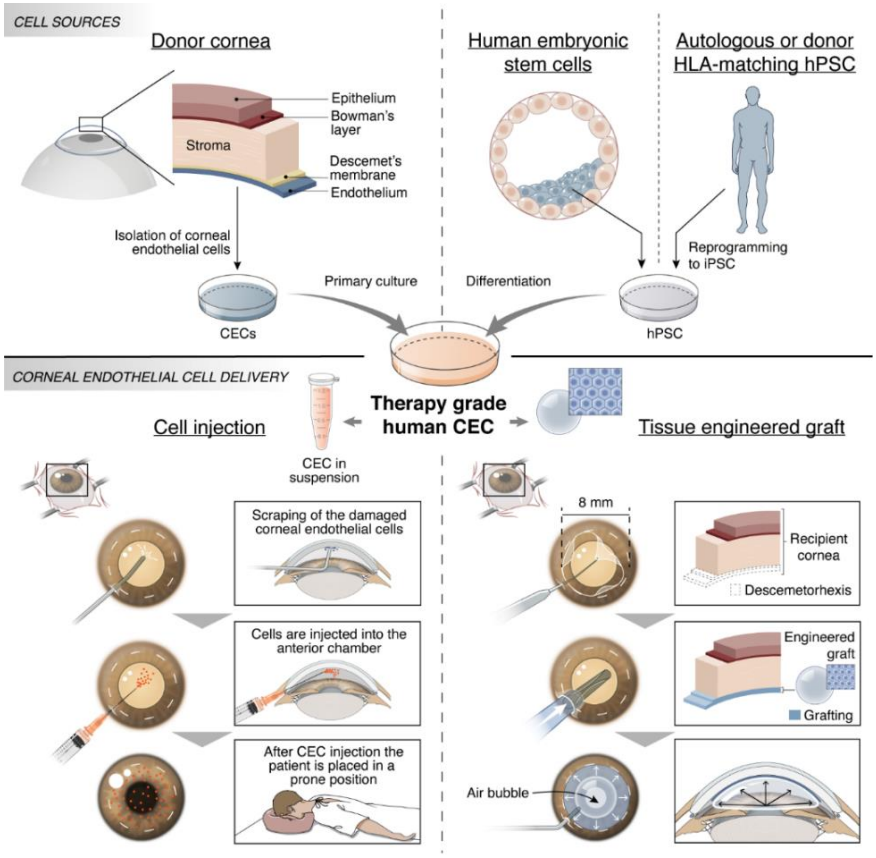

Figure 8. Regardless of the origin of the therapy-grade CECs, whether primary cultured or pluripotent stem cell–derived, it is crucial to develop strategies to deliver them alive and with sufficient potential to adhere to the posterior part of the cornea. Currently, the approaches studied for the delivery of CECs are cell injection into the anterior chamber of the eye and the use of different substrates to bioengineer corneal endothelial grafts. This schematic overview highlights the differences of such approaches for the efficient delivery of CECs.

Interestingly, two different protocols for CEC primary expansion, with or without transforming growth factor β inhibitor SB431542, and two different techniques for removing damaged corneal endothelium were used.[140] Moreover, one recipient received an injection of 5×10^5 cells while the other recipients received a cell injection of 1×10^6 cells introducing another variable factor during the clinical trial. The recipients' CEC densities 24 weeks after injection ranged from 947 to 2833

cells/mm^2 with an average density of 1924 cells/mm^2 [59] which decreased to an average CEC density of 1257 cells/mm^2 after 5 years.[139] It would be interesting to understand how donor and patient characteristics could influence this parameter and if the use of postoperative ROCK inhibitors could reduce the loss of CECs after their injection.

In cases of advanced FECD, where the Descemet's membrane is altered by the presence of guttae, the CEC attachment and monolayer formation is highly impaired.[141,142] This can induce complications when treating these subjects with cell injection. In the clinical trial by Kinoshita and colleagues, seven patients with FECD were treated, and the guttae did not seem to improve after 2 and 5 years.

Okumura and colleagues performed a proof-of-concept study where they compared the outcomes of CEC injection in two rabbit model groups: in the first group the CECs were scraped leaving the Descemet's membrane intact, and in the second group, a 4 mm diameter Descemetorhexis was performed.[143] After 14 days, corneal thickness and transparency in both groups was comparable, although recovery in the descemetorhexis group was slower.[143] In a recent study by Mehta and colleagues, CEC injection was also performed in two rabbit models: in the first group the CECs were scraped leaving the Descemet's membrane intact, whereas in the second group a complete Descemetorhexis was performed.[136] Interestingly, after three weeks, corneas in the complete Descemetorhexis group that received a CEC injection remained swollen with an approximate thickness of 850 μm, whereas in the group where Descemet's membrane was left intact, and received a CEC injection, decreased to 582 μm.[136] These studies suggest that the presence of Descemet's membrane in the recipient cornea is crucial for a successful outcome of CEC injection. Nevertheless, partially removing altered parts of Descemet's membrane in a controlled manner followed by a CEC injection could be an option for treating FECD.

Cell injection is not yet an efficient method regarding the number of cells used. Namely, the number of CECs commonly used, 1×10^6 cells per cornea, is approximately 4 to 5 times higher than the cell count in the healthy human corneal endothelium. Based on our calculations, CECs isolated from a single donor can be expanded to 5×10^6 to 10×10^6 cells at confluence by the second passage. Adopting the cell injection numbers from Kinoshita's clinical trial, 1×10^6 cells per cornea, 5–10 patients could be hypothetically treated with one single donor. Improving cell adherence and survival during this procedure would reduce the number of cells needed to treat one diseased cornea, allowing more patients to benefit from this technique. This can be complemented by strategies such as the isolation of CECs from tissues deemed unsuitable for transplant for direct cell injection (Ong et al. 2020,[78] *Section 3.1. Primary culture of corneal endothelial cells*).

Furthermore, it is necessary to understand how non-adhered CECs distribute. To date, there are few studies showing the biodistribution of injected CECs and the effect they may have both within the recipient's eye and systemically. Brunette and colleagues described the deposition of cells behind the eye lens capsule after CEC injection.[129] The capacity of CECs to cross the eye's trabecular meshwork to systemically disperse in the body appears to be unlikely.[144] Although one patient suffered severe glaucoma after CEC injection, it was likely secondary to steroid use, and while the trabecular meshwork did not reveal blockage after gonioscopy, CECs could have been removed by macrophages that subsequently blocked drainage. Finally, it could be possible that the regeneration of the corneal endothelium in the patients with Fuchs' endothelial corneal dystrophy is due to the patient's own CECs, triggered by the ROCK inhibitor and not by the injected cells. To exclude this possibility, a control group consisting of a DSO/DWEK procedure with and without ROCK inhibitor may be considered in future studies.

There are currently three ongoing clinical trials using cell injection of primary cultured human CECs worldwide, which will soon provide valuable new data to

advance towards the implementation of this technology in the therapeutic setting. These comprise a phase I clinical trial (identification number NCT04191629) which studies the delivery of primary cultured CECs with ferromagnetic beads in Mexico, and two phase III clinical trials (identification numbers UMIN000034334 and UMIN000012534) to further study CEC injection in Japan.

Tissue engineered corneal endothelium

Another strategy to deliver CECs is the use of carriers or scaffolds to make bioengineered corneal endothelial grafts (Figure 9). The appeal of this strategy is that the cells could be delivered to the correct place in a controlled manner, having already formed a confluent cell monolayer that is ready to start functioning. Moreover, the use of cell carriers or scaffolds would also reduce the number of cells needed compared to cell injection, thereby increasing the number of patients that could benefit from the therapy. Based on our calculations, where CECs from a single donor can be expanded to 5×10^6 to 10×10^6 cells, and considering that a corneal endothelial graft should be composed of approximately 2×10^5 CECs, we estimate that 25 to 50 patients could be treated from a single donor with this delivery method. Contrary to cell injection, where its potential to treat FECD is still uncertain, this delivery strategy could be applied to treat most corneal diseases, similar to DSAEK or DMEK. Nevertheless, this approach presents additional challenges compared to cell injection.

To bioengineer a corneal endothelial graft, the substrate or material needs to conform to specific requisites. It should be strong enough to undergo surgical manipulation without breaking, but possess a thickness comparable to DSAEK or DMEK. The selected scaffold should be transparent and its refractive index close to 1.38 to match the cornea,[1] and be permeable to ions, nutrients and metabolic remnants such as lactic acid. Equally important, it needs to promote CEC adhesion and phenotype, but should also adhere to the recipients' corneal stroma. It is imperative that the selected carrier does not trigger fibrotic reactions which can damage the recipients' eye.

Although not essential, biodegradability is an appealing feature so that the transplanted cells would generate their own Descemet's membrane while the carrier slowly degrades over time.

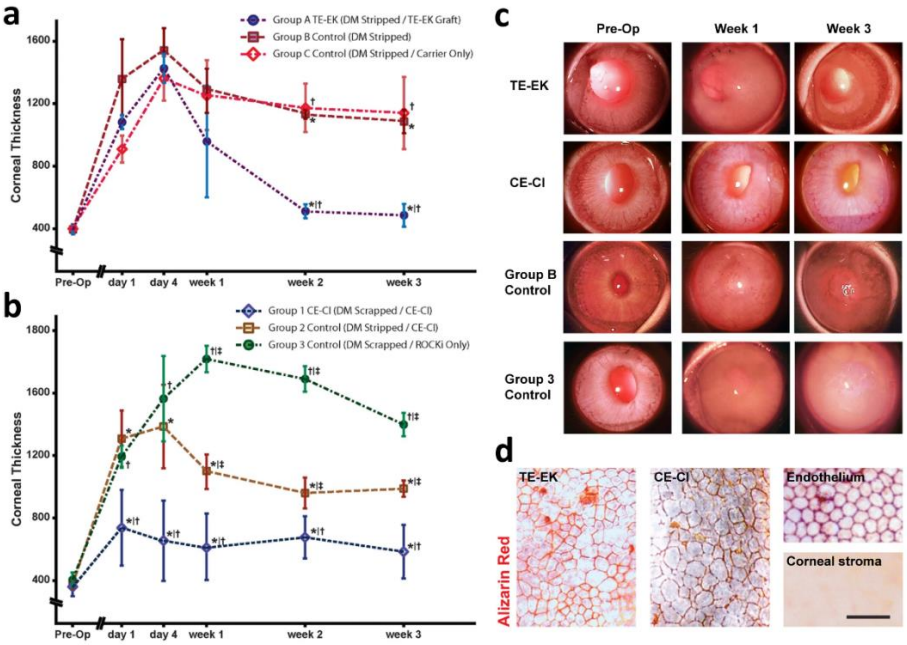

Figure 9. The functional evaluation of two CEC delivery methods suggests that CECs can be both successfully delivered using a cell injection or a cell carrier. Primary cultured human CECs were delivered to two bullous keratopathy rabbit models using either a stromal CEC carrier (TE-EK) or a cell injection (CE-CI) and showed comparable corneal edema reduction (A and B). In Group B control the corneal endothelium was stripped without receiving any treatment. In Group C control the corneal endothelium was stripped following a transplant with the carrier without cells. In Group 2 control the corneal endothelium was stripped following an injection with CECs. In Group 3 control the endothelium was scrapped following treatment with Y-27632 ROCK inhibitor eye drops. Slit lamp images of rabbit eyes before clinical intervention (pre-op) and 1 and 3 weeks after clinical intervention show transparency recovery in corneas treated with either CE-CI or TE-EK (C). Flat-mount Alizarin red staining of rabbit corneas receiving treated with TE-EK or CE-CI show the presence of CECs mosaic (D). Sections of rabbit corneal endothelium and rabbit corneal stroma were also stained as controls (D). This Figure was adapted from Peh et al. 2019.[136] Licensed under a Creative Commons Attribution 4.0 International License (CC BY 4.0) https://creativecommons.org/licenses/by-nc-nd/4.0/.

There are currently two main classifications of carriers for CECs, namely biologic scaffolds derived from tissues and synthetic or artificial scaffolds. Alternatively, some research groups are trying to develop bioengineered endothelial monolayer sheets, comprising only CECs and their extracellular matrix by culturing the cells on thermoresponsive gel substrates. In this section, we discuss the main advantages of the different strategies for bioengineering corneal endothelial grafts.

Biologic scaffolds

Biologic scaffolds are tissue-derived CEC carriers commonly generated by decellularization of biological membranes or decellularization and modification of biological matrices, resulting in a scaffold that can be used as a cell carrier (Table 1). Bovine corneal posterior lamellae,[145] porcine Descemet's membrane,[146] modified porcine corneal stroma,[96] and modified fish-scales[147] have been used as scaffolds for CECs. Nevertheless, their xenogeneic origin might rouse skepticism because of the associated risk they could contain remnants of cellular material but also might not provide the best support for human cells.

As an alternative to xenogeneic sources, decellularized human tissues and biological membranes have also been used as scaffolds for CECs. Modified donor corneal stroma[136,148–152] (Figure 10), amniotic membrane,[153–155] lens anterior capsule,[156–160] and Descemet's membrane[160] have been used as sources for generating CEC carriers.

Considering data from pre-clinical studies, stromal scaffolds have been the most successful in reverting corneal edema and recovering cornea transparency in rabbits.[136,148,151] Conversely, lens anterior capsule carriers triggered strong fibrotic reactions in minipig eyes'[161] and amniotic membranes did not fully revert corneal edema in cats.[154] There is currently an ongoing phase I clinical trial in Singapore (identification number NCT04319848) for delivering primary cultured CECs using decellularized and modified human corneal stromal carriers to patients suffering

from corneal endothelial disease. This study is at an early recruitment phase and more information will be available in the coming years.

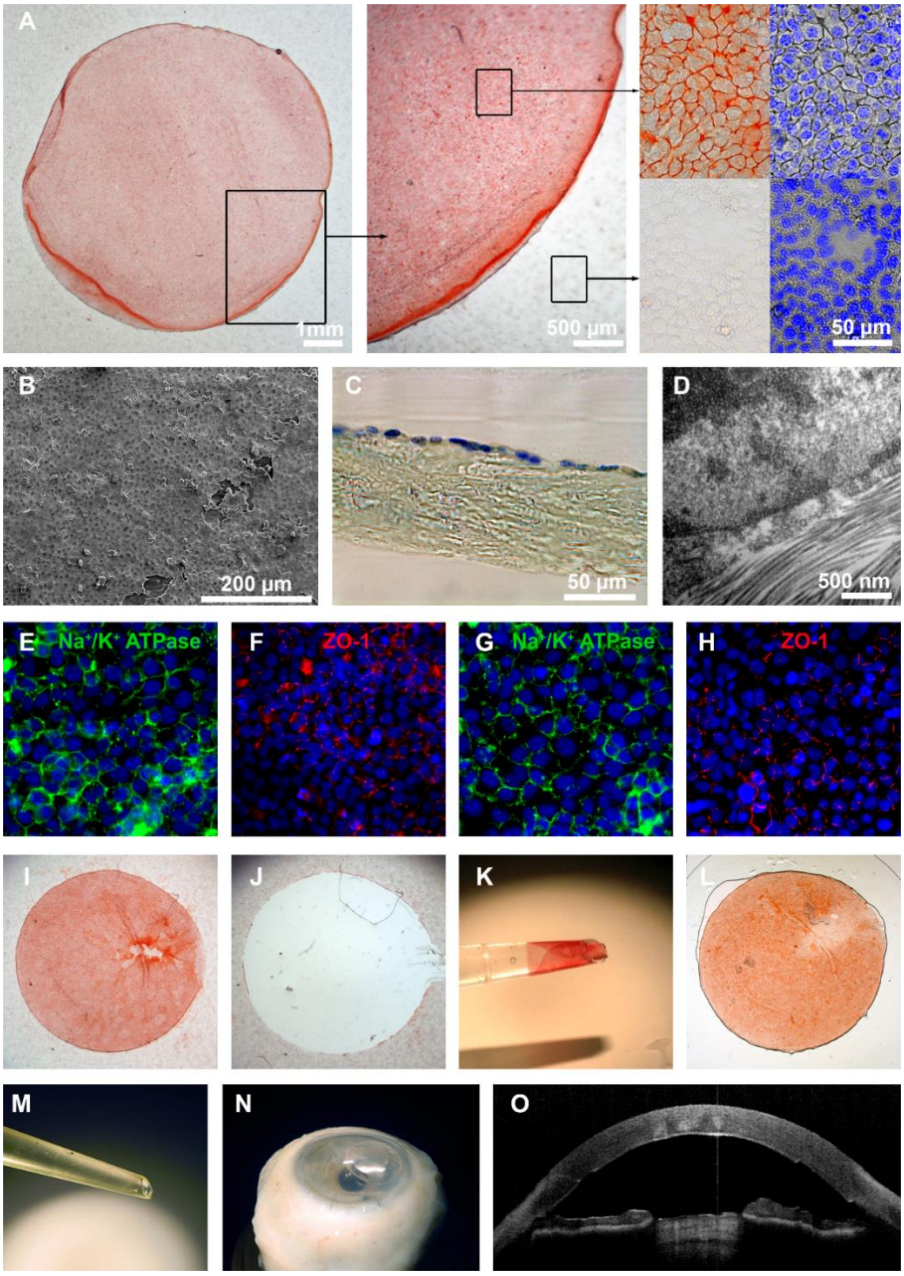

(Figure 10 - legend on next page)

The attraction of using biological scaffolds rests with their somatic origin, as there is no better biocompatibility than that of a native tissue. Nevertheless, biological carriers present some other hurdles. Generating CEC carriers from donor tissue will always be dependent on donor availability and require adequate tissue banking. Countries lacking this infrastructure may have difficulties in using tissue-derived CEC carriers. Furthermore, the donor-to-donor variability may influence the final characteristics of the generated carriers and it is uncertain of how this will affect the final therapy.

Figure 10. Bioengineered human corneal endothelial graft. Human CEC stained with Alizarin Red on a human stromal cell carrier (A). Only the CECs grown on the stromal carrier show the characteristic red staining caused by calcium deposits in the tight junction regions of the bioengineered endothelial graft. Cell nuclei were stained with Hoechst 33342. Scanning electron microscopy (B) and semi-thin sections stained with toluidine blue (C) showed a uniform cell monolayer on the stromal cell carrier. Transmission electron microscopy confirmed the adherence of the CEC on the stromal collagen fibers (D). Na^+/K^+ ATPase and ZO-1 immunofluorescence staining were comparable in CECs grown in tissue culture plastic (E and F) and CECs grown on the human stromal carrier (G and H). (I) Shows another bioengineered endothelial graft stained with Alizarin Red. The bioengineered endothelial graft could be successfully detached from the culture tissue plastic (J), rolled and loaded in an insertion cartridge (K), and released through the narrow opening of the insertion cartridge (L) without showing morphological alterations. After culture of CEC the bioengineered graft was loaded in an injector (M) and grafting was simulated in an *ex vivo* cadaver human eye globe (N). OCT measurement revealed that the bioengineered graft followed and adjusted to the posterior curvature of the recipient cornea (O). This figure was obtained from He et al. 2016.[150]

Polymer scaffolds

Polymer scaffolds are CEC carriers that can be generated from naturally occurring polymers derived from biological sources or from synthetic polymers. Using different approaches such as crosslinking,[162] spin-coating,[163] and electrospinning,[164] these materials can be fabricated into CEC carriers with properties resulting from both the polymer and the fabrication techniques (Table 1). The main advantages of polymer scaffolds are the independence from donor tissue and the ability to generate an abundant amount of material in a rapid and reproducible way to create a highly defined product for clinical use. Nevertheless, using carriers from non-physiological origins may result in adverse reactions.

Commonly used naturally occurring polymers have been collagen, including collagen vitrigel,[44,159,165–172] collagen-derived gelatin,[173,174] and silk fibroin.[175–182] The data have been variable, and animal experiments have revealed the main shortcomings of these carriers. For example, collagen carriers have difficulties staying attached to the recipients' corneal stroma, and the scaffolds tend to detach after 2 weeks.[170] Other studies with collagen-derived carriers did not monitor carrier integration beyond two weeks after implantation[165,166] leaving the graft integration question unanswered.

Similarly, gelatin-based scaffolds also present integration problems; a study reported that four weeks after implantation, 60% of the transplanted scaffolds detached from the recipients' corneal stroma.[174] Silk fibroin scaffolds have also been tested in animal models, nevertheless they triggered fibrotic reactions on recipient rabbits' corneal stroma[175] making them ineligible for therapeutic use. There is an urgent need to overcome the previously mentioned shortcomings of these carriers in order to translate them into the clinical setting.

Many synthetic polymers have also been studied as CECs carriers. Examples of synthetic polymers used have been polycaprolactone (PCL),[183] poly(ethylene glycol)

(PEG),[184] polylactic acid (PLA),[185] chitosan,[186] gelatin methacrylate (GelMA),[187] chemically modified agarose,[188] and combinations of polymers such as silk fibroin–glycerin[189] and chitosan–PCL.[190,191] These synthetic approaches purport to allow a degree of design flexibility of the material to fit the clinical purpose as well as offering the consistency that biologic scaffolds cannot.

Despite promising results in terms of the physical properties of the carrier, cell survival, adherence, and phenotype maintenance, there is only one *in vitro* study performed using primary cultured CECs.[187] The biocompatibility characterization of the other studied carriers has been performed by using immortalized cell lines[183,185,192,193] or primary cultured CECs from non-human origin.[186,189–191] To better understand if the generated carriers are a good platform for regenerative medicine, it is compulsory to demonstrate biocompatibility and phenotype maintenance with primary cultured human CECs. Animal experiments are crucial to demonstrate that the generated scaffolds can integrate in the recipient's corneal stroma without triggering a fibrotic reaction.

Bioengineered endothelial monolayer sheets

Conversely, different groups are studying the possibility to deliver CECs in the form of bioengineered endothelial monolayer sheets. The appeal of this method is that the grafts are assembled by the cells' own extracellular matrix, generating a fully biocompatible construct with a decreased risk of adverse reactions upon implantation (Table 1).

To generate such sheets, CECs are cultured on thermoresponsive polymer substrates. After cell confluency has been reached, and through a decrease of temperature, the CEC monolayer is detached from the thermoresponsive culture surface, resulting in a highly compacted cell sheet, or ultrathin corneal endothelial graft.[194–199] These bioengineered endothelial monolayer sheets appear to be an elegant approach to deliver CECs into the cornea. Moreover, they present a biocompatibility advantage

compared to the cell carriers. However, these ultrathin cell sheets are particularly fragile and their manipulation inside the eye can be technically challenging. It is of utmost importance to develop techniques to enable their accurate and reproducible delivery into the recipient cornea. Loading such sheets on gelatin or hyaluronic acid carriers has been proposed to reduce their manipulation.[200–202] Nevertheless, this approach shares similarities with the use of CEC carriers and their potential biocompatibility and integration problems.

Table 1. Studied corneal endothelial cell carrier types, developmental stage and preparation methods

References	Type of carrier Stage of development	Preparation method	Endothelialization
Biologic scaffolds - Decellularized tissues			
Arnalich-Montiel et al. 2019[152]	Human corneal stroma lamellae DSAEK in rabbits	1. Cryostat cutting (150 μm) 5–6 lamellae per cornea 2. Decellularization (SDS, DNAse)	Human. Primary culture
Bayyoud et al. 2012[145]	Bovine corneal stroma lamellae In vitro	1. Microkeratome cutting Undefined thickness 2. Decellularization (Tris–EDTA, SDS and Aprotinin)	Human. Primary culture
Choi et al. 2010[149]	Human corneal stroma lamellae In vitro	1. Microtome cutting (120–200 μm) 3-4 lamellae per cornea 2. Decellularization (Triton and NH_4OH)	Human. Primary culture
He et al. 2016[150]	Human corneal stroma lamellae Simulation of DSAEK on a post–mortem human eyeball	1. Femtosecond laser cutting (<100 μm) 10–12 lamellae per cornea 2. Decellularization (ethanol. SDS, DNAse I)	Human. B4G12 cell line
Honda et al. 2009[148]	Human corneal stroma lamellae DSAEK in rabbits	1. Dissection with tissue dissection scalpel (100–150 μm) 2–3 lamellae per cornea 2. No decellularization	Human. Primary culture
Parekh et al. 2018[147]	Tilapia fish scale In vitro	1. Protease/surfactant/DNase/RNAse/surfactant/acetic acid/nitric acid decalcification Average thickness: 100–120 μm	Human. Primary culture
Peh et al. 2017[151]	Human corneal stroma lamellae DSAEK in rabbits **Clinical Trial (NCT04319848)**	1. Femtosecond laser cutting (100 μm) Single posterior lamella with its Descemet's membrane 2. Freezing but no decellularization	Human. Primary culture
Zhang et al. 2014[96]	Porcine corneal stroma lamellae DSAEK in rabbits	1. Dissection with tissue dissection knives Undefined thickness 2. Decellularization (freeze-drying + air-drying)	Human. hESC-derived

Biologic scaffolds - Decellularized membranes			
Diao and Hong 2015[146]	Porcine Descemet's membrane In vitro	1. Microkeratome cutting + air bubble Descemet's detachment 2. Decellularization (EDTA + cell scrapping)	No endothelialization
Fan et al. 2011 and 2013[153,154]	Human amniotic membrane Animal experiments in cats (penetrating keratoplasty covered with endothelialized amniotic membrane)	1. Manual cutting of human amniotic membrane 2. Decellularization (trypsin–EDTA + cell scraping)	Human. Immortalized cell line
Ishino et al. 2004[155]	Human amniotic membrane Animal experiments in rabbits (penetrating keratoplasty covered with endothelialized amniotic membrane)	Decellularization (mechanical, EDTA)	Human. Primary culture
Kopsachilis et al. 2012[156]	Human crystalline lens anterior capsule In vitro	1. Manual cutting on post-mortem lens 2. Decellularization (trypsin–EDTA, distilled water)	Human. Primary culture
Spinozzi et al. 2019 and 2020[159,160] **Telinius et al. 2020**[161]	Human crystalline lens anterior capsule Ex vivo simulation of DMEK on human cornea on artificial anterior chamber (Spinozzi) DMEK in Gottingen minipigs (Telinius)	1. Manual cutting on post-mortem lens 2. Decellularization (ethanol, trypsin-EDTA, sponge mechanics)	Human. Primary culture
Spinozzi et al. 2020[160]	Human Descemet's membrane Ex vivo simulation of DMEK on human cornea on artificial anterior chamber	1. Descemet's membrane trephining (Ø 8.0 mm) and stripping 2. Decellularization (ethanol, trypsin–EDTA, sponge mechanics)	Human. Primary culture
Van den Bogerd et al. 2018[158]	Human crystalline lens anterior capsule In vitro	1. Manual cutting on post-mortem lens 2. Decellularization (trypsin–EDTA, distilled water)	Human. Primary culture
Yoereuk et al. 2009[157]	Human crystalline lens anterior capsule In vitro	1. Manual cutting on post-mortem lens 2. Decellularization (trypsin–EDTA)	Human. Primary culture

Polymeric scaffolds – naturally occurring polymers			
Aghaei-Ghareh-Bolagh et al. 2019[179]	Silk fibroin and tropoelastin Biocompatibility by implantation under the skin in mice	Mixture of 75% human tropoelastin and 25% silk fibroin Flat moulding and heating at 160°C for 8 hours. Thickness: 28–93 µm	Human. B4G12 line
Bourget et al. 2016[172]	Extracellular matrix self-assembled in vitro by keratocytes Collagens I,V,VI,XII, lumican and decorin In vitro	1. Corneal keratocyte culture of a newborn child 2. Two–layer assembly for increasing strength Thickness: 40 µm	Human. Primary culture
Choi et al. 2018[178]	Silk fibroin + lysophosphatidic acid In vitro	Film of natural silk fibroin + 8% lysophosphatidic acid Cross-linked by methanol and UV Thickness: 6–8 µm	Rabbit. Primary culture
Kim et al. 2015, 2016 and 2018[180-182]	- Silk fibroin + Human collagen I 2015 - Silk fibroin + aloe vera extract 2016 - Silk Fibroin + β Carotene 2018 In vitro (2015, 2016, 2018) DMEK in rabbits (2016)	Manufacture of a natural silk fibroin film. Coating with human Collagen I, unknown thickness 2015 Manufacture of a film composed of silk fibroin + 3% aloe vera extract. Thickness: 6–8 µm 2016 Mixture of silk fibroin and β Carotene. Methanol cross-linking/rinsing unknown thickness 2018	Rabbit. Primary culture
Kimoto et al. 2014[174]	Gelatin A DSAEK in monkeys	Moulding of a curved and cross-linked sheet by heating to 140°C Thickness: 20 µm	Monkey. Primary culture
Koizumi et al. 2007[170]	Collagen I Vitrigel DSAEK in monkeys	Commercially available collagen I vitrigel scaffold.	Monkey. Primary culture
Levis et al. 2012[169]	Rat tail collagen I Real Architecture For 3D Tissues (RAFT) In vitro + DSAEK simulation of the material alone in a porcine eyeball ex vivo	1. Hydrogel of 80% rat tail collagen I + 10% minimum essential medium + 10% endothelial culture medium 2. Compression dehydration on smooth, flat plastic Thickness: 60–200 µm	Human. B4G12 cell line and primary culture
Madden et al. 2011[177]	Silk fibroin In vitro	Manufacture of a natural silk fibroin film from the cocoons of Bombyx mori. Fabrication by PDMS casting. Coating with collagen IV (origin?) Thickness: 5 µm	Human. B4G12 line and primary culture
Mimura et al. 2004[44]	Collagen I DSAEK in rabbits	1. Cross-linked collagen network (origin?) 2. Alkaline solution/drying/UV sterilization/rehydration Thickness: 40–50 µm	Human. Primary culture

Palchesko et al. 2016[171]	Collagen IV + laminin on the surface of a collagen I disc In vitro	Complex 7–step process Collagen I gel (unspecified origin), human placenta collagen IV, mouse sarcoma cell laminin. Thickness: 10 µm	Bovine and human. Primary culture
Ramachandran et al. 2020[176]	Silk fibroin In vitro	Manufacture of a natural silk fibroin film from the cocoons of Bombyx mori. Fabrication by PDMS casting. Coating with FNC coating® Thickness: 15 µm	Human. Primary and HCEnC-21T cell line
Spinozzi et al. 2019[159]	Collagen I Simulation of DSEK (and not DMEK because it is too sticky) on human cornea on an artificial anterior chamber	Collagen sheets (unspecified origin) Thickness: 20 µm	Porcine. Primary culture
Vázquez et al. 2016[168]	Human Collagen I DMEK in rabbits	Molding of collagen I membrane extracted from clinical grade human bone. Cross-linking UV Thickness: 20 µm	Rabbit and Human. Primary Culture
Vázquez et al. 2017[175]	Silk Fibroin DMEK in rabbits	Manufacture of a natural silk fibroin film from the cocoons of Bombyx mori. Thickness: 10 µm	Rabbit and Human. Primary Culture
Watanabe et al. 2011[173]	Gelatin hydrogel A (porcine) In vitro	Preparation of gelatin films: drying and coating with collagen IV (origin?) Thickness: 50 µm	Human. Primary culture
Yamaguchi et al. 2016[167]	Atellocollagen DSAEK in rabbits	Commercially available Atelocollagen hydrogel scaffold (CM-24). Coating with Viscosat®	Human. Primary culture
Yoshida et al. 2014 and 2017[165,166]	Atelocollagen clinical-grade porcine -Biocompatibility of the material alone (without CECs) in the rabbit cornea and in the anterior chamber 2014 -DMEK in rabbits 2017	Collagen I Vitrigel by moulding a curved sheet and UV cross–linking. Atelocollagen (Nippon Meat Packers,Inc, Osaka, Japan) Thickness: 20 µm	Human. Primary culture

Polymeric scaffolds – synthetic polymers			
Chen et al. 2015[193]	Silk fibroin + poly (L-lactic acid-co-ε-caprolactone) (P(LLA-CL)) In vitro	Silk fibroin electroweaving + P(LLA–CL) (25 :75) Thickness: 56 ± 4.20 μm	Human. B4G12 line
Kruse et al. 2017[183]	PCL and Poly(lactic-co-glycolic) acid (PLGA) In vitro	Electrospinning of a membrane by a prototype machine PCL or PLGA solution + chloroform Disinfected with isopropanol Thickness: 109 ± 17 μm	Human. HCEC-12 line
Liang et al. 2011[186]	Chitosan hydrogel, hydroxypropyl chitosan (HPCTS) and sodium alginate dialdehyde. Open surgery in rabbits	Mixture of the 3 components that gels at room temperature Encapsulation of suspended endothelial cells	Rabbit. Primary culture
Ozcelik et al. 2014[184]	Poly (ethylene glycol) hydrogel (PEG) Biocompatibility by simulation of cell–free DSEK in sheep	1. Solution of glycerol ethylate+sebacoul chloride+ α, ω-dihydroxypoly (ε–caprolactone) (PCL)+ dichloromethane 2. Cross-linked by hydrochloric acid and alcohol Thickness: 50 μm	Sheep. Primary culture
Rizwan et al. 2017[187]	Gelatin methacrylate (GelMa) In vitro Biocompatibility of the material (without endothelial cells) in the anterior chamber of rabbits	UV-crosslinked hydrogel of gelatin A and methacrylate Surface microstructured by molding to facilitate cell adhesion Thickness: 138 ± 5 μm	Human. Primary culture
Salehi et al. 2014[192]	Nanofibers of poly (glycerol sebacate) (PGS) and polycaprolactone (PCL) In vitro	Electro-woven matrix manufacturing of PGS and PCL Nanofiber size: 300–500 nm Thickness unknown	Human. HCEC-12 line
Seow et al. 2019[188]	Agarosse corsslinked with GRGD, lysine, poly-lysine or gelatin In vitro	Mold casting of chemically cross linked agarose materials Thickness: 15–20 μm	Rabbit. Primary culture
Song et al. 2019[189]	Silk Fibroin + Glycerin In vitro	Film of natural silk fibroin + 1% glycerol Crystallized by methanol Thickness: 7 μm	Rabbit. Primary culture
Van Hoorick et al. 2020[185]	Poly D-L-lactic acid (PDLLA)-gelatin In vitro	Multi-step spin coating of: Gelatin A, PDLLA, gelatin B. Membrane harvesting by gelatin A solution in 40°C water bath Thickness: 0.8–1 μm	Human. B4G12 line
Wang et al. 2012[190]	Chitosan + polycaprolactone (PCL) In vitro	1. Mixture of 75% chitosan and 25% polycaprolactone 2. NaOH drying/neutralization/rinse/ethanol 70%/UV sterilization	Bovine. Primary culture
Young et al. 2014[191]	Chitosan + polycaprolactone (PCL) In vitro	Preparation of chitosan+polycaprolactone solutions/evaporation/NaOH treatment/70% ethanol sterilization/UV treatment/Rinsing	Bovine. Primary culture

Bioengineered endothelial monolayer sheets			
Hsiue et al. 2006[200] **Lai et al. 2013**[201]	Gelatin A Animal experimentation in rabbits	Cell culture on pNIPAAm thermoresponsive gel to generate ultrathin corneal endothelial grafts Gelatin disc used as transplant substrate (Thickness: 700–800 μm). Endothelial sheet glued upside down on the disc and inserted to have the cells directly against the cornea. The gelatin is then resorbed	Human. Primary culture
Ide et al. 2006[198]	NONE In vitro	Cell culture on poly(N–isopropylacrylamide) (pNIPAAm), which is heat-sensitive and allows the endothelium to be detached in a ultrathin corneal endothelial graft by lowering the temperature to 20°C	Human. Primary culture
Lai et al. 2015[202]	Recombinant hyaluronic acid Animal experimentation in rabbits	Cell culture on PIPAAm thermoresponsive polymer to generate ultrathin corneal endothelial grafts Cross-linked hyaluronic acid disc used as transplant substrate (Thickness: 700 μm). Endothelial sheet glued upside down on the disc and inserted to have the cells directly against the cornea. The hyaluronic acid is then resorbed	Rabbit. Primary culture
Madathil et al. 2014[197]	NONE In vitro	Cell culture on NGMA thermoresponsive polymer (pNIPAAm + glycydyl methacrylate), which is heat-sensitive and allows the endothelium to be detached in a ultrathin corneal endothelial graft by lowering the temperature to 20°C	Rabbit. Primary culture
Sumide et al. 2006[196]	NONE In vivo. PK in rabbit models, ultrathin endothelial graft is attached on recipient's dissected corneal stromal bed and then re-inserted in the recipient eye	Cell culture on poly(N–isopropylacrylamide) (pNIPAAm), which allows the endothelium to be detached in a ultrathin corneal endothelial graft by lowering the temperature to 20°C	Human. Primary culture
Teichman et al. 2013 and 2015[194,195]	NONE Lamina coating and chondroitin sulfate In vitro	Cell culture on a heat-sensitive support of poly (vinyl methyl ether) (PVME) and vinyl methyl ether and maleic acid (PVMEMA) coated with laminin, chondroitin–6–sulfate and cyclo(arginine–glycine–aspartic acid–D–tyrosine-lysine) cRGD peptides. Ultrathin corneal endothelial graft is detached by lowering the temperature to 20°C	Human. HCEC-12 line

Acellular corneal endothelial graft substitutes

Development of surgical techniques such as DSO or DWEK revealed that in specific cases of FECD, the regeneration of corneal endothelium could be achieved without the use of a donor endothelial graft, challenging the current state-of-the-art. Nevertheless, DSO/DWEK are limited to early-stage disease in relatively young patients and recovery is long and unpredictable. Endothelial graft substitutes comprising of synthetic or tissue-derived matrices could aim to promote corneal healing when implanted after DSO/DWEK procedures. With this technique, no donor graft would be required. The potential advantage is that acellular corneal endothelial graft substitutes may promote or facilitate proliferation and migration of peripheral CECs to repopulate acellular regions, and also support corneal deturgescence and edema reduction upon implantation.

Mehta and colleagues were the first to report the use of acellular corneal endothelial graft substitutes in 2017.[203] In their study, the corneal endothelium was stripped off rabbit eyes and decellularized human Descemet's membrane was introduced similarly to a DMEK procedure, a process called Descemet membrane transfer. The animal group receiving allogenic decellularized Descemet's membrane showed an increased corneal endothelial migration and a faster edema reduction compared to the control group which did not received an allogeneic transplant (Figure 11). There is currently an ongoing clinical trial in Singapore studying such technique in humans (identification number NCT03275896). The first clinical results were recently published, and the first transplantation of a 4 mm diameter decellularized Descemet's membrane into a patient was successful in improving the patient's best-corrected Snellen visial acquity from 6/18 to 6/7.5 at 6 months after transplant.[204] Moreover, corneal thickness was reduced from 603 μm to 569 μm and central CEC density was 889 cells/mm^2 [204]. This first proof-of-concept study paves the way to study acellular corneal endothelial graft substitutes to promote CEC healing and edema reduction.

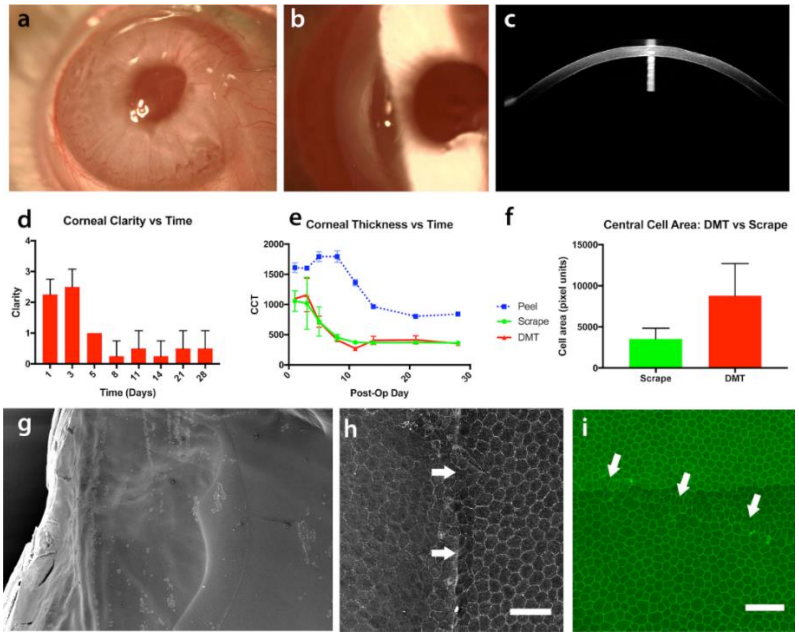

Figure 11. Descemet's membrane transfer (DMT) on a rabbit model. Eleven days after DMT the corneas appeared to be clear in the center (A). A small opaque area could be seen in the periphery of the Descemet's graft, at the descemetorhexis edge (B). Optical coherence tomography showed that corneal thickness of rabbits receiving a Descemet's membranes transplant did not differ from control animals (C). Rabbit eyes showed a central corneal clarity of 0 or 1 8 days after DMT (D). Corneal thickness recovery of eyes receiving DMT was comparable to the animal control group were the cells were scraped, leaving a region of the Descemet's membrane denuded (scrape) and significantly better compared to the animal control group that underwent a descemetorhexis (peel) (E). Central endothelial cell area was greater in the corneas receiving DMT compared to the scrape group (F). Scanning electron microscopy revealed that CECs could migrate over the Descemet's membrane graft, forming a complete monolayer (G). CEC bridged over the edge of the Descemet's membrane graft edge, indicated with white arrows (H). Immunofluorescence analysis of ZO-1 revealed that the bridging CECs formed an uninterrupted cell monolayer over the transferred Descemet's membrane (I). Scale bar: 50 μm (H)

A second approach proposed the use of a synthetic graft substitute to reverse corneal endothelial disease. There is currently an ongoing randomized multi-center clinical trial (identification number NCT03069521) aimed to evaluate if a Contomac Ci26-based implant (EndoArt), is successful in reversing corneal edema and promoting sight recovery. The EndoArt implant was designed to prevent fluid infiltration into

the cornea, thereby preventing and reversing corneal edema. While the data on this study are still restricted, preliminary results from eight patients with chronic corneal edema are encouraging.[205] Out of these eight patients, seven presented a reduction of corneal edema and recovery of transparency after EndoArt implantation. In one patient, surgery failed due to hypotomy and a rescue penetrating keratoplasty was performed. In the seven successful surgeries the construct detached from the recipients' cornea and had to be repositioned by rebubbling until correctly attached to the cornea (Figure 12). The cornea remained clear in the seven patients for up to 4 months.

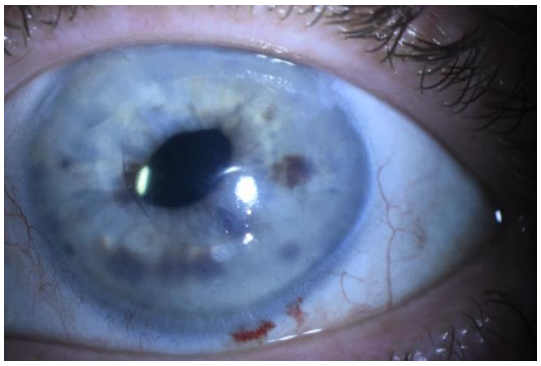

Figure 12. Slit lamp image of a patient's eye one day after EndoArt implantation. Courtesy of Dr Ruth Lapid-Gortzak, Amsterdam University Medical Center, the Netherlands.

Despite initial positive results, the exact timespan over which the cornea will remain transparent and whether corneal edema will reoccur remains uncertain. Furthermore, more data are needed to determine the precise detachment rate and if corneal nutrition will be affected in the long-term due to the impermeability of the construct. Improvements in the material attachment to the recipients' cornea would be required to enable widely acceptance of such device. Moreover, based on currently available data, CECs are unable to migrate over the EndoArt, the effect of which remains to be seen. Overall, although acellular graft substitutes offer an attractive solution to current tissue shortage, future studies are needed to determine if they are successful enough to be implemented in a large scale clinical setting and for what indication.

Pharmacological modulation of the corneal endothelium

The pharmacological modulation of the corneal endothelium to promote cell survival, proliferation and migration has also been studied as a potential treatment for corneal endothelial disease, showing promising preliminary results (Table 2). The appeal of this therapeutic modality is that the patients' endothelium could regenerate with a minimal procedure of intracameral or topical delivery of a drug. While it might seem that the risks of using a pharmacological modulation of the corneal endothelium are rather low, as it would always be possible to perform a rescue DMEK/DSAEK if the patients are not recovering after a reasonable treatment time window to avoid subepithelial or stromal scarring, it is important to monitor possible infiltrations of the trabecular meshwork or development of iridocorneal endothelial type syndrome caused by the therapeutic drug.

ROCK inhibitors are one of the most promising candidates for treating corneal endothelial disease. ROCK is a protein kinase downstream of the effector GTPase Rho, which plays a crucial role in cytoskeleton regulation. The first drug candidate identified was Y-27632, which showed potential to trigger CEC repair and survival *in vitro*.[61,206] After showing success in reducing corneal edema and recovering visual acuity in rabbit and monkey bullous keratopathy models,[207,208] a first clinical trial was performed in Japan (identification number UMIN000003625). This trial comprised two different groups. First, a group of eight patients were treated, four with FECD and four with bullous keratopathy. Briefly, the damaged CECs were surgically removed gently, preserving the Descemet's membrane. After this minimal surgical procedure, the eight patients were treated with topical delivery of 10 mM Y-27632 using eye drops six times a day for 7 days. Cornea thickness was reported at 3 and 6 months after treatment. In the four patients suffering from central corneal edema caused by FECD, a decrease of corneal thickness, from an average of 740 μM to an average of 640 μm was reported after 6 months. Conversely, the corneal thickness did not reduce after the treatment with Y-27632 in the four patients with

bullous keratopathy and diffuse corneal edema.[207,208] The second group consisted of three patients suffering from bullous keratopathy after cataract surgery, where the Descemet's membrane was partially detached and lost. These patients were directly treated with topical delivery of 1 mM Y-27632 six times a day for 4 months and four times a day for 2 months using eye drops.[209] After 3 months of treatment, the corneal edema was reduced from values of 900–610 μm to values of 580–503 μm and visual acuity recovered to 20/20 in 2 patients and 20/25 in one patient.[209] These studies implied the success of the therapy depends on the disease background and highlight the importance of developing a controlled dosage and treatment duration.

Ripasudil, another ROCK inhibitor, has also shown success in reducing corneal edema and recovering corneal clarity in a bullous keratopathy rabbit model.[210] Y-27632 and Ripasudil target the ATP-dependent kinase domains of ROCK1 and ROCK2 with an IC_{50} of 0.11 M and 0.051 M for ROCK1 and 0.17 M and 0.019 M for ROCK2 respectively.[211] The increased efficacy and affinity of Ripasudil compared to Y-27632 for ROCK1 and ROCK2, indicated by the lower IC_{50}, is due to the addition of a fluorine atom in the isoquinoline moiety.[212,213] Both ROCK inhibitors show a comparable ocular distribution reaching the highest concentration in the cornea 15 to 30 min after instillation.[211] *In vitro* studies suggest that ripasudil might promote an increase in cell proliferation, migration and adhesion,[214] thus causing the regeneration of the corneal endothelium. In 2016, a first-in-human study was performed in Australia. Two patients with FECD who underwent a DSO/DWEK procedure and did not experience corneal clearing after 2 and 3 months were treated with topical delivery of ripasudil 0.4% eye drops 6 times a day for 2 weeks. One month after treatment, the CECs had repopulated the bare stroma of both patients and corneal opacity was reduced.[215] In the same study, another eye that did not clear 2 months after a DSO/DWEK procedure was treated with the topical delivery of 10 μM Y-27632 using eye drops six times a day for 2 weeks without success.

ROCK inhibitors have shown success in clinical trials, but the number of patients involved in these studies is very low, though there are a number of studies currently recruiting. In order to conclude if ROCK inhibitors have a beneficial effect treating corneal endothelial disease, there is the urgent need to perform larger randomized control trials with a DWEK control group and specifically defined dosing and therapeutic length.

Furthermore, there is the need to understand each disease case such that we are able to identify which patients will benefit from the therapy and which patients are not suitable candidates. Crucial considerations could be patient age, genetic background, the stage of the disease, the absence/presence or amount of bullae, the peripheral CEC density, and the shape and size of the Descemetorhexis. Part of this challenge is that the biological action of ROCK inhibitors is not well understood, for example whether they increase cell survival, proliferation or migration.

There are currently four ongoing phase II, randomized and double-blinded clinical trials using topical delivery of Ripasudil for treating FECD. A first study in Germany (identification number NCT03575130) will involve 21 participants and study the topical delivery of Ripasudil 0.4% eye drops after a DWEK procedure six times per day for 2–4 weeks. The control group will undergo a DWEK procedure and will be treated with placebo artificial tears. A second clinical trial in the United States (identification number NCT03813056) will involve 72 participants and will study the benefits of Ripasudil 0.4% eye drops delivered six times per day for 2–4 weeks after a DMEK procedure. The control group will undergo a DMEK procedure and will be treated with placebo artificial tears. A third study (identification number NCT03249337) will compare Ripasudil dosing regimen of 3 times a day with 6 times a day in patients who underwent a DSO/DWEK procedure for FECD. Finally, a fourth international multicenter trial (identification number NCT04250207) will involve 60 participants and will study the topical delivery of two different doses of Ripasudil (K-321 solution) eye drops after a DWEK procedure on FECD patients.

Half the controls that will undergo DWEK will receive placebo only and the other half will receive twice daily placebo and twice daily Ripasudil. These studies will give more insight into the use of ROCK inhibitors for treating corneal endothelial disease.

To date, ROCK inhibitors have been the most studied drugs for treating corneal endothelial disease, but there is also promising research exploring other pharmacological tools to promote corneal endothelial regeneration. Different growth factors such as epidermal growth factor,[216] platelet-derived growth factor[217] and fibroblast growth factors[218] have been studied to promote migration and proliferation of CECs for tissue regeneration. Nevertheless, their potential benefit comes with the risk of causing an undesired EndMT.[52,219] Research in this field identified an engineered FGF-1 molecule, TTHX1114,[220] which has shown potential *in vitro* and *in vivo* to trigger corneal endothelial regeneration without any relevant side effects (United States patent registry number US 2016/0263.190 A1). There is currently an ongoing phase I/II clinical trial in the United States (identification number NCT04520321) studying the safety and efficacy of TTHX1114 for treating corneal endothelial disease. This study is at an early recruitment phase.

There has also been research specifically focusing on the pharmacological modulation of FECD. It is known that the extracellular environment of FECD increases the risk of an endothelial to mesenchymal transition leading to a loss of function of the corneal endothelium.[142] One of the better understood factors causing this transition is the increase of TGF-β.[52,219] TGF- β inhibitors can reduce the endothelial to mesenchymal transition of CECs *in vitro*[221] suggesting the potential of these pharmacological tools to treat patients with FECD.

Another characteristic of the pathological profile of FECD is the cell death due to an increase in oxidative stress.[222] N-acetyl cysteine (NAC), a scavenger of reactive oxygen species, has been shown to reduce CEC death *in vitro* and in a transgenic

COL8A2$^{L450W/L450W}$ mouse model[223,224] and CEC ultraviolet damage model.[225] Nevertheless, the *COL8A2* transgenic model does not develop corneal edema and the animal model developed by Liu et al.[225] is a UV damage model, not a model of FECD. Sulforaphane has also been identified as an oxidative stress reducer by phosphorylating and activating Nrf2, a transcription factor that promotes expression of antioxidative stress proteins, and has been shown to decrease CEC apoptosis *in vitro.*[226,227] Oxotremorine, a selective muscarinic acetylcholine receptor agonist, and mefenamic acid, a nonsteroidal anti-inflammatory drugs, have also shown to decrease oxidative stress and increase survival in human CECs *in vitro.*[228] These data suggest that pharmacological tools could be used as a potential treatment for Fuchs' endothelial corneal dystrophy. However, there is a clear need for double blinded randomized controlled clinical trials to generate higher level evidence.

Table 2. Studied drugs and their developmental stage for the treatment of corneal endothelial disease

Drugs for the treatment of corneal endothelial disease					
Drug	**Drug class**	**Possible mechanism of action**	**Developmental stage**	**Ongoing clinical trials**	**References**
Y-27632	Inhibitor of Rho-associated, coiled–coil–containing, protein kinase 1	Increase in CEC survival, proliferation and/or migration	In humans Completed clinical trial: UMIN000003625	No	Okumura et al. 2013, 2015[207,209] Koizumi et al. 2013[208]
Ripasudil	Inhibitor of Rho–associated, coiled–coil–containing protein kinase 1	Increase in CEC survival, proliferation and/or migration	In humans	Yes NCT03575130, NCT03813056, NCT04250207, and NCT03249337	Okumura et al. 2016[210] Moloney et al. 2017[215] Schlötzer-Schrehardt et al. 2020[214]
TTHX1114	Engineered human fibroblast growth factor 1 protein	Promotion of CEC proliferation	In humans	Yes NCT04520321	Xia et al. 2012[220]
SB431542	Inhibitor of the TGF–β type I receptors ALK5, ALK4 and ALK7	Decrease of endothelial to mesenchymal transition	In vitro (immortalized human CEC lines)	No	Okumura et al. 2017[221]
Sulforaphane	Nrf2 transcription factor activator	Oxidative stress and apoptosis reduction	In vitro (immortalized human CEC lines)	No	Ziaei et al. 2013[226]
N-acetyl cysteine (NAC)	Scavanger of reactive oxygen species	Oxidative stress and apoptosis reduction	In vitro (immortalized human CECs) In vivo (early onset FECD mouse model)	No	Halilovic et al. 2016[224] Kim et al. 2014[223] Liu et al. 2020[225]
Oxotremorine	Selective muscarinic acetylcholine receptor agonist	Oxidative stress and apoptosis reduction	In vitro (bovine CECs)	No	Kim et al 2017[228]
Mefenamic acid	Nonsteroidal anti-inflammatory drug inhibitor of cyclooxygenase 1 and 2	Oxidative stress and apoptosis reduction	In vitro (bovine CECs)	No	Kim et al. 2017[228]

Genetic modulation of the corneal endothelium

One of the leading causes of corneal endothelial disease are genomic alterations in patients, which the gene or protein subsequently affect CECs. Developing tools for correcting these genetic alterations or avoiding their associated effects could potentially reduce the need for corneal transplantation, making more corneal donor tissue available for other purposes.

There are currently four corneal endothelial dystrophies with a clear genetic origin, namely: polymorphous corneal dystrophy (PPCD), congenital hereditary endothelial dystrophy (CHED), X-linked endothelial dystrophy (XCED), and FECD.[229] The first three are rare,[229] while FECD, a disease of autosomal dominant nature with incomplete penetrance, has a global estimated prevalence of 4–5% in people above 40 years old[230] and is the leading indication for corneal transplantation worldwide.[231] The development of a genetic modulation therapy to specifically treat FECD could have a major impact on reducing the need for corneal donor tissue.

The pathophysiology of FECD has been extensively reviewed elsewhere.[230,231] Although alterations in different genes, among them *SLC4A11*, *ZEB1* or *COL8A2*, have been associated with the disease, the most common genetic alteration is an intronic CTG trinucleotide repeat expansion in the transcription factor 4 (*TCF4*) gene.[230,231] The role of the CTG repeat expansion has been thoroughly reviewed elsewhere.[230] The CTG repeat expansion has a prevalence in Fuchs' patients ranging from 26% to 79%, depending on group ethnicity,[230] which positions the CTG trinucleotide repeat expansion in the *TCF4* gene as the most viable genetic target for developing a genetic modulation therapy. While there is not yet a clearly identified genetic mechanism to explain the effect of this trinucleotide expansion on the *TCF4* gene, there is evidence for three hypotheses: a dysregulated TCF4 protein expression leading to a protein loss–of–function, RNA repeat–mediated toxicity, or toxic repeat peptide generated by repeat–associated non–AUG dependent (RAN) translation.[230]

In this section, we discuss the possible therapeutic approaches for corneal endothelial genetic modulation based on the altered *TCF4* gene origin of FECD.

Gene augmentation

Gene augmentation consists of the delivery of a functioning copy of a specific defective gene aimed to correct a disease caused by a protein loss of function. The most commonly used systems for nucleic acid transfer have traditionally been viral vectors, such as adeno associated viral vectors (AAVs) and adenoviral vectors (AVs).[232] AAV serotypes AAV-7, AAV-8 and AAV-9 have shown strong tropism for ocular tissues,[233] being good candidates for such approach. The size of *TCF4* messenger RNA, around 8000 bp, is a key consideration for developing viral delivery methods. *TCF4* can be too large to be delivered with specific AAV serotypes.[234] Specific AAV serotypes, namely AAV-5 have been successful in deliverying genes up to 8900 bp[235] and could be used to deliver a functioning copy of *TCF4* messenger RNA to CECs. Non-viral delivery strategies such as liposomal gene delivery or DNA–protein conjugates have also been studied.[232] Lessons learnt from gene augmentation therapies focused on treating other eye diseases[236] could facilitate the generation of a gene augmentation therapy if the corneal endothelial disease origin was closely related to an altered protein expression. Given that the cells are arrested in G1 phase, the CECs are an attractive target for gene therapies as the cells do not divide and are therefore more likely to retain their delivered material. Furthermore, the immune-privileged nature of the eye provides an advantage of likely allowing the repeated delivery of gene therapy products. Gene augmentation studies on retinal congenital blindness due to *RPE65* deficiency have shown that the repeated subretinal administration of an AAV-based gene therapy in the contralateral eye did not cause immune reactions even if the recipient presented circulating anti-AAV antibodies.[237,238] Other studies have also assessed the low presence of AAV neutralizing antibodies in the aqueous humor in humans[239,240] and after the subretinal delivery of AAV-based gene therapy treatment in dogs.[241] These data suggest that repeated delivery of a gene therapy product in the anterior chamber is unlikely to

generate immune reactions that could affect the therapy efficacy or the recipient's eye. Nevertheless, further studies are required to understand the possible immune reactions following repeated administration of gene therapy products in the anterior eye chamber.

Antisense oligonucleotide-based modulation

Antisense oligonucleotides are a strategy for treating genetic diseases caused by either RNA repeat–mediated toxicity or the generation of toxic repeat peptides by RAN translation. Antisense oligonucleotides such as small interference RNA (siRNA) or micro RNA (miRNA) are complementary sequences to messenger RNA (mRNA) that trigger their blockage or elimination.[242] Designing specific antisense oligonucleotide strategies targeting the mRNA transcripts containing the CUG trinucleotide expansion would allow the removal of their associated deleterious effects, as only the non-expansion containing allele would be translated.

Three reports have studied the use of antisense oligonucleotides in order to reverse CTG expansion associated toxicity for FECD.[243–245] These studies demonstrated that antisense oligonucleotides could diminish the toxic effects associated to the CUG expansion in *TCF4* mRNA in human CEC lines.[243–245] Moreover, the delivery and uptake of antisense oligonucleotides was assessed *ex vivo* in human corneas[244] and *in vivo* using mouse models.[243,246] Nevertheless, *in vivo* functionality and reduction of the disease associated phenotype has not yet been assessed.

Antisense oligonucleotide therapies could be an elegant approach to treat FECD, nevertheless there are some key aspects that need to be taken into consideration. Namely, it is crucial to develop an efficient delivery method. The therapeutic RNA must be delivered to the back of the cornea either by topical delivery or intracameral injection without compromising its structure and the antisense oligonucleotide must be targeted and internalized by the CECs. Furthermore, an antisense oligonucleotide therapy will require life-long treatment as RNA oligonucleotides degrade quickly *in*

vivo, meaning that the therapeutic agent will have to be delivered on repetitive basis. Apart from the effect on a patient's daily life, it is necessary to determine the cost-effectiveness of such therapeutic approaches. Finally, antisense oligonucleotides targeting CTG repeat could also bind to the same repeat elsewhere in the genome, potentially evoking an undesired off-target effect.

CRISPR/Cas9-based modulation

Nucleases offer the possibility to modulate genomic regions by cleaving specific targets and promote cellular responses for DNA damage repair. With the use of nucleases, genomic regions can be removed, and/or genes can be modified or inserted if a DNA template sequence is co-delivered with the desired nuclease.[236] The ease of target modulation and the high specificity for sequence cleavage of clustered regularly interspaced short palindromic repeats (CRISPR)/Cas9 system compared to other programmable nucleases such as zinc finger nucleases and meganucleases[247] positions CRISPR/Cas9 as the preferred genome editing tool to reach therapeutic use. CRISPR/Cas9 for genome editing and gene regulation has been thoroughly described elsewhere.[248,249]

CRISPR/Cas9 could potentially be used to remove CTG expansions in the *TCF4* gene in order to revert the mutation causing Fuchs' endothelial corneal dystrophy regardless of the genetic mechanism causing the disease and the number of CTG repeats present. Efforts for developing CRISPR/Cas9 therapies to correct other diseases caused by trinucleotide expansion, such as Huntington's disease,[250,251] paves the way for this approach.

Being a relatively new approach, studies published using CRISPR/Cas9 technology to correct genetic alterations related to corneal endothelial dystrophies are currently very limited. In 2020, Rong and colleagues demonstrated the possibility to reduce the accumulation of *TCF4* mRNA containing the CUG expansion by targeting it with an endonuclease defective Cas9, similar to an antisense oligonucleotide therapy

technology known as CRISPR interference.[252] In a different strategy, Uehara and coworkers demonstrated that the removal of *COL8A2* gene allele containing a missense mutation using CRISPR/Cas9 prevented a mouse model from developing early onset Fuchs' endothelial corneal dystrophy.[253] While still in an early stage, these first studies have set the basis for the continued development of this approach.

While CRISPR/Cas9 is a promising therapeutic tool for the treatment of corneal endothelial dystrophies, it is important to highlight some of its limitations. For example, it is necessary to develop a delivery platform of both the Cas9 protein and single guide RNA, assuring that both can reach the CECs in the back of the cornea. This delivery platform should be administered topically or via an intracameral injection. Despite outperforming other nucleases in high-fidelity targeting, CRISPR/Cas9 could still cut or edit off-targets. It will be crucial to study the potential off-target effects that such therapy could generate in the cornea and eye in order to assure its safety.

General considerations

There are crucial aspects that must be considered for designing a successful genetic modulation strategy, which have been extensively reviewed elsewhere,[254] some of which need to be addressed for developing a successful genetic modulation strategy for treating corneal endothelial dystrophies. It will be important to elucidate the main genetic mechanism behind the corneal endothelial dystrophy in order to strategically design a successful therapy, as each genetic modulation strategy is best-suited to certain genetic disease mechanisms. Furthermore, defining the relationship between genotype and disease phenotype is of utmost importance. For example, there are no readily available techniques to determine the size of known trinucleotide repeats in CECs apart from gene sequencing, which is impossible to perform without a biopsy of the corneal endothelium and should be avoided due to potential tissue damage. It is crucial to develop such techniques in order to detect genetic alterations related to

corneal dystrophies as well as characterizing the effect of genetic modulation therapies.

The current lack of *in vitro* and *in vivo* models for FECD also hamper the research of genome modulation strategies. The development of *in vitro* and animal disease models presenting the genetic and phenotypic characteristics of late-onset FECD is paramount to study delivery and safety, including genotoxicity studies, but also to determine clinically meaningful end-point parameters to assess the efficacy of the selected approach.

Finally, while genetic modulation of the corneal endothelium could correct the genotype behind the disease, it will not necessarily treat existing symptomatology. For this reason, it remains to be understood when it would be most successful and feasible to treat patients, and whether it must be done before symptomatology appears, for example by performing a genetic background check on a presymptomatic patient, or at an early disease stage, when symptoms start to develop.

Societal challenges and ethical perspective

There is currently a global donor corneal tissue shortage, whereby only one in seventy patients worldwide have access to donor tissue for transplant. Underlying this figure is an imbalance between corneal blindness and access to corneal transplantation in different regions. Most of Western European countries, Northern American countries, Brazil, Singapore and Australia do not suffer from severe tissue donor shortage.[11] In fact, countries such as the United States of America, Italy or the Netherlands are net exporters of corneal donor tissue. On the other hand, African, Asian, and some South American and Middle Eastern countries suffer from great tissue scarcity [11]. The reasons behind such tissue scarcity are the lack of infrastructure that would allow cornea tissue donation, processing and storage, such

as tissue banks but also cultural reasons that prevent tissue donation among citizens. It is essential to understand this unbalanced global map while developing therapies for treating corneal endothelial disease.

Corneal endothelial regenerative medicine aims to create an alternative to corneal transplantation, which would especially benefit the countries suffering from major tissue scarcity problems. Unlike Europe and the United States, where bullous keratopathy and FECD are the major indications for corneal transplantation,[11] the main indication for corneal transplantation in countries suffering from major tissue scarcity are infectious keratitis and trauma[11,255] and these cannot be treated by corneal endothelial regenerative therapies. Nevertheless, 18% and 22% of the corneal transplantations in Africa and Asia, respectively, are still indicated for corneal endothelial disease.[255] Alleviating this burden would liberate donor corneas for other indications.

Corneal endothelial regenerative medicine approaches also raise questions from a societal perspective. Cell and gene therapies will likely be more expensive than corneal transplantation. As a reference, the Holoclar autologous stem cell therapy for treating limbal stem cell deficiency has a selling price of USD 105,000 per eye in Europe[256] and Voretigene neparvovec, commercially known as Luxturna, a gene therapy for correcting the defective *RPE65* gene in retinal cells has a selling price of USD 850,000 per patient in the UK.[257] Cost effectiveness of CEC therapies could be addressed by the use of cell carriers. A recent analysis by Mehta and colleagues suggested the selling price of a tissue-engineered CEC graft could be comparable to a donor graft.[258] From the patient perspective, at present, the only therapy for advanced disease is corneal transplantation. CEC injection could potentially address donor shortage and avoid the limitations of DMEK such as graft dislocation, and technically challenging surgery, especially in cases such as failed grafts and poor visibility. Currently, most patients are diagnosed and treated after a significant loss of CECs. Gene therapy could halt and potentially reverse the degeneration of CECs

in early FECD patients, obviating the need for transplantation. In turn, FECD patients with central guttae and clear periphery could benefit from Descemet stripping only in combination with ROCK inhibitors that obviate the need for allogeneic donor tissue or long-term use of steroids and associated side effects.

Any regenerative therapies will require cGMP facilities to produce the therapeutic product and will be strictly quality controlled by the national regulatory authorities. The field of translational medicine, while it purports to "bring the bench to bedside" the reality is significantly more complicated than that in reality. After a successful clinical trial, any therapeutic product must either provide a very strong rationale for a return on investment to elicit commercial interest or face a future where it can neither be produced under the European Union Hospital Exemption, a European Union regulation foreseen in Regulation (EC)1394/2007 with defined minimal criteria intended to provide patients the possibility to benefit from an innovative individual treatment in the absence of valid therapeutic alternatives, nor clear the hurdles of Marketing Authority. In fact, the very first ATMP to achieve marketing approval in Europe, ChondroCelect, a product composed mainly of autologous chondrocytes, has already been withdrawn from the market due to the high cost associated with its production rendering it difficult to attain reimbursement. While advances in technology and scale could reduce costs in future, regenerative therapies are only foreseeable in richer self-sufficient countries, with few exceptions of countries such as Japan, which suffers from donor shortage and has a cell therapy program. As the costs of treatment become more reasonable in the future, however, such advanced therapies will become more accessible and feasible for countries that suffer most from tissue scarcity.

The current view is that an expensive therapy in a country that is self-sufficient in donor tissue should provide an improvement upon the therapeutic outcome of the existing therapy. For a cellular or genetic therapy for corneal endothelial disease, they should therefore be benchmarked against the price and outcomes of the current

DMEK. CEC therapies could allow better control of the number of live cells delivered compared to manually dissected or peeled grafts. Bioengineered grafts could be seeded with a higher CEC density (≥3,000 cells/mm^2), potentially increasing graft survival. Moreover, to effectively tackle the worldwide donor tissue scarcity, it is necessary to promote a global approach. If a cellular or genetic therapy is employed in a country that is self-sufficient in terms of corneal transplants, this would generate a local donor cornea surplus. Countries with major tissue scarcity would indirectly benefit from such a situation as they would be able to import sufficient corneas. Finally, affordable logistic solutions to transport bioengineered endothelial grafts and frozen CECs suspensions over long distances could allow countries lacking a GMP infrastructure to benefit from CEC therapies.

On the other hand, DSO combined with pharmacological modulation and acellular grafts present distinct advantages compared to endothelial keratoplasty, CEC, or genetic therapies. Their relatively low cost and the minimal infrastructure needed could allow their implementation, especially in countries with severe donor tissue scarcity, thereby reducing the need for corneal transplantation. Moreover, the use of regenerative approaches in self-sufficient countries could indirectly benefit countries in need by freeing donor tissue for use. Nevertheless, both DSO and acellular grafts have drawbacks compared to DMEK or cell therapies. DSO is unlikely to benefit patients with advanced Fuchs disease or bullous keratopathy, and the long-term outcomes of such interventions remain to be determined. Furthermore, in case of DSO failure, the corneal edema will worsen, and it will require access to donor corneas as only an endothelial graft will be able to improve it, a major drawback in countries suffering from tissue scarcity. Moreover, DSO is only suitable for FECD patients, and most patients in developing countries have bullous keratopathy.

Regenerative therapies should be weighed or combined with the global development of efficient eye bank infrastructures and ocular surgery facilities as well as promoting organ donations though legislation and education of populations that are reluctant to

donate organs due to religious, cultural or other concerns. The current worldwide shortage of donor corneas, which is expected to increase as the population grows older, can only be tackled with a global effort and a communal attitude.

Approaches for corneal endothelium regenerative medicine regulatory framework in the European Union: from bench to bedside

To make the successful translation of the therapies discussed in this review from bench to bedside, it is imperative to consider the regulatory framework and strategy at an early stage of development. In the European Union, there is specific guidance on good manufacturing practices and clinical development of therapies to assure quality and safety of the product. Depending on the approach taken for corneal endothelial regeneration, a therapy can be classified as a medical device, an advanced therapeutic medicinal products (ATMP), or a medicinal product. The different classifications have a significant impact on the regulatory path to the patient.

Medical devices are products or equipment intended for a medical use, and are generally regulated on a Member State level according to Regulation (EC) 2017/745. Acellular corneal endothelial graft substitutes or endothelial keratoprostheses would be considered medical devices, nevertheless classification boundaries might vary on a case-by-case approach. Regulation (EC) 2017/745 issued by the European Commission regulates medical devices repealing the previous Directive 93/42/EEC which regulated medical devices at national level. The European Medicines Agency (EMA) has no responsibility for the regulation of medical devices unless the medical device contains a medicinal product as an ancillary substance in which case scientific opinions are provided.

ATMPs are medicinal products based on cells or gene transfer and can be classified as cell therapeutic medicinal product (CTMP), gene therapeutic medicinal product (GTMP) or tissue engineering product (TEP). The EMA regulates ATMPs via a centralized procedure under the ATMP Regulation (EC) 1394/2007. As it currently stands, a CEC-based therapy, whether delivered as cell injection or as part of a tissue engineered corneal endothelial graft, will be categorized as an ATMP. On the other hand, genetic modulation approaches would only be categorized as ATMPs if the active substance is a biological medicinal product, meaning it is produced or extracted from a biological source. Examples for this would be gene delivery via viral vectors or plasmids. It is important to highlight that CRISPR-Cas9 based therapies would be considered ATMPs if delivered via viral or plasmid vector, but if delivered as a Cas9 recombinant protein together with a synthetic guide RNA, they would potentially fall outside the ATMP framework and could be classified as medicinal products. Nevertheless, there is no precedent for such case yet, and every case should be assessed individually. The boundaries for product classifications can change over time and should always be determined for the specific product.

A substance or a combination of substances with properties to restore, correct or modify physiological conditions in humans are considered medicinal products. The EMA regulates medicinal products under Directive 2001/83/EC. This includes recombinant proteins and pharmaceuticals that can be used for modulation of the corneal endothelium, but also synthetic oligonucleotides.

Apart from categorizing the different approaches, other regulations are needed for the translation of such therapies to the clinic. Regarding clinical trials, their implementation and conduction within the European Union is controlled by the Clinical Trials Information System (CTIS) under the Regulation (EC) 536/2014. Nevertheless, the competences for approval and supervision of clinical trials remain in hands of Member States. A manufacturing authorization issued by Member State national authorities is required for all stages of the clinical trials. And there are

specific requirements that need to be addressed for ATMPs. Namely, Regulation (EC) 536/2014 establishes that investigational medicinal products (IMPs) need to comply with Good Manufacturing Practices (GMP) to assure the safety and reliability of the clinical trial. GMP manufacturing should be considered at an early pre-clinical developmental stage to enable successful transition towards the clinical setting. Furthermore, every batch of the treatment used for the clinical trial needs to be certified by a qualified person within national authorities.

Directive 2009/120/EC establishes a case by case risk-based approach when assessing the potential benefits of an ATMP therapy for market authorization. The risk analysis may consider the cell source (xenogeneic, allogenic or autologous), cell proliferation capacity, cell manipulation, functionality, and preclinical and clinical data regarding functionality, safety and efficacy of a cell therapy. Directive 2010/84/EC defines a pharmacovigilance system to collect, detect, assess, and monitor possible adverse effects. Finally, directives 2004/23/EC, 2006/17/EC and 2006/86/EC provide guidance for process donation, procurement, testing, storage and traceability in case a therapy originates from human tissues.

To facilitate navigation through the regulatory framework and understand the requirements needed at every developmental stage, researchers and developers are encouraged to seek advice at an early preclinical stage as well as during later clinical development. Within the EMA, legal and regulatory scientific guidance can be enquired through the EMA innovation taskforce and the small and medium enterprise (SME) office. Moreover, the scientific advice working party of the EMA can provide scientific advice and guide researchers throughout the different steps of a therapy development process, based on a case-by-case approach. National advice can also be requested from certain member states of the European Union. The request of early guidance by researchers or developers will provide the necessary tools to understand the requirements for the approval of specific products at every development stage and allow a smooth navigation through the regulatory framework.

Finally, experience learned with the marketing approval of other ophthalmologic therapies, such as the process for marketing authorization of Holoclar [259,260], might be valuable guidance to understand the requirements that should be met to prove safety and efficacy of a therapy so that a positive benefit–risk balance can be achieved.

Conclusions and future directions

Advances in protocols for the expansion of primary human CECs and their *in vivo* delivery are challenging the current one donor–one patient paradigm. It is very likely that research will develop protocols to successfully culture older donor corneas but also increase the number of CEC that can be obtained from a single donor. Furthermore, future research on the derivation of CECs from pluripotent stem cells may generate a new cell source for therapy, thereby obviating the need for allogeneic donors. A current clinical trial in Japan using iPSC–derived corneal epithelial cells for treating patients with limbal stem cell deficiency (UMIN000036539) could set the ground for future pluripotent stem cell–based therapies to treat corneal diseases.

Future results on the ongoing CEC–based clinical trials in Japan and Singapore will provide deeper understanding on the feasibility of CECs delivery methods. It is highly possible that the amount of CEC used in cell injection can be reduced compared to the currently used million cells/eye, which will allow to increase the number of patients treated from a single donor. Moreover, the ongoing clinical trials will help defining clinical endpoints for CEC therapies, highly relevant for regenerative medicine therapies as they are an integral part of the regulatory approval.[261] Finally, synthetic CEC carriers would enable a more cost–effective, limitless and standardized alternative.

Acellular corneal endothelial grafts provide an alternative therapeutic approach that will be dramatically cheaper, and especially beneficial in developing countries.

Future clinical trials will help to understand how long a cornea can be kept transparent using such devices.

Lamellar corneal transplantation is presently the default procedure to treat corneal endothelial disease. With an increase in the available therapeutic arsenal, it is critical to select the best treatment option for each patient. In the coming years, research will allow deeper understanding of what spectrums of corneal endothelial disease could be successfully treated with each approach. It is possible that young patients with long CTG repeats in the *TCF4* gene and early to moderate FECD could be candidates for genetic modulation. On the other hand, FECD patients with a good peripheral corneal endothelium could be treated with ROCK inhibitors alone or in combination with DSO/DWEK. Severe bullous keratopathy and advanced FECD could be treated by lamellar keratoplasty or cell therapy delivered by injection for bullous keratopathy cases or using a carrier for FECD cases. A personalized medicine approach will allow greater access for more people to therapy and tackle global donor shortage.

Funding

P.C., R.M.M.N, V.L.S.L, and M.M.D. were funded to perform this work by Chemelot InSciTe under the EyeSciTe consortium.

Acknowledgements

The authors graciously thank Dr Kerstin Wickstrom (Icelandic Medicines Agency) for the valuable feedback on section: *9. Approaches for corneal endothelium regenerative medicine regulatory framework in the European Union: from bench to bedside.*

References

1. Patel, S., Alió, J. L. & Pérez-Santonja, J. J. Refractive index change in bovine and human corneal stroma before and after LASIK: A study of untreated and re-treated corneas implicating stromal hydration. *Investig. Ophthalmol. Vis. Sci.* **45**, 3523–3530 (2004).

2. Johnson, D. H., Bourne, W. M. & Campbell, R. J. The Ultrastructure of Descemet's Membrane: I. Changes with age in Normal Corneas. *Arch. Ophthalmol.* **100**, 1942–1947 (1982).

3. Kabosova, A. *et al.* Compositional differences between infant and adult human corneal basement membranes. *Investig. Ophthalmol. Vis. Sci.* **48**, 4989–4999 (2007).

4. Yam, G. H. *et al.* Characterization of Human Transition Zone Reveals a Putative Progenitor-Enriched Niche of Corneal Endothelium. *Cells* **8**, 1244 (2019).

5. Amano, S., Yamagami, S., Mimura, T., Uchida, S. & Yokoo, S. Corneal Stromal and Endothelial Cell Precursors. *Cornea* **25**, S73–S77 (2006).

6. He, Z. *et al.* Revisited microanatomy of the corneal endothelial periphery: New evidence for continuous centripetal migration of endothelial cells in humans. *Stem Cells* **30**, 2523–2534 (2012).

7. Whikehart, D. R., Parikh, C. H., Vaughn, A. V., Mishler, K. & Edelhauser, H. F. Evidence suggesting the existence of stem cells for the human corneal endothelium. *Mol. Vis.* **11**, 816–824 (2005).

8. Bonanno, J. A. Molecular mechanisms underlying the corneal endothelial pump. *Exp. Eye Res.* **95**, 2–7 (2012).

9. Bonanno, J. A. Identity and regulation of ion transport mechanisms in the corneal endothelium. *Prog. Retin. Eye Res.* **22**, 69–94 (2003).

10. Zheng, T., Le, Q., Hong, J. & Xu, J. Comparison of human corneal cell density by age and corneal location: An in vivo confocal microscopy study. *BMC Ophthalmol.* **16**, 109 (2016).

11. Gain, P. *et al.* Global survey of corneal transplantation and eye banking. *JAMA Ophthalmol* **134**, 167–173 (2016).

12. Thompson, R. W., Price, M. O., Bowers, P. J. & Price, F. W. Long-term graft survival after penetrating keratoplasty. *Ophthalmology* **110**, 1396–1402 (2003).

13. Mannis, M. J. *et al.* The effect of donor age on penetrating keratoplasty for endothelial disease: Graft survival after 10 years in the cornea donor study. *Ophthalmology* **120**, 2419–2427 (2013).

14. Price, M. O., Mehta, J. S., Jurkunas, U. V. & Price, F. W. Corneal endothelial dysfunction: Evolving understanding and treatment options. *Prog. Retin. Eye Res.* **82**, 100904 (2021).

15. Dunker, S. L. *et al.* Practice patterns of corneal transplantation in Europe. *J. Cataract Refract. Surg.* **47**, 865-869 (2021).

16. Dunker, S. L. *et al.* Real-World Outcomes of DMEK: A Prospective Dutch registry study. *Am. J. Ophthalmol.* **222**, 218–225 (2021).

17. Melles, G. R. J., Ong, T. S., Ververs, B. & Van Der Wees, J. Descemet membrane endothelial keratoplasty (DMEK). *Cornea* **25**, 987–990 (2006).

18. Dunker, S. L. *et al.* Descemet Membrane Endothelial Keratoplasty versus Ultrathin Descemet Stripping Automated Endothelial Keratoplasty: A Multicenter Randomized Controlled Clinical Trial. *Ophthalmology* **127**, 1152–1159 (2020).

19. Hos, D. *et al.* Immune reactions after modern lamellar (DALK, DSAEK, DMEK) versus conventional penetrating corneal transplantation. *Prog. Retin. Eye Res.* **73**, 100768 (2019).

20. Birbal, R. S. *et al.* Five-Year Graft Survival and Clinical Outcomes of 500 Consecutive Cases After Descemet Membrane Endothelial Keratoplasty. *Cornea* **39**, 290–297 (2020).

21. Newman, L. R. *et al.* Preloaded Descemet Membrane Endothelial Keratoplasty Donor Tissue: Surgical Technique and Early Clinical Results. *Cornea* **37**, 981–986 (2018).

22. Català, P. *et al.* Transport and Preservation Comparison of Preloaded and Prestripped-Only DMEK Grafts. *Cornea* **39**, 1407–1414 (2020).

23. Romano, V. *et al.* Comparison of preservation and transportation protocols for preloaded Descemet membrane endothelial keratoplasty. *Br. J. Ophthalmol.* **102**, 549–555 (2018).

24. Parekh, M., Ruzza, A., Ferrari, S., Busin, M. & Ponzin, D. Preloaded tissues for Descemet membrane endothelial keratoplasty. *Am. J. Ophthalmol.* **166**, 120–125 (2016).

25. Busin, M. *et al.* Clinical Outcomes of Preloaded Descemet Membrane Endothelial Keratoplasty Grafts With Endothelium Tri-Folded Inwards. *Am. J. Ophthalmol.* **193**, 106–113 (2018).

26. Tran, K. D. *et al.* Evaluation and quality assessment of prestripped, preloaded descemet membrane endothelial keratoplasty grafts. *Cornea* **36**, 484–490 (2017).

27. Böhm, M. *et al.* Cost-effectiveness analysis of preloaded versus non-preloaded Descemet membrane endothelial keratoplasty for the treatment of Fuchs endothelial corneal dystrophy in an academic centre. *Br. J. Ophthalmol.* **In Press**, (2021).

28. Lie, J. T., Lam, F. C., Groeneveld-Van Beek, E. A., Van Der Wees, J. & Melles, G. R. J. Graft preparation for hemi-Descemet membrane endothelial keratoplasty (hemi-DMEK). *Br. J. Ophthalmol.* **100**, 420–424 (2016).

29. Zygoura, V. *et al.* Quarter-descemet membrane endothelial keratoplasty (quarter-dmek) for fuchs endothelial corneal dystrophy: 6 months clinical outcome. *Br. J. Ophthalmol.* **102**, 1425–1430 (2018).

30. Gadhvi, K. A. *et al.* Eye Banking: One Cornea for Multiple Recipients. *Cornea* **39**, 1599–1603 (2020).

31. Heindl, L. M. *et al.* Split cornea transplantation for 2 recipients: A new strategy to reduce corneal tissue cost and shortage. *Ophthalmology* **118**, 294–301 (2011).

32. Shah, R. D., Randleman, J. B. & Grossniklaus, H. E. Spontaneous corneal clearing after Descemet's stripping without endothelial replacement. *Ophthalmology* **119**, 256–260 (2012).

33. Arbelaez, J. G., Price, M. O. & Price, F. W. Long-term follow-up and complications of stripping Descemet membrane without placement of graft in eyes with Fuchs endothelial dystrophy. *Cornea* **33**, 1295–1299 (2014).

34. Borkar, D. S., Veldman, P. & Colby, K. A. Treatment of fuchs endothelial dystrophy by descemet stripping without endothelial keratoplasty. *Cornea* **35**, 1267–1273 (2016).

35. Thuret, G. *et al.* One threat, different answers: The impact of COVID-19 pandemic on cornea donation and donor selection across Europe. *Br. J. Ophthalmol.* **Online ahe**, (2020).

36. Baum, J. L., Niedra, R., Davis, C. & Yue, B. Y. J. T. Mass culture of human corneal endothelial cells. *Arch Ophthalmol* **97**, 1136–1140 (1979).

37. Yue, B. Y. J. T., Sugar, J., Gilboy, J. E. & Elvart, J. L. Growth of human corneal endothelial cells in culture. *Invest Ophthalmol Vis Sci* **30**, 248–253 (1989).

38. Tripathi, R. C. & Tripathi, B. J. Human trabecular endothelium, corneal endothelium, keratocytes, and scleral fibroblasts in primary cell culture. A comparative study of growth characteristics, morphology, and phagocytic activity by light and scanning electron microscopy. *Exp. Eye Res.* **35**, 611–624 (1982).

39. Fabricant, R. N., Alpar, A. J., Centifano, Y. M. & Kaufman, H. E. Epidermal growth factor receptors on corneal endothelium. *Arch Ophthalmol* **99**, 305–308 (1981).

40. Engelmann, K., Bohnke, M. & Friedl, P. Isolation and long-term cultivation of human corneal endothelial cells. *Investig. Ophthalmol. Vis. Sci.* **29**, 1656–1662 (1988).

41. Engelmann, K. & Friedl, P. Optimization of culture conditions for human corneal endothelial cells. *Vitr. Cell Dev Biol* **25**, 1065–1072 (1989).

42. Engelmann, K. & Friedl, P. Growth of human corneal endothelial cells in a serum-reduced medium. *Cornea* **14**, 62–70 (1995).

43. Amano, S., Mimura, T., Yamagami, S., Osakabe, Y. & Miyata, K. Properties of corneas reconstructed with cultured human corneal endothelial cells and human corneal stroma. *Jpn. J. Ophthalmol.* **49**, 448–452 (2005).

44. Mimura, T. *et al.* Cultured human corneal endothelial cell transplantation with a collagen sheet in a rabbit model. *Invest Ophthalmol Vis Sci* **45**, 2992–2997 (2004).

45. Mimura, T. *et al.* Transplantation of corneas reconstructed with cultured adult human corneal endothelial cells in nude rats. *Exp. Eye Res.* **79**, 231–237 (2004).

46. Mimura, T., Yokoo, S., Araie, M., Amano, S. & Yamagami, S. Treatment of rabbit bullous keratopathy with precursors derived from cultured human corneal endothelium. *Investig. Ophthalmol. Vis. Sci.* **46**, 3637–3644 (2005).

47. Chen, K.-H., Azar, D. & Joyce, N. C. Transplantation of adult human corneal endothelium ex vivo: A morphologic study. *Cornea* **20**, 731–737 (2001).

48. Joyce, N. C. & Zhu, C. Human corneal endothelial cell proliferation. Potential for use in regenerative medicine. *Cornea* **23**, 8–19 (2004).

49. Zhu, C. & Joyce, N. C. Proliferative response of corneal endothelial cells from young and older donors. *Invest Ophthalmol Vis Sci* **45**, 1743–1751 (2004).

50. Li, W. *et al.* A novel method of isolation, preservation, and expansion of human corneal endothelial cells. *Invest Ophthalmol Vis Sci* **48**, 614–620 (2007).

51. Peh, G. S. L., Toh, K.-P., Wu, F.-Y., Tan, D. T. & Mehta, J. S. Cultivation of human corneal endothelial cells isolated from paired donor corneas. *PLoS One* **6**, e28310 (2011).

52. Roy, O., Leclerc, V. B., Bourget, J. M., Thériault, M. & Proulx, S. Understanding the process of corneal endothelial morphological change in vitro. *Investig. Ophthalmol. Vis. Sci.* **56**, 1228–1237 (2015).

53. Jäckel, T., Knels, L., Valtink, M., Funk, R. H. W. & Engelmann, K. Serum-free corneal organ culture medium (SFM) but not conventional minimal essential organ culture medium (MEM) protects human corneal endothelial cells from apoptotic and necrotic cell death. *Br. J. Ophthalmol.* **95**, 123–130 (2011).

54. Peh, G. S. L. *et al.* Propagation of human corneal endothelial cells: A novel dual media approach. *Cell Transpl.* **24**, 287–304 (2015).

55. Bartakova, A., Kuzmenko, O., Alvarez-Delfin, K., Kunzevitzky, N. J. & Goldberg, J. L. A cell culture approach to optimized human corneal endothelial cell function. *Investig. Ophthalmol. Vis. Sci.* **59**, 1617–1629 (2018).

56. Frausto, R. F. *et al.* Phenotypic and functional characterization of corneal endothelial cells during in vitro expansion. *Sci. Rep.* **10**, 7402 (2020).

57. Parekh, M. *et al.* Human corneal endothelial cells from older donors can be cultured and passaged on cell-derived extracellular matrix. *Acta Ophthalmol.* **In Press**, 1–11 (2020).

58. Parekh, M. *et al.* Passaging capability of human corneal endothelial cells derived from old donors with and without accelerating cell attachment. *Exp. Eye Res.* **189**, 107814 (2019).

59. Kinoshita, S. *et al.* Injection of Cultured Cells with a ROCK Inhibitor for Bullous Keratopathy. *N. Engl. J. Med.* **378**, 995–1003 (2018).

60. Peh, G. S. L. *et al.* The effects of rho-associated kinase inhibitor Y-27632 on primary human corneal endothelial cells propagated using a dual media approach. *Sci. Rep.* **5**, 1–10 (2015).

61. Pipparelli, A. *et al.* ROCK Inhibitor Enhances Adhesion and Wound Healing of Human Corneal Endothelial Cells. *PLoS One* **8**, 1–19 (2013).

62. Vianna, L. M. M. *et al.* Use of human serum for human corneal endothelial cell culture. *Br. J. Ophthalmol.* **99**, 267–271 (2015).

63. Feizi, S. *et al.* Effect of amniotic fluid on the invitro culture of human corneal endothelial cells. *Exp. Eye Res.* **122**, 132–140 (2014).

64. Nakahara, M. *et al.* Corneal Endothelial Expansion Promoted by Human Bone Marrow Mesenchymal Stem Cell-Derived Conditioned Medium. *PLoS One* **8**, 1–10 (2013).

65. Shima, N., Kimoto, M., Yamaguchi, M. & Yamagami, S. Increased proliferation and replicative lifespan of isolated human corneal endothelial cells with L-ascorbic acid 2-phosphate. *Investig. Ophthalmol. Vis. Sci.* **52**, 8711–8717 (2011).

66. Okumura, N. *et al.* Inhibition of TGF-β Signaling Enables Human Corneal Endothelial Cell Expansion In Vitro for Use in Regenerative Medicine. *PLoS One* **8**, (2013).

67. Peh, G. S. L. *et al.* Optimization of human corneal endothelial cell culture: Density dependency of successful cultures in vitro. *BMC Res. Notes* **6**, 2–10 (2013).

68. Miyata, K. *et al.* Effect of donor age on morphologic variation of cultured human corneal endothelial cells. *Cornea* **20**, 59–63 (2001).

69. Choi, J. S. *et al.* Factors affecting successful isolation of human corneal endothelial cells for clinical use. *Cell Transplant.* **23**, 845–854 (2014).

70. He, J., Kakazu, A. H., Bazan, N. G. & Bazan, H. E. P. Aspirin-triggered lipoxin A4 (15-epi-LXA4) increases the endothelial viability of human corneas storage in Optisol-GS. *J. Ocul. Pharmacol. Ther.* **27**, 235–241 (2011).

71. Joyce, N. C., Zhu, C. C. & Harris, D. L. Relationship among oxidative stress, dna damage, and proliferative capacity in human corneal endothelium. *Investig. Ophthalmol. Vis. Sci.* **50**, 2116–2122 (2009).

72. Joyce, N. C., Harris, D. L. & Zhu, C. C. Age-related gene response of human corneal endothelium to oxidative stress and DNA damage. *Investig. Ophthalmol. Vis. Sci.* **52**, 1641–1649 (2011).

73. Parekh, M. *et al.* Culturing Discarded Peripheral Human Corneal Endothelial Cells From the Tissues Deemed for Preloaded DMEK Transplants. *Cornea* **38**, 1175–1181 (2019).

74. Parekh, M., Ahmad, S., Ruzza, A. & Ferrari, S. Human corneal endothelial cell cultivation from old donor corneas with forced attachment. *Sci. Rep.* **7**, 1–12 (2017).

75. Frausto, R. F., Le, D. J. & Aldave, A. J. Transcriptomic analysis of cultured corneal endothelial cells as a validation for their use in cell replacement therapy. *Cell Transplant.* **25**, 1159–1176 (2016).

76. Chng, Z. *et al.* High Throughput Gene Expression Analysis Identifies Reliable Expression Markers of Human Corneal Endothelial Cells. *PLoS One* **8**, 1–15 (2013).

77. Parekh, M. *et al.* Increasing Donor Endothelial Cell Pool by Culturing Cells from Discarded Pieces of Human Donor Corneas for Regenerative Treatments. *J. Ophthalmol.* **2525384**, (2019).

78. Ong, H. S. *et al.* A Novel Approach of Harvesting Viable Single Cells from Donor Corneal Endothelium for Cell-Injection Therapy. *Cells* **9**, 1428 (2020).

79. Takahashi, K. & Yamanaka, S. Induction of Pluripotent Stem Cells from Mouse Embryonic and Adult Fibroblast Cultures by Defined Factors. *Cell* **126**, 663–676 (2006).

80. Taylor, C. J., Peacock, S., Chaudhry, A. N., Bradley, J. A. & Bolton, E. M. Generating an iPSC bank for HLA-matched tissue transplantation based on known donor and recipient HLA types. *Cell Stem Cell* **11**, 147–152 (2012).

81. Lwigale, P. Y. Corneal Development: Different Cells from a Common Progenitor. *Prog. Mol. Biol. Transl. Sci.* **134**, 43–59 (2015).

82. McCabe, K. L. *et al.* Efficient generation of human embryonic stem cell-derived corneal endothelial cells by directed differentiation. *PLoS One* **10**, e0145266 (2015).

83. Ali, M., Khan, S. Y., Kabir, F., Gottsch, J. D. & Riazuddin, S. A. Comparative transcriptome analysis of hESC- and iPSC-derived corneal endothelial cells. *Exp Eye Res* **176**, 252–257 (2018).

84. Grönroos, P., Ilmarinen, T. & Skottman, H. Directed differentiation of human pluripotent stem cells towards corneal endothelial-like cells under defined conditions. *Cells* **10**, 331 (2021).

85. Zhao, J. J. & Afshari, N. A. Generation of human corneal endothelial cells via in vitro ocular lineage restriction of pluripotent stem cells. *Invest Ophthalmol Vis Sci* **57**, 6878–6884 (2016).

86. Song, Q. *et al.* Directed differentiation of human embryonic stem cells to corneal endothelial cell-like cells: A transcriptomic analysis. *Exp Eye Res* **151**, 107–114 (2016).

87. Chen, P. *et al.* Treatment with retinoic acid and lens epithelial cell-conditioned medium in vitro directed the differentiation of pluripotent stem cells towards corneal endothelial cell-like cells. *Exp Ther Med* **9**, 351–360 (2015).

88. Ju, C., Zhang, K. & Wu, X. Derivation of corneal endothelial cell-like cells from rat neural crest cells in vitro. *PLoS One* **7**, e42378 (2012).

89. Hatou, S. *et al.* Functional corneal endothelium derived from corneal stroma stem cells of neural crest origin by retinoic acid and Wnt/β-catenin signaling. *Stem Cells Dev* **22**, 828–839 (2013).

90. Fukuta, M. *et al.* Derivation of mesenchymal stromal cells from pluripotent stem cells through a neural crest lineage using small molecule compounds with defined media. *PLoS One* **9**, 1–25 (2014).

91. Lovatt, M. *et al.* Directed differentiation of periocular mesenchyme from human embryonic stem cells. *Differentiation* **99**, 62–69 (2018).

92. Wagoner, M. D. *et al.* Feeder-free differentiation of cells exhibiting characteristics of corneal endothelium from human induced pluripotent stem cells. *Biol. Open* **7**, 1–10 (2018).

93. Chambers, S. M. *et al.* Highly efficient neural conversion of human ES and iPS cells by dual inhibition of SMAD signaling. *Nat. Biotechnol.* **27**, 275–280 (2009).

94. Kriks, S. *et al.* Dopamine neurons derived from human ES cells efficiently engraft in animal models of Parkinson's disease. *Nature* **480**, 547–551 (2011).

95. Pasca, A. M. *et al.* Functional cortical neurons and astrocytes from human pluripotent stem cells in 3D culture. *Nat. Methods* **12**, 671–678 (2015).

96. Zhang, K., Pang, K. & Wu, X. Isolation and transplantation of corneal endothelial cell–like cells derived from in-vitro-differentiated human embryonic stem cells. *Stem Cell Dev* **23**, 1340–1354 (2014).

97. Hanson, C. *et al.* Transplanting embryonic stem cells onto damaged human corneal endothelium. *World J. Stem Cells* **9**, 127–132 (2017).

98. Li, Z. *et al.* Rapid differentiation of multi-zone ocular cells from human induced pluripotent stem cells and generation of corneal epithelial and endothelial cells. *Stem Cell Dev* **28**, 454–463 (2019).

99. Chen, X. *et al.* Directed differentiation of human corneal endothelial cells from human embryonic stem cells by using cell-conditioned culture media. *Investig. Ophthalmol. Vis. Sci.* **59**, 3028–3036 (2018).

100. Menendez, L. *et al.* Directed differentiation of human pluripotent stem cells to neural crest stem cells. *Nat. Protoc.* **8**, 203–212 (2013).

101. Kumar, S. & Duester, G. Retinoic acid signaling in perioptic mesenchyme represses Wnt signaling via induction of Pitx2 and Dkk2. *Dev. Biol.* **340**, 67–74 (2010).

102. Ding, V., Chin, A., Peh, A., Mehta, J. S. & Choo, A. Generation of novel monoclonal antibodies for the enrichment and characterization of human corneal endothelial cells (hCENC) necessary for the treatment of corneal endothelial blindness. *MAbs* **6**, 1439–1452 (2014).

103. Shao, C., Fu, Y., Lu, W. & Fan, X. Bone marrow-derived endothelial progenitor cells: A promising therapeutic alternative for corneal endothelial dysfunction. *Cells Tissues Organs* **193**, 253–263 (2011).

104. Inagaki, E. *et al.* Skin-derived precursors as a source of progenitors for corneal endothelial regeneration. *Stem Cell Transl Med* **6**, 788–798 (2017).

105. Shen, L. *et al.* Therapy of corneal endothelial dysfunction with corneal endothelial cell-like cells derived from skin-derived precursors. *Sci. Rep.* **7**, 13400 (2017).

106. Yamashita, K. *et al.* Corneal endothelial regeneration using mesenchymal stem cells derived from human umbilical cord. *Stem Cells Dev.* **27**, 1097–1108 (2018).

107. Joyce, N. C., Harris, D. L., Markov, V., Zhang, Z. & Saitta, B. Potential of human umbilical cord blood mesenchymal stem cells to heal damaged corneal endothelium. *Mol Vis* **18**, 547–64 (2012).

108. Parekh, M. *et al.* Effects of corneal preservation conditions on human corneal endothelial cell culture. *Exp. Eye Res.* **179**, 93–101 (2019).

109. Yamamoto, A. *et al.* A physical biomarker of the quality of cultured corneal endothelial cells and of the long-term prognosis of corneal restoration in patients. *Nat. Biomed. Eng.* **3**, 953–960 (2019).

110. Van den Bogerd, B. *et al.* Corneal endothelial cells over the past decade: Are we missing the mark(er)? *Transl. Vis. Sci. Technol.* **8**, (2019).

111. Bai, H. *et al.* The Na+, K+ ATPase β1 subunit regulates epithelial tight junctions via MRCKα. *JCI Insight* **6**, e134881 (2021).

112. Sugi, K., Musch, M. W., Field, M. & Chang, E. B. Inhibition of NA+,K+-ATPase by interferon γ down-regulates intestinal epithelial transport and barrier function. *Gastroenterology* **120**, 1393–1403 (2001).

113. He, Z. *et al.* 3D map of the human corneal endothelial cell. *Sci Rep* **6**, 29047 (2016).

114. Okumura, N. *et al.* Cell surface markers of functional phenotypic corneal endothelial cells. *Investig. Ophthalmol. Vis. Sci.* **55**, 7610–7618 (2014).

115. Dorfmueller, S. *et al.* Isolation of a recombinant antibody specific for a surface marker of the corneal endothelium by phage display. *Sci. Rep.* **6**, 21661 (2016).

116. Toda, M. *et al.* Production of homogeneous cultured human corneal endothelial cells indispensable for innovative cell therapy. *Investig. Ophthalmol. Vis. Sci.* **58**, 2011–2020 (2017).

117. Ueno, M. *et al.* Gene signature-based development of ELISA assays for reproducible qualification of cultured human corneal endothelial cells. *Investig. Ophthalmol. Vis. Sci.* **57**, 4295–4305 (2016).

118. Miyai, T. *et al.* Karyotype changes in cultured human corneal endothelial cells. *Mol. Vis.* **14**, 942–950 (2008).

119. Hamuro, J. *et al.* Cultured human corneal endothelial cell aneuploidy dependence on the presence of heterogeneous subpopulations with distinct differentiation phenotypes. *Investig. Ophthalmol. Vis. Sci.* **57**, 4385–4392 (2016).

120. Taapken, S. M. *et al.* Karotypic abnormalities in human induced pluripotent stem cells and embryonic stem cells. *Nat. Biotechnol.* **29**, 313–314 (2011).

121. Peterson, S. E. *et al.* Normal human pluripotent stem cell lines exhibit pervasive mosaic aneuploidy. *PLoS One* **6**, e23018 (2011).

122. Garcia-Martinez, J., Bakker, B., Schukken, K. M., Simon, J. E. & Foijer, F. Aneuploidy in stem cells. *World J. Stem Cells* **8**, 216–222 (2016).

123. Ting, D. S. J., Peh, G. S. L., Adnan, K. & Mehta, J. S. Translational and Regulatory Challenges of Corneal Endothelial Cell Therapy: A Global Perspective. *Tissue Eng. Part B Rev.* **In Press**, (2021).

124. Aboalchamat, B., Engelmann, K., Böhnke, M., Eggli, P. & Bednarz, J. Morphological and functional analysis of immortalized human corneal endothelial cells after transplantation. *Exp. Eye Res.* **69**, 547–553 (1999).

125. Rolev, K., O'Donovan, D. G., Coussons, P., King, L. & Rajan, M. S. Feasibility Study of Human Corneal Endothelial Cell Transplantation Using an In Vitro Human Corneal Model. *Cornea* **37**, 778–784 (2018).

126. Guindolet, D. *et al.* Storage of porcine cornea in an innovative bioreactor. *Investig. Ophthalmol. Vis. Sci.* **58**, 5907–5917 (2017).

127. Koizumi, N., Okumura, N. & Kinoshita, S. Development of new therapeutic modalities for corneal endothelial disease focused on the proliferation of corneal endothelial cells using animal models. *Exp. Eye Res.* **95**, 60–67 (2012).

128. Rolev, K., Coussons, P., King, L. & Rajan, M. Experimental models of corneal endothelial cell therapy and translational challenges to clinical practice. *Exp. Eye Res.* **188**, 107794 (2019).

129. Bostan, C. *et al.* In vivo functionality of a corneal endothelium transplanted by cell-injection therapy in a feline model. *Investig. Ophthalmol. Vis. Sci.* **57**, 1620–1634 (2016).

130. Faye, P. A. *et al.* Focus on cell therapy to treat corneal endothelial diseases. *Exp. Eye Res.* **204**, 108462 (2021).

131. Zhang, B., Korolj, A., Lai, B. F. L. & Radisic, M. Advances in organ-on-a-chip engineering. *Nat. Rev. Mater.* **3**, 257–278 (2018).

132. Mimura, T. *et al.* Magnetic attraction of iron-endocytosed corneal endothelial cells to Descemet's membrane. *Exp. Eye Res.* **76**, 745–751 (2003).

133. Mimura, T. *et al.* Necessary prone position time for human corneal endothelial precursor transplantation in a rabbit endothelial deficiency model. *Curr. Eye Res.* **32**, 617–623 (2007).

134. Okumura, N. *et al.* ROCK inhibitor converts corneal endothelial cells into a phenotype capable of regenerating in vivo endothelial tissue. *Am. J. Pathol.* **181**, 268–277 (2012).

135. Okumura, N., Kinoshita, S. & Koizumi, N. Cell-based approach for treatment of corneal endothelial dysfunction. *Cornea* **33**, S37–S41 (2014).

136. Peh, G. S. L. *et al.* Functional Evaluation of Two Corneal Endothelial Cell-Based Therapies: Tissue-Engineered Construct and Cell Injection. *Sci. Rep.* **9**, 6087 (2019).

137. Patel, S. V., Bachman, L. A., Hann, C. R., Bahler, C. K. & Fautsch, M. P. Human corneal endothelial cell transplantation in a human ex vivo model. *Investig. Ophthalmol. Vis. Sci.* **50**, 2123–2131 (2009).

138. Moysidis, S. N. *et al.* Magnetic field-guided cell delivery with nanoparticle-loaded human corneal endothelial cells. *Nanomedicine Nanotechnology, Biol. Med.* **11**, 499–509 (2015).

139. Numa, K. *et al.* Five-Year Follow-up of First Eleven Cases Undergoing Injection of Cultured Corneal Endothelial Cells for Corneal Endothelial Failure. *Ophthalmology* **In Press**, (2020).

140. Van Den Bogerd, B., Ni Dhubhghaill, S. & Zakaria, N. Cultured cells and ROCK inhibitor for bullous keratopathy. *N. Engl. J. Med.* **379**, 1184–1185 (2018).

141. Rizwan, M. *et al.* In Vitro Topographical Model of Fuchs Dystrophy for Evaluation of Corneal Endothelial Cell Monolayer Formation. *Adv. Healthc. Mater.* **5**, 2896–2910 (2016).

142. Kocaba, V. *et al.* Association of the gutta-induced microenvironment with corneal endothelial cell behavior and demise in fuchs endothelial corneal dystrophy. *JAMA Ophthalmol.* **136**, 886–892 (2018).

143. Okumura, N. *et al.* Feasibility of cell-based therapy combined with descemetorhexis for treating Fuchs endothelial corneal dystrophy in rabbit model. *PLoS One* **13**, e0191306 (2018).

144. Okumura, N. *et al.* Rho kinase inhibitor enables cell-based therapy for corneal endothelial dysfunction. *Sci. Rep.* **6**, 26113 (2016).

145. Bayyoud, T. *et al.* Decellularized bovine corneal posterior lamellae as carrier matrix for cultivated human corneal endothelial cells. *Curr. Eye Res.* **37**, 179–186 (2012).

146. Diao, Y. M. & Hong, J. Feasibility and safety of porcine Descemet's membrane as a carrier for generating tissue-engineered corneal endothelium. *Mol. Med. Rep.* **12**, 1929–1934 (2015).

147. Parekh, M., Van Den Bogerd, B., Zakaria, N., Ponzin, D. & Ferrari, S. Fish scale-derived scaffolds for culturing human corneal endothelial cells. *Stem Cells Int.* **2018**, 8146834 (2018).

148. Honda, N., Mimura, T., Usui, T. & Amano, S. Descemet stripping automated endothelial keratoplasty using cultured corneal endothelial cells in a rabbit model. *Arch. Ophthalmol.* **127**, 1321–1326 (2009).

149. Choi, J. S. *et al.* Bioengineering endothelialized neo-corneas using donor-derived corneal endothelial cells and decellularized corneal stroma. *Biomaterials* **31**, 6738–6745 (2010).

150. He, Z. *et al.* Cutting and decellularization of multiple corneal stromal lamellae for the bioengineering of endothelial grafts. *Investig. Ophthalmol. Vis. Sci.* **57**, 6639–6651 (2016).

151. Peh, G. S. L. *et al.* Regulatory Compliant Tissue-Engineered Human Corneal Endothelial Grafts Restore Corneal Function of Rabbits with Bullous Keratopathy. *Sci. Rep.* **7**, 1–17 (2017).

152. Arnalich-Montiel, F. *et al.* Treatment of corneal endothelial damage in a rabbit model with a bioengineered graft using human decellularized corneal lamina and cultured human corneal endothelium. *PLoS One* **14**, 1–16 (2019).

153. Fan, T. *et al.* Establishment of a continuous untransfected human corneal endothelial cell line and its biocompatibility to denuded amniotic membrane. *Mol. Vis.* **17**, 469–480 (2011).

154. Fan, T. *et al.* Transplantation of tissue-engineered human corneal endothelium in cat models. *Mol. Vis.* **19**, 400–407 (2013).

155. Ishino, Y. *et al.* Amniotic membrane as a carrier for cultivated human corneal endothelial cell transplantation. *Investig. Ophthalmol. Vis. Sci.* **45**, 800–806 (2004).

156. Kopsachilis, N., Tsinopoulos, I., Tourtas, T., Kruse, F. E. & Luessen, U. W. Descemet's membrane substrate from human donor lens anterior capsule. *Clin. Exp. Ophthalmol.* **40**, 187–194 (2012).

157. Yoeruek, E., Saygili, O., Spitzer, M. S., Tatar, O. & Bartz-Schmidt, K. U. Human anterior lens capsule as carrier matrix for cultivated human corneal endothelial cells. *Cornea* **28**, 416–420 (2009).

158. Van den Bogerd, B., Ní Dhubhghaill, S. & Zakaria, N. Characterizing human decellularized crystalline lens capsules as a scaffold for corneal endothelial tissue engineering. *J. Tissue Eng. Regen. Med.* **12**, e2020–e2028 (2018).

159. Spinozzi, D. *et al.* Evaluation of the Suitability of Biocompatible Carriers as Artificial Transplants Using Cultured Porcine Corneal Endothelial Cells. *Curr. Eye Res.* **44**, 243–249 (2019).

160. Spinozzi, D. *et al.* In Vitro Evaluation and Transplantation of Human Corneal Endothelial Cells Cultured on Biocompatible Carriers . *Cell Transplant.* **29**, 096368972092357 (2020).

161. Telinius, N. *et al.* Göttingen Minipig is not a Suitable Animal Model for in Vivo Testing of Tissue-Engineered Corneal Endothelial Cell-Carrier Sheets and for Endothelial Keratoplasty. *Curr. Eye Res.* **45**, 945–949 (2020).

162. Maitra, J. & Shukla, V. K. Cross-linking in hydrogels - a review. *Am. J. Polym. Sci.* **4**, 25–31 (2014).

163. Lawrence, C. J. & Zhou, W. Spin coating of non-Newtonian fluids. *J. Nonnewton. Fluid Mech.* **39**, 137–187 (1991).

164. Schiffman, J. D. & Schauer, C. L. A Review : Electrospinning of Biopolymer Nanofibers and their Applications A Review : Electrospinning of Biopolymer Nanofibers and their Applications. *Polym. Rev.* **48**, 317–352 (2008).

165. Yoshida, J. *et al.* Development and Evaluation of Porcine Atelocollagen Vitrigel Membrane With a Spherical Curve and Transplantable Artificial Corneal Endothelial Grafts. *Investig. Ophthalmol. Vis. Sci.* **55**, 4975–4981 (2014).

166. Yoshida, J. *et al.* Transplantation of Human Corneal Endothelial Cells Cultured on Bio-Engineered Collagen Vitrigel in a Rabbit Model of Corneal Endothelial Dysfunction. *Curr. Eye Res.* **42**, 1420–1425 (2017).

167. Yamaguchi, M. *et al.* Optimization of Cultured Human Corneal Endothelial Cell Sheet Transplantation and Post- Operative Sheet Evaluation in a Rabbit Model. *Curr. Eye Res.* **41**, 1178–1184 (2016).

168. Vazquez, N. *et al.* Human Bone Derived Collagen for the Development of an Artificial Corneal Endothelial Graft. In Vivo Results in a Rabbit Model. *PLoS One* **11**, e0167578 (2016).

169. Levis, H. J. *et al.* Plastic Compressed Collagen as a Novel Carrier for Expanded Human Corneal Endothelial Cells for Transplantation. *PLoS One* **7**, e50993 (2012).

170. Koizumi, N. *et al.* Cultivated Corneal Endothelial Cell Sheet Transplantation in a Primate Model. *Investig. Ophthalmol. Vis. Sci.* **48**, 4519–4526 (2007).

171. Palchesko, R. N., Funderburgh, J. L. & Feinberg, A. W. Engineered Basement Membranes for Regenerating the Corneal Endothelium. *Adv. Healthc. Mater.* **5**, 2942–2950 (2016).

172. Bourget, J. M. & Proulx, S. Characterization of a corneal endothelium engineered on a self-assembled stromal substitute. *Exp. Eye Res.* **145**, 125–129 (2016).

173. Watanabe, R., Hayashi, R., Kimura, Y., Tanaka, Y. & Nishida, K. A Novel Gelatin Hydrogel Carrier Sheet for Corneal Endothelial Transplantation. *Tissue Eng. Part A* **17**, 2213–2219 (2011).

174. Kimoto, M. *et al.* Development of a Bioengineered Corneal Endothelial Cell Sheet to Fit the Corneal Curvature. *Investig. Ophthalmol. Vis. Sci.* **55**, 2337–2343 (2014).

175. Vazquez, N. *et al.* Silk Fibroin Films for Corneal Endothelial Regeneration: Transplant in a Rabbit Descemet Membrane Endothelial Keratoplasty. *Investig. Ophthalmol. Vis. Sci.* **58**, 3357–3365 (2017).

176. Ramachandran, C., Gupta, P., Hazra, S. & Mandal, B. B. In Vitro Culture of Human Corneal Endothelium on Non-Mulberry Silk Fibroin Films for Tissue Regeneration. *Transl. Vis. Sci. Technol.* **9**, 12 (2020).

177. Madden, P. W. *et al.* Biomaterials Human corneal endothelial cell growth on a silk fi broin membrane. *Biomaterials* **32**, 4076–4084 (2011).

178. Choi, J. H. *et al.* Biofunctionalized lysophosphatidic acid/silk fibroin film for cornea endothelial cell regeneration. *Nanomaterials* **8**, 290 (2018).

179. Aghaei-Ghareh-Bolagh, B. *et al.* Optically robust, highly permeable and elastic protein films that support dual cornea cell types. *Biomaterials* **188**, 50–62 (2019).

180. Kim, E. Y. *et al.* Bioengineered neo-corneal endothelium using collagen type-I coated silk fibroin film. *Colloids Surfaces B Biointerfaces* **136**, 394–401 (2015).

181. Kim, D. K., Sim, B. R. & Khang, G. Nature-Derived Aloe Vera Gel Blended Silk Fibroin Film Scaffolds for Cornea Endothelial Cell Regeneration and Transplantation. *ACS Appl. Mater. Interfaces* **8**, 15160–15168 (2016).

182. Kim, D. K., Sim, B. R., Kim, J. I. & Khang, G. Functionalized silk fibroin film scaffold using β-Carotene for cornea endothelial cell regeneration. *Colloids Surfaces B Biointerfaces* **164**, 340–346 (2018).

183. Kruse, M. *et al.* Electro-spun Membranes as Scaffolds for Human Corneal Endothelial Cells. *Curr. Eye Res.* **43**, 1–11 (2018).

184. Ozcelik, B. *et al.* Biodegradable and biocompatible poly(ethylene glycol)-based hydrogel films for the regeneration of corneal endothelium. *Adv. Healthc. Mater.* **3**, 1496–1507 (2014).

185. Van Hoorick, J. *et al.* Designer Descemet Membranes Containing PDLLA and Functionalized Gelatins as Corneal Endothelial Scaffold. *Adv. Healthc. Meterials* **9**, 2000760 (2020).

186. Liang, Y. *et al.* Fabrication and characters of a corneal endothelial cells scaffold based on chitosan. *J Mater Sci Mater Med* **22**, 175–183 (2011).

187. Rizwan, M. *et al.* Biomaterials Sequentially-crosslinked bioactive hydrogels as nano-patterned substrates with customizable stiffness and degradation for corneal tissue engineering applications. *Biomaterials* **120**, 139–154 (2017).

188. Seow, W. Y., Kandasamy, K., Peh, G. S. L., Mehta, J. S. & Sun, W. Ultrathin, Strong, and Cell-Adhesive Agarose-Based Membranes Engineered as Substrates for Corneal Endothelial Cells. *ACS Biomater. Sci. Eng.* **5**, 4067–4076 (2019).

189. Song, J. E. *et al.* Characterization of surface modified glycerol/silk fibroin film for application to corneal endothelial cell regeneration. *J. Biomater. Sci. Polym. Ed.* **30**, 263–275 (2019).

190. Wang, T., Wang, I., Lu, J. & Young, T. Novel chitosan-polycaprolactone blends as potential scaffold and carrier for corneal endothelial transplantation. *Mol. Vis.* **18**, 255–264 (2012).

191. Young, T., Wang, I., Hu, F. & Wang, T. Fabrication of a bioengineered corneal endothelial cell sheet using chitosan/polycaprolactone blend membranes. *Colloids Surfaces B Biointerfaces* **116**, 403–410 (2014).

192. Salehi, S. *et al.* Poly (glyverol sebacate_-poly (e-caprolactone) blend nanofibrous scaffold as intrinsic bio- and immunocompatible system for corneal repair. *Acta Biomater.* **50**, 370–380 (2017).

193. Chen, J. *et al.* Electrospun nanofibrous SF/P (LLA-CL) membrane: a potential substratum for endothelial keratoplasty. *Int. J. Nanomedicine* **10**, 3337–3350 (2015).

194. Teichmann, J. *et al.* Acta Biomaterialia Human corneal endothelial cell sheets for transplantation : Thermo-responsive cell culture carriers to meet cell-specific requirements. *Acta Biomater.* **9**, 5031–5039 (2013).

195. Teichmann, J. *et al.* Thermo-responsive cell culture carriers based on poly (vinyl methyl ether) — the effect of biomolecular ligands to balance cell adhesion and stimulated detachment. *Sci. Technol. Adv. Mater.* **16**, 045003 (2015).

196. Sumide, T. *et al.* Functional human corneal endothelial cell sheets harvested from temperature-responsive culture surfaces. *FASEB J.* **20**, 392–4 (2006).

197. Madathil, B. K., Rajanasari, P., Kumar, A. & Kumary, T. V. N-Isopropylacrylamide-co-glycidylmethacrylate as a Thermoresponsive Substrate for Corneal Endothelial Cell Sheet Engineering. *Biomed Res. Int.* **2014**, 450672 (2014).

198. Ide, T. *et al.* Structural characterization of bioengineered human corneal endothelial cell sheets fabricated on temperature-responsive culture dishes. *Biomaterials* **27**, 607–614 (2006).

199. Lai, J., Chen, K., Hsu, W., Hsiue, G. & Lee, Y. Bioengineered Human Corneal Endothelium for Transplantation. *Arch Ophthalmol* **124**, 1441–1448 (2006).

200. Hsiue, G., Lai, J., Chen, K. & Hsu, W. A Novel Strategy for Corneal Endothelial Reconstruction with a Bioengineered Cell Sheet. *Transplantation* **81**, 473–476 (2006).

201. Lai, J. *et al.* Characterization of Cross-Linked Porous Gelatin Carriers and Their Interaction with Corneal Endothelium: Biopolymer Concentration Effect. *PLoS One* **8**, e54058 (2013).

202. Lai, J., Cheng, H. & Ma, D. H. Investigation of Overrun-Processed Porous Hyaluronic Acid Carriers in Corneal Endothelial Tissue Engineering. *PLoS One* **10**, e0136067 (2015).

203. Bhogal, M., Lwin, C. N., Seah, X. Y., Peh, G. & Mehta, J. S. Allogeneic descemet's membrane transplantation enhances corneal endothelial monolayer formation and restores functional integrity following descemet's stripping. *Investig. Ophthalmol. Vis. Sci.* **58**, 4249–4260 (2017).

204. Soh, Y. Q. & Mehta, J. S. Regenerative Therapy for Fuchs Endothelial Corneal Dystrophy. *Cornea* **37**, 523–527 (2018).

205. Daphna, O. & Marcovich, A. L. EndoArt: Multi center ongoing study of innovative artificial implant designed to treat corneal edema. in *38th Congress of the European Society of Chataract and Refractive Surgeons* **2-4 Octobe**, (2020).

206. Okumura, N. *et al.* Enhancement on primate corneal endothelial cell survival in vitro by a rock inhibitor. *Investig. Ophthalmol. Vis. Sci.* **50**, 3680–3687 (2009).

207. Okumura, N. *et al.* The ROCK inhibitor eye drop accelerates corneal endothelium wound healing. *Investig. Ophthalmol. Vis. Sci.* **54**, 2439–2502 (2013).

208. Koizumi, N. *et al.* Rho-associated kinase inhibitor eye drop treatment as a possible medical treatment for fuchs corneal dystrophy. *Cornea* **32**, 1167–1170 (2013).

209. Okumura, N. *et al.* Effect of the Rho Kinase inhibitor Y-27632 on corneal endothelial wound healing. *Investig. Ophthalmol. Vis. Sci.* **56**, 6067–6074 (2015).

210. Okumura, N. *et al.* Effect of the rho-associated kinase inhibitor eye drop (Ripasudil) on corneal endothelial wound healing. *Investig. Ophthalmol. Vis. Sci.* **57**, 1284–1292 (2016).

211. Isobe, T. *et al.* Effects of K-115, a Rho-kinase inhibitor, on aqueous humor dynamics in rabbits. *Curr. Eye Res.* **39**, 813–822 (2014).

212. Kaneko, Y. *et al.* Effects of K-115 (Ripasudil), a novel ROCK inhibitor, on trabecular meshwork and Schlemms canal endothelial cells. *Sci. Rep.* **6**, 19640 (2016).

213. Liao, J. K., Seto, M. & Noma, K. Rho kinase (ROCK) inhibitors. *J. Cardiovasc. Pharmacol.* **50**, 17–24 (2007).

214. Schlötzer-Schrehardt, U. *et al.* Potential functional restoration of corneal endothelial cells in Fuchs endothelial corneal dystrophy by ROCK inhibitor (Ripasudil). *Am. J. Ophthalmol.* **In Press**, 185–199 (2020).

215. Moloney, G. *et al.* Descemetorhexis without grafting for fuchs endothelial dystrophy-supplementation with topical ripasudil. *Cornea* **36**, 642–648 (2017).

216. Hoppenreijs, V. P. T., Pels, E., Vrensen, G. F. J. M., Oosting, J. & Treffers, W. F. Effects of human epidermal growth factor on endothelial wound healing of human corneas. *Investig. Ophthalmol. Vis. Sci.* **33**, 1946–1957 (1992).

217. Hoppenreijs, V. P. T., Pels, E., Vrensen, G. F. J. M. & Treffers, W. F. Effects of platelet-derived growht factor on endothelial wound healing in human corneas. *Investig. Ophthalmol. Vis. Sci.* **35**, 150–161 (1994).

218. Lu, J. *et al.* TGF-β2 inhibits AKT activation and FGF-2-induced corneal endothelial cell proliferation. *Exp. Cell Res.* **312**, 3631–3640 (2006).

219. Wendt, M. K., Tian, M. & Schiemann, W. P. Deconstructing the mechanisms and consequences of TGF-β-induced EMT during cancer progression. *Cell Tissue Res.* **347**, 85–101 (2012).

220. Xia, X., Babcock, J. P., Blaber, S. I., Harper, K. M. & Blaber, M. Pharmacokinetic Properties of 2nd-Generation Fibroblast Growth Factor-1 Mutants for Therapeutic Application. *PLoS One* **7**, e48210 (2012).

221. Okumura, N. *et al.* Activation of TGF-β signaling induces cell death via the unfolded protein response in Fuchs endothelial corneal dystrophy. *Sci. Rep.* **7**, 6801 (2017).

222. Jurkunas, U. V., Bitar, M. S., Funaki, T. & Azizi, B. Evidence of oxidative stress in the pathogenesis of fuchs endothelial corneal dystrophy. *Am. J. Pathol.* **177**, 2278–2289 (2010).

223. Kim, E. C., Meng, H. & Jun, A. S. N-Acetylcysteine increases corneal endothelial cell survival in a mouse model of Fuchs endothelial corneal dystrophy. *Exp. Eye Res.* **127**, 20–25 (2014).

224. Halilovic, A. *et al.* Menadione-Induced DNA Damage Leads to Mitochondrial Dysfunction and Fragmentation during Rosette Formation in Fuchs Endothelial Corneal Dystrophy. *Antioxidants Redox Signal.* **24**, 1072–1083 (2016).

225. Liu, C. *et al.* Ultraviolet A light induces DNA damage and estrogen-DNA adducts in Fuchs endothelial corneal dystrophy causing females to be more affected. *Proc. Natl. Acad. Sci. U. S. A.* **117**, 573–583 (2020).

226. Ziaei, A., Schmedt, T., Chen, Y. & Jurkunas, U. V. Sulforaphane decreases endothelial cell apoptosis in Fuchs endothelial corneal dystrophy: A novel treatment. *Investig. Ophthalmol. Vis. Sci.* **54**, 6724–6734 (2013).

227. Lovatt, M., Kocaba, V., Hui Neo, D. J., Soh, Y. Q. & Mehta, J. S. Nrf2: A unifying transcription factor in the pathogenesis of Fuchs' endothelial corneal dystrophy. *Redox Biol.* **37**, 101763 (2020).

228. Kim, E. C. *et al.* Screening and characterization of drugs that protect corneal endothelial cells against unfolded protein response and oxidative stress. *Investig. Ophthalmol. Vis. Sci.* **58**, 892–900 (2017).

229. Aldave, A. J., Han, J. & Frausto, R. F. Genetics of the corneal endothelial dystrophies: An evidence-based review. *Clin. Genet.* **84**, 109–119 (2013).

230. Fautsch, M. P. *et al.* TCF4-mediated Fuchs endothelial corneal dystrophy: Insights into a common trinucleotide repeat-associated disease. *Prog. Retin. Eye Res.* 100883 (2020). doi:10.1016/j.preteyeres.2020.100883

231. Ong Tone, S. *et al.* Fuchs endothelial corneal dystrophy: The vicious cycle of Fuchs pathogenesis. *Prog. Retin. Eye Res.* 100863 (2020). doi:10.1016/j.preteyeres.2020.100863

232. Robbins, P. D. & Ghivizzani, S. C. Viral vectors for gene therapy. *Pharmacol. Ther.* **80**, 35–47 (1998).

233. Lebherz, C., Maguire, A., Tang, W., Bennett, J. & Wilson, J. M. Novel AAV serotypes for improved ocular gene transfer. *J. Gene Med.* **10**, 375–382 (2008).

234. Wu, Z., Yang, H. & Colosi, P. Effect of genome size on AAV vector packaging. *Mol. Ther.* **18**, 80–86 (2010).

235. Allocca, M. *et al.* Serotype-dependent packaging of large genes in adeno-associated viral vectors results in effective gene delivery in mice. *J. Clin. Invest.* **118**, 1955–1964 (2008).

236. Moore, C. B. T., Christie, K. A., Marshall, J. & Nesbit, M. A. Personalised genome editing – The future for corneal dystrophies. *Prog. Retin. Eye Res.* **65**, 147–165 (2018).

237. Bennett, J. *et al.* AAV2 gene therapy readministration in three adults with congenital blindness. *Sci. Transl. Med.* **4**, 120ra15 (2012).

238. Annear, M. J. *et al.* Gene therapy in the second eye of RPE65-deficient dogs improves retinal function. *Gene Ther.* **18**, 53–61 (2011).

239. Andrzejewski, S., Moyle, P. M., Stringer, B. W., Steel, J. C. & Layton, C. J. Neutralisation of adeno-associated virus transduction by human vitreous humour. *Gene Ther.* **28**, 242–255 (2021).

240. Lee, S. *et al.* Relationship between neutralizing antibodies against adeno-associated virus in the vitreous and serum: Effects on retinal gene therapy. *Transl. Vis. Sci. Technol.* **8**, (2019).

241. Amado, D. *et al.* Safety and efficacy of subretinal readministration of a viral vector in large animals to treat congenital blindness. *Sci. Transl. Med.* **2**, (2010).

242. Rinaldi, C. & Wood, M. J. A. Antisense oligonucleotides: The next frontier for treatment of neurological disorders. *Nat. Rev. Neurol.* **14**, 9–22 (2018).

243. Zarouchlioti, C. *et al.* Antisense Therapy for a Common Corneal Dystrophy Ameliorates TCF4 Repeat Expansion-Mediated Toxicity. *Am. J. Hum. Genet.* **102**, 528–539 (2018).

244. Hu, J. *et al.* Oligonucleotides targeting TCF4 triplet repeat expansion inhibit RNA foci and mis-splicing in Fuchs' dystrophy. *Hum. Mol. Genet.* **27**, 1015–1026 (2018).

245. Hu, J. *et al.* Duplex RNAs and ss-siRNAs Block RNA Foci Associated with Fuchs' Endothelial Corneal Dystrophy. *Nucleic Acid Ther.* **29**, 73–81 (2019).

246. Chau, V. Q. *et al.* Delivery of Antisense Oligonucleotides to the Cornea. *Nucleic Acid Ther.* **30**, 207–214 (2020).

247. Cox, D. B. T., Platt, R. J. & Zhang, F. Therapeutic genome editing: Prospects and challenges. *Nat. Med.* **21**, 121–131 (2015).

248. Wang, H., La Russa, M. & Qi, L. S. CRISPR/Cas9 in genome editing and beyond. *Annu. Rev. Biochem.* **85**, 227–264 (2016).

249. Jiang, F. & Doudna, J. A. CRISPR – Cas9 structures and mechanisms. *Annu. Rev. Biophys.* **46**, 505–529 (2017).

250. Shin, J. W. *et al.* Permanent inactivation of Huntington's disease mutation by personalized allele-specific CRISPR/Cas9. *Hum. Mol. Genet.* **25**, 4566–4576 (2016).

251. Yang, S. *et al.* CRISPR/Cas9-mediated gene editing ameliorates neurotoxicity in mouse model of Huntington's disease. *J. Clin. Invest.* **127**, 2719–2724 (2017).

252. Rong, Z., Gong, X., Hulleman, J. D., Corey, D. R. & Mootha, V. V. Trinucleotide repeat-targeting dCas9 as a therapeutic strategy for fuchs' endothelial corneal dystrophy. *Transl. Vis. Sci. Technol.* **9**, 47 (2020).

253. Uehara, H. *et al.* Start codon disruption with CRISPR/Cas9 prevents murine Fuch's endothelial corneal dystrophy. *bioRxiv* **Preprint**, (2020).

254. Anguela, X. M. & High, K. A. Entering the modern era of gene therapy. *Annu. Rev. Med.* **70**, 273–288 (2019).

255. Matthaei, M. *et al.* Changing indications in penetrating keratoplasty: A systematic review of 34 years of global reporting. *Transplantation* **101**, 1387–1399 (2017).

256. Shukla, V., Seoane-Vazquez, E., Fawaz, S., Brown, L. & Rodriguez-Monguio, R. The Landscape of Cellular and Gene Therapy Products: Authorization, Discontinuations, and Cost. *Hum. Gene Ther. Clin. Dev.* **30**, 102–113 (2019).

257. Yanuzzi, N. A. & Smiddy, W. E. Cost-effectiveness of voretigene neparvovec-rzyl therapy. *JAMA Ophthalmol.* **137**, 1123–4 (2019).

258. Tan, T. E. *et al.* A cost-minimization analysis of tissue-engineered constructs for corneal endothelial transplantation. *PLoS One* **9**, e100563 (2014).

259. Pellegrini, G. *et al.* From discovery to approval of an advanced therapy medicinal product-containing stem cells, in the EU. *Regen. Med.* **11**, 407–420 (2016).

260. Pellegrini, G. *et al.* Navigating Market Authorization: The Path Holoclar Took to Become the First Stem Cell Product Approved in the European Union. *Stem Cells Transl. Med.* **7**, 146–154 (2018).

261. Schlereth, S. L. *et al.* New Technologies in Clinical Trials in Corneal Diseases and Limbal Stem Cell Deficiency: Review from the European Vision Institute Special Interest Focus Group Meeting. *Ophthalmic Res.* **64**, 145–167 (2021).

3

Transport and preservation comparison of preloaded and prestripped-only DMEK grafts

This chapter has been published as:

Català, P., Vermeulen, W., Rademakers, T., van den Bogaerdt, A., Kruijt, P.J., Nuijts, R.M.M.A., LaPointe, V.L.S., Dickman, M.M. Transport and preservation comparison of preloaded and prestripped-only DMEK grafts. *Cornea*. 2020; 39 (11): 1407-1414

Abstract

This study compares the effect of the transport of conventionally pre-stripped DMEK tissue with the DMEK RAPID preloaded transport system from Geuder AG (Heidelberg, Germany). Endothelial cell loss, tissue integrity, endothelial cell phenotype and viability were assessed and compared. Twelve DMEK grafts were pre-stripped by the cornea bank and transported using two conditions: conventional flask (n=6) or a preloaded transport cartridge (DMEK RAPID, n=6). After transport, tissues were analyzed for cell density, denuded areas, immunolocalization of corneal endothelial markers ZO-1, CD166 and Na/K ATPase, histology analysis and cell viability staining with Hoechst, calcein AM and ethidium homodimer. Endothelial cell loss (10.35% vs. 9.15%) did not differ between transport conditions. Histological analysis confirmed the integrity of the Descemet's membrane and endothelial cell layer with both transport conditions. Similarly, the corneal endothelial cell mosaic was conserved in both conditions. The ZO-1 tight junctions confirmed the integrity of the confluent corneal endothelial cell monolayer. CD166 and Na^+/K^+ ATPase detection with immunofluorescence was also comparable. A similar percentage of dead cells was reported in both conditions (18.1% vs. 16.73%). Moreover, the surface covered with calcein-positive cells (59.02% vs. 61.95%) did not differ between transport conditions. Our results suggest that DMEK grafts can be prestripped, preloaded into a novel transport cartridge and shipped to the clinic with comparable endothelial cell loss, phenotypical marker expression and viability to conventional pre-stripped donor tissue.

Introduction

Descemet membrane endothelial keratoplasty (DMEK) has emerged as the treatment of choice for corneal endothelial dysfunction owing to excellent visual recovery and low risk of rejection.[1–5] Eye bank-prepared tissue has helped to reduce intraoperative complications related to tissue preparation. However, the final steps of tissue preparation, namely separating the donor tissue from the corneal button, staining with trypan blue, rinsing with balanced salt solution, and loading into an injector, are left to the surgeon. The recent development of preloaded DMEK transport systems has the potential to reduce costly operation theatre time and the risk of iatrogenic tissue damage. Moreover, they will allow eye banks to send only the tissue necessary for DMEK surgery, optimizing donor availability for other purposes.[6,7] To date, two preloaded DMEK transport protocols have been developed and studied.[8–10] These allow the transport of pre-stripped DMEK tissue in either a modified Jone's tube[8] or a modified lens insertion carrier.[9] More recently, Geuder AG (Heidelberg, Germany) has developed a method, for transporting the pre-stripped DMEK tissue in a preloaded glass cannula similar to the one used for its injection in the operation theater. The aim of this study is to compare the DMEK RAPID preloaded transport method, developed by Geuder AG, with the conventional pre-stripped method used to date. Determining whether the DMEK tissue arrives equally viable for transplant in both conditions is necessary before the implementation of this preloaded transport system in the clinical setting.

Materials and methods

Ethical statement

This research was performed in compliance with the tenets of the Helsinki Declaration. Twelve human cadaveric corneoscleral tissues (Table 1), which were unsuitable for transplantation due to medical history reasons, such as high-risk behavior, were obtained from the Cornea Department of the ETB-BISLIFE Multi Tissue Center (Beverwijk, the Netherlands) following consent from the next of kin of all deceased donors.

Shipping conditions

All tissues were preserved post-mortem in organ culture media at 31°C before use. Organ culture media comprised the following: minimum essential medium (Biowest, Nuaillé, France) supplemented with 20 mM HEPES (Sigma, Saint Louis, MO, USA), 26 mM sodium bicarbonate (Sigma, Saint Louis, MO, USA), 2% (v/v) newborn calf serum (ThermoFisher Scientific, Waltham, MA, USA), 10 IU/mL penicillin, 0.1 mg/mL streptomycin and 0.25 µg/mL amphotericin (Sigma, Saint Louis, MO, USA). The tissues were processed and transported in two different conditions: The first condition used was the conventional method used for shipping DMEK tissue grafts, in which the pre-stripped endothelial tissue was laid-flat on the corneal stromal bed. The second condition was the preloaded DMEK RAPID from Geuder (Geuder AG, Heidelberg, Germany) (Figure 1), in which the corneal endothelium was pre-stripped with the endothelial cells facing outwards and was loaded in a Geuder preloadable glass cannula for DMEK (Geuder AG, Heidelberg, Germany).

During transportation, the tissue was conserved in transport media (organ culture media with 6% (w/v) dextran (Sigma, Saint Louis, MO, USA)) at ambient temperature in line with clinical practice. Transport of the DMEK tissues was performed within the Netherlands, from the ETB-BISLIFE Multi Tissue Center in

Beverwijk (North Holland) to the Maastricht University Medical Center+ (Limburg). All tissues were received and analyzed 36 – 48 h after the DMEK pre-stripping only or preloading.

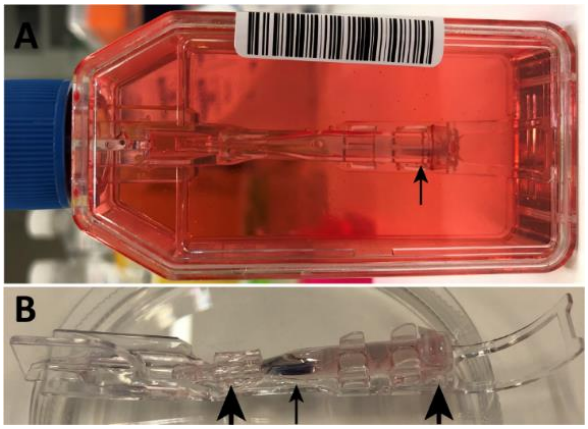

Figure 1. Representative images of DMEK tissue in the pre-loaded transport condition using the DMEK RAPID Geuder system. A is the cartridge with preloaded DMEK tissue in the transport flask containing transport media. B is the cartridge with transport support for the pre-loaded DMEK tissue. Full arrows indicate the stained DMEK tissue roll in the Geuder cartridge. Arrow heads indicate two liquid permeable plugs that allow gentle washing steps and staining of the graft within the transport cartridge.

Preparation of tissue for transport

The corneas (n=12) were vacuum fixed in a punch base. The corneal endothelium was first trephined using a 10 mm diameter trephine (e.janach, Como, Italy) and the Descemet membrane was gently stripped leaving it attached to the cornea by a hinge. After the first stripping, the DMEK graft was left to lay on top of the corneal stromal bed and further trephined using a 8.5 mm diameter trephine (Moria, Doylestown, PA, USA). For the pre-stripped only transport method (n=6), the 8.5 mm diameter DMEK graft was left on top of the corneal stroma attached by a hinge. The pre-stripped cornea was then transported in a glass bottle containing approximately 50 mL of transport media. The average total time required for preparation of pre-stripped only DMEK tissue was 20 min. For the preloaded transport method (n=6), the 8.5 mm DMEK graft was separated from the cornea and rolled with the

endothelial side facing outwards. The endothelial roll was then stained by dragging it through a drop of trypan blue solution (0.4%), washed with BSS, transferred to a 35 mm culture dish with transport media and gently suctioned using a syringe into a preloadable glass cannula for DMEK containing transport media (Geuder AG, Heidelberg, Germany). The loaded glass cannula was sealed with plastic plugs at both the funnel and rear sides and transferred to a T25 tissue culture flask (Corning, Corning, NYS, USA) completely filled with approximately 70 mL of transport media for transport. The total time required for the preparation of preloaded transport DMEK tissue was approximately 30 min. Tissue marking for graft orientation was not used in this study as tissue marking may be more traumatic to preloaded tissue.[11]

Study design

This study included twelve donor corneas, six in the pre-stripped only DMEK group and six in the preloaded DMEK group. From each group, three whole DMEK rolls (n=6) were used for viability staining. The remaining DMEK rolls (n=6) were used as following: two DMEK rolls from each group (n=4) were divided, one half was used for immunofluorescence and the other half used for hematoxylin and eosin staining. The remaining rolls (n=2) were used for immunofluorescence (Figure 2).

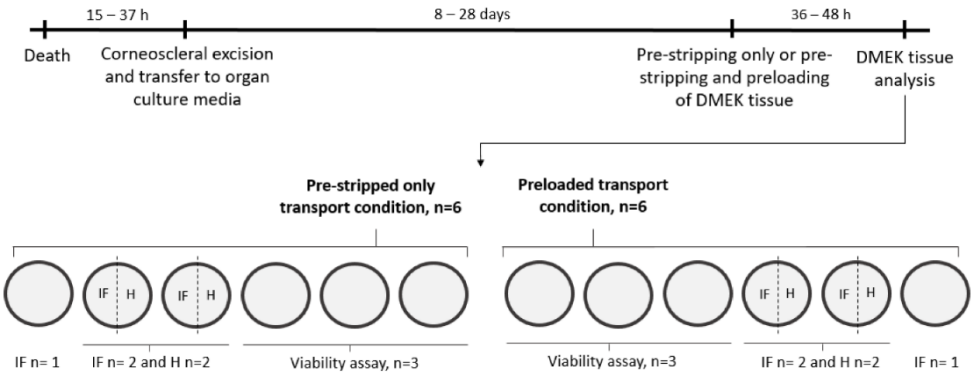

Figure 2. Schematic representation of timings and tissue use in this study. IF: immunofluorescence assay, H: histology.

Table 1. Donor information. ECD: endothelial cell density (cells/mm^2)

Cornea number	Age	Sex	Hours between death and excision	Days in preservation	Cause of death	ECD before stripping	ECD after stripping	ECD after transport	Experiment
Preloaded 01	34	M	15	22	Stroke	3000	3000	2500	Phase contrast, histology, immunofluorescence
Preloaded 02	58	M	16	28	Non-specified	2700	2700	2500	Phase contrast, histology, immunofluorescence
Preloaded 03	76	F	20	16	Stroke	2600	2600	2400	Phase contrast, immunofluorescence
Preloaded 04	62	M	26	26	Respiratory failure	2800	2800	2800	Viability assay
Preloaded 05	68	F	37	8	Aortic aneurysm	2800	2800	2600	Viability assay
Preloaded 06	69	M	32	25	Septicemia	2500	2500	2100	Viability assay
Prestripped-only 01	34	M	15	22	Stroke	3100	3100	2700	Phase contrast, histology, immunofluorescence
Prestripped-only 02	57	F	27	27	Hemorrhage	2300	2300	2000	Phase contrast, histology, immunofluorescence
Prestripped-only 03	76	F	20	16	Stroke	2600	2600	2400	Phase contrast, immunofluorescence
Prestripped-only 04	66	F	29	21	Chronic obstructive pulmonary disease	2800	2800	2600	Viability assay
Prestripped-only 05	76	F	26	22	Acute myocardial infraction	2900	2900	2400	Viability assay
Prestripped-only 06	69	M	32	25	Septicemia	2700	2700	2500	Viability assay

Tissue analysis with phase contrast microscopy

All tissues (n=12) were analyzed before and after Descemet's membrane stripping at the Cornea Department of ETB-BISLIFE to determine the cell density and identify possible denuded areas using an upright microscope. Following transport, the preloaded DMEK rolls were released into a 35 mm culture dish filled with BSS ophthalmic irrigation solution (Alcon, MO, USA) and pre-stripped only DMEK tissues were fully stripped. DMEK tissues for immunofluorescence and histology were stained with 0.4% trypan blue solution for 30 s and washed with BSS ophthalmic irrigation solution (Alcon, MO, USA), then unfolded on a glass slide and analyzed with an Eclipse TS100 microscope (Nikon, Tokyo, Japan) to determine the cell density and denuded areas (n=6). The tissues for viability assay (n=6) were immediately incubated with the viability assay.

Histological analysis

Four corneal endothelial rolls (two of each transport condition, n=4), were fixed in 4% paraformaldehyde (PFA) for 20 min at ambient temperature. After fixation, the tissues were halved, with one half used for histological analysis and the other for immunofluorescence analysis. The half used for histological analysis was placed overnight in a Citadel 2000 automated tissue processor (ThermoFisher Scientific, Waltham, MA, USA) and embedded in paraffin. The paraffin-embedded endothelial rolls were sectioned using a Microm HM 355S microtome (ThermoFisher Scientific, Waltham, MA, USA) and mounted on glass slides. The mounted sections were then stained for hematoxylin and eosin in order to identify any morphological changes in the Descemet's membrane and endothelium integrity. In brief, samples were first dewaxed with xylene and rehydrated with decreasing series of ethanol (100%, 96%, 70%, 50%) following by water. After rehydration, the tissue samples were stained with hematoxylin Gill III (Sigma, Saint Louis, MO, USA) for 5 min following a wash with running water for 5 min. Then, the samples were stained with eosin (Sigma, Saint Louis, MO, USA) for 1 min, dehydrated with increasing series of ethanol (70%, 96%, 100%) and then cleared with xylene. Finally, the samples were

mounted using DPX mounting media (Sigma, Saint Louis, MO, USA). Descemet's membrane thickness was analyzed using the ImageJ software distributor Fiji.[12] Briefly, a line was drawn across the Descemet's membrane with the line-drawing tool and measured to determine the thickness of the membrane.

Immunofluorescence analysis

Two full DMEK tissues (one of each transport condition, n=2) and the four remaining halves of fixed DMEK tissues (two of each transport condition, n=4), were used for immunofluorescence analysis. The tissues were stained for ZO-1, Na^+/K^+ ATPase and CD166 (n=3 for each transport condition). Briefly, the DMEK tissues were fixed in 4% PFA for 20 min at ambient temperature and the cells were permeabilized with 0.2% Triton X-100 in PBS for 10 min. After permeabilization, non-specific antibody interactions were blocked with 2% BSA solution in PBS for 1 h at ambient temperature. Tissues were incubated overnight at 4°C with primary antibodies diluted in 2% BSA solution. After primary antibody incubation, tissues were washed three times in PBS and then incubated with secondary antibodies and Hoechst 33342 for 50 min at ambient temperature in the dark. The DMEK tissues were then washed three times in PBS and mounted with coverslips with ProLong Gold antifade reagent (Thermo Fisher Scientific Waltham, MA, USA). Cells were examined on an Eclipse Ti-E inverted microscope equipped with a spinning disk (Nikon, Tokyo, Japan). All the information of the primary and secondary antibodies used can be found in Table 2.

Endothelial cell triple staining for viability

Six DMEK tissue`s (three of each transport condition), were triple-stained with Hoechst 33342, ethidium homodimer-1 and calcein AM to determine the viability of the corneal endothelial cells after transport as previously described.[13] Briefly, the tissues were first washed in BBS solution to remove serum esterase from the media. The whole endothelial rolls were then incubated in a BBS solution containing 4 µM ethidium homodimer-1, 2 µM calcein AM and 3 µM Hoechst 33342 (Thermo Fisher

Scientific, Waltham, MA, USA) for 45 min at ambient temperature in the dark. After the incubation, the corneal endothelial rolls were unfolded on a glass slide and flat mounted using relaxation incisions without mounting media. A tile scan of the whole corneal endothelium was performed on an Eclipse Ti-E inverted widefield microscope (Nikon, Tokyo, Japan). The percentage of dead cells (nuclei stained with ethidium homodimer) compared to the total number of cells (nuclei stained with Hoechst) found in the unfolded corneal endothelial rolls was calculated using ImageJ software distributor Fiji[12]. To perform the particle analysis, the images were converted to binary format and the stained cell nuclei were selected by circularity (circularity range 0.3 – 1) and size (size range: 25 – 670 μm^2) and counted. The surface percentage covered with calcein AM and the denuded areas were also calculated using Fiji. For calcein AM quantification, the images were converted to binary and the percentage of area covered was calculated. For the denuded areas, the denuded regions were manually selected and their surface area was measured.

Table 2. Primary and secondary antibody details

Antibody/stain	Manufacturer	Reference number	Concentration
Mouse anti-CD166 primary	BD Biosciences	559260	2.5 µg/mL
Rabbit anti-Zona Occludens 1 (ZO-1) primary	Thermo Fisher Scientific	402200	2.5 µg/mL
Mouse anti-Na^+/K^+ ATPase primary	Abcam	Ab7671	10 µg/mL
Goat anti-mouse Alexa Fluor 488 secondary	Thermo Fisher Scientific	A11001	5 µg/mL
Donkey anti-rabbit Alexa Fluor 568 secondary	Thermo Fisher Scientific	A10042	5 µg/mL
Hoechst 33342	Thermo Fisher Scientific	H1399	1 µg/mL

Statistical analysis

R Statistical Software[14] (v. 3.2.4) was used for statistical analysis. Descriptive values are shown as mean ± standard deviation. Data were analyzed to check for statistical significance using a Student's t-test, considering samples with equal variances and a 0.05 significance level.

Results

Donor characteristics

Baseline donor characteristics did not differ between both transport conditions. The average donor age for the pre-stripped only and preloaded transport conditions was 63 (±15.87) and 61.2 (±14.68) years, respectively. The interval between death and tissue retrieval was 24.83 (±6.24) hours for the pre-stripped only and 24.33 (±8.91) hours for the preloaded condition. The average days in culture media of the donor tissue for pre-stripped only and preloaded conditions were 22.17 (±3.76) and 20.83 (±7.55) days, respectively.

Tissue preparation

Eye bank pre-stripping (n=12) and preloading (n=6) were performed by one experienced technician and was successful in all cases.

Tissue analysis after shipping

All tissues (n=12) were received without evident damage. One of the preloaded DMEK tissues lost the trypan blue coloring and was not visible inside the cannula; the remaining five maintained the trypan blue coloring on arrival. All tissues analyzed with light microscopy (n=3 per transport condition) preserved the integrity of the corneal endothelial cell mosaic regardless of the transport condition (Figure 3A, C). The DMEK tissues had minimally denuded areas in the periphery, which were comparable in both transport conditions (Figure 3B, D). Baseline endothelial cell count and cell loss did not differ between transport conditions. There was also no significant difference in central endothelial cell count (cells/mm^2) before and after transport in both conditions (pre-stripped only: 2733 ±273 vs. 2450 ±243; preloaded: 2733 ±175 vs. 2483 ±232).

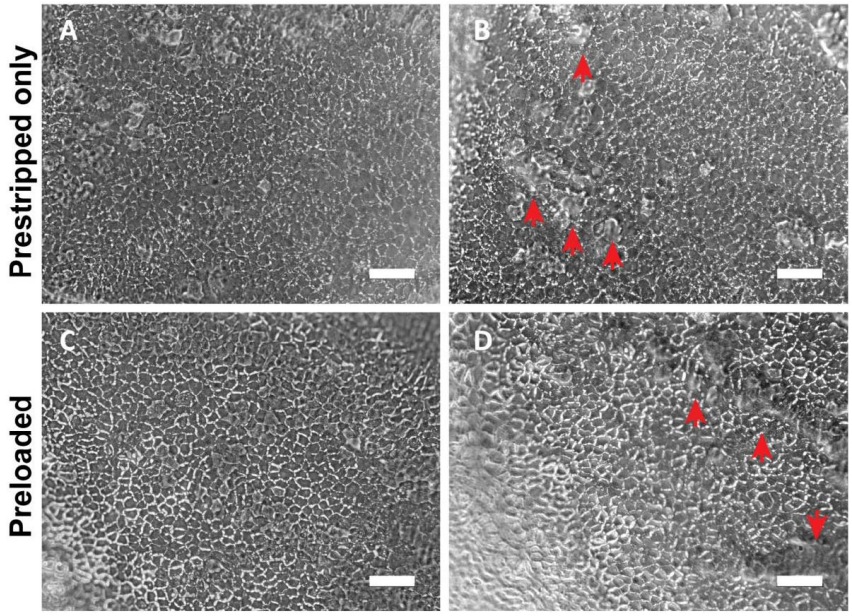

Figure 3. Representative phase contrast images following transport of pre-stripped only (upper row) and preloaded (lower row) DMEK rolls. A and C are images of the central part of the corneal endothelial rolls, showing that the cell morphology and confluency were unaffected by either transport condition. B and D show minimally denuded areas (arrow heads) in the periphery of tissues transported in both conditions. Scale bar: 100 μm.

Histological analysis of DMEK tissues

The hematoxylin and eosin staining of the DMEK tissue transported in both conditions showed the presence and integrity of a monolayer of endothelial cells on the Descemet's membrane (Figure 4). Descemet's membrane thickness was statistically similar in both conditions, namely 3.67 μm (±0.21) for preloaded and 3.86 μm (±0.18) for pre-stripped only. These data indicated no macroscopic alterations in the Descemet's membrane or the endothelial cells for either transport condition.

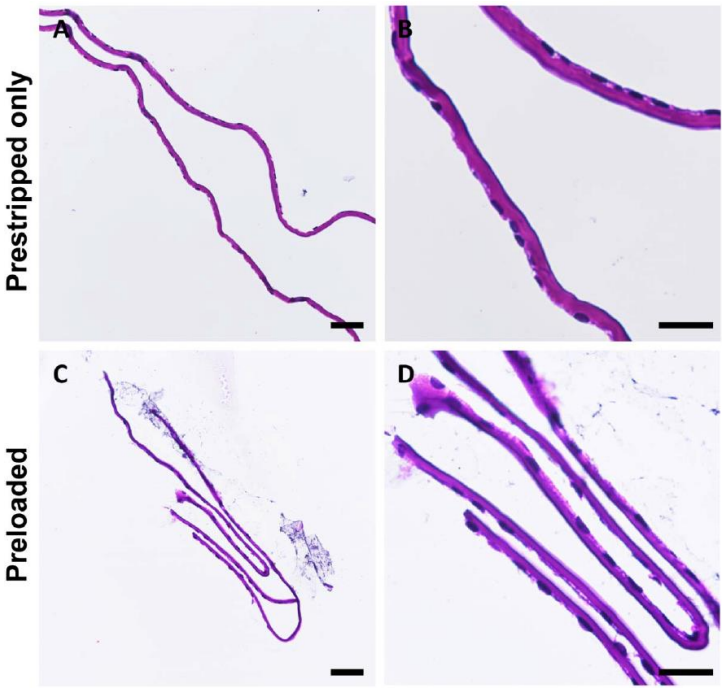

Figure 4. Representative images of hematoxylin and eosin stained sections of corneal endothelial DMEK tissues transported as either pre-stripped only or preloaded endothelial roll. The thickness of the Descemet's membrane in the endothelial rolls was comparable in both conditions, namely 3.67 µm (±0.21) for preloaded and 3.86 µm (±0.18) for conventional, p= 0.48. Moreover, a monolayer of cell nuclei stained with hematoxylin was present on the Descemet's membrane in both conditions. B and D are a zoomed region of interest from images A and C, respectively. Scale bar: A and C: 50 µm; B and D: 25 µm.

Immunofluorescence analysis of corneal endothelial phenotypical markers on DMEK tissue

Samples transported in both conditions were analyzed to detect the presence of CD166, Na^+/K^+ ATPase and ZO-1 proteins (Figure 5). The phenotype markers for the corneal endothelium CD166 and Na^+/K^+ ATPase showed a similar expression in both conditions (Figure 5A, B, D, E). Moreover, the presence and expression of ZO-1, indicates the integrity of the cell monolayer and the maintenance of these tight junctions after the DMEK processing in both conditions (Figure 5C, F). The data

obtained indicated that the phenotypical markers of corneal endothelial cells were maintained in both conditions after transport.

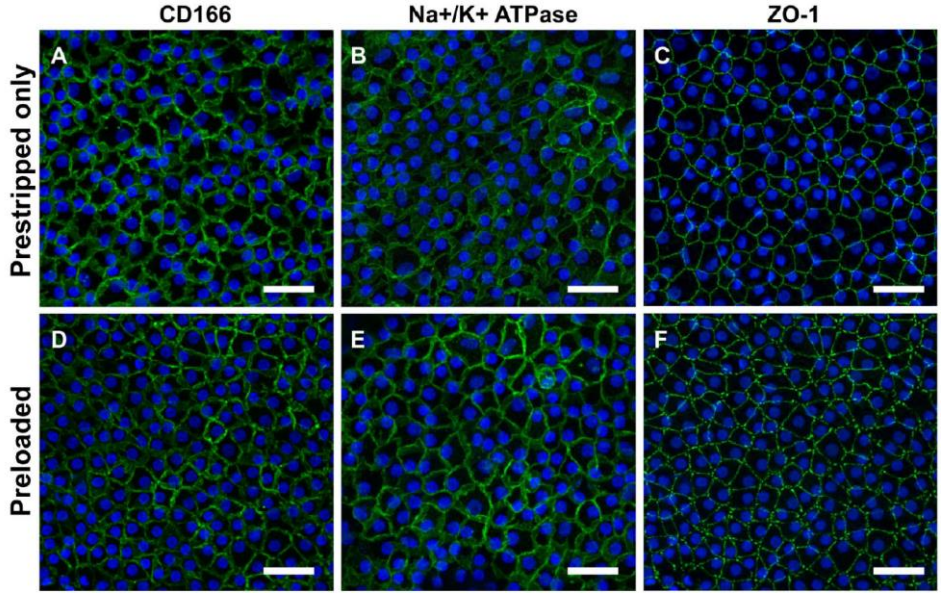

Figure 5. Representative images of immunofluorescence stainings of phenotypical and functional protein markers (green) of the corneal endothelial DMEK tissues transported in both pre-stripped only and preloaded conditions. Cell nuclei (blue) were stained with Hoechst. A and D are immunofluorescence analysis for CD166, B and E for Na^+/K^+ ATPase and C and F for ZO-1. All the protein markers expression was comparable in both transport conditions, and showed integrity of the tight junctions in the corneal endothelial monolayer in both conditions. Scale bars: 50 µm.

Viability staining for DMEK tissues

The viability triple staining with Hoechst, calcein AM and ethidium homodimer were used to assess the viability of the DMEK tissues transported in both conditions (Figure 6). The whole-DMEK tissue staining of calcein AM (Figure 6C, G) and ethidium homodimer (Figure 6D, H) were similar in tissues transported in both conditions. The percentage of dead cells, calcein-covered area and denuded areas was calculated with Fiji analysis software and was statistically similar in DMEK tissue transported in either condition. The percentage of dead cells was 16.73% (±7.45) for the preloaded transport and 18.1% (±5.01) for the pre-stripped only

transport condition. The calcein-covered surface in the preloaded condition was 61.95% (±7.63) and in the pre-stripped only condition was 59.02% (±8.58). The denuded areas were 8.11% (±3.2) in the preloaded condition and 5.83% (±1.61) in the pre-stripped only condition. These data reveals that the transport condition had no effect on the viability of the DMEK tissue for transplantation.

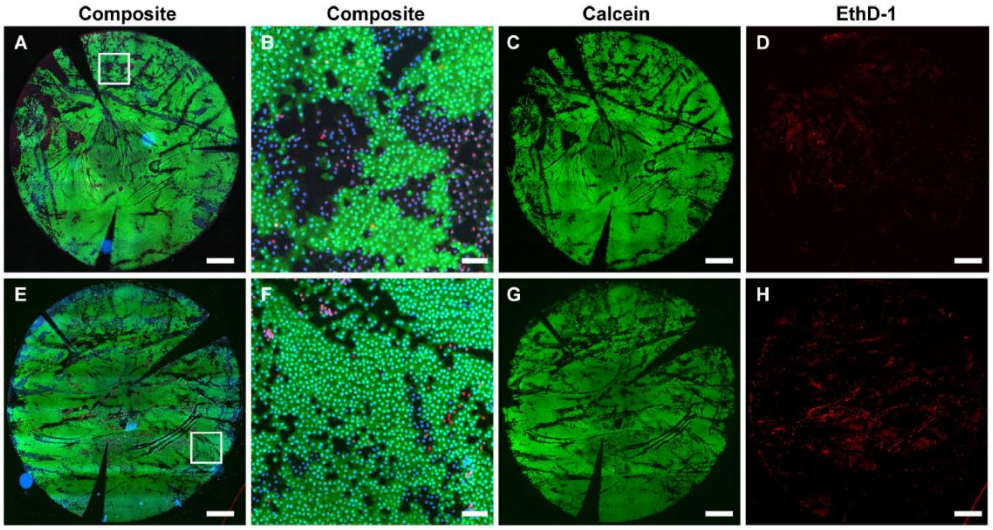

Figure 6. Representative images of live/dead triple staining of full corneal endothelial DMEK tissues transported in both pre-stripped only (A-C) and preloaded (E-H) transport conditions. A and E are merged images of Hoechst (blue), calcein (green) and ethidium homodimer (red). B and F are zoomed in of the regions indicated in A and E with a square. C and G are calcein fluorescent regions. D and H are ethidium homodimer fluorescent regions. The percentage of dead cells is statistically equal in DMEK tissue transported in either condition, being 16.73% (±7.45) for the preloaded transport condition and 18.1% (±5.01) for the pre-stripped only transport condition, p=0.81. Furthermore, the calcein-covered surface (green surface) and the denuded areas (acellular areas) appear to be equal in DMEK tissue transported in either condition. The calcein-covered surface in the preloaded condition was 61.95% (±7.63) whereas in the pre-stripped only condition was 59.02% (±8.58), p= 0.68. The denuded areas were 8.11% (±3.2) in the preloaded condition and 5.83% (±1.61) in the pre-stripped only condition, p= 0.33 . n=3 preloaded, n=3 pre-stripped only. Scale bar: A, C, D, E, G and H: 1 mm; B and F: 100 µm.

Discussion

In this laboratory study, we compared the DMEK RAPID transport system from Geuder AG with conventional eye bank pre-stripped DMEK. Our results show no significant difference in endothelial cell density, tissue histology, surface marker expression and endothelial cell viability, suggesting this system is suitable for clinical use.

Previous studies describe different methods to preload DMEK grafts at the eye bank.[8–10] These allow the transport of pre-stripped DMEK tissue in either a modified Jone's tube[8] or a modified lens insertion carrier.[9] Unlike the other preloaded transport systems, the DMEK RAPID employs a smooth-surface and smooth-edged borosilicate glass cartridge that allows the surgeon to inject the sensitive donor tissue directly into the patient's anterior chamber without manipulation of the endothelium through an astigmatism neutral incision.[15–17] Moreover, the high transparency of the glass cannula enables correct orientation of the lamella to be controlled during surgery.

Storage and transport were not associated with significant central endothelial cell loss in both conditions, despite the use of Dextran due to eye bank regulations.[18,19] The denuded areas in the periphery of the donor grafts (Figure 3), irrespective of transport conditions, likely represent stress lines caused by pre-stripping and/or tissue handling during experiments. Histological analysis (Figure 4) confirmed the integrity of Descemet's membrane and endothelial cell layer and revealed no difference in Descemet's membrane thickness (3.67 µm vs 3.86 µm) between transport conditions. Regarding the endothelial cell phenotype, in both conditions the corneal endothelial cell mosaic was conserved. The ZO-1 tight junctions detected with immunofluorescence (Figure 5C, F) confirmed the integrity of the confluent corneal endothelial cell monolayer. CD166 and Na^+/K^+ ATPase detection with immunofluorescence (Figure 5A, B, D, F) was also comparable in both conditions,

confirming the maintenance of corneal endothelial specific proteins (CD166) and metabolic functional endothelial transporters (Na^+/K^+ ATPase) in both conditions.

The viability assay showed similar percentage of dead cells in both transport methods (18.1% vs. 16.73%). Moreover, the calcein-covered surface (59.02% vs. 61.95%) did not differ between transport conditions. A comparable percentage of cells in both transport conditions were still alive but not metabolically active, reflected by the lack of calcein-associated fluorescence and the lack of ethidium homodimer nuclear staining. This cell population was only recognized thanks to the triple staining (Hoechst, calcein AM and ethidium homodimer) used in these experiments. Viability studies performed only with calcein AM would not recognize this population of cells. The findings reported in this study are in line with previous publications on preloaded tissue for DMEK using a modified Jone's tube[8] or a modified lens insertion carrier[9]. The cell viability determined by the calcein-covered surface ranged from 37.8% to 70.1% with these transport techniques.[10] Compared to the previously studied preloaded techniques, the Geuder transport system shows favorable cell viability (61.95%) compared to the modified Jone's tube (61.95% vs 37.8%) and a comparable cell viability to the modified lens insertion carrier (61.95 vs 70.1%).[10] Given the limited number of suitable tissues, the current study focused on the effects of the new transport system from Geuder in comparison to conventional pre-stripped only method. A future side-by-side comparison of existing preloaded DMEK transport methods would give further clinically relevant data.

With this study, it can be concluded that the DMEK RAPID preloaded transport system delivers DMEK donor tissue with comparable endothelial cell density, phenotypical marker expression and viability to conventional prestripped donor tissue. Implementation of this system could facilitate the transition to DMEK for novice surgeons, shorten the duration of surgery, and takes advantage of the tissue preparation skills of eye bank professionals to minimize iatrogenic endothelial cell loss.

Funding

This study was funded by Chemelot InSciTe under the EyeSciTe consortium.

References

1. Price, M. O., Giebel, A. W., Fairchild, K. M. & Price, F. W. Descemet's membrane endothelial keratoplasty. Prospective multicenter study of visual and refractive outcomes and endothelial survival. *Ophthalmology* **116**, 2361–2368 (2009).

2. Guerra, F. P., Anshu, A., Price, M. O., Giebel, A. W. & Price, F. W. Descemet's membrane endothelial keratoplasty: Prospective study of 1-year visual outcomes, graft survival, and endothelial cell loss. *Ophthalmology* **118**, 2368–2373 (2011).

3. Dickman, M. M. *et al.* Changing practice patterns and long-term outcomes of endothelial versus penetrating keratoplasty: A prospective dutch registry study. *Am. J. Ophthalmol.* **170**, 133–142 (2016).

4. Ham, L., Balachandran, C., Verschoor, C. A., Van Der Wees, J. & Melles, G. R. J. Visual rehabilitation rate after isolated descemet membrane transplantation: Descemet membrane endothelial keratoplasty. *Arch. Ophthalmol.* **127**, 252–255 (2009).

5. Rodríguez-Calvo-De-Mora, M. *et al.* Clinical outcome of 500 consecutive cases undergoing Descemet's membrane endothelial keratoplasty. *Ophthalmology* **122**, 464–470 (2015).

6. Gain, P. *et al.* Global survey of corneal transplantation and eye banking. *JAMA Ophthalmol.* **134**, 167–173 (2016).

7. Tan, D. T. H., Dart, J. K. G., Holland, E. J. & Kinoshita, S. Corneal transplantation. *Lancet* **379**, 1749–1761 (2012).

8. Tran, K. D. *et al.* Evaluation and quality assessment of prestripped, preloaded descemet membrane endothelial keratoplasty grafts. *Cornea* **36**, 484–490 (2017).

9. Parekh, M., Ruzza, A., Ferrari, S., Busin, M. & Ponzin, D. Preloaded tissues for Descemet membrane endothelial keratoplasty. *Am. J. Ophthalmol.* **166**, 120–125 (2016).

10. Romano, V. *et al.* Comparison of preservation and transportation protocols for preloaded Descemet membrane endothelial keratoplasty. *Br. J. Ophthalmol.* **102**, 549–555 (2018).

11. Newman, L. R. *et al.* Minimizing Endothelial Cell Loss Caused by Orientation Stamps on Preloaded Descemet Membrane Endothelial Keratoplasty Grafts. *Cornea* **38**, 233–237 (2019).

12. Schindelin, J. *et al.* Fiji: An open-source platform for biological-image analysis. *Nat. Methods* **9**, 676–682 (2012).

13. Pipparelli, A. *et al.* Pan-corneal endothelial viability assessment: Application to endothelial grafts predissected by eye banks. *Investig. Ophthalmol. Vis. Sci.* **52**, 6018–6025 (2011).

14. R Core Team. R: A language and environment for statistical computing. (2013).

15. Szurman, P. *et al.* Novel liquid bubble dissection technique for DMEK lenticule preparation. *Graefe's Arch. Clin. Exp. Ophthalmol.* **254**, 1819–1823 (2016).

16. Yoeruek, E., Bayyoud, T., Hofmann, J. & Bartz-Schmidt, K. U. Novel maneuver facilitating Descemet membrane unfolding in the anterior chamber. *Cornea* **32**, 370–373 (2013).

17. Sarnicola, C. *et al.* Cannula-assisted technique to unfold grafts in descemet membrane endothelial keratoplasty. *Cornea* **38**, 275–279 (2019).

18. Thuret, G., Manissolle, C., Campos-Guyotat, L., Guyotat, D. & Gain, P. Animal compound-free medium and poloxamer for human corneal organ culture and deswelling. *Investig. Ophthalmol. Vis. Sci.* **46**, 816–822 (2005).

19. Yoeruek, E., Hofmann, J. & Bartz-Schmidt, K. U. Comparison of swollen and dextran deswollen organ- cultured corneas for descemet membrane dissection preparation: Histological and ultrastructural findings. *Investig. Ophthalmol. Vis. Sci.* **54**, 8036–8040 (2013).

4

Single cell transcriptomics reveal the heterogeneity of the human cornea to identify novel markers of the limbus and stroma

This chapter has been published as:

Català, P., Groen, N., Dehnen, J.A., Soares, E., van Velthoven, A.J.H., Nuijts, R.M.M.A., Dickman, M.M., LaPointe, V.L.S. Single cell transcriptomics reveals the heterogeneity of the human cornea to identify novel markers of the limbus and stroma. *Sci Rep*. 2021; 11: 21727

Abstract

The cornea is the clear window that lets light into the eye. It is composed of five layers: epithelium, Bowman's layer, stroma, Descemet's membrane and endothelium. The maintenance of its structure and transparency are determined by the functions of the different cell types populating each layer. Attempts to regenerate corneal tissue and understand disease conditions requires knowledge of how cell profiles vary across this heterogeneous tissue. We performed a single cell transcriptomic profiling of 19,472 cells isolated from eight healthy donor corneas. Our analysis delineates the heterogeneity of the corneal layers by identifying cell populations and revealing cell states that contribute in preserving corneal homeostasis. We identified expression of *CAV1*, *HOMER3* and *CPVL* in the corneal epithelial limbal stem cell niche, *CKS2*, *STMN1* and *UBE2C* were exclusively expressed in highly proliferative transit amplifying cells, *CXCL14* was expressed exclusively in the suprabasal/superficial limbus, and and *NNMT* was exclusively expressed by stromal keratocytes. Overall, this research provides a basis to improve current primary cell expansion protocols, for future profiling of corneal disease states, to help guide pluripotent stem cells into different corneal lineages, and to understand how engineered substrates affect corneal cells to improve regenerative therapies.

Introduction

The healthy cornea is a transparent and avascular tissue that allows light to enter the eye and accounts for most of its refractive power. The cornea is composed of five layers: its outer surface is a stratified sheet of corneal epithelial cells that reside on the Bowman's layer, a collagen-based acellular membrane synthesized by the stromal keratocytes. The keratocytes populate the corneal stroma, the middle layer of the cornea that is composed of structured collagen fibers and other extracellular matrix proteins. The corneal endothelium forms a thin monolayer of tightly packed hexagonal cells that line in the innermost surface of the cornea and reside in close contact to the stroma on the Descemet's membrane.

Corneal structure and transparency are governed by the functions of the cell types populating each layer. Epithelial cells act as a biological barrier to block the passage of foreign material and provide a smooth surface that absorbs nutrients. Keratocytes maintain extracellular matrix homeostasis responsible for the cornea's biomechanical and optical properties, and endothelial cells serve as active pumps transporting ions, metabolites and fluid to maintain corneal hydration and transparency.

Selective replacement of dysfunctional single corneal layers with that of a donor,[1] the autologous transplantation of primary cultured corneal epithelial limbal stem cells,[2] and the treatment of endothelial dysfunctions with primary cultured allogeneic corneal endothelial cells[3] are already a therapeutic reality. Gaining deeper understanding of corneal cell profiles and their transcriptomic signatures can be highly relevant for the improvement of such therapies.

In order to further understand the cellular complexity of this heterogeneous tissue, we provide a high-quality single-cell ribonucleic acid sequencing (scRNAseq) dataset from 19,472 corneal cells isolated from four female and four male donors.

With it, we depict the diverse cell populations and provide a comprehensive cell atlas of the healthy human cornea. The transcriptomic cell census identified subpopulations with different roles in the maintenance of corneal homeostasis and provides a baseline to improve primary cell expansion protocols, for future profiling of corneal disease states, to help guide pluripotent stem cells into different corneal lineages, and to understand how engineered substrates affect corneal cells to improve regenerative therapies. Furthermore, this dataset identified markers exclusively expressed in cells comprising the limbal epithelial stem cell niche, highly proliferating epithelial cells, and stromal keratocytes which could be used as reference to improve current corneal cell replacement therapies.

Materials and methods

Ethical statement

This study was performed in compliance with the tenets of the Declaration of Helsinki. Ten human donor corneas (Table 1) deemed unsuitable for transplantation were obtained from the Saving Sight Eye Bank (Kansas City, MO, USA) and the ETB-BISLIFE Multi-Tissue Center (Beverwijk, the Netherlands) were used for this study. Both male and female donor corneas, with ages ranging from 22 to 79 years and preserved either in Optisol-GS at 4°C or in Organ culture media at 31°C were used. Organ culture media comprised the following: minimum essential medium supplemented with 20 mM HEPES, 26 mM sodium bicarbonate, 2% (v/v) newborn calf serum (Thermo Fisher Scientific), 10 IU/mL penicillin, 0.1 mg/mL streptomycin and 0.25 μg/mL amphotericin. The tissues used for scRNAseq had no history of ocular disease, chronic systemic disease or infection such as HIV or hepatitis B.

Manual dissection of the corneal tissue

Eight donor corneas were dissected for scRNAseq. First, cells were isolated from six corneas that were manually dissected to separate the epithelial, stromal and the endothelial layers to ensure the gentlest possible enzymatic dissociation of each layer. The corneas were vacuum fixed in a punch base (e.janach) endothelial-cell side up, stained with trypan blue solution (0.4%) for 30 s and washed with BSS ophthalmic irrigation solution. The corneal endothelium was then gently lifted following the Schwalbe line using a DMEK cleavage hook (e.janach) and fully stripped using angled McPherson tying forceps. The remaining tissue was trephined using a 9.5 mm Ø Barron vacuum punch (Katena) in order to separate the epithelium and stroma from the scleral ring. The remaining two corneas were used for limbus isolation. A surgical scalpel was used to cut the limbus into approximately 1 × 2 mm fragments, which were then rinsed with PBS.

Table 1. Donor cornea information

Cornea	Gender	Age (years)	Preservation	Eye bank	Experiment
01	Female	62	Optisol (4°C for 5 days)	Saving Sight	9.5 mm Ø trephined cornea scRNAseq
02	Male	22	Optisol (4°C for 6 days)	Saving Sight	9.5 mm Ø trephined cornea scRNAseq
03	Male	75	Optisol (4°C for 10 days)	Saving Sight	9.5 mm Ø trephined cornea scRNAseq
04	Female	48	Optisol (4°C for 8 days)	Saving Sight	9.5 mm Ø trephined cornea scRNAseq
05	Male	75	Organ culture media (31°C for 21 days)	ETB-BISLIFE	9.5 mm Ø trephined cornea scRNAseq
06	Female	75	Organ culture media (31°C for 15 days)	ETB-BISLIFE	9.5 mm Ø trephined cornea scRNAseq
07	Female	71	Organ culture media (31°C for 18 days)	ETB-BISLIFE	Limbus scRNAseq
08	Male	79	Organ culture media (31°C for 14 days)	ETB-BISLIFE	Limbus scRNAseq
09	Female	78	Organ culture media (31°C for 7 days)	ETB-BISLIFE	Immunofluorescence
10	Male	71	Organ culture media (31°C for 8 days)	ETB-BISLIFE	Immunofluorescence

Tissue dissociation to single cells

The six manually dissected corneal tissues were enzymatically treated to obtain single cell suspensions. The stripped corneal endothelium was incubated with 2 mg/mL collagenase (Sigma) solution in human endothelial serum free media (SFM) (Thermo Fisher Scientific) for 1–2 h at 37°C followed by a 10 min incubation with Accutase (Thermo Fisher Scientific) at 37°C to obtain a single cell suspension. The cells were centrifuged for 5 min at 800 × g and resuspended in 0.5 mL of human endothelial SFM media.

The corneal epithelium–stroma tissues were treated with 1.5 mg/mL collagenase and 0.2 mg/mL bovine testis hyaluronidase (Sigma) in DMEM/F12 (Thermo Fisher

Scientific) for approximately 1 h at 37 °C. The released corneal epithelium was suctioned with a P1000 micropipette and further treated with Accutase for 10 min at 37°C to obtain a single cell suspension of corneal epithelial cells. The cells were centrifuged for 5 min at 800 × g and resuspended in 0.5 mL of DMEM/F12. The remaining corneal stroma was treated with 1.5 mg/mL collagenase and 0.2 mg/mL bovine testis hyaluronidase in DMEM/F12 for 5–7 h to obtain a single cell suspension of corneal keratocytes. After the incubation, the cells were centrifuged for 5 min at 800 × g and resuspended in 0.5 mL of DMEM/F12 media.

The limbus fragments isolated from the two corneas for limbal isolation were digested with four trypsinization cycles. In each cycle, the limbus fragments were incubated in 10 mL of 0.05% trypsin/0.01% EDTA (Thermo Fisher Scientific) at 37°C for 30 min. The trypsin containing dissociated cells were transferred to a 50 mL centrifuge tube containing 10 mL DMEM/F12 media and centrifuged for 5 min at 300 × g, after which the cells were resuspended in 0.5 mL of DMEM/F12 media. The undigested limbal fragments were placed again in 10 mL of 0.05% trypsin/0.01% EDTA for the following trypsinization cycle. The cells isolated from the limbus of the two donor corneas were pooled for the following steps.

Methanol cell fixation

After dissociation, the single cell suspensions were passed through a 100 μm Ø cell strainer, centrifuged for 5 min at 300 × g and resuspended in 1 mL ice-cold PBS to eliminate any medium remnants. Next, the cells were again centrifuged for 5 min at 300 × g and resuspended in ice-cold PBS at a ratio of 200 μL PBS per 1×10^6 cells followed by the dropwise addition of ice-cold methanol, at a ratio of 800 μL per 1×10^6 cells. The cells were stored at -80°C until sequencing.

Single-cell RNA sequencing (scRNAseq)

Single-cell mRNA sequencing was performed at Single Cell Discoveries according to standard 10x Genomics 3’ V3.1 chemistry protocol. Prior to loading the cells on

the 10x Chromium controller, cells were rehydrated in rehydration buffer. Cells were then counted to assess cell integrity and concentration. Approximately 9,000 cells (comprising 3,000 cells from each of the three layers) from corneas 01, 02, 03 and 04 were separately loaded by layer and cornea. Furthermore, 3,000 cells (1,000 cells from each of the three layers) from corneas 05 and 06, and 3,000 cells from corneas 07 and 08 (from the limbal samples) were separately loaded by cornea. The resulting sequencing libraries were prepared following a standard 10x Genomics protocol.

Bioinformatic analysis of scRNA-seq data

BCL files resulting from sequencing were transformed to FASTQ files with 10x Genomics Cell Ranger mkfastq. FASTQ files were mapped with Cell Ranger count. During sequencing, Read 1 was assigned 28 base pairs, and were used for identification of the Illumina library barcode, cell barcode and UMI. R2 was used to map the human reference genome GRCh38. Filtering of empty barcodes was done in Cell Ranger. The data from all samples were loaded in R (version 3.6.2) and processed using the Seurat package (version 3.2.0).[56] More specifically, cells with at least 1000 UMIs per cell and less than 20% mitochondrial gene content were retained for analysis. The data of all 10x libraries was merged and processed together. The merged dataset was normalized for sequencing depth per cell and log-transformed using a scaling factor of 10,000. The patient effect was corrected using the integration function of Seurat and used for dimensionality reduction and clustering of all cells or cells selected per layer. Cells were clustered using graph-based clustering and the original Louvain algorithm was utilized for modularity optimization. The differentially expressed genes per cluster were calculated using the Wilcoxon rank sum test and used to identify cell types. Putative doublets were computationally identified using scDblFinder (v1.2.0).[57]

Primary culture of limbal cells

Human primary limbal cells were harvested from corneal tissue of cadaveric donors (ages ranging from 36 to 79 years) with informed consent. Human limbal cells were cultured as previously described.[58,59] In short, a surgical scalpel was used to cut the limbus of the corneas into approximately 1 × 2 mm fragments, which were then rinsed with PBS. The limbus fragments were then incubated in 10 mL of 0.05% trypsin/0.01% EDTA (Thermo Fisher Scientific) at 37°C for 30 min. The trypsin containing dissociated cells were transferred to a 50 mL centrifuge tube containing 10 mL culture media and centrifuged for 5 min at 300 × g, after which the cells were resuspended in 0.5 mL of culture media. The undigested limbal fragments were placed again in 10 mL of 0.05% trypsin- EDTA for another trypsinization cycle. Culture medium consisted of 2:1 mixture of DMEM/F12 media (Thermo Fisher Scientific) supplemented with 2 mM GlutaMAX (Thermo Fisher Scientific), 10% fetal bovine serum (Thermo Fisher Scientific), 125 IU/L insulin (Humulin R, Lilly), 0.2 mM adenine (Merck), 1,1 μM hydrocortisone (Merck), 8.5 ng/ml cholera toxin (Sigma), 2 nM triiodothyronine (Sigma), 10 ng/ml epidermal growth factor (Amsbio), and 100 IU/mL penicillin-streptomycin (Thermo Fisher Scientific). The limbal cells were plated on a feeder layer of lethally irradiated 3T3-J2 fibroblasts (fibroblast feeder-layer density 40,000 cells/cm^2). The 3T3-J2 fibroblast immortalized cells line was a kind gift of Prof. Howard Green (Harvard Medical School, Boston, MA, USA). When confluent, limbal epithelial stem cells were passaged by 0.05% trypsin/0.01% EDTA (Thermo Fisher Scientific) treatment and seeded at a density of 15,000 cells/cm^2 in a Nunc chamber slide (Thermo Fisher Scientific).

Immunofluorescence

Two human donor corneas and primary cultured limbal cells were used for immunofluorescence analysis. The corneas were cut in half transversally, embedded in a cryomold containing Tissue-Tek O.C.T. compound, snap frozen in liquid nitrogen, and stored at -80°C until sectioning. For sectioning, 10 μm consecutive

sections were cut on an adhesive cryofilm type 3C(16UF) using a modified Kawamoto method[60], to help preserve the morphology of the tissue during sectioning. The sections were left to dry for 10 min prior to use. The corneal sections and the primary limbal cells cultured on a chamber slide were fixed with 4% paraformaldehyde, permeabilized with 0.1% Triton X-100 in PBS for 10 min and blocked with 2% BSA solution in PBS for 1 h followed by overnight incubation at 4°C with primary antibodies diluted in 2% BSA blocking solution: mouse monoclonal [1F5D3] anti-Ube2c (1:100 dilution; Thermo Fisher Scientific), mouse monoclonal [1F7G5] anti-CKS2 (1:100 dilution; Thermo Fisher Scientific; 37-0300), rabbit polyclonal anti-P63 (p63α) (1:100 dilution; Cell Signaling Technology; 4892), rabbit polyclonal anti-CPVL (1:100 dilution; Thermo Fisher Scientific), rabbit polyclonal anti-HOMER3 (1:250 dilution; Atlas Antibodies), rabbit polyclonal anti-CXCL14 (1:200 dilution; Thermo Fisher Scientific), rabbit polyclonal anti-caveolin1 (1:300 dilution; Abcam; ab2910), rabbit monoclonal [EP1573Y] anti-Stathmin 1 (1:100 dilution; Abcam), and mouse monoclonal [4A4] anti-P63 (ΔNp63) (1:100 dilution; Abcam; ab735). The tissue sections and primary limbal cells were washed five times and incubated with secondary antibodies diluted in 2% BSA blocking solution, goat anti-rabbit A488 (1:300 dilution; Thermo Fisher Scientific) or goat anti-mouse A568 (1:300 dilution; Thermo Fisher Scientific), for 50 min at ambient temperature in the dark. Cell nuclei were stained with 0.5 μg/mL DAPI for 10 min. The samples were washed five times in PBS, mounted with coverslips with Fluoromount G mounting medium (Thermo Fisher Scientific) and examined on a Nikon Eclipse Ti-E inverted microscope equipped with a X-Light V2-TP spinning disk (Crest Optics).

Results

Five major cell clusters were identified in the corneal tissue

Six donor corneas and the limbi of two donor corneas (Table 1) were manually dissected and dissociated into single cells for single-cell RNA sequencing. After filtering low quality cells, the transcriptome profiles of 19,472 cells were further analyzed (Figure 1a).

Data of the 19,472 sequenced cells were embedded in a uniform manifold approximation and projection (UMAP) and unbiased low resolution clustering revealed five major cell clusters (Figure 1b, left). The expression of specific corneal layer marker (keratin 5 (*KRT5)* for epithelium[4], keratocan (*KERA)* for stromal cells[5], and transporter-like protein 11 (*SLC4A11)* for endothelium[6]) identified the three main layers within the five identified clusters (Figure 1c). Differential gene expression profiling of the clusters further confirmed the identification of a corneal epithelial cell cluster comprising 5,964, a corneal stromal cell cluster comprising 12,344 cells, a corneal endothelial cell cluster comprising 842 cell, and non-corneal clusters of blood/lymphatic vessel endothelial cells comprising 36 cells, and immune cells comprising 216 cells (Figure 2). Cell clusters from the three corneal cell layers were further classified separately at higher resolution in different corneal layer–specific subclusters (Figure 1b, right).

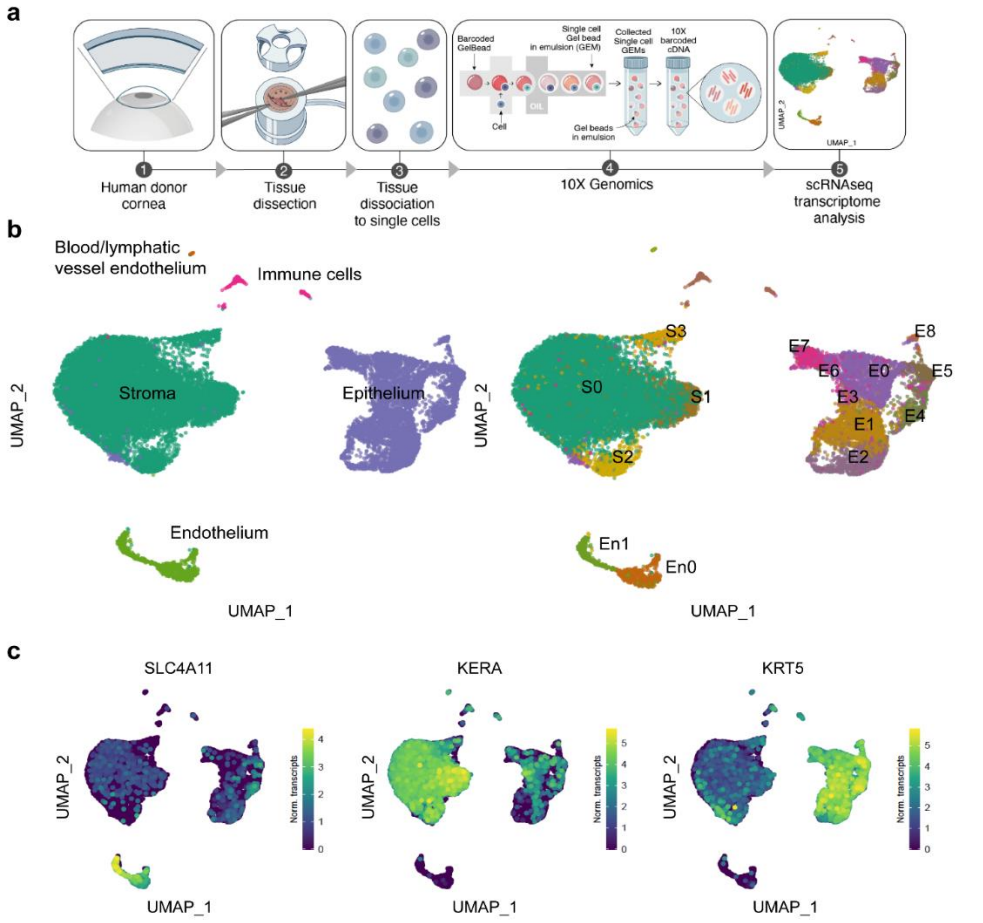

Figure 1. Cell clusters from all three corneal layers and two additional clusters of immune and blood/lymphatic endothelial cells were identified with scRNAseq analysis. Experimental overview for scRNAseq (a). UMAP of the 19,472 sequenced cells with the identified five major cell clusters (b, left). Cell clusters from the three corneal cell layers were further subclustered in different cell subpopulations (b, right). Single cell expression level UMAP of specific corneal layer markers supports cell cluster identification (c): *SLC4A11* is corneal endothelial specific, *KERA* is corneal stromal specific, and *KRT5* is corneal epithelial specific.

Nine cell clusters were identified within the corneal epithelium

A major cluster of 5,964 corneal epithelial cells was identified and further analysis revealed nine subclusters (E0-8, Figure 3a). Differential gene expression profiling was used for further identification of the subclusters. Cluster E3 presented a high

expression of stromal cell markers *KERA*, lumican (*LUM*), and aldehyde dehydrogenase 3 member A1 (*ALDH3A1*),[5,7,8] as well as a reduced expression of corneal epithelial marker keratin 12 (*KRT12*)[9,10] compared to the other epithelial subclusters (Figure 3b and Supplementary Figure S1). Putative doublet analysis of cluster E3 suggested epithelial–stromal keratocyte cell doublets (Supplementary Figure S2). Cluster E7 was identified as conjunctival epithelial cells based on high expression of conjunctival markers such as keratin 13 (*KRT13*), keratin 15 (KRT15), and keratin 19 (*KRT19*),[11,12] and the low expression of the corneal epithelial marker *KRT12* (Figure 3b and Supplementary Figure S1).

Cells forming clusters E6, E8 and E8 showed increased expression of corneal limbal markers keratin 14 (*KRT14*)[13,14], *KRT15*,[15,16] and S100 calcium binding protein A2 (*S100A2)*[17] compared to the other identified clusters suggesting their location in the corneal limbus (Figure 3b and Supplementary Figure S1). Interestingly, cluster E6 showed an increased expression of the superficial epithelium limbus marker[17] S100 calcium binding protein A8 (*S100A8*) compared with clusters E0 and E8 and a reduced expression of the basal corneal epithelial cell markers connexin 26 (*GJB2*), connexin 30 (*GJB6*), and integrin β4 (*ITGB4*),[18–20] (Figure 3b and Supplementary Figure S1) leading to its identification as a population of wing/superficial epithelial cells in the limbus or peripheral cornea. Cluster E0 presented an increased expression of *GJB6*, and *GJB2*, which are predominantly found in basal corneal epithelium[18] suggesting these cells formed a basal corneal epithelial cell population in the limbal stem cell niche or peripheral cornea (Figure 3b and Supplementary Figure S1). Finally, the high expression of mitogenic factors Ki-67 (*MKI67*)[21], survivin (*BIRC5*)[22] and H2A histone family member X (*H2AFX*)[23] in cluster E8, as well as the differential expression of transit-amplifying cell marker CD109[24], suggested that cluster E8 was formed by highly proliferative transit-amplifying cells in the limbal stem cell niche or peripheral cornea (Figure 3b and Supplementary Figure S1). No quiescent limbal epithelial stem cells expressing *ABCB5*, *ABCG2* and *CD200*[24–27] were identified in this dataset (Supplementary Figure S1).

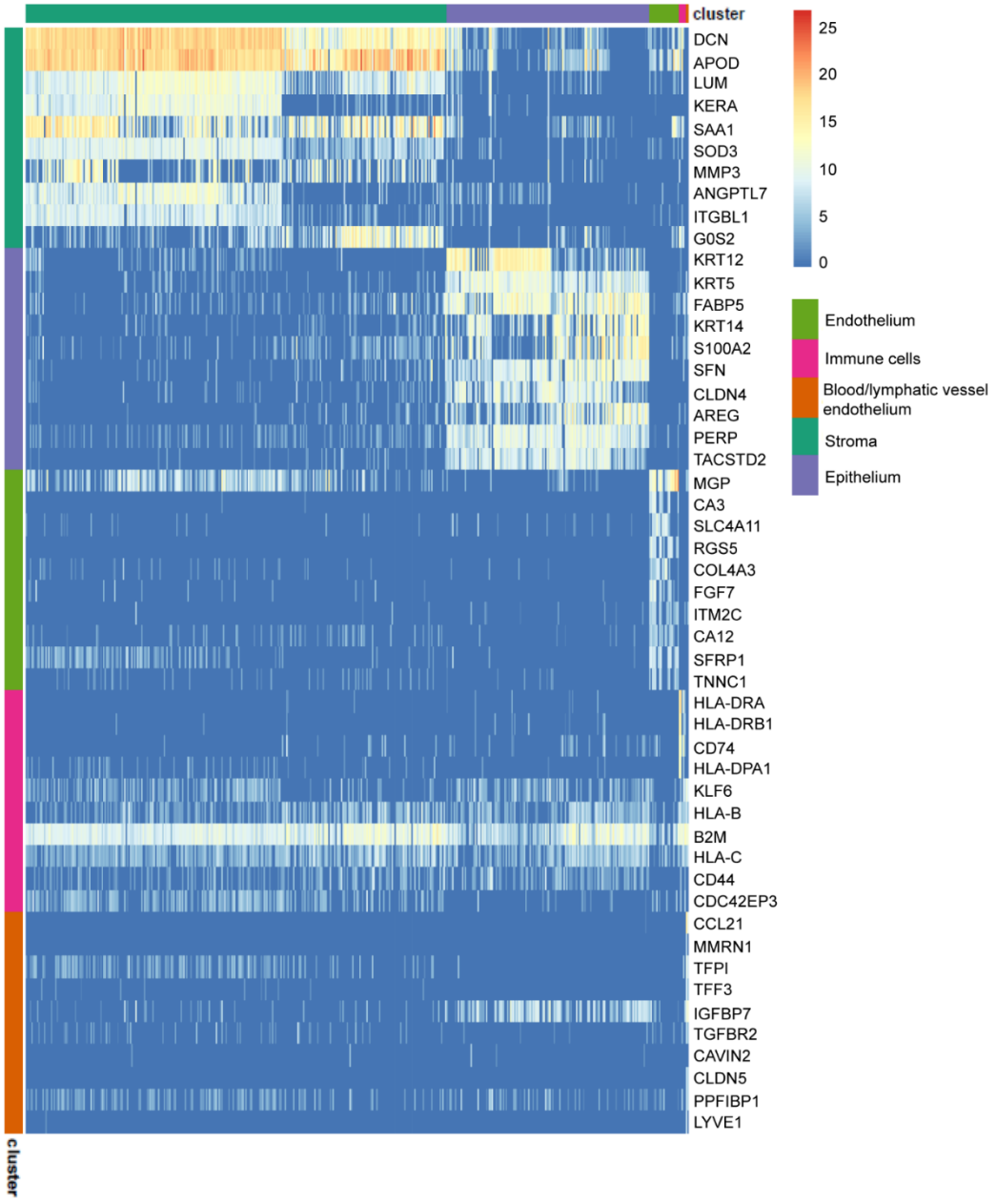

Figure 2. The heatmap of the top 10 differentially expressed genes for each cluster showed distinct transcriptomic profiles for the five major cell clusters and allowed cell cluster identification.

Cluster E5 presented high expression of *GJB6* and *ITGB4* associated with basal epithelium[18] and *KRT12*, and *KRT3* associated with terminally differentiated corneal epithelium[27–29], along with a reduced expression of *KRT14* compared to clusters E6, E8, and E0, and no expression of *KRT15*, suggesting these cells were corneal epithelial basal cells originating from the limbus (Figure 3b and Supplementary Figure S1). Cluster E1 was identified as post-mitotic and terminally differentiated migratory epithelial cells based on the expression of genes associated with cell migration such as *RHOV*[30] and tight junction formation and obliteration *CLDN7*[31] together with a high expression of corneal epithelial cell markers *KRT12*, *KRT3*, and *KRT5*. This cluster retained a low expression level of *KRT14*, implying their limbal origin (Figure 3b and Supplementary Figure S1).

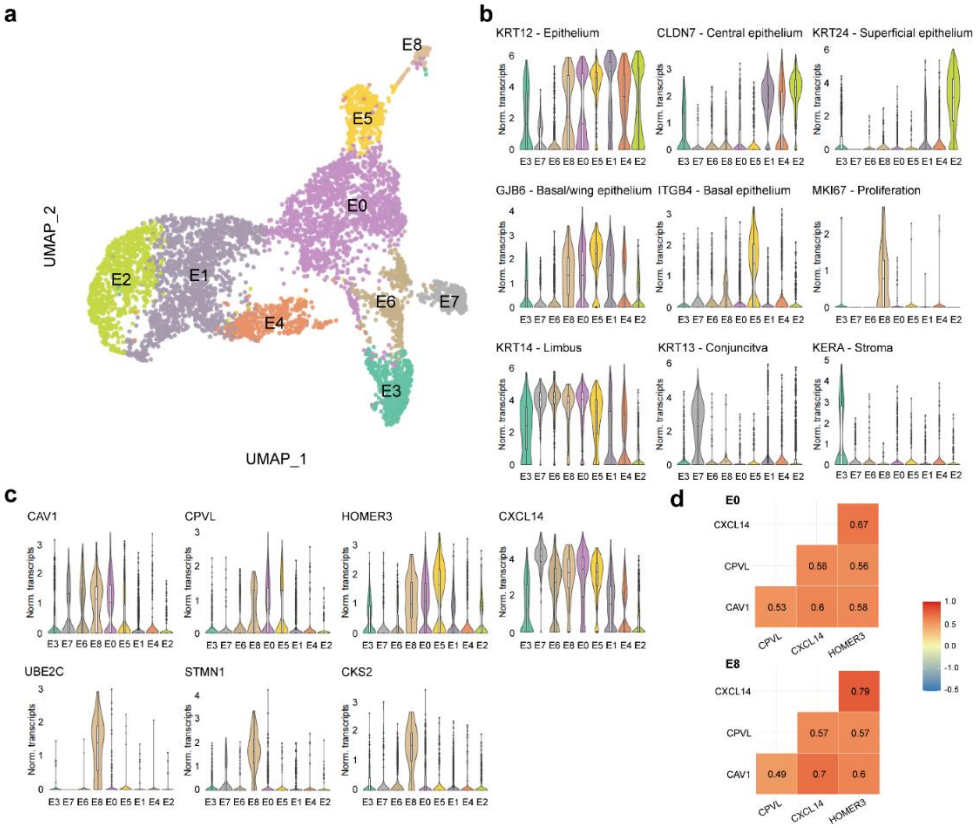

(Figure 3 - legend on next page)

Cluster E4 was composed of cells with a high expression of *KRT12*, *KRT3*, and *KLF5* suggesting this cluster was terminally differentiated cells from the central corneal epithelium (Figure 3b and Supplementary Figure S1). The cells forming cluster E2 presented a high expression of *KRT12*, *KRT24*, and *CXCL17* associated with wing/superficial central epithelium (Figure 3b and Supplementary Figure S1).

scRNAseq reveals novel specific markers for the corneal limbal stem cell niche and transit-amplifying cells

Differential gene expression analysis of the basal corneal limbal epithelial cells (cluster E0), and the transit-amplifying cells (cluster E8), showed that genes encoding for caveolin-1 (*CAV1*), probable serine carboxypeptidase (*CPVL*), homer scaffolding protein 3 (*HOMER3*), and C-X-C motif chemokine 14 (*CXCL14*) were highly expressed in both clusters (Figure 3c), suggesting they could be markers of the human limbal stem cell niche. Moreover, the expression of the markers highly correlated in clusters E0 and E8 (Figure 3d), again suggesting their identity of corneal epithelial cells located in the limbal stem cell niche. Interestingly, a cluster of basal corneal epithelial cells (cluster E5) retained some expression of the identified markers, in line with the limbal origin annotated for this cluster.

Figure 3. A major cluster of 5,964 corneal epithelial cells was identified with scRNAseq analysis. The UMAP revealed nine different cell subclusters: a cluster of basal limbal epithelial cells (E0), a cluster of migratory epithelial cells (E1), a cluster of wing/superficial epithelial cells (E2), a cluster of stromal-epithelial doublets (E3), a cluster of central epithelial cells (E4), a cluster of basal central epithelial cells originating from the limbus (E5), a cluster of wing epithelial cells in the limbus (E6), a cluster of conjunctival cells (E7), and a cluster of highly proliferative transit-amplifying cell (E8) (a). Violin plots show marker genes for corneal epithelium (KRT12), central (*CLDN7*), superficial (*KRT24*), suprabasal (*GJB6*), basal (*ITGB4*), and limbal (*KRT14*) corneal epithelium, as well as proliferation (*MKI67*), conjunctival (*KRT13*) and stromal (*KERA*) markers, for the identification of cell subclusters (b). Differential gene expression identified novel epithelial limbal niche–specific markers and proliferative epithelial cell–specific markers, and are visualized as violin plots (c). Correlation analysis confirmed the co-expression of limbal niche–specific markers in peripheral/limbal epithelial cell populations (d).

To confirm these findings, expression of the markers in the corneal epithelial limbus and central cornea was assessed by immunofluorescence (Figure 4 and Supplementary Figure S3). Caveolin-1 and CXCL14 were expressed in the limbus of the cornea, whereas caveolin-1 was minimally expressed and CXCL14 absent in the central cornea (Figure 4 and Supplementary Figure S3). Interestingly, CXCL14 was expressed in the suprabsal/superficial limbus and not in the limbal stem cell niche. Central basal corneal epithelial cells retained minimal expression of both ΔNp63 and caveolin-1 (Figure 4 and Supplementary Figure S3), suggesting their limbal origin. In contrast, HOMER3 and CPVL were expressed both in the limbus and in the central cornea, where central basal epithelial cells appeared to have higher expression (Figure 4 and Supplementary Figure S3). Caveolin-1 expression was further validated on human primary cultured corneal limbal epithelial cells, where it was expressed in ΔNp63-positive limbal epithelial stem cells (Supplementary Figure S4).

Differential gene expression analysis on the transit-amplifying cells (cluster E8) revealed that the expression of *CKS2*, *STMN1*, and *UBE2C* was exclusive to this cluster. Expression of cyclin-dependent kinase 2, stathmin-1, and ubiquitin conjugating enzyme E2 C, was exclusive to the limbus and absent in the central cornea (Figure 4, Supplementary Figure S3, and Supplementary Figure S5). Cyclin-dependent kinase 2 was further validated on human primary cultured corneal limbal epithelial cells, where it was expressed in in p63α-positive limbal epithelial stem cells (Supplementary Figure S6).

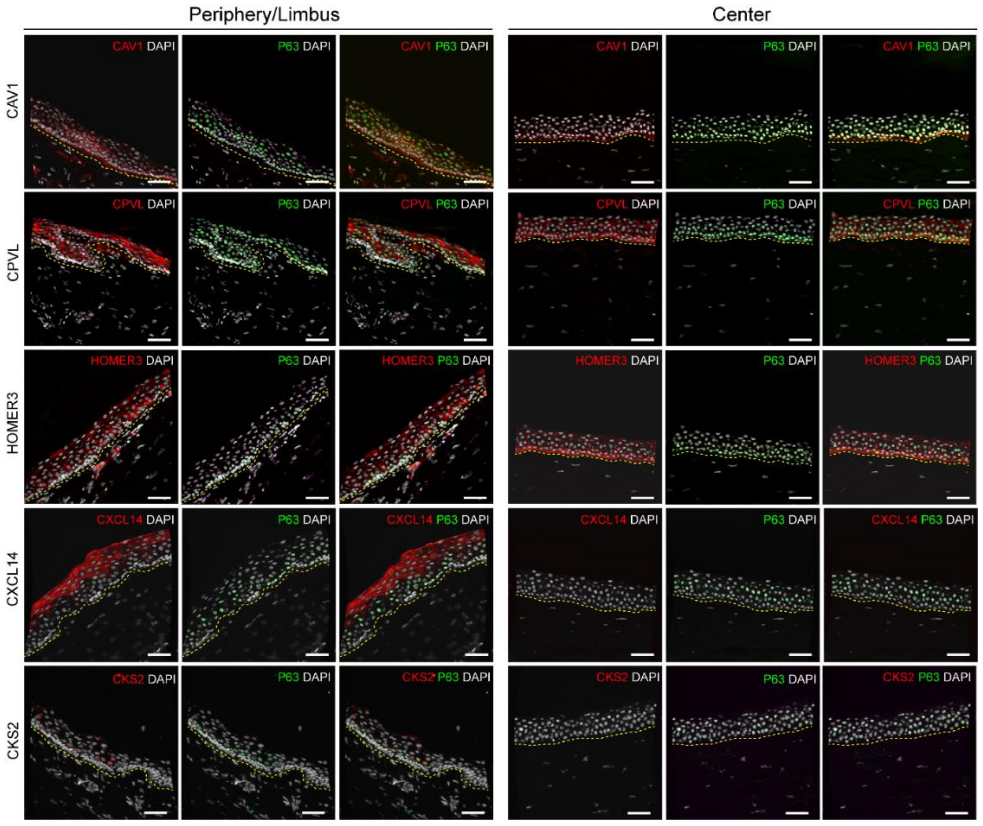

Figure 4. Immunofluorescence of caveolin-1 (*CAV1*), CXCL14 and CKS2 (red) on human corneal tissue cryosections confirmed differential protein expression in the limbus/periphery, and absence (CKS2, and CXCL14) or minimal expression (caveolin-1) in the central cornea. Basal corneal epithelial cells retained minimal expression of both ΔNp63 and caveolin-1, suggesting their limbal origin. HOMER3 and CPVL were expressed in the limbus, but also in the central cornea, where central basal epithelial cells appeared to have higher expression. P63 (ΔNp63 or p63α) was used as a corneal epithelial limbal cell marker (green). Cell nuclei were stained with DAPI (white). The yellow dashed line indicates the boundary between epithelium (above) and stroma (below). Scale bars represent 50 μm.

Four cell clusters were identified within the corneal stroma

A major cluster of 12,344 corneal stromal cells was identified, and further analysis revealed four different subclusters of corneal stromal cells (S0-S3, Figure 5a). High expression of stromal keratocyte markers LUM, *KERA*, or *ALDH3A1*[5,7,8] suggested that clusters S0, S1 and S2 were stromal keratocytes (Figure 5b). Cluster S2 showed

increased expression of extracellular matrix proteins such as *COL12A1*, *COL6A2*, *COL6A1*, and *LAMB2* suggesting these were activated keratocytes that played a crucial role in maintaining the corneal stromal extracellular matrix (Figure 5b and Supplementary Figure S7). Cluster S3 showed a decreased expression of keratocyte markers *LUM*, *KERA*, and *ALDH3A1* and increased expression of the fibroblastic marker *CD44*[32–34] compared to clusters S0, S1 and S2 (Figure 5b and Supplementary Figure S7). The myofibroblast-specific marker, α-smooth muscle actin (*ACTA2*),[35,36] was not detected in cluster S3 (Supplementary Figure S7), suggesting it is composed of keratocytes that are in transition to stromal myofibroblasts.

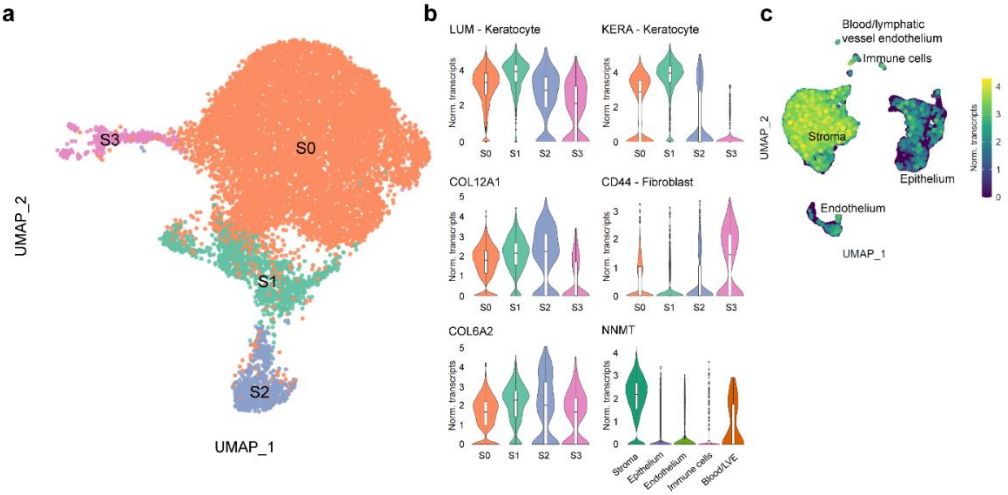

Figure 5. A major cluster of 12,344 corneal stromal cells was identified with scRNAseq analysis. The UMAP revealed four different cell subclusters, three keratocyte clusters (S0-S2), with one having a high extracellular matrix protein secretion profile (S2) and a cluster of keratocytes transitioning to stromal myofibroblasts (S3) (a). Violin plots show marker genes for stromal keratocytes (*KERA* and *LUM*), stromal fibroblasts (*CD44*), collagen (*COL6A2* and *COL12A1*) secretion for the identification of cell subclusters, and *NNMT* expression exclusive to the stroma within the cornea (b). Single cell expression level UMAP of NNMT further confirms differential expression of *NNMT* in the stromal cluster (c).

Finally, differential gene expression analysis of the major stromal cluster compared to the clusters associated with the corneal epithelial and endothelial layers identified that the expression of nicotinamide N-methyltransferase (*NNMT*) was exclusive to the corneal stromal cluster, suggesting that this gene could be used as a novel corneal stromal marker (Figure 5b and c).

Two cell clusters were identified within the corneal endothelium

A major cluster of 842 corneal endothelial cells was identified and further analysis revealed two different subclusters of corneal endothelial cells (En0-1, Figure 6a). Both clusters showed expression of corneal endothelial cell markers CD166 (*ALCAM*) and sPrdx1 (*PRDX1*)[37,38] and functional markers Na^+/K^+ ATPase (*ATP1A1*)[6] and sodium bicarbonate transporter-like protein 11 (*SLC4A11*)[6] confirming the corneal endothelial phenotype (Figure 6b and Supplementary Figure S7). Differential expression analysis revealed that cluster En0 possessed a lower expression of tight junction protein zona occludens-1 (*TJP1*)[6] and focal adhesion regulator microtubule-actin cross-linking factor-1 (*MACF1*)[39] compared to cluster En1 (Figure 6b), suggesting cells in cluster En0 could preferentially migrate upon corneal endothelial damage to contribute to tissue repair. Furthermore, cluster En1 possessed a higher expression of *COL4A3* (Figure 6b) suggesting these cells could play an important role on Descemet's membrane homeostasis. Interestingly, both clusters retained expression of *PITX2*, a periocular mesenchyme marker associated with progenitor endothelial cells.[40,41] No endothelial fibroblasts were identified, evidenced by the absence of *ACTA2* and *CD44* (Supplementary Figure S8).

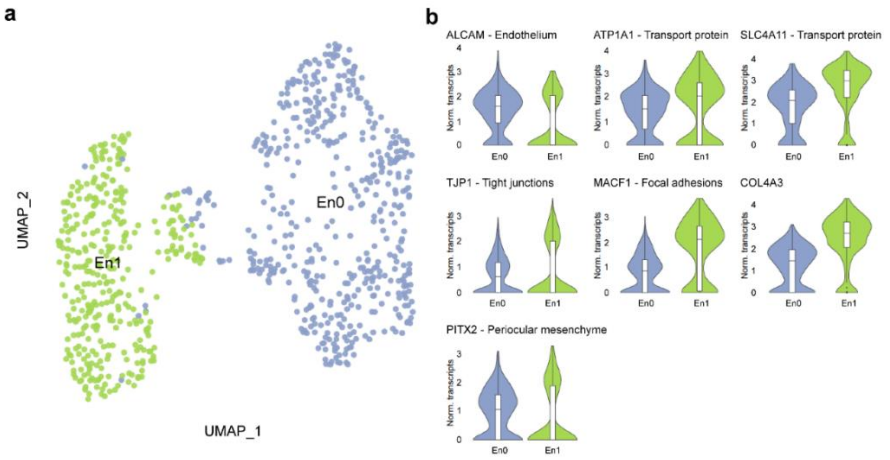

Figure 6. A major cluster of 842 corneal endothelial cells was identified with scRNAseq analysis. The UMAP revealed two different endothelial cell subclusters, a cell cluster with high collagen synthesis (En2) and another cell cluster with low tight junction and focal adhesion protein expression (En1) (a). Violin plots show marker genes for corneal endothelium (*ALCAM*), ion and bicarbonate transporters (*ATP1A1* and *SLC4A11* respectively), tight junction proteins (*TJP1*), focal adhesion protein regulator (*MACF1*), collagen secretion (*COL4A3*) and periocular mesenchyme (*PITX2*) (b).

Discussion

Gaining transcriptomic information at the single cell level of human corneal cells enables a greater understanding of this heterogeneous tissue. In this study, we have performed a scRNAseq analysis of the healthy cornea to create a comprehensive cell atlas of the human cornea (Figure 7). Moreover, scRNAseq analysis enabled the identification of novel markers of the limbal epithelial stem cell niche, transit-amplifying cells, and stromal keratocytes. The data generated can serve as a reference cell atlas with a major impact in the further improvement and development of cell replacement therapies or regenerative medicine approaches for treating corneal blindness. This research further complements scRNAseq analysis of the developing human cornea[42] and of the human corneal limbus[43,44].

The corneal epithelium appeared to be the most heterogeneous corneal layer with 9 identified cell clusters. The transcriptomic signature of epithelial cells from the basal, wing and superficial layers of both central and limbus/peripheral cornea were identified. A population of conjunctival epithelial cells was detected (cluster E7; Figure 3), likely representing contamination from the dissection process. Moreover, a cluster of highly proliferative transit-amplifying cells (cluster E8) was detected. No quiescent limbal epithelial stem cells expressing *ABCB5, TCF4, CD200* and *ABCG2* were identified (Supplementary Figure S1). This result is in line with the study of Li et al., where out of 16,360 cells specifically isolated from the adult corneal limbus region, only 69 cells were identified as limbal epithelial stem cells, corresponding with 0.4% of the total sequenced cells.[43] Because our data present sequencing information of 5,964 corneal epithelial cells, it is possible that there might not have been enough sequencing depth to detect such a rare population. Moreover, and in line with these results, in a recent study by Dou et al., expression of ABCB5 and ABCG2 was also minimally detected 47,627 cells isolated from the human corneal limbus, and was also associated to limitations in the sequencing depth.[44] These are opposing findings to the results presented by Collin et al. 2021,

where a major cluster of 893 (4%) limbal progenitor/stem cells was detected in a pool of 21,343 sequenced cells isolated from corneoscleral buttons.[42]

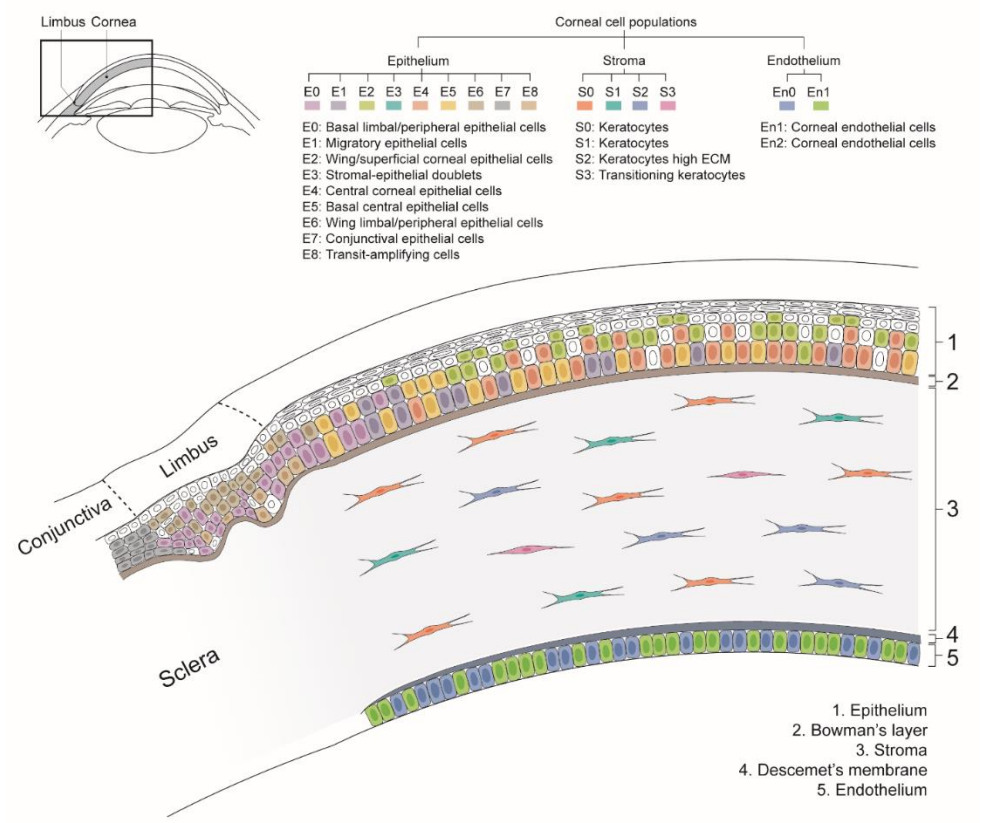

Figure 7. scRNAseq data analysis identified nine epithelial, four stromal and two endothelial corneal cell clusters. This figure presents a summary of the cell type and location of each cluster in the healthy human cornea, generating a comprehensive cell census of the healthy human cornea. In the epithelium: a cluster of basal limbal epithelial cells (E0), a cluster of migratory epithelial cells (E1), a cluster of wing/superficial epithelial cells (E2), a cluster of stromal-epithelial doublets (E3), a cluster of central epithelial cells (E4), a cluster of basal central epithelial cells originating from the limbus (E5), a cluster of wing epithelial cells in the limbus (E6), a cluster of conjunctival cells (E7), and a cluster of highly proliferative transit-amplifying cell (E8). In the stroma: three keratocyte clusters (S0-S2), with one having a high extracellular matrix protein secretion profile (S2) and a cluster of keratocytes transitioning to stromal myofibroblasts (S3). In the endothelium: a cell cluster with high collagen synthesis (En2), and a cell cluster with low tight junction and focal adhesion protein expression (En1).

Differential analysis identified the expression of *CAV1*, *HOMER3*, *CXCL14*, and *CPVL* to be exclusive to cell clusters comprising the corneal epithelial stem cell niche (Figure 3). In line with our findings, Collin et al. recently reported the exclusivity of *CXCL14* and *CPVL* to the corneal epithelial stem cell niche.[42] Immunofluorescence analysis confirmed the expression of caveolin-1 and CXCL14 in the limbus, and their absence in the central cornea (Figure 4). Nevertheless, CXCL14 was expressed in the superficial layers of the limbus but not the limbal stem cell niche. HOMER3 and CPVL were both expressed in the limbus, and in the central cornea, where central basal epithelial cells appeared to retain higher expression of these markers (Figure 4). We further validated the finding of caveolin-1 with immunofluorescence in primary cultured limbal stem cells (Supplementary Figure S4). These results suggest that caveolin-1 could be used for the identification of epithelial limbal stem cells, with the advantage that it is a cell membrane marker, whereas p63 is expressed in the nucleus. This could open the door to isolating and enriching these cells for regenerative therapies.

Furthermore, our study also revealed novel makers specific to transit-amplifying cells, namely *CKS2*, *STMN1*, and *UBE2C*. We further validated these findings with immunofluorescence, and confirmed their expression in the limbus and periphery of human corneas. Furthermore, expression of CKS2 was also assessed in primary cultured limbal stem cells (Supplementary Figure S6), suggesting this is a suitable marker for identifying highly proliferative transit-amplifying cells. Interestingly, primary limbal cells expressing a lower level amount of ΔNp63 and p63α, based on fluorescence intensity, also showed a reduced expression of caveolin-1 and cyclin-dependent kinase 2 respectively (Supplementary Figures S4 and S6). Interestingly, two recent studies also reported STMN1 and UBE2C to be specific markers of limbal transit amplifying cells.[43,45] Finally, in a 2019 single cell transcriptome study, Kaplan et al. hypothesized that the stemness of mouse limbal epithelial stem cells could be regulated through autophagy.[46] The identification of caveolin-1, a facilitator of caveolin-mediated endocytosis, as a marker of the human corneal limbus in our study

could support this hypothesis. Nevertheless, further research is required to confirm this theory.

It is important to highlight that as previously reported, the corneal epithelium sheds superficial layers when corneas are preserved in media[47] and it is very likely that this cell atlas does not fully portray the most superficial layer of corneal epithelial cells. Two types of cornea preservation conditions, namely in Optisol-GS medium and organ culture medium, were used for this research, in line with clinical practice in the United States of America and Europe, respectively. No major differences in cell clustering were found between preservation conditions.

Three clusters of the corneal stroma were identified as corneal keratocytes (clusters S0, S1 and S2; Figure 5). Cluster S2 was identified as cells with a key role in extracellular protein secretion to maintain the homeostasis of the stroma. Furthermore, we identified a cluster (S3) of keratocytes transitioning to myofibroblasts, though a fully differentiated myofibroblast phenotype expressing alpha smooth muscle actin was not identified. Interestingly, our analysis did not identify a population of corneal stromal stem cells expressing *ABCB5* and *ABCG2*, as previously identified by Funderburgh and colleagues. [48–50] Our hypothesis is that the expression of these genes is induced by the primary expansion of corneal keratocytes and is not found in the cornea.[48–50] Finally, differential gene expression analysis identified that the expression of *NNMT* was exclusive to the corneal stroma, suggesting this could be used as a novel marker to identify corneal stromal cells. Interestingly, the study by Li et al. reported differential expression of NNMT in a cluster of 69 quiescent limbal stem cells expressing *ABCB5* and *ABCG2*.[43] As previously mentioned, perhaps due to limitations in sequencing depth, we did not find a population of limbal stem cells expressing *ABCB5* and *ABCG2*, and therefore unable to confirm these results. Since Li and colleagues did not include a population of corneal stromal cells in their differential analysis, it also explains why *NNMT* was not detected as a stromal marker in their study. It is possible that *NNMT* is expressed

specifically in both ABCB5^{+}/ABCG2^{+} quiescent limbal stem cells and in corneal stromal cells.

Two cell clusters were identified forming the corneal endothelium (Figure 6). Both clusters showed high expression of corneal endothelial markers such as CD166 (*ALCAM*), sPrdx1 (*PRDX1*), ZO-1 (*TJP1*), or *SLC4A11*, confirming the endothelial phenotype. Nevertheless, expression of *CD200*, reported as corneal endothelial cell marker in a previous study,[51] was not detected in our dataset, suggesting it might not be a specific marker for corneal endothelial cells. Despite sharing great similarity, one of the clusters (En1) expressed more extra cellular matrix proteins, suggesting that these cells could play a crucial role on maintaining the Descemet's membrane. Cell cluster En0 showed lower expression of tight junction proteins and focal adhesions, suggesting these cells could preferentially migrate upon corneal endothelial damage and contribute to tissue repair via migration or cytosolic expansion. Interestingly, our study did not detect a population of precursor endothelial cells, as discussed in previous studies.[52,53] Nevertheless, both corneal endothelial cell clusters detected retained expression of *PITX2*, a marker associated with neural crest-derived corneal endothelial cell precursors.[40,41] These data suggests that it is highly possible that a progenitor-like state is not exclusive to the peripheral corneal endothelium but to cells across the endothelium.

Interestingly, no corneal endothelial fibroblasts were detected in this study, indicated by the lack of expression of fibroblastic markers α-smooth muscle actin (*ACTA2*) and *CD44* (Supplementary Figure S8), which is in contrast to a previous report.[42] It is likely that the bulk enzymatic corneoscleral tissue desegregation performed by Collin et al., affected the susceptible corneal endothelial cells, causing endothelial cells transcriptomic bias portrayed in scRNAseq dataset, as showed in other studies.[54,55] We performed a more gentle approach to obtain single endothelial cells for sequencing, first dissecting the tissue and mechanically stripping the endothelium

from the cornea, and then treating the endothelial cells with a shorter enzymatic digestion.

Overall, this study provides significant information to help understand the heterogeneity of the healthy human cornea, as well as understanding the gene expression stratification across cells present in the same corneal layer, while providing novel markers to identify specific cell types. Moreover, this transcriptomic cell atlas offers a baseline for future studies with the aim of regenerating corneal tissue or further developing corneal cell replacement therapies.

Funding

This research was funded by Chemelot InSciTe under the EyeSciTe consortium and ZonMw Enabling Technology Hotels grant 435005012.

Acknowledgements

The authors thank Annika Jeschke and Timo Rademakers (Maastricht University) for the assistance in the immunofluorescence experiments and the sample cryosectioning. The authors thank Single Cell Discoveries (Utrecht, the Netherlands) for the single cell sequencing services provided. The authors thank ETB-BISLIFE: Multi Tissue Center and Saving Sight Kansas City for providing research-grade human corneas.

Data availability

The scRNAseq dataset presented in this study has been uploaded to the Gene Expression Omnibus (GEO accession: GSE186433) and can be accessed using this link: https:// www.ncbi.nlm.nih.gov/geo/query/acc.cgi?acc=GSE186433. All the datasets presented in this study are available in DataVerseNL and can be accessed using this link: https://doi.org/10.34894/X7ZSDZ.

References

1. Price, M. O., Mehta, J. S., Jurkunas, U. V. & Price, F. W. Corneal endothelial dysfunction: Evolving understanding and treatment options. *Prog. Retin. Eye Res.* **82**, 100904 (2021).

2. Pellegrini, G., Rama, P., Di Rocco, A., Panaras, A. & De Luca, M. Concise review: Hurdles in a successful example of limbal stem cell-based regenerative medicine. *Stem Cells* **32**, 26–34 (2014).

3. Català, P. *et al.* Approaches for corneal endothelium regenerative medicine. *Prog. Retin. Eye Res.* In Press (2021).

4. Ramos, T., Scott, D. & Ahmad, S. An Update on Ocular Surface Epithelial Stem Cells: Cornea and Conjunctiva. *Stem Cells Int.* **2015**, 601731 (2015).

5. Foster, J. W., Gouveia, R. M. & Connon, C. J. Low-glucose enhances keratocyte-characteristic phenotype from corneal stromal cells in serum-free conditions. *Sci. Rep.* **5**, 10839 (2015).

6. Van den Bogerd, B. *et al.* Corneal endothelial cells over the past decade: Are we missing the mark(er)? *Transl. Vis. Sci. Technol.* **8**, (2019).

7. Fernández-Pérez, J. & Ahearne, M. Influence of Biochemical Cues in Human Corneal Stromal Cell Phenotype. *Curr. Eye Res.* **44**, 135–146 (2019).

8. Pei, Y., Reins, R. Y. & McDermott, A. M. Aldehyde dehydrogenase (ALDH) 3A1 expression by the human keratocyte and its repair phenotypes. *Exp. Eye Res.* **83**, 1063–1073 (2006).

9. Hayashi, R. *et al.* Co-ordinated ocular development from human iPS cells and recovery of corneal function. *Nature* **531**, 376–380 (2016).

10. Ouyang, H. *et al.* WNT7A and PAX6 define corneal epithelium homeostasis and pathogenesis. *Nature* **511**, 358–361 (2014).

11. Van Velthoven, A. J. H. *et al.* Increased Cell Survival of Human Primary Conjunctival Stem Cells in Dimethyl Sulfoxide-Based Cryopreservation Media. *Biopreserv. Biobank.* **19**, 67–72 (2021).

12. Ramirez-Miranda, A., Nakatsu, M. N., Zarei-Ghanavati, S., Nguyen, C. V. & Deng, S. X. Keratin 13 is a more specific marker of conjunctival epithelium than keratin 19. *Mol. Vis.* **17**, 1652–1661 (2011).

13. Eghtedari, Y. *et al.* Keratin 14 expression in epithelial progenitor cells of the developing human cornea. *Stem Cells Dev.* **25**, 699–711 (2016).

14. Cheng, C. C., Wang, D. Y., Kao, M. H. & Chen, J. K. The growth-promoting effect of KGF on limbal epithelial cells is mediated by upregulation of ΔNp63α through the p38 pathway. *J. Cell Sci.* **122**, 4473–4480 (2009).

15. Nasser, W. *et al.* Corneal-Committed Cells Restore the Stem Cell Pool and Tissue Boundary following Injury. *Cell Rep.* **22**, 323–331 (2018).

16. Yoshida, S. *et al.* Cytokeratin 15 can be used to identify the limbal phenotype in normal and diseased ocular surfaces. *Investig. Ophthalmol. Vis. Sci.* **47**, 4780–4786 (2006).

17. Li, J. *et al.* S100A expression in normal corneal-limbal epithelial cells and ocular surface squamous cell carcinoma tissue. *Mol. Vis.* **17**, 2263–2271 (2011).

18. Shurman, D. L., Glazewski, L., Gumpert, A., Zieske, J. D. & Richard, G. In vivo and in vitro expression of connexins in the human corneal epithelium. *Investig. Ophthalmol. Vis. Sci.* **46**, 1957–1965 (2005).

19. Stepp, M. A. Corneal integrins and their functions. *Exp. Eye Res.* **83**, 3–15 (2006).

20. Schlötzer-Schrehardt, U. & Kruse, F. E. Identification and characterization of limbal stem cells. *Exp. Eye Res.* **81**, 247–264 (2005).

21. Sun, X. & Kaufman, P. D. Ki-67: more than a proliferation marker. *Chromosoma* **127**, 175–186 (2018).

22. Wang, C., Zheng, X., Shen, C. & Shi, Y. MicroRNA-203 suppresses cell proliferation and migration by targeting BIRC5 and LASP1 in human triple-negative breast cancer cells. *J. Exp. Clin. Cancer Res.* **31**, 1–8 (2012).

23. Andäng, M. *et al.* Histone H2AX-dependent GABAA receptor regulation of stem cell proliferation. *Nature* **451**, 460–464 (2008).

24. Bojic, S. *et al.* CD200 Expression Marks a Population of Quiescent Limbal Epithelial Stem Cells with Holoclone Forming Ability. *Stem Cells* **36**, 1723–1735 (2018).

25. Ksander, B. R. *et al.* ABCB5 is a limbal stem cell gene required for corneal development and repair. *Nature* **511**, 353–357 (2014).

26. de Paiva, C. S., Chen, Z., Corrales, R. M., Pflugfelder, S. C. & Li, D. O riginal A rticle ABCG2 Transporter Identifies a Population of Clonogenic. *Stem Cells* **23**, 63–73 (2005).

27. Bonnet, C. *et al.* Human limbal epithelial stem cell regulation, bioengineering and function. *Prog. Retin. Eye Res.* (2021). doi:10.1016/j.preteyeres.2021.100956

28. He, J. *et al.* Tissue engineered corneal epithelium derived from clinical-grade human embryonic stem cells. *Ocul. Surf.* **18**, 672–680 (2020).

29. Kitazawa, K. *et al.* PAX6 regulates human corneal epithelium cell identity. *Exp. Eye Res.* **154**, 30–38 (2017).

30. Hodge, R. G. & Ridley, A. J. Regulation and functions of RhoU and RhoV. *Small GTPases* **11**, 8–15 (2020).

31. Yoshida, Y., Ban, Y. & Kinoshita, S. Tight junction transmembrane protein claudin subtype expression and distribution in human corneal and conjunctival epithelium. *Investig. Ophthalmol. Vis. Sci.* **50**, 2103–2108 (2009).

32. Li, X. *et al.* CD44 is involved in SMAD signaling by TGFb in keratocytes. *Investig. Ophthalmol. Vis. Sci.* **50**, 4539 (2009).

33. Choong, P. F., Mok, P. L., Cheong, S. K. & Then, K. Y. Mesenchymal stromal cell-like characteristics of corneal keratocytes. *Cytotherapy* **9**, 252–258 (2007).

34. Acharya, P. S. *et al.* Fibroblast migration is mediated by CD44-dependent TGFβ activation. *J. Cell Sci.* **121**, 1393–1402 (2008).

35. Jester, J. V. *et al.* Myofibroblast differentiation of normal human keratocytes and hTERT, extended-life human corneal fibroblasts. *Investig. Ophthalmol. Vis. Sci.* **44**, 1850–1858 (2003).

36. Wilson, S. E. Corneal myofibroblasts and fibrosis. *Exp. Eye Res.* **201**, 108272 (2020).

37. Ding, V., Chin, A., Peh, A., Mehta, J. S. & Choo, A. Generation of novel monoclonal antibodies for the enrichment and characterization of human corneal endothelial cells (hCENC) necessary for the treatment of corneal endothelial blindness. *MAbs* **6**, 1439–1452 (2014).

38. Okumura, N. *et al.* Cell surface markers of functional phenotypic corneal endothelial cells. *Investig. Ophthalmol. Vis. Sci.* **55**, 7610–7618 (2014).

39. Ning, W. *et al.* The CAMSAP3-ACF7 Complex Couples Noncentrosomal Microtubules with Actin Filaments to Coordinate Their Dynamics. *Dev. Cell* **39**, 61–74 (2016).

40. Chen, L. *et al.* Ap-2β is a downstream effector of PITX2 required to specify endothelium and establish angiogenic privilege during corneal development. *Investig. Ophthalmol. Vis. Sci.* **57**, 1072–1081 (2016).

41. Kumar, S. & Duester, G. Retinoic acid signaling in perioptic mesenchyme represses Wnt signaling via induction of Pitx2 and Dkk2. *Dev. Biol.* **340**, 67–74 (2010).

42. Collin, J. *et al.* A single cell atlas of human cornea that defines its development, limbal progenitor cells and their interactions with the immune cells. *Ocul. Surf.* **In Press**, (2021).

43. Li, D. Q. *et al.* Single-cell transcriptomics identifies limbal stem cell population and cell types mapping its differentiation trajectory in limbal basal epithelium of human cornea. *Ocul. Surf.* **20**, 20–32 (2021).

44. Dou, S. *et al.* Molecular identity of human limbal heterogeneity involved in corneal homeostasis and privilege: Single-cell RNA sequencing of human limbus. *Ocul. Surf.* **21**, 206–220 (2021).

45. Li, J.-M. *et al.* Single-Cell Transcriptomics Identifies a Unique Entity and Signature Markers of Transit-Amplifying Cells in Human Corneal Limbus. *Investig. Opthalmology Vis. Sci.* **62**, 36 (2021).

46. Kaplan, N. *et al.* Single-cell RNA transcriptome helps define the limbal/ corneal epithelial stem/early transit amplifying cells and how autophagy affects this population. *Investig. Ophthalmol. Vis. Sci.* **60**, 3570–3583 (2019).

47. Guindolet, D. *et al.* Epithelial regeneration in human corneas preserved in an active storage machine. *Transl. Vis. Sci. Technol.* **10**, 31 (2021).

48. Du, Y., Funderburgh, M. L., Mann, M. M., SundarRaj, N. & Funderburgh, J. L. Multipotent Stem Cells in Human Corneal Stroma. *Stem Cells* **23**, 1266–1275 (2005).

49. Du, Y. *et al.* Secretion and organization of a cornea-like tissue in vitro by stem cells from human corneal stroma. *Investig. Ophthalmol. Vis. Sci.* **48**, 5038–5045 (2007).

50. Wu, J., Du, Y., Mann, M. M., Funderburgh, J. L. & Wagner, W. R. Corneal stromal stem cells versus corneal fibroblasts in generating structurally appropriate corneal stromal tissue. *Exp. Eye Res.* **120**, 71–81 (2014).

51. Cheong, Y. K. *et al.* Identification of cell surface markers glypican-4 and CD200 that differentiate human corneal endothelium from stromal fibroblasts. *Investig. Ophthalmol. Vis. Sci.* **54**, 4538–4547 (2013).

52. Yam, G. H. *et al.* Characterization of Human Transition Zone Reveals a Putative Progenitor-Enriched Niche of Corneal Endothelium. *Cells* **8**, 1244 (2019).

53. Van den Bogerd, B., Dhubhghaill, S. N., Koppen, C., Tassignon, M. J. & Zakaria, N. A review of the evidence for in vivo corneal endothelial regeneration. *Surv. Ophthalmol.* **63**, 149–165 (2018).

54. Mattei, D. *et al.* Enzymatic dissociation induces transcriptional and proteotype bias in brain cell populations. *Int. J. Mol. Sci.* **21**, 7944 (2020).

55. Denisenko, E. *et al.* Systematic assessment of tissue dissociation and storage biases in single-cell and single-nucleus RNA-seq workflows. *Genome Biol.* **21**, 130 (2020).

56. Stuart, T. *et al.* Comprehensive Integration of Single-Cell Data. *Cell* **177**, 1888–1902 (2019).

57. Germain, P.-L. scDblFinder: scDblFinder. R package version 1.2.0. (2020).

58. Pellegrini, G. *et al.* Long-term restoration of damaged corneal surfaces with autologous cultivated corneal epithelium. *Lancet* **349**, 990–993 (1997).

59. Rama, P. *et al.* Limbal Stem-Cell Therapy and Long-Term Corneal Regeneration. *N. Engl. J. Med.* **363**, 147–155 (2010).

60. Kawamoto, T. & Kawamoto, K. Preparation of thin frozen sections from nonfixed and undecalcified hard tissues using kawamoto's film method. *Methods Mol Biol* **2230**, 259–281 (2021).

Supplementary Information

Supplementary Figure S1

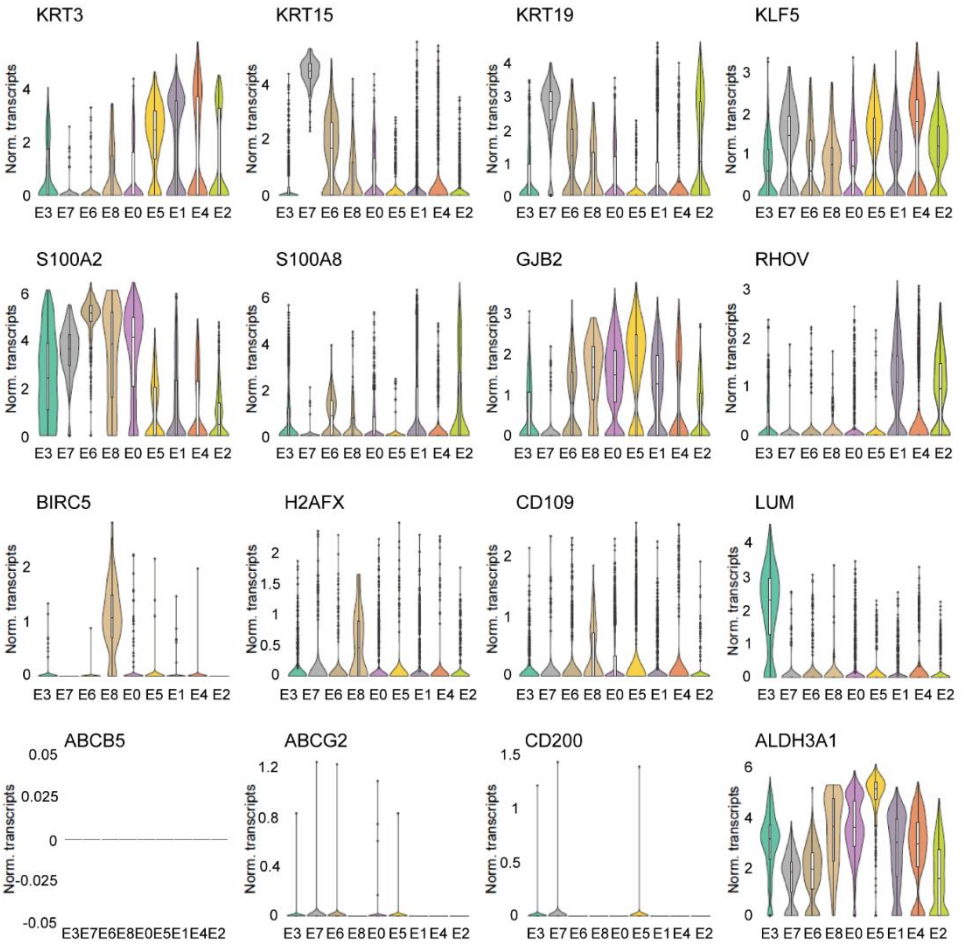

Supplementary Figure S1. Violin plots show additional marker genes for the identification of corneal epithelial clusters.

Supplementary Figure S2

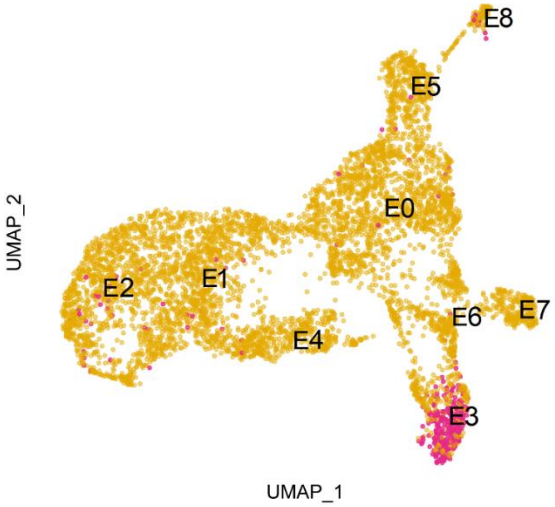

Supplementary Figure S2. Putative doublets were computationally identified using scDblFinder (v1.2.0) and epithelial cell cluster E3 was identified as a cluster of stromal-epithelial doublets.

Supplementary Figure S3

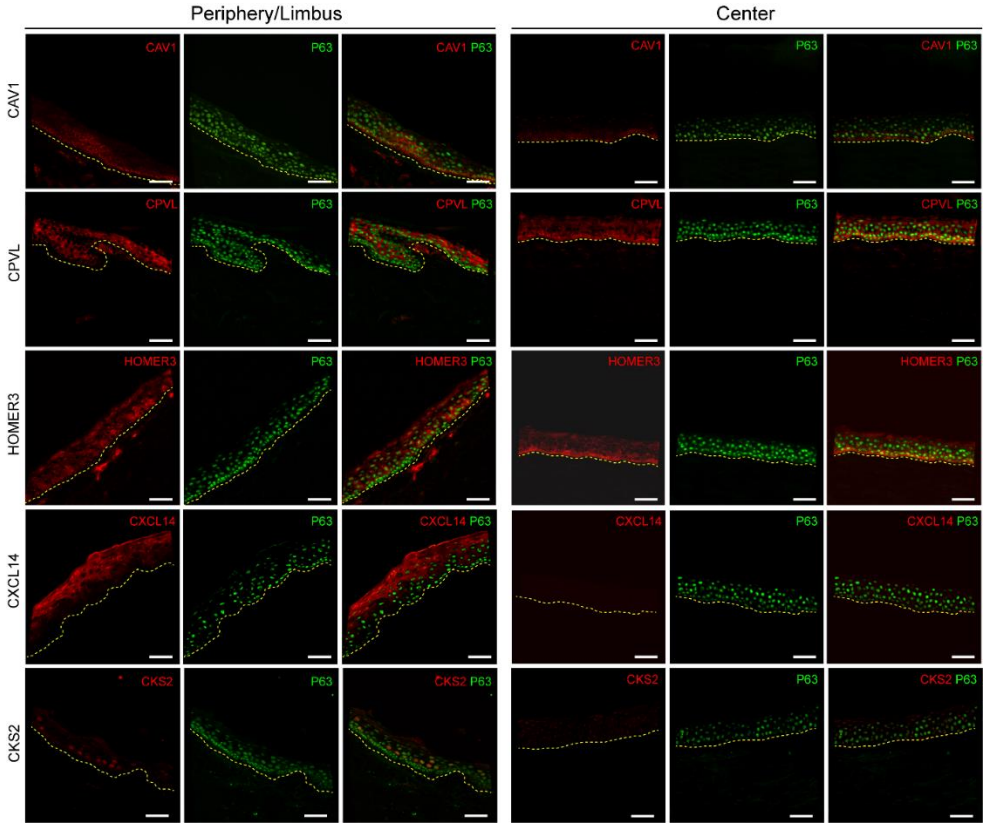

Supplementary Figure S3. Immunofluorescence of caveolin-1 (*CAV1*), CXCL14 and CKS2 (red) on human corneal tissue cryosections confirmed differential protein expression in the limbus/periphery, and absence (CKS2, and CXCL14) or minimal expression (caveolin-1) in the central cornea. Basal corneal epithelial cells retained minimal expression of both ΔNp63 and caveolin-1, suggesting their limbal origin. HOMER3 and CPVL were expressed in the limbus, but also in the central cornea, where central basal epithelial cells appeared to have higher expression. P63 (ΔNp63 or p63α) was used as a corneal epithelial limbal cell marker (green). The yellow dashed line indicates the boundary between epithelium (above) and stroma (below). Scale bars represent 50 μm.

Supplementary Figure S4

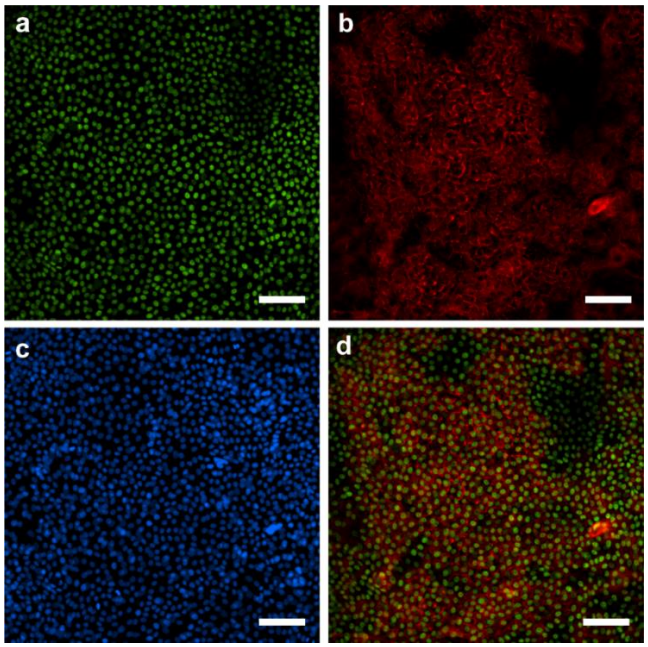

Supplementary Figure S4. Immunofluorescence analysis of caveolin-1 (*CAV1*) expression in primary cultured human corneal limbal epithelial stem cells. Limbal epithelial stem cells expressing ΔNp63 (a, green) also showed expression of caveolin-1 (b, red), as observed in the image overlay (d). Cell nuclei were stained with DAPI (c). These results suggest caveolin-1 could be a selective marker for corneal limbal stem cells. Scale bars represent 100 μm.

Supplementary Figure S5

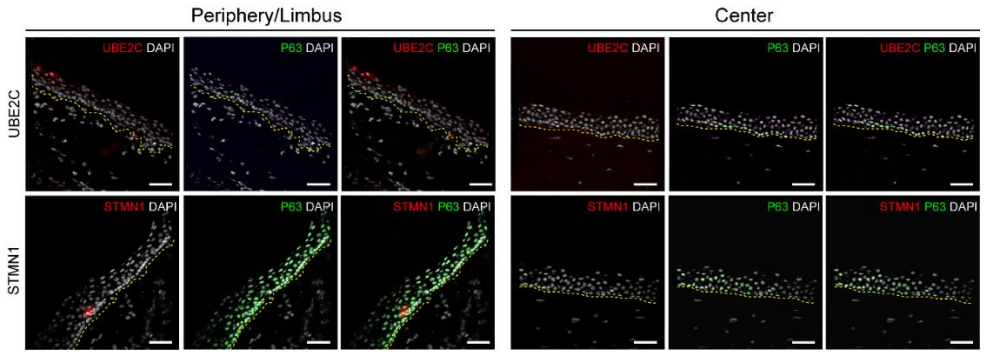

Supplementary Figure S5. Immunofluorescence of UBE2C and stathmin-1 (STMN1) on human corneal tissue cryosections confirmed differential protein expression in the limbus/periphery, and absence in the central cornea. P63 (ΔNp63 or p63α) was used as a corneal epithelial limbal cell marker (green). Cell nuclei were stained with DAPI (white). The yellow dashed line indicates the boundary between epithelium (above) and stroma (below). Scale bars represent 50 μm.

Supplementary Figure S6

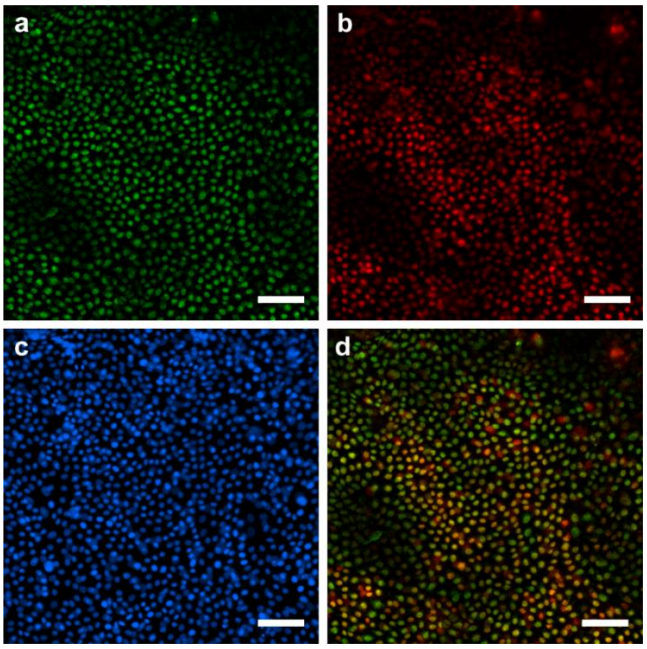

Supplementary Figure S6. Immunofluorescence analysis of cyclin-dependent kinase 2 (*CKS2*) expression in primary cultured human corneal limbal epithelial stem cells. Limbal epithelial stem cells expressing p63α (a, green) also showed expression of *CKS2* (b, red), as observed in the image overlay (d). Cell nuclei were stained with DAPI (c). Scale bars represent 100 μm.

Supplementary Figure S7

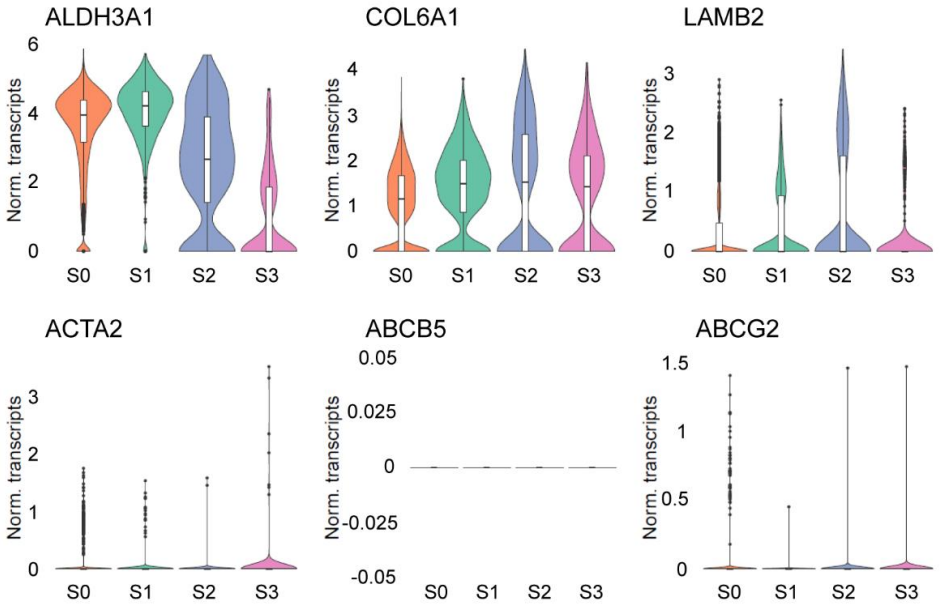

Supplementary Figure S7. Violin plots show additional marker genes for the identification of corneal stromal clusters.

Supplementary Figure S8

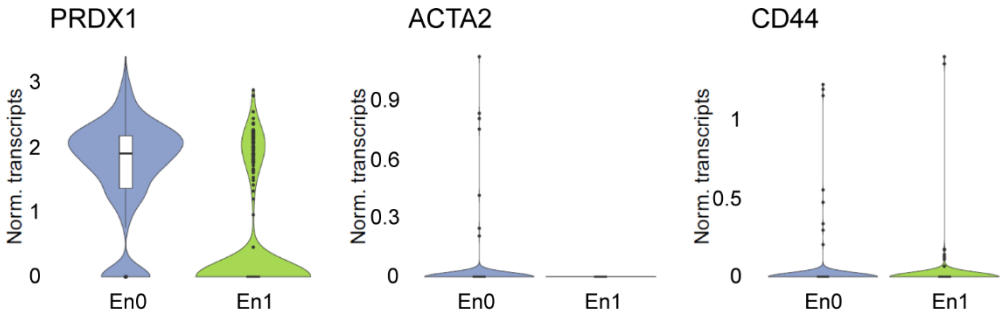

Supplementary Figure S8. Violin plots show additional marker genes for the identification of corneal endothelial clusters.

Supplementary Figure S9

In line with the study by Collin et al. 2021,[1] our scRNAseq study shows differential expression of SARS-CoV-2 entry receptors *ACE2*, *TMPRSS2*, *TMPRSS4*[2-4] in the corneal epithelium, and *NRP1*[5] in both corneal epithelium and stroma. This results are in line with the hypothesis of the cornea as a potential SARS-CoV-2 entry site (Supplementary Figure S7). Finally, the lack of SARS-CoV-2 entry receptors in the corneal endothelium (Supplementary Figure S7), the most often selectively transplanted corneal layer, supports the safety of donor tissue for endothelial keratoplasty.

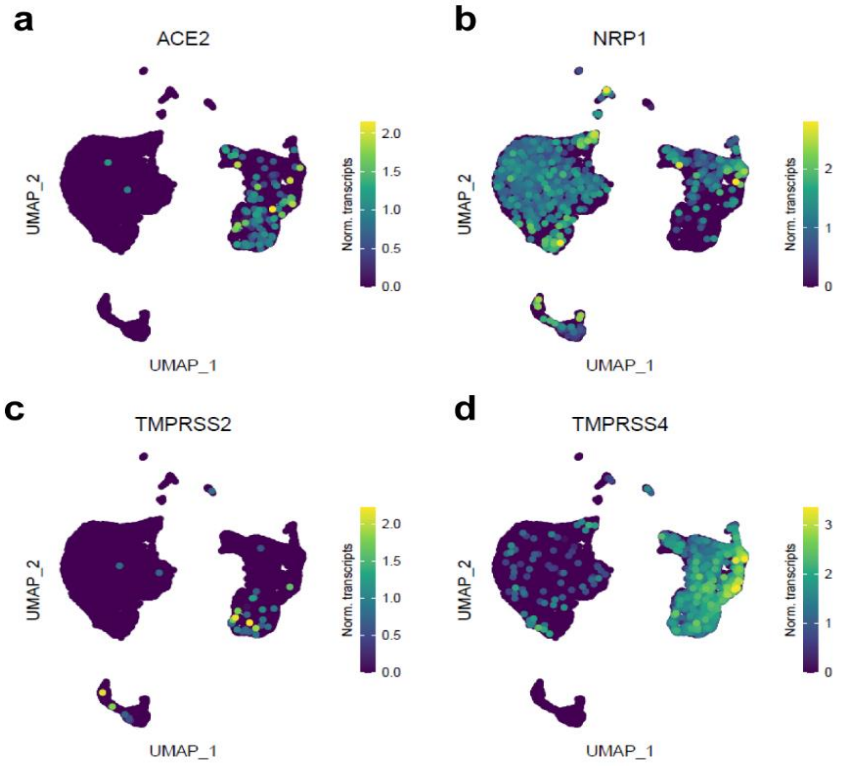

Supplementary Figure S9. Single cell transcriptome expression level UMAP of SARS-CoV-2 cell receptor *ACE2* (a) and receptor-associated *NRP1* (b), *TMPRSS2* (c), and *TMPRSS4* (d) protein expressing genes.

Supplementary references

1. Collin, J. *et al.* Co-expression of SARS-CoV-2 entry genes in the superficial adult human conjunctival, limbal and corneal epithelium suggests an additional route of entry via the ocular surface. *Ocul. Surf.* **19**, 190–200 (2021).

2. Yan, R. *et al.* Structural basis for the recognition of SARS-CoV-2 by full-length human ACE2. *Science.* **367**, 1444–1448 (2020).

3. Hoffmann, M. *et al.* SARS-CoV-2 Cell Entry Depends on ACE2 and TMPRSS2 and Is Blocked by a Clinically Proven Protease Inhibitor. *Cell* **181**, 271–280 (2020).

4. Zang, R. *et al.* TMPRSS2 and TMPRSS4 mediate SARS-CoV-2 infection of human small intestinal enterocytes. *Sci. Immunol.* **5**, eabc3582 (2020).

5. Cantuti-Castelvetri, L. *et al.* Neuropilin-1 facilitates SARS-CoV-2 cell entry and infectivity. *Science.* **370**, 856–860 (2020).

5

A single-cell RNA-seq analysis unravels the heterogeneity of primary cultured corneal endothelial cells

This chapter has been published as:

Català, P., Groen, N., LaPointe, V.L.S., Dickman, M.M. A single-cell RNA-seq analysis unravels the heterogeneity of primary cultured corneal endothelial cells. *Sci Rep.* 2023; 13: 9361

Abstract

The primary culture of donor-derived human corneal endothelial cells (CECs) is a promising cell therapy. It confers the potential to treat multiple patients from a single donor, alleviating the global donor shortage. Nevertheless, this approach has limitations preventing its adoption, particularly culture protocols allow limited expansion of CECs and there is a lack of clear parameters to identify therapy-grade CECs. To address this limitation, a better understanding of the molecular changes arising from the primary culture of CECs is required. Using single-cell RNA sequencing on primary cultured CECs, we identify their variable transcriptomic fingerprint at the single cell level, provide a pseudo temporal reconstruction of the changes arising from primary culture, and suggest markers to assess the quality of primary CEC cultures. This research depicts a deep transcriptomic understanding of the cellular heterogeneity arising from the primary expansion of CECs and sets the basis for further improvement of culture protocols and therapies.

Introduction

The cornea is the transparent window transmitting light into the eye. The inner part of this avascular tissue is covered by a monolayer of hexagonal corneal endothelial cells (CECs)[1] that maintain corneal transparency and hydration by their pump and barrier function.[2] Human CECs are arrested in a non-proliferative state and lack regenerative capacity. Consequently, damage to CECs due to surgery, inherited diseases, or acquired conditions results in irreversible corneal oedema, impairing vision.[3]

Corneal transplantation is the current therapy for treating corneal endothelium dysfunction. Still, only one donor cornea is available for every 70 patients in need, leaving 12.7 million people awaiting treatment worldwide.[4] A first landmark clinical trial showed that primary cultivated CECs can restore corneal transparency, breaking the one-donor–one-recipient paradigm.[5,6] Encouraged by the long-term success of this therapy,[7] clinical trials are ongoing in Japan (UMIN000034334 and UMIN000012534), Mexico (NCT04191629) and Singapore (NCT04319848) to assess the therapeutic potential of cultured CECs.

Nonetheless, the transplantation of cultured CECs has limitations preventing its wider adoption. Primary CEC cultures are only successful when derived from donors younger than 45 years of age, limiting the pool of donor corneas suitable for this technique. Furthermore, cultures become heterogeneous over time, and significant alterations diminishing the cell phenotype and functionality are observed after the second passage.[8] Notably, there is a lack of clear parameters to identify therapy-grade cells.[9] Recently, cell morphology[10] and a set of markers: CD44, CD105, CD24, and CD133, also referred to as the E-ratio, have been used as exclusion criteria for therapy-grade CECs.[11] If we were able to identify additional or other cell-specific markers we could selectively assess and enrich for therapy-grade CECs.

To deconstruct the heterogeneity and gain knowledge on the alterations arising from the primary culture of CECs , we used single-cell RNA sequencing (scRNA-Seq) to profile 42,220 primary human CECs from six corneas of three donors at five time points over three passages in culture. Our analysis revealed that the culture diversified over time into heterogeneous subpopulations including cells less desirable for therapy that were entering a senescent or fibrotic state. We identified markers that can be used in combination to assess for therapy-grade cells and enrich for desired cell populations. Pseudo time analysis further uncovered the different trajectories arising during culture. Together, our study sheds light on the various routes followed by CECs in culture, identifies novel markers to increase culture efficiency, and presents a roadmap to improve culture protocols.

Materials and methods

Research-grade donor human corneas and ethical statement

This study was performed in compliance with the tenets of the Declaration of Helsinki. All research-grade human donor corneas used for primary culture were obtained from the Lions Eye Institute for Transplant & Research (Tampa, USA), with informed consent from the next of kin. The research involving human-derived corneas was performed in accordance to Maastricht University and Dutch national regulations. All corneas had an endothelial cell density of at least 2800 cells/mm^2, deemed unsuitable for transplantation, and were preserved in Optisol-GS at 4°C for up to 14 days prior to their use (Table 1).

Table 1. Donor cornea information. COD= cause of death, GI= Gastrointestinal, MVA= motor vehicle accident, ECD= endothelial cell density, OS= oculus sinister, OD= oculus dexter.

Donor	Sex	Age (years)	Preservation time (days)	COD	ECD OS/OD (cells/mm^2)
Donor 1	Male	34	12	Trauma	3195/2917
Donor 2	Male	29	11	GI bleed	2832/2878
Donor 3	Female	27	14	MVA	2861/3159

Isolation and culture of primary human corneal endothelial cells

Six paired corneas, from two male and one female donor aged 27 to 34 years, were used for isolation and primary culture of endothelial cells. Donors had no history of ocular disease, chronic systemic disease, or pathological infection such as HIV, Hepatitis B and C, HTLV-I/II, syphilis, or SARS-CoV-2.

Prior to isolation, the endothelial–Descemet's corneal layer was manually stripped as follows: the corneas were vacuum fixed in a punch base (e.janach) endothelial cell side up and trephined with a 10 mm Ø corneal punch at a fixed depth of 100 μm (e.janach). To delimit the endothelial trephined line, corneas were stained with a trypan blue solution (0.4%) for 30 s, and washed with balanced salt solution sterile irrigating solution (BSS; Alcon). The corneal endothelium was then gently lifted

using a DMEK cleavage hook (e.janach) and fully stripped using angled McPherson tying forceps.

Human corneal endothelial cells were isolated and cultured as previously reported.[5] Briefly, the stripped endothelium–Descemet's layer was incubated with 2 mg/ml collagenase A (Roche) solution in human endothelial serum free media (SFM) (Thermo Fisher Scientific) for 2–5 h at 37°C followed by a 5 min incubation in TrypLE express (Thermo Fisher Scientific) to generate small clumps of corneal endothelial cells. Cells from each cornea were seeded equally across 2 wells of a 24-well plate coated with fibronectin collagen (FNC) coating mix (Athena Enzyme Systems) in M5 stabilization media (human endothelial SFM (Thermo Fisher Scientific) supplemented with 5% fetal bovine serum (FBS), 100 U/mL penicillin–streptomycin, and 0.25 μg/mL amphotericin B) supplemented with 10 μM Y-27632 (STEMCELL Technologies). Subsequently, corneal endothelial cells were cultured in M4 proliferation medium (1:1 Ham's F12 (Thermo Fisher Scientific) and M199 (Thermo Fisher Scientific) supplemented with 5% FBS, 20 μg/mL ascorbic acid (Sigma), 1 × ITS (Thermo Fisher Scientific), 10 ng/mL human recombinant bFGF (Sigma), and 10 μM Y-27632 (STEMCELL Technologies)); media was refreshed every other day. Upon reaching 90% confluency, after approximately 8–10 days of culture, cells were cultured in M5 stabilization media for 7 days. After this, corneal endothelial cells were treated with TripLE express and passaged into wells pre-coated with FNC-coating mix at a seeding density of 10,500 cells/cm^2 in M5 stabilization medium. All cell culture was performed in incubators with humidified atmosphere of 37°C and 5% CO_2.

Preparation of single cell suspension and methanol fixation

Cells from five different culture time points were methanol fixed for sequencing. Namely, cells at days 2 and 5 of culture after isolation in M4 proliferation media at passage 0, and cells at confluency after 7 days of culture in M5 stabilization media, at passages 0, 1, and 2.

To generate a single cell suspension, primary cultured corneal endothelial cells were treated with TripLE express for approximately 30 min at 37°C. Then cells were centrifuged for 5 min at 800 × *g* and resuspended in 1 mL ice-cold Dulbecco's phosphate-buffered saline (DPBS). Next, the cells were centrifuged for 5 min at 800 × *g* and resuspended in ice-cold DPBS at a ratio of 200 μL DPBS/1 × 10^6 cells, followed by the dropwise addition of ice-cold methanol at a ratio of 800 μL DPBS/ 1 × 10^6 cells. The fixed cell suspensions were stored at -80°C until sequencing.

Single-cell RNA sequencing

scRNAseq of primary cultured CECs was performed at Single Cell Discoveries (Utrecht, the Netherlands) following standard 10× Genomics 3' V3.1 chemistry protocol. Cells were rehydrated and loaded on the 10× Chromium controller as follows. Approximately 10,000 cells were loaded per each sample specified in Table 2. The resulting sequencing libraries were prepared following a standard 10× Genomics protocol and sequenced with an Illumina NovaSeq 6000 platform; read length: 150 bp, paired-end.

Table 2. 10x genomics sample loading and library information

Library	Donor and time point (cell count ratio)
G1	Donor 3 day 5 proliferation + donor 2 confluency passage 0 (1:3)
G2	Donor 3 confluency passage 0 + donor 2 day 5 proliferation (3:1)
G3	Donor 3 confluency passage 1 + donor 1 day 2 proliferation (3:1)
G4	Donor 3 confluency passage 2 + donor 2 day 2 proliferation (3:1)
G5	Donor 1 confluency passage 0
G6	Donor 1 confluency passage 1
G7	Donor 1 confluency passage 2
G8	Donor 2 confluency passage 1
G9	Donor 2 confluency passage 2

Bioinformatic analysis of scRNA-seq data

The BCL files resulting from sequencing were transformed to FASTQ files with 10× Genomics Cell Ranger mkfastq following its mapping with Cell Ranger count.

During sequencing, Read 1 was assigned 28 bp, and were used for identification of the Illumina library barcode, cell barcode and unique molecular identifier (UMI). R2 was used to map the human reference genome GRCh38. Filtering of empty barcodes was done in Cell Ranger. The data from all samples were loaded in R (version 4.2.0)[12] and processed using the Seurat package (version 4.1.1).[13] More specifically, for each library a UMI cutoff was used to filter out low quality cells because of the differences between the libraries (*i.e.* g1 – 500, g2 – 3000, g3 – 500, g4 – 1313, g5 – 4000, g6 – 4000, g7 – 4000, g8 – 4000, g9 – 4000) (Table 2). Additionally, cells with less than 10% mitochondrial gene content were retained for analysis. The data of all 10× libraries were merged and processed together. The merged dataset was normalized for sequencing depth per cell and log-transformed using a scaling factor of 10,000. The multiplexed samples were demultiplexed based on their snp profile using Souporcell.[14] Briefly, the bam file and barcodes of each library were used as input together with the reference genome GRCh38. Besides the default parameters, the number of clusters was set to the number of multiplexed samples per library. The demultiplexing information for each cell was added to the metadata object in Seurat. The patient and library effect was corrected using Harmony,[15] as implemented in Seurat and used for dimensionality reduction and clustering of all cells. Cells were clustered using graph-based clustering and the original Louvain algorithm was utilized for modularity optimization. The differentially expressed genes per cluster were calculated using the Wilcoxon rank sum test and used to identify cell types. Putative doublets were computationally identified using scDblFinder (version 1.2.0)[16] but did not compose a separate cluster and therefore were not removed from the dataset (Figure S9). Pseudo time analysis was performed using the Monocle-3 package (version 1.0.0).[17] Gene set enrichment analysis was performed on lists of differentially regulated genes without prefiltering step. Gene lists were preranked using the signed -log10 (P adj) and subjected to enrichment analysis using fgsea package (version 1.22.0)[18] and gage (version 2.46.1)[19] with curated and hallmark gene sets from MSigDB Collections (version 7.5.1).[20,21] To prune selectively the resulting pathways and GO terms, enrichment was considered when up- or

downregulated gene sets were detected using both methods. The CEC dataset was integrated with the previously published cornea atlas.[22] The library effect was corrected for using harmony, followed by dimensionality reduction. The cluster information from the separate analysis was used to overlay in 2D space. The cell type of the atlas cells was predicted using the CEC confluency dataset using the cell label transfer functionality from Seurat.

Immunofluorescence

Primary cultured CECs at time point confluency passage 2 deriving from all three donors were used for immunofluorescence analysis. CECs were fixed in 4% PFA for 15 min at ambient temperature and the cells were permeabilized with 0.1% (v/v) Triton X-100 in phosphate buffered saline (PBS) for 10 min. After permeabilization, non-specific antibody interactions were blocked with blocking buffer (2% (w/v) BSA solution in PBS) for 1 h at ambient temperature. CECs were incubated overnight at 4°C with primary antibodies mouse monoclonal anti-CD166 [3A6] (1:200 dilution, BD Biosciences), rabbit polyclonal anti-ZO1 (1:100 dilution, Thermo Fisher Scientific), mouse monoclonal anti-CD44 [Hermes-3] (1:400 dilution, Abcam), rabbit polyclonal anti-VMO1 (1:100 dilution, Prestige Antibodies), rabbit polyclonal anti-THBS2 (1:100 dilution, Abcam), rabbit monoclonal anti-CD10 [EPR22867-118] (1:100 dilution, Abcam), rabbit monoclonal anti-NCAM1 [CAL53] (1:100 dilution, Abcam), and rabbit polyclonal anti-CGNL1 (1:200 dilution, Atlas antibodies) diluted in blocking buffer. After primary antibody incubation, tissues were washed three times in PBS and then incubated with secondary antibodies goat anti-mouse A488 (1:400 dilution; Thermo Fisher Scientific), and donkey anti-rabbit A568 (1:400 dilution; Thermo Fisher Scientific) diluted in blocking buffer for 50 min at ambient temperature in the dark. Cell nuclei were stained with 1 μg/mL Hoechst 33342 (Thermo Fisher Scientific) for 10 min. The CEC samples were then washed three times in PBS and examined on an Eclipse Ti-E inverted microscope (Nikon) equipped with an X-Light V2-TP spinning disk (Crest Optics).

Statistical and quantitative analysis of scRNAseq data

All the statistical analysis for scRNAseq were performed in R (version 4.2.0) with the packages described in the methods detail section. Briefly, differentially expressed genes were detected using a Wilcoxon Rank-Sum test, statistical significance was defined as $p < 0.01$. GSEA revealed differentially enriched gene sets from MSigDB Collections, statistical significance was defined as $p < 0.05$.

Results

scRNAseq reveals different subpopulations of CECs arising from primary culture

Six paired human corneas, from two male and one female donor (Table 1), were used for isolation, primary culture, and scRNAseq of CECs (Figure 1A). Cells from five different time points in culture were loaded for sequencing as specified in Table 2. Namely, cells at days 2 and 5 of culture after their isolation in M4 proliferation media at passage 0, and cells at passages 0, 1, and 2, at confluency after 7 days of culture in M5 stabilization media. The cultures showed characteristic CEC morphology over time (Figure 1B, Figure S1) and expressed the desired CEC proteins such as CD166 and zonula occludens-1 (ZO-1) (Figure 1c).

After filtering for cells with a minimum of 1,000 transcripts, the transcriptome profiles of 42,220 cells were embedded in a uniform manifold approximation and projection (UMAP). Cells from all donors were distributed homogeneously across the UMAP (Figure S2). Unbiased low-resolution clustering revealed six major cell clusters (Figure 2A), all of which expressed CEC markers *ALCAM* (CD166), *PRDX6*, *SLC4A11*, *PITX2*, and *ATP1A1*,[9,23,24] confirming their endothelial identity (Figure 2B). The absence of keratocyte markers *CD34*, *KERA*, and *ALDH1A1*,[25,26] and epithelial markers *KRT12*, *KRT14*, and *PAX6*[27,28] confirmed the absence of contaminating cell types from corneal stroma and epithelium (Figure S3). Differential gene expression profiling was used for cluster identification.

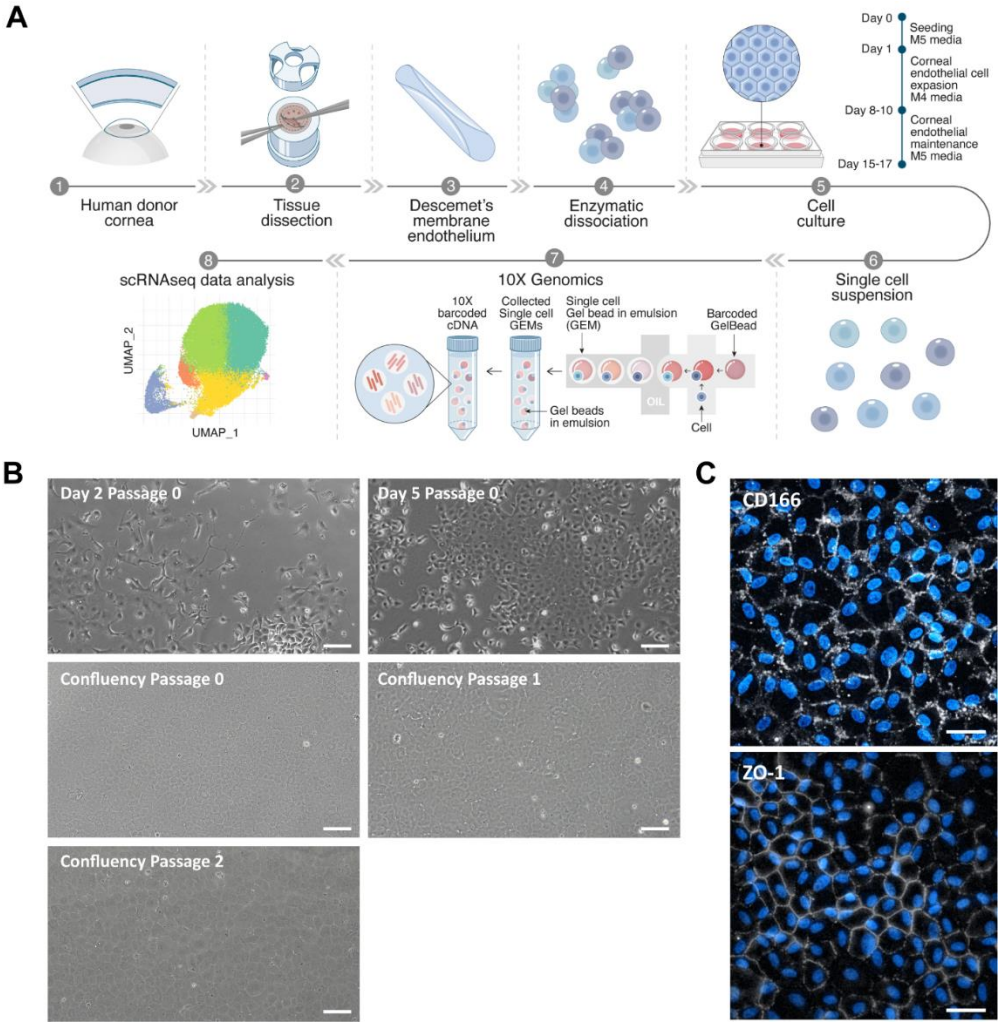

Figure 1. Human CECs were successfully isolated and cultured for scRNAseq

(A) Schematic representation of the experimental overview.

(B) Phase contrast images of CEC over the different time points selected for scRNAseq confirm the desired hexagonal morphology of the cells. Scale bars represent 100 μm.

(C) Immunofluorescence assessment of CEC markers CD166 and ZO-1 confirm the phenotype of the primary cultured cells at passage 2. Scale bars represent 50 μm.

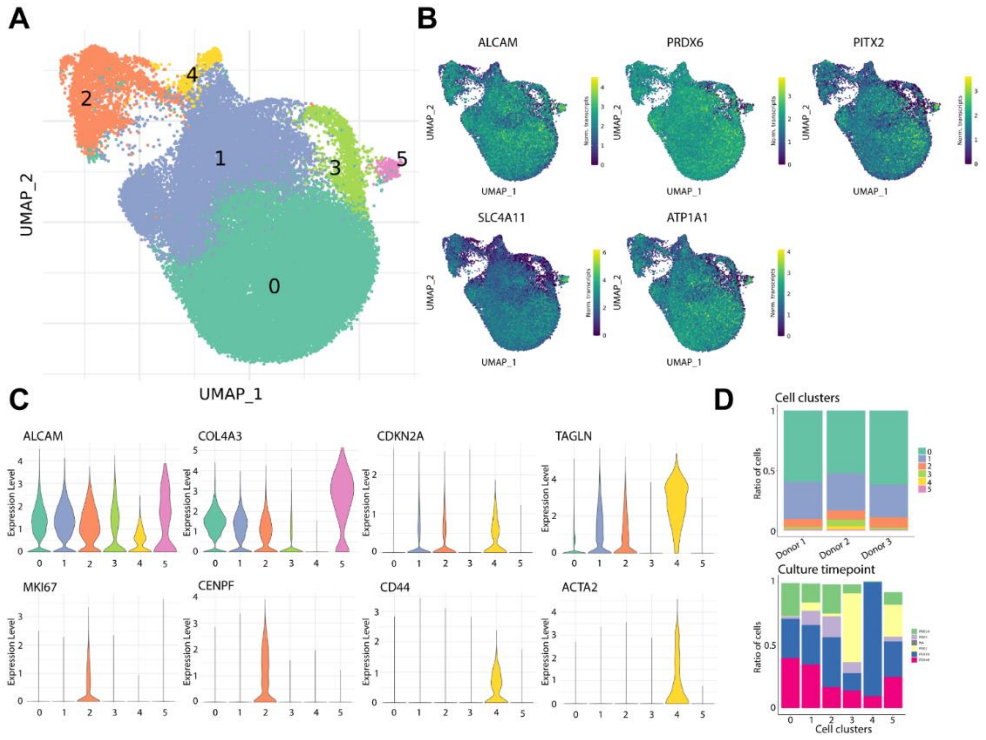

Figure 2. scRNAseq analysis reveals distinct clusters of primary cultured CECs

(A) UMAP of the 42,220 sequenced cells reveals six cell clusters.

(B) Gene expression UMAP of typical CEC markers namely *ALCAM* (CD166), *PRDX6*, *PITX2*, *SLC4A11*, and *ATP1A1* confirms the endothelial identity of the sequenced cells.

(C) Violin plots of show gene expression for markers of endothelium (*ALCAM*, *COL4A3*), senescence (*CDKN2A*, *TAGLN*), proliferation (*MKI67*, *CENPF*), and fibrosis (*CD44*, *ACTA2*).

(D) Bar charts show the distribution of cells of each donor per cluster (top) and the time point composition of each cluster (bottom).

Clusters 0 and 5 presented increased differential gene expression of typical CEC markers, *SLC4A11*, *COL4A3*,[23] *CDH2*,[29] and *ALCAM*, compared to the other sequenced cells, suggesting these clusters were composed of therapy-grade CECs (Figure 2C and S4). Cluster 1 was identified as CECs transitioning towards a senescent phenotype due to the high differential expression of senescence markers such as *MT2A*,[30] *CDKN2A* (p16),[31] and *TAGLN* [32] (Figure 2C and S4). Cluster 2 was

composed of highly proliferative CECs expressing *MKI67*, [33] *CENPF*, [34] and *PTTG1*[35] (Figure 2C). Cluster 4 was composed of fibrotic CECs with increased differential expression of *ACTA2* (α-smooth muscle actin (SMA)),[36] *CD44*,[37] and *COL6A1*[38] (Figure 2C and S4). Finally, our analysis revealed that cluster 3 was mainly composed of cells in passage 0 (at both day 2 and day 5) (Figure 2D) that differentially expressed ribosomal-associated genes (Figure S5). This finding suggested that cells at an early culture stage clustered together due to the necessary adaptation to *in vitro* culture conditions and the use of proliferation media, which led us to further explore the cells that had been cultured to confluency in passages 0, 1 and 2.

scRNAseq reveals seven distinct subpopulations of primary cultured CECs at therapeutically relevant time points

To identify the meaningful differences at therapeutically relevant time points and remove the clustering bias introduced by the adaptation to primary culture conditions after cell isolation, we separately analyzed the CECs at confluency in passages 0, 1, and 2. These time points are the most therapeutically relevant, as CECs are most suitable for therapy after 7 days in M5 stabilization media up to passage 2.[8,39]

After removing sub-confluent cells from day 2 and day 5 (in passage 0) of culture, the transcriptome profiles of 37,158 CECs at confluency in passages 0, 1, and 2 were embedded in a UMAP. Unbiased low-resolution clustering revealed seven cell clusters (Figure 3A) with distinct transcriptomic signatures. Cells from all donors were distributed homogeneously across the UMAP (Figure S6). Differential gene expression analysis was used for identification of each cell cluster (C0–C6).

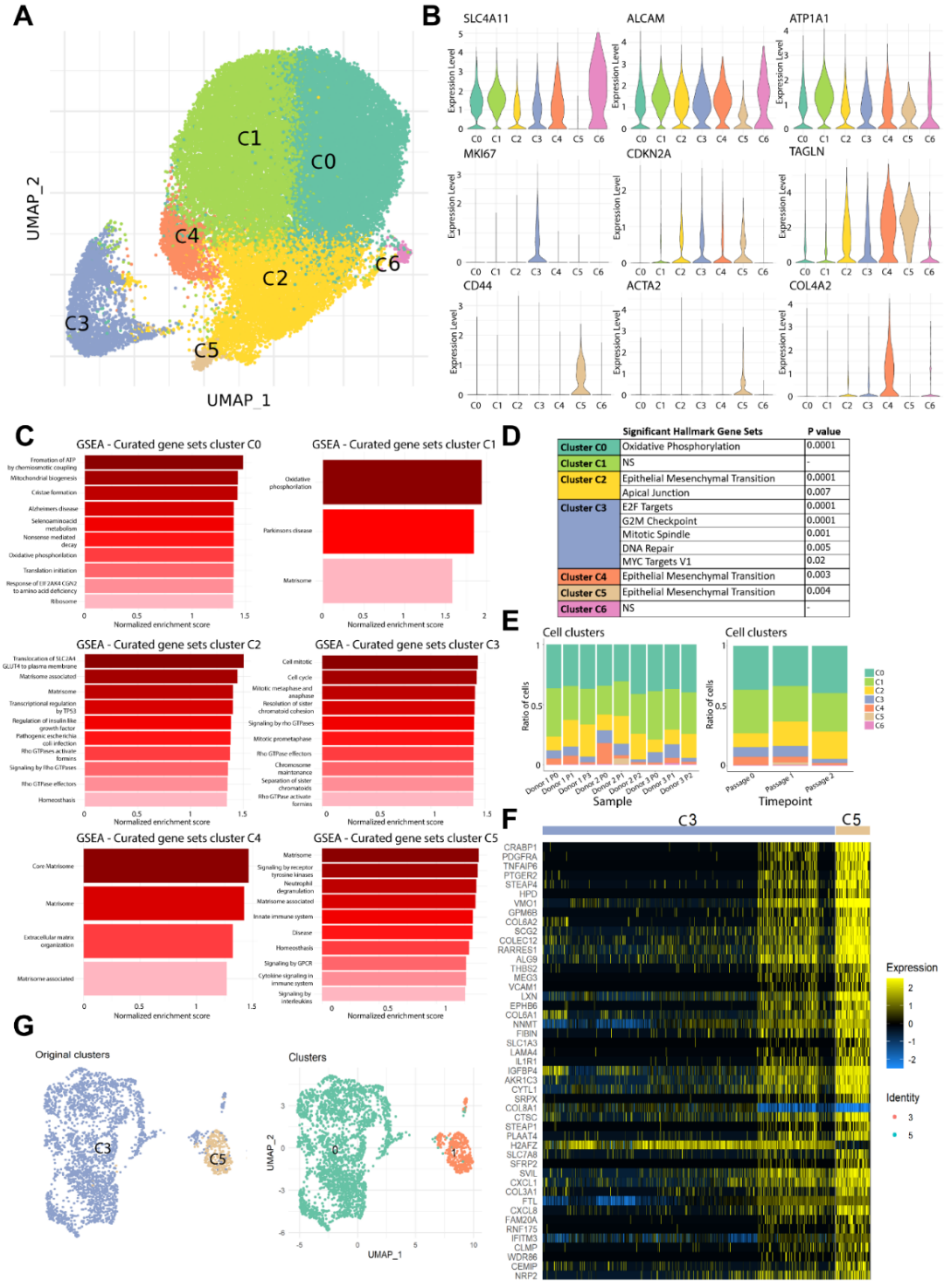

	Significant Hallmark Gene Sets	P value
Cluster C0	Oxidative Phosphorylation	0.0001
Cluster C1	NS	-
Cluster C2	Epithelial Mesenchymal Transition	0.0001
	Apical Junction	0.007
Cluster C3	E2F Targets	0.0001
	G2M Checkpoint	0.0001
	Mitotic Spindle	0.001
	DNA Repair	0.005
	MYC Targets V1	0.02
Cluster C4	Epithelial Mesenchymal Transition	0.003
Cluster C5	Epithelial Mesenchymal Transition	0.004
Cluster C6	NS	-

(Figure 3 - legend on next page)

Increased differential expression of typical CEC markers, such as *COL4A6*,[23] *SLC4A11*, *ATP1A1*, *COL4A3*, and *CDH2* suggested that clusters C0 and C1 were composed of therapy-grade CECs (Figure 3B and S7). Further analysis by gene set enrichment analysis (GSEA) revealed that highly metabolically active cells comprised these clusters (Figure 3C), with a distinct hallmark for oxidative phosphorylation in cluster C0 (Figure 3D). These markers are also found in native functioning human CECs, suggesting these cells were therapy-grade CECs. Cluster C3 was composed of proliferating CECs with differential high expression of *MKI67* (KI-67), *CENPF*, and *PTTG1* (Figure 3B and S7). GSEA further confirmed enriched gene sets and significant hallmarks related to cell proliferation (Figure 3C, D).

Figure 3. scRNAseq analysis reveals seven distinct CEC clusters at therapeutically relevant time points

(A) UMAP of the 37,158 cells at confluency time points reveals seven cell clusters.

(B) Violin plots show gene expression for markers of endothelium (*SLC4A11*, *ALCAM*, *ATP1A1*), proliferation (*MKI67*), senescence (*CDKN2A*, *TAGLN*), fibrosis (*CD44*, *ACTA2*), and extracellular matrix production (*COL4A2*).

(C) Gene set enrichment analysis (GSEA) reveal differentially expressed gene sets across cell clusters ($p < 0.05$).

(D) Significant differentially expressed hallmark gene sets across clusters ($p < 0.05$) show endothelial to mesenchymal transition in lower quality CEC clusters C2, C4 and C5; and proliferation hallmarks in cluster C3.

(E) Bar charts show composition of cell clusters across the different sequenced samples (left), and across the different time points (right).

(F) Heatmap of the top 50 differentially expressed genes across clusters C3 and C5 ($p < 0.01$) shows a subpopulation of CEC within cluster C3 that highly resembles the cells comprising cluster C5.

(G) UMAP of the reclustering analysis of cell clusters C3 and C5 with original clusters (left) and newly detected clusters (right).

Clusters C2 and C4 were composed of CECs with increased differential expression of senescence related genes. Namely, *CDKN2A* (p16), *TAGLN*, and *MT2A* (Figure 3B and S7) in cluster C2 and *CDKN1A* (p21),[40] *CDKN2A* (p16), and *TAGLN* in cluster C4 (Figure 3B and S7), suggesting these cells were transitioning towards an undesirable senescent and fibrotic phenotype. Cluster C4 had a high extracellular matrix production suggested by the differential high expression of *COL4A1*, *COL4A2*, *COL5A1*, and *FBLN5* in cells that maintained the expression of endothelial markers such as *SLC4A11*, and *COL4A3* (Figure 3B and S7).

In contrast, cells in cluster C2 presented a low expression of CEC markers such as *ALCAM*, *SLC4A11*, *CDH2*, and *ATP1A1* (Figure 3B and S7). GSEA revealed that both clusters C2 and C4 had a significant hallmark for epithelial to mesenchymal transition (Figure 3D), confirming these cells were transitioning towards senescence and fibrosis. GSEA revealed that cluster C2 was enriched for genes related to alterations in the matrisome production, upregulation of p53 pathway, and upregulation on Rho GTPase pathway, which are known to regulate cellular senescence[41,42] (Figure 3C), and cluster C4 expression was enriched for genes related to matrisome, extracellular matrix organization and matrisome associated genes suggesting a remodeling of the extracellular matrix (Figure 3C). Cluster C5 was composed of fibrotic cells differentially expressing the fibrosis-associated markers *COL6A1*, *COL6A3*, *CD44*, and *ACTA2* (Figure 3B). The cells in cluster C5 had diminished expression of *ALCAM* (CD166) and lacked *SLC4A11* expression, two CEC markers. GSEA further suggested enriched expression of genes related to the matrisome and matrisome associated processes and increased signaling by G-coupled protein receptors and receptor tyrosine kinase (Figure 3C), with a significant hallmark for epithelial to mesenchymal transition for cells in cluster C5 (Figure 3D). Finally, Cluster C6 was composed of CECs with differential high expression of typical endothelial markers such as *SLC4A11*, *COL4A3*, and *CDH2* (Figure 3B) suggesting they were therapy-grade CECs. These cells differentially expressed higher *GOLGA8A* and *GOLGA8B*, suggesting a possible increase in secretory

pathways. GSEA did not reveal significant upregulation of gene sets nor significant hallmarks compared to other clusters.

Longer culture times decrease proliferation and increase transitioning to senescence

Our scRNAseq data analysis revealed that at longer culture time points, namely confluency in passage 2, there was an increase in the number of cells transitioning to a senescent/fibrotic phenotype (cluster C2 and C4) and a decrease in the number of proliferative cells (cluster C3) compared to earlier time points (Figure 3E). Interestingly, the number of cells in cluster C4 decreased over culture time (Figure 3E) while cells in cluster C2 increased over time. This could be because the cells in C4 are early senescent cells and transition to later senescent cells in cluster C2. Regarding fibrotic CECs in cluster C5, these cells were detected as early as passage 1, but were also present in passage 2 at lower prevalence compared to passage 1. Finally, the prevalence ratio of therapy grade CECs (cluster C0 and C1) was maintained over time points (Figure 3E) showing the presence of therapy-grade CECs over all culture passages.

scRNAseq subclustering analysis revealed two distinct transcriptomic profiles of proliferating cells

The CEC marker *ALCAM*, and the fibrotic markers *CD44* and *ACTA2* were heterogeneously expressed across different cells comprising proliferative cluster C3 (Figure S8), suggesting it contained a subcluster of highly proliferative fibrotic CECs. Correlation and differential expression analysis revealed similarities between a subcluster of C3 with the fibrotic cells present in cluster C5 (Figure 3F). This was confirmed by a reclustering analysis of only clusters C3 and C5, which showed that a small subpopulation of cells originating from cluster C3 clustered together with the cells originating from cluster C5 (Figure 3G). This finding confirms the presence of a subpopulation of highly proliferative fibrotic CECs within cluster C3.

Primary cultured CECs resemble native human CECs

To assess how comparable primary cultured CECs are to native human CECs, we integrated the transcriptome of cells cultured to confluency in passages 0, 1, and 2 with a previously published cornea scRNAseq atlas.[22] To do so, the cluster information from both the CECs in the cornea cell atlas and this study were overlaid in 2D space (Figure 4A). The clustering analysis revealed that the CEC clusters originating from the native human corneal endothelium (Atlas En0 and Atlas En1) clustered adjacent to primary CEC clusters C6, C1 and C0, suggesting these cell clusters share comparable transcriptomic profiles (Figure 4A).

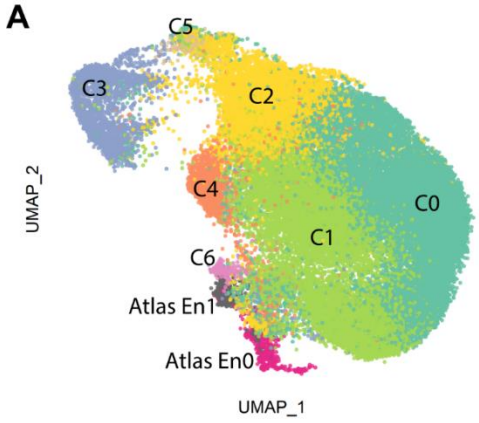

B

	CEC atlas count	CEC atlas fraction
Cluster C0	3	0.4%
Cluster C1	454	53.9%
Cluster C2	0	0%
Cluster C3	0	0%
Cluster C4	5	0.6%
Cluster C5	0	0%
Cluster C6	380	45.1%

Figure 4. Therapy grade primary cultured CECs resemble human native CECs.

(A) Integrated data UMAP of primary cultured CECs at confluency and native human CECs from the previously published cornea cell atlas (Catala et al. 2021). The integration analysis shows that native CECs (Atlas 0 and Atlas 1) cluster adjacent to high quality primary cultured CEC clusters (clusters C0, C1, and C6) suggesting clusters C0, C1 and C6 can be considered therapy-grade primary cultured CECs.

(B) The cell type of the atlas CECs was predicted using the CEC confluency dataset using the cell label transfer functionality from Seurat. 99.4% of the atlas cells were attributed to clusters C0, C1 and C6, further suggesting the therapeutic standard of these clusters.

To further understand the similarity of native human CEC to primary cultured cells, we performed a cluster prediction analysis of the atlas CECs using the clustering analysis of cells at confluency. The prediction analysis revealed that 99.4% of the atlas CECs were associated to clusters C1 (53.9%), C6 (45.1%), and C0 (0.4%) (Figure 4B), suggesting these clusters are similar to native human CECs and could be used for therapeutic purposes. Furthermore, our prediction analysis found that no native CECs were associated with the senescent and fibrotic clusters C2 and C5, or the proliferative cluster C3 (Figure 4B).

Pseudo time reconstruction and evaluation reveal the dynamics of CEC profiles arising from primary expansion

To assess how the cells transition between clusters over time, we performed a pseudo time reconstruction of the cells at confluency in passages 0, 1, and 2. Our first analysis revealed that the CECs originating from clusters C0, C1, and C6, transitioned into the senescent cells in cluster C2, and then became the fibrotic cells in cluster C5 (Figure 5A). Interestingly, the last cluster the pseudo time trajectory identified were the proliferative cells in cluster C3. We hypothesize this is due to the presence of a side population of fibrotic proliferative cells within cluster C3 (Figure 3F, G), which might interfere with the pseudo time trajectory analysis. To reduce such bias and identify gene trends over the pseudo time trajectory, we performed a pseudo time analysis of the confluent cells excluding cluster C3 (Figure 5B). In line with the first analysis, the pseudo time trajectory revealed that the CECs from clusters C0, C1, and C6 transitioned into the transitioning senescent cells in cluster C2, and then the fibrotic cells in cluster C5 (Figure 5B) showing that primary cultured CECs transition towards senescence and fibrosis over culture time.

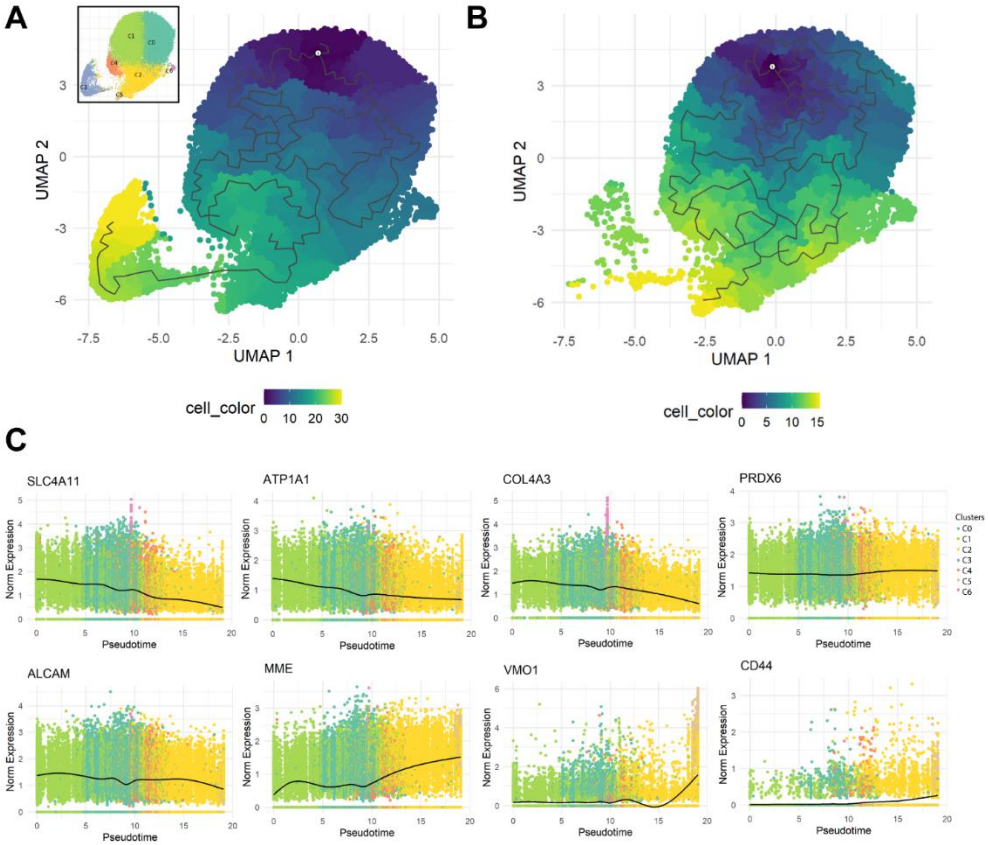

Figure 5. Pseudo temporal trajectory reconstruction reveals the dynamics of primary cultured CECs.

(A) Monocle 3 pseudo temporal trajectory reconstruction on UMAP reduction of the scRNAseq confluency time points reveals the CEC cluster dynamics over primary culture. UMAP reduction is colored by pseudo time bins with dark blue being the earliest and yellow corresponding to late.

(B) Monocle 3 pseudo temporal trajectory reconstruction on UMAP reduction of the scRNAseq confluency time points excluding proliferative cluster C3 reduces bias and reveals the temporal dynamics of the CEC clusters at confluence level. UMAP reduction is colored by pseudo time bins with dark blue being the earliest and yellow corresponding to late.

(C) Pseudo time reconstruction reveals differential gene expression trends over CEC clusters. Our analysis revealed a reduction over time of CEC markers *SLC4A11*, *ATP1A1*, *COL4A3*, and *ALCAM*, while *PRDX6* expression was constant. Conversely, *CD44*, *MME*, and *VMO1* expression significantly increased over time.

The pseudo time reconstruction revealed that the expression of functional markers such as *SLC4A11* and *ATP1A1* was reduced over time, showing that senescent (cluster C2 and C4) and fibrotic (cluster C5) cells had a highly reduced expression of crucial functional markers (Figure 5C). Moreover, pseudo time reconstruction also revealed reduced expression of *COL4A3* and *ALCAM* over time (Figure 5C). Interestingly, the expression of *PRDX6*, a known marker of CECs, remained constant and did not decrease over time in the senescent (C2 and C4) and fibrotic (C5) clusters (Figure 5C). Besides crucial CEC markers, our analysis also revealed a significant increase of *CD44* expression over time in clusters C2 and C5 CECs. Furthermore, the expression of *MME* (CD10) and *VMO1* in the pseudo time analysis was increased in the senescent and fibrotic clusters C2 and C5 (Figure 5C). These genes were also differentially expressed in lower quality clusters C2 and C5, respectively, and can be candidates to assess quality of primary cultured CECs.

scRNAseq transcriptomic profiles for quality assessment of primary cultured CEC correlate with protein level expression

The differential gene expression across CEC clusters and the pseudo time reconstruction both showed that the quality of the primary cultured CEC could be evaluated with a specific set of markers to differentiate therapy-grade CEC (clusters C0, C1, and C6), from lower quality CECs transitioning towards a senescent or fibrotic phenotype (clusters C2 and C5). The expression of *ALCAM* (CD166), *CGNL1* (cingulin-like protein 1), and *NCAM1* (CD56) were higher in the clusters comprising therapy-grade CECs (clusters C0 and C1), and lower in the cells in clusters C2 and C5 (Figure 6A). Additionally, the expression of *CD44*, *MME* (CD10), *VMO1*, and *THBS2* were higher in the fibrotic cells in cluster C5 and lower in the cells in clusters C0, C1, and C6 (Figure 6A), representing markers that could be used to exclude low quality CECs.

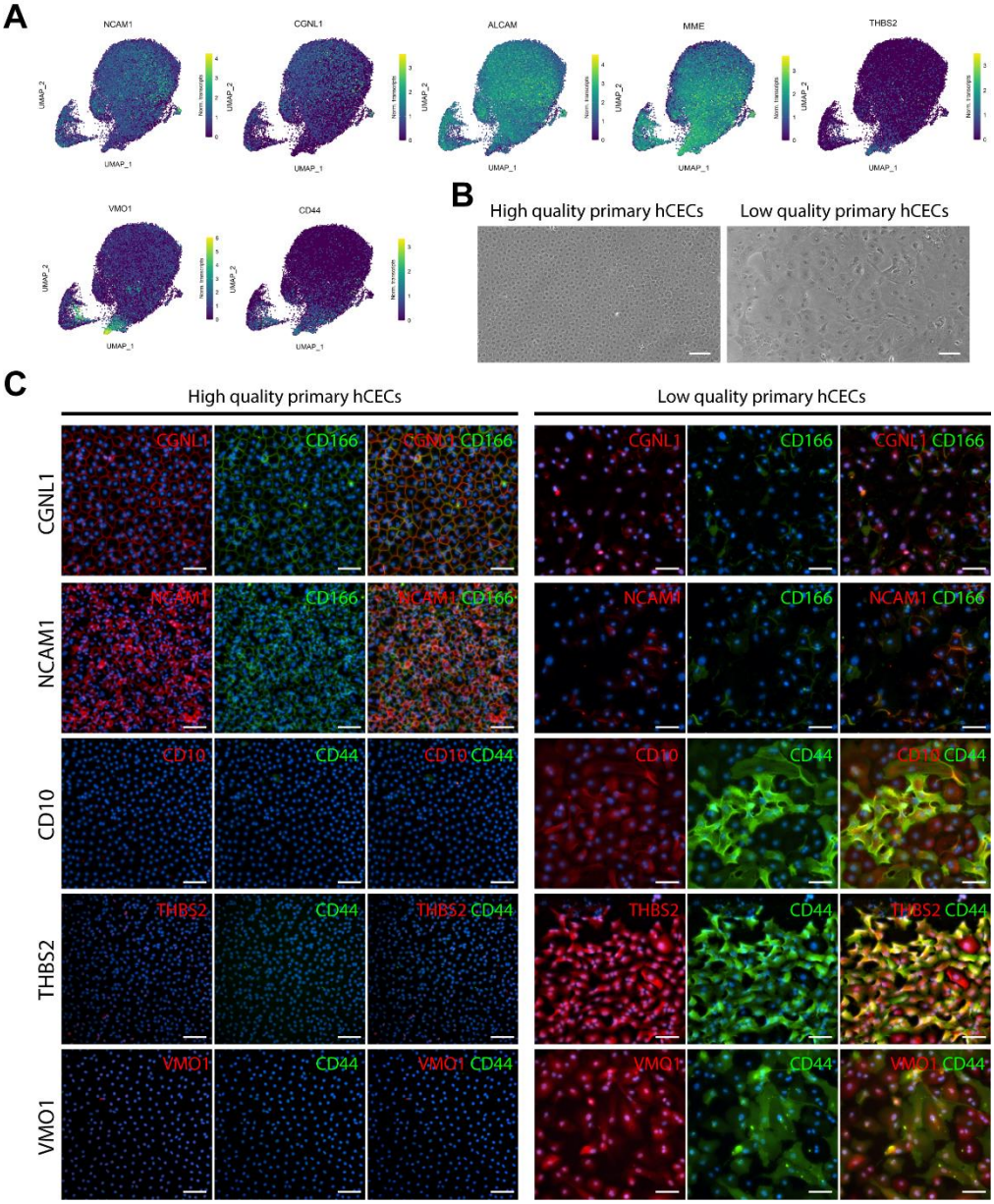

(Figure 6 - legend on next page)

To confirm the findings at the transcriptomic level were also present at the protein level, we assessed protein expression on primary CEC cultures with a characteristic hexagonal morphology associated with therapy-grade CECs and on primary CEC cultures composed of cells with spindle shape morphology, a characteristic of cells undergoing an endothelial to mesenchymal transition, referred as low quality primary CECs (Figure 6B). Immunofluorescence analysis confirmed that CGLN1, NCAM1 (CD56) and ALCAM (CD166) were exclusively expressed by good quality CECs and not expressed in the cultures containing CECs with an altered morphology (Figure 6C). Furthermore, immunofluorescence analysis also confirmed that CD44, MME (CD10), THBS2, and VMO1 were exclusively expressed by low quality CECs and not expressed in high quality CEC cultures (Figure 6C).

Figure 6. scRNAseq analysis suggests specific markers for CEC quality assessment.

(A) Gene expression UMAP of differentially expressed markers in clusters of therapy-grade CECs (clusters C0 and C1) and clusters of senescent/fibrotic CECs (cluster C5). *NCAM1*, *CGNL1*, and *ALCAM* were differentially expressed in clusters CO and C1 ($p < 0.01$). *MME* and *CD44* were differentially expressed in clusters C2 and C5. *THBS2* and *VMO1* were differentially expressed in cluster C5 ($p < 0.01$).

(B) Phase contrast images of a high quality therapy-grade CEC culture showing the typical hexagonal cell morphology and a low quality culture of primary human CECs showing the characteristic morphological alterations of an endothelial to mesenchymal transition. Scale bars represent 100 μm.

(C) Immunofluorescence analysis shows expression of CD166 (green), NCAM1 (red), and CGNL (red) in high quality CEC cultures (N=2) and absence of expression in lower quality CEC cultures (N=2). Immunofluorescence analysis shows expression of CD44 (green), MME (CD10) (red), THBS2 (red), and VMO1 (red) in lower quality CEC cultures (N=2) and the absence of expression in high quality CEC cultures (N=2). Cell nuclei were stained with Hoechst 33342 (blue). Scale represent 100 μm.

Discussion

In this study, we present a single-cell roadmap of human CECs in culture, revealing the diverse trajectories of individual cells. Our scRNAseq census of 42,200 primary cultured CECs revealed the presence of 7 clusters in therapeutically relevant time points, including therapy-grade CECs expressing *SLC4A11*, *ALCAM*, and *COL4A3* (clusters C0, C1 and C6); highly proliferative CECs expressing *MKI67* and *CENPF* (cluster C3); lower quality CECs entering senescence and EMT expressing *CDKN1A*, *CDKN2A*, and *TAGLN* (clusters C2 and C4); as well as fibrotic CECs expressing *CD44*, and *ACTA2* (cluster C5). We assessed to which extent CECs in culture resemble native human CECs and analyzed how these CEC populations diverge over culture time, giving insights into the alterations arising during primary culture. Moreover, our transcriptomic profiling provides an array of combinatorial markers to differentiate therapy-grade CEC from cells undergoing senescence and EMT, thereby paving the way for improving culture protocols and guiding the selection of cells for therapy. The transcriptomic data we obtained will help better our understanding of the mechanisms involved in the alterations occurring during primary culture of CECs leading to a loss of function and phenotype.

Our analysis showed that proliferating sub-confluent CECs sequenced at day 2 and day 5 clustered together (cluster 3), with high differential expression of ribosomal-related genes. We hypothesize that this is most likely due to their necessary adaptation to *in vitro* culture conditions and the use of proliferation media, which biased the first clustering. These findings led us to separately explore the 37,158 cells at confluency in passages 0, 1, and 2. Our analysis revealed three clusters of therapy-grade CEC (clusters C0, C1, and C6) based on the high differential expression of functional CEC markers *SLC4A11* and *ATP1A1* and the CEC markers *ALCAM*, *PRDX6*, and *COL4A3*. These cells were the majority in all passages, comprising 70% of all the sequenced cells. GSEA revealed that cells in C0 and C1

were metabolically active with increased expression of genes related to oxidative phosphorylation, in line with the crucial activity and function of CECs.[43]

The integration analysis of the dataset from this study with native CECs from a previously published cornea cell atlas revealed that native CECs clustered close to clusters C0, C1 and C6, suggesting the similarity of these cells. Cluster prediction analysis on native CECs revealed that these cells would group within clusters C1 (53.9%), C6 (45.1%), and C0 (0.4%). The low 0.4% prediction for cluster C0 is interesting because the primary cultured cells still expressed high levels of endothelial markers, namely *SLC4A11*, *ATP1A1*, *ALCAM*, and *PRDX6*. We hypothesize the low prediction might be due to a slight increase in ribosomal protein expression or a difference in the number of genes/cell which can be a technical sampling variation compared to clusters C1 and C6, which skews the cell clustering. Overall, our data shows that CECs in clusters C0, C1, and C6 are good quality CECs and are a suitable source for therapy. And while our dataset shows that cells in clusters C1 and C6 more closely resemble native human CECs that cells in cluster C0, it does not mean that cells in cluster C0 are unsuitable for therapy, but that they are distinguishable from native corneal endothelium.

Our scRNAseq analysis also revealed the presence of two clusters composed of senescent cells that were transitioning towards a mesenchymal phenotype (clusters C2 and C4). Our pseudo time reconstruction showed these cells were originating from the therapy-grade clusters C0, C1, and C6. This finding shows the transition to senescence of CECs during primary culture. Senescent cells in cluster C2 had reduced expression of key functional markers such as *SLC4A11*, *ATP1A1*, and *ALCAM*. This finding is in line with a recently published report that demonstrated a decrease of *SLC4A11* in lower-quality primary CECs.[43] The total number of senescent cells (clusters C2 and C4) increased over culture time, suggesting the CECs transitioned towards senescence over extended culture times. Cells comprising cluster C4 decreased over culture time, indicating that they either transition into

senescent cells in cluster C2 or represent an end-point cluster, where cells tend to die over time. GSEA revealed that cells in cluster C2 had differential gene expression, specifically an increase in genes involved in the p53 and Rho GTPase pathways, suggesting these pathways might play a key role on the senescence and endothelial to mesenchymal transition of primary cultured CECs. P53 is a known senescence regulator,[41,44] and its inhibition could delay the cellular senescence in primary CECs. A study in 2013 revealed that the inhibition of p53 was associated with improved morphology and higher expression of CEC markers, namely collagen type 8, Na/K ATPase, and N-cadherin, in primary cultured CECs.[45] Furthermore, our findings suggest that the inhibition of the Rho GTPase pathway can play a key role in delaying cellular senescence, further confirming that the use of Rho-associated protein kinase (ROCK) inhibitors such as Y-27632 might be a pivotal factor in the protocols for primary expansion of therapy-grade CECs. Indeed, previous studies have used Y-27632 for the primary expansion of CECs.[6,46–48] Based on these findings, we therefore recommend the use of ROCK inhibitors during the primary expansion of CECs.

Our scRNAseq analysis revealed that a cluster of CECs (cluster C5) expressing characteristic fibrotic markers ACTA2 and CD44 originated from the senescent cells at clusters C2, suggesting a transition from senescence to endothelial to mesenchymal transition phenotype. While fibrotic markers were found in later time points, we did observe that cells comprising cluster C5 appeared as early as passage 1, but were then reduced by passage 2. This finding could be due to the sequencing sampling limitation of 10,000 cells per sample, making it highly possible that this small fibrotic cell population was not sequenced from a culture of hundreds of thousands of cells. Our second hypothesis is that after passaging, the fibrotic cells could not successfully adhere, causing a reduction of this cell population and enriching for good quality cells.

Our findings showed that extended culture times decreased the proliferation potential of CECs, shown by a reduction in the number of cells in the proliferation cluster C3 across passages. Moreover, we detected the presence of a subpopulation of undesired proliferative fibrotic cells that could potentially overgrow the culture of CECs over extended culture periods. In our view, these results show that with the current protocols, culturing CECs further than passage 2 is incompatible with their therapeutic use, a recommendation in line with previous studies that suggested passage 2 as the threshold time point to assure the therapeutic suitability of primary cultured CECs.[8,39,49]

Selecting and assessing the quality of the primary cultured CECs are a crucial aspect to ensure a safe and efficacious therapy. Based on our differential expression analysis and pseudo time reconstruction, we show that therapy-grade CEC should be identified by the expression of CD166 and NCAM1 membrane proteins together with CGNL1, a membrane-associated protein to cellular tight junctions; lack of expression of altered extracellular matrix, namely VMO1 and THBS2; and lack of expression of membrane proteins CD44 and CD10. While the membrane protein markers suggested by our analysis would allow sorting for therapy-grade CECs, we believe is equally important to characterize CEC culture quality based on expression of other fundamental proteins such as aberrant extracellular matrix production. Future studies are required to understand how the expression of these markers correlate to therapeutic success. Similar to our suggestion to analyze markers for therapy-grade CECs ($CD166^+$, $NCAM1^+$, $CGNL1^+$, $CD44^-$, $CD10^-$, $VMO1^-$, and $THBS2^-$), Kinoshita and colleagues proposed the combinatorial marker expression referred as the E-ratio ($CD166^+$, $CD44^-$, $CD133^-$, $CD24^-$, and $CD105^-$) to assess for therapy-grade CECs. We and they both detected increased CD166 expression in therapy-grade CECs and CD44 exclusively expressed in lower quality senescent and transitioning CECs. By contrast, our analysis revealed that *CD24* and *ENG* (CD105) were heterogeneously and minimally expressed across clusters in some CECs, and we did not detect expression of *PROM1* (CD133) in any cluster. These differences

might be due to the lack of correlation between transcript and protein detection. Future studies analyzing such differences can shed light on the suitability of markers to assess or enrich for therapy-grade CECs.

While primary cultured CECs have been traditionally assessed as bulk entities without accounting for their heterogeneity, our study analyses them at the single-cell level over five culture time points in three different passages. Our study provides significant information to help understand the changes arising from the culture of human CECs, portraying their cellular heterogeneity as well as characterizing their variability over extended culture times. These results provide a pivotal dataset that can help identify and characterize the undesired cell populations arising from primary culture in the attempt to improve current protocols. Our results also show the importance of supplementing media for CEC expansion with ROCK inhibitors to reduce cellular senescence. Furthermore, based on the results reported in this study, we propose a combination of markers to assess the quality of primary cultured CECs. Overall, this transcriptomic cell analysis offers a baseline for future studies with the aim of improving CEC-based therapies.

Funding

This research was partly funded by the Bayer Ophthalmology Research Awards 2021 and Chemelot InSciTe under the EyeSciTe consortium.

Acknowledgements

The authors thank Single Cell Discoveries (Utrecht, the Netherlands) for the single cell sequencing services provided. The authors thank the Lions Eye Institute for Transplant & Research (Tampa, FL, USA) for providing research-grade human corneas.

Data availability

The scRNAseq dataset presented in this study and the R scripts will be made publically available in the gene expression omnibus, DataVerseNL, and GirHub upon manuscript acceptance.

References

1. DelMonte, D. W. & Kim, T. Anatomy and physiology of the cornea. *J. Cataract Refract. Surg.* **37**, 588–598 (2011).

2. Bonanno, J. A. Molecular mechanisms underlying the corneal endothelial pump. *Exp. Eye Res.* **95**, 2–7 (2012).

3. Price, M. O., Mehta, J. S., Jurkunas, U. V. & Price, F. W. Corneal endothelial dysfunction: Evolving understanding and treatment options. *Prog. Retin. Eye Res.* **82**, 100904 (2021).

4. Gain, P. *et al.* Global survey of corneal transplantation and eye banking. *JAMA Ophthalmol.* **134**, 167–173 (2016).

5. Peh, G. S. L. *et al.* Propagation of human corneal endothelial cells: A novel dual media approach. *Cell Transpl.* **24**, 287–304 (2015).

6. Kinoshita, S. *et al.* Injection of cultured cells with a ROCK inhibitor for bullous keratopathy. *N. Engl. J. Med.* **378**, 995–1003 (2018).

7. Numa, K. *et al.* Five-year follow-up of first eleven cases undergoing injection of cultured corneal endothelial cells for corneal endothelial failure. *Ophthalmology* **128**, 504–514 (2021).

8. Frausto, R. F. *et al.* Phenotypic and functional characterization of corneal endothelial cells during in vitro expansion. *Sci. Rep.* **10**, 7402 (2020).

9. Català, P. *et al.* Approaches for corneal endothelium regenerative medicine. *Prog. Retin. Eye Res.* **87**, 100987 (2022).

10. Yamamoto, A. *et al.* A physical biomarker of the quality of cultured corneal endothelial cells and of the long-term prognosis of corneal restoration in patients. *Nat. Biomed. Eng.* **3**, 953–960 (2019).

11. Ueno, M. *et al.* Superiority of mature differentiated cultured human corneal endothelial cell injection therapy for corneal endothelial failure. *Am. J. Ophthalmol.* **237**, 267–277 (2022).

12. R Core Team. R: A language and environment for statistical computing. (2013).

13. Stuart, T. *et al.* Comprehensive integration of single-cell data. *Cell* **177**, 1888–1902 (2019).

14. Heaton, H. *et al.* Souporcell: robust clustering of single-cell RNA-seq data by genotype without reference genotypes. *Nat. Methods* **17**, 615–620 (2020).

15. Korsunsky, I. *et al.* Fast, sensitive and accurate integration of single-cell data with Harmony. *Nat. Methods* **16**, 1289–1296 (2019).

16. Germain, P.-L. scDblFinder: scDblFinder. R package version 1.2.0. (2020).

17. Cao, J. *et al.* The single-cell transcriptional landscape of mammalian organogenesis. *Nature* **566**, 496–502 (2019).

18. Korotkevich, G. *et al.* Fast gene set enrichment analysis. *BioRxiv* (2021). doi:https://doi.org/10.1101/060012

19. Luo, W., Friedman, M. S., Shedden, K., Hankenson, K. D. & Woolf, P. J. GAGE: Generally applicable gene set enrichment for pathway analysis. *BMC Bioinformatics* **10**, 161 (2009).

20. Subramanian, A. *et al.* Gene set enrichment analysis: A knowledge-based approach for interpreting genome-wide expression profiles. *Proc. Natl. Acad. Sci. U. S. A.* **102**, 15545–15550 (2005).

21. Liberzon, A., Birger, C., Ghandi, M., Mesirov, J. P. & Tamayo, P. The molecular signatures database (MSigDB) hallmark gene set collection. *Cell Syst.* **1**, 417–425 (2015).

22. Català, P. *et al.* Single cell transcriptomics reveals the heterogeneity of the human cornea to identify novel markers of the limbus and stroma. *Sci. Rep.* **11**, 21727 (2021).

23. Van den Bogerd, B. *et al.* Corneal endothelial cells over the past decade: Are we missing the mark(er)? *Transl. Vis. Sci. Technol.* **8**, (2019).

24. Català, P. *et al.* Transport and preservation comparison of preloaded and prestripped-only DMEK grafts. *Cornea* **39**, 1407–1414 (2020).

25. Foster, J. W., Gouveia, R. M. & Connon, C. J. Low-glucose enhances keratocyte-characteristic phenotype from corneal stromal cells in serum-free conditions. *Sci. Rep.* **5**, 10839 (2015).

26. Fernández-Pérez, J. & Ahearne, M. Influence of biochemical cues in human corneal stromal cell phenotype. *Curr. Eye Res.* **44**, 135–146 (2019).

27. Hayashi, R. *et al.* Co-ordinated ocular development from human iPS cells and recovery of corneal function. *Nature* **531**, 376–380 (2016).

28. Ouyang, H. *et al.* WNT7A and PAX6 define corneal epithelium homeostasis and pathogenesis. *Nature* **511**, 358–361 (2014).

29. He, Z. *et al.* 3D map of the human corneal endothelial cell. *Sci Rep* **6**, 29047 (2016).

30. Malavolta, M. *et al.* Changes in Zn homeostasis during long term culture of primary endothelial cells and effects of Zn on endothelial cell senescence. *Exp. Gerontol.* **99**, 35–45 (2017).

31. Enomoto, K., Mimura, T., Harris, D. L. & Joyce, N. C. Age differences in cyclin-dependent kinase inhibitor expression and Rb hyperphosphorylation in human corneal endothelial cells. *Investig. Ophthalmol. Vis. Sci.* **47**, 4330–4340 (2006).

32. Benadjaoud, M. A. *et al.* Deciphering the dynamic molecular program of radiation-induced endothelial senescence. *Int. J. Radiat. Oncol. Biol. Phys.* **112**, 975–985 (2022).

33. Sun, X. & Kaufman, P. D. Ki-67: more than a proliferation marker. *Chromosoma* **127**, 175–186 (2018).

34. Varis, A., Salmela, A. L. & Kallio, M. J. Cenp-F (mitosin) is more than a mitotic marker. *Chromosoma* **115**, 288–295 (2006).

35. Ersvær, E. *et al.* Prognostic value of mitotic checkpoint protein BUB3, cyclin B1, and pituitary tumor-transforming 1 expression in prostate cancer. *Mod. Pathol.* **33**, 905–915 (2020).

36. Rao, B. K., Malathi, N., Narashiman, S. & Rajan, S. T. Evaluation of myofibroblasts by expression of alpha smooth muscle actin: A marker in fibrosis, dysplasia and carcinoma. *J. Clin. Diagnostic Res.* **8**, 14–17 (2014).

37. Hamuro, J. *et al.* Metabolic plasticity in cell state homeostasis and differentiation of cultured human corneal endothelial cells. *Investig. Ophthalmol. Vis. Sci.* **57**, 4452–4463 (2016).

38. Oouchi, Y., Watanabe, M., Ida, Y., Ohguro, H. & Hikage, F. Rosiglitasone and ROCK inhibitors modulate fibrogenetic changes in TGF-β2 treated human conjunctival fibroblasts (HconF) in different manners. *Int. J. Mol. Sci.* **22**, (2021).

39. Peh, G. S. L. *et al.* Functional evaluation of two corneal endothelial cell-based therapies: tissue-engineered construct and cell injection. *Sci. Rep.* **9**, 6087 (2019).

40. Matthaei, M., Meng, H., Meeker, A. K., Eberhart, C. G. & Jun, A. S. Endothelial Cdkn1a (p21) overexpression and accelerated senescence in a mouse model of Fuchs endothelial corneal dystrophy. *Investig. Ophthalmol. Vis. Sci.* **53**, 6718–6727 (2012).

41. Rufini, A., Tucci, P., Celardo, I. & Melino, G. Senescence and aging: The critical roles of p53. *Oncogene* **32**, 5129–5143 (2013).

42. Orgaz, J. L., Herraizy, C. & Sanz-Moreno, V. Rho GTPases modulate malignant transformation of tumor cells. *Small GTPases* **5**, e983867 (2014).

43. Deguchi, H. *et al.* Intracellular pH affects mitochondrial homeostasis in cultured human corneal endothelial cells prepared for cell injection therapy. *Sci. Rep.* **12**, 1–14 (2022).

44. Mijit, M., Caracciolo, V., Melillo, A., Amicarelli, F. & Giordano, A. Role of p53 in the regulation of cellular senescence. *Biomolecules* **10**, 420 (2020).

45. Sha, X., Liu, Z., Song, L., Wang, Z. & Liang, X. Human amniotic epithelial cell niche enhances the functional properties of human corneal endothelial cells via inhibiting P53-survivin-mitochondria axis. *Exp. Eye Res.* **116**, 36–46 (2013).

46. Peh, G. S. L. *et al.* The effects of rho-associated kinase inhibitor Y-27632 on primary human corneal endothelial cells propagated using a dual media approach. *Sci. Rep.* **5**, 1–10 (2015).

47. Parekh, M. *et al.* Human corneal endothelial cells from older donors can be cultured and passaged on cell-derived extracellular matrix. *Acta Ophthalmol.* **In Press**, 1–11 (2020).

48. Okumura, N. *et al.* Enhancement on primate corneal endothelial cell survival in vitro by a rock inhibitor. *Investig. Ophthalmol. Vis. Sci.* **50**, 3680–3687 (2009).

49. Frausto, R. F., Le, D. J. & Aldave, A. J. Transcriptomic analysis of cultured corneal endothelial cells as a validation for their use in cell replacement therapy. *Cell Transplant.* **25**, 1159–1176 (2016).

Supplementary Information

Supplementary Figure S1

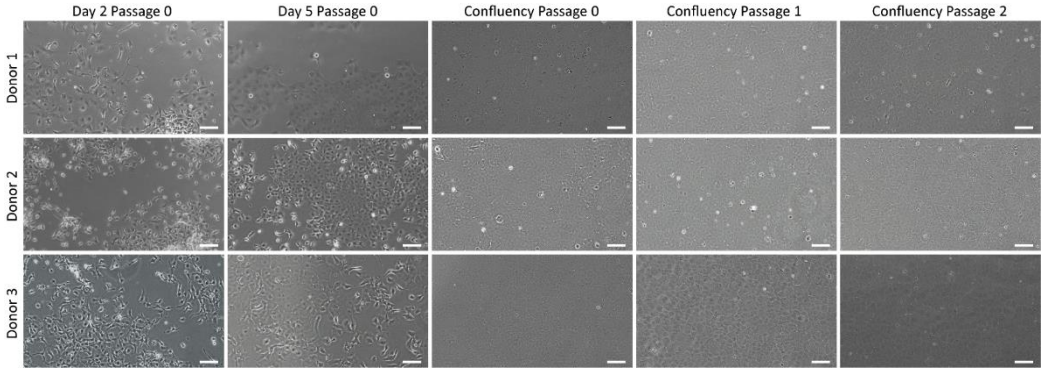

Figure S1. Phase contrast images of each donor time point used for scRNAseq, related to Figure 1. Phase contrast imaging shows desired endothelial morphology in all of the sequenced samples. Scale bar represents 100 μm.

Supplementary Figure S2

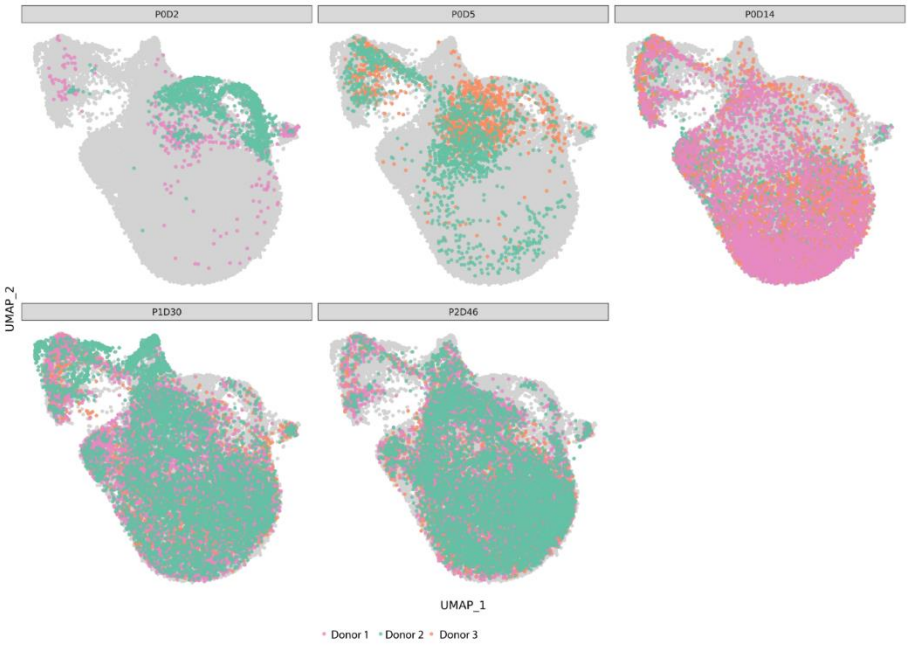

Figure S2. UMAP projection of cells per time point, related to Figure 2. Cell distribution UMAP per each time point further confirms that cluster is composed of CEC at early culture time points. Each donor is represented by color confirming the donor distribution across cell clusters. P0D2: day 2 in proliferation media. P0D5: day 5 in proliferation media. P0D14: passage 0 maintenance media. P1D30: passage 1 maintenance media. P2D46: passage 2 maintenance media.

Supplementary Figure S3

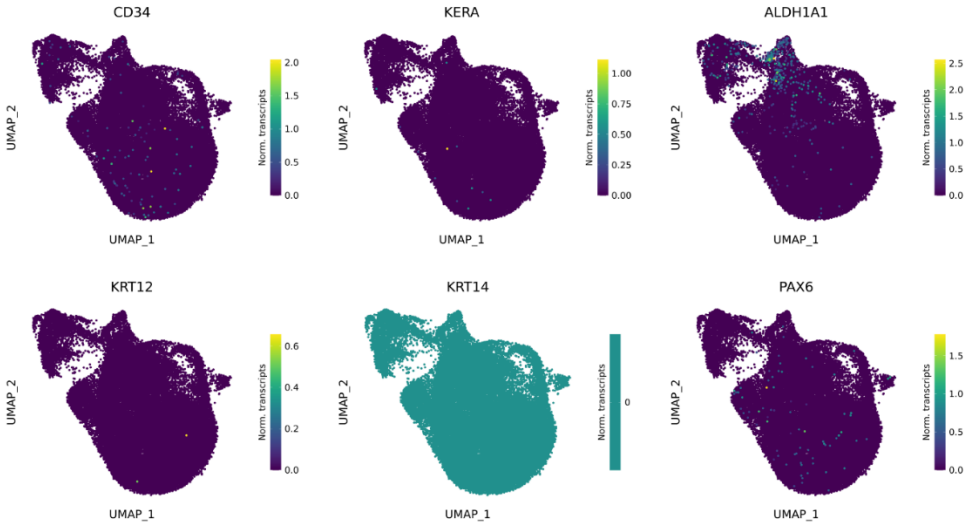

Figure S3. scRNAseq revealed absence of stroma and epithelial contamination, related to Figure 2. Gene expression UMAP of stromal markers *KERA*, *LUM*, and *ALDH1A1* and epithelial markers *KRT12*, *KRT14*, and *PAX6* confirmed absence of contaminant corneal side-populations in the primary culture.

Supplementary Figure S4

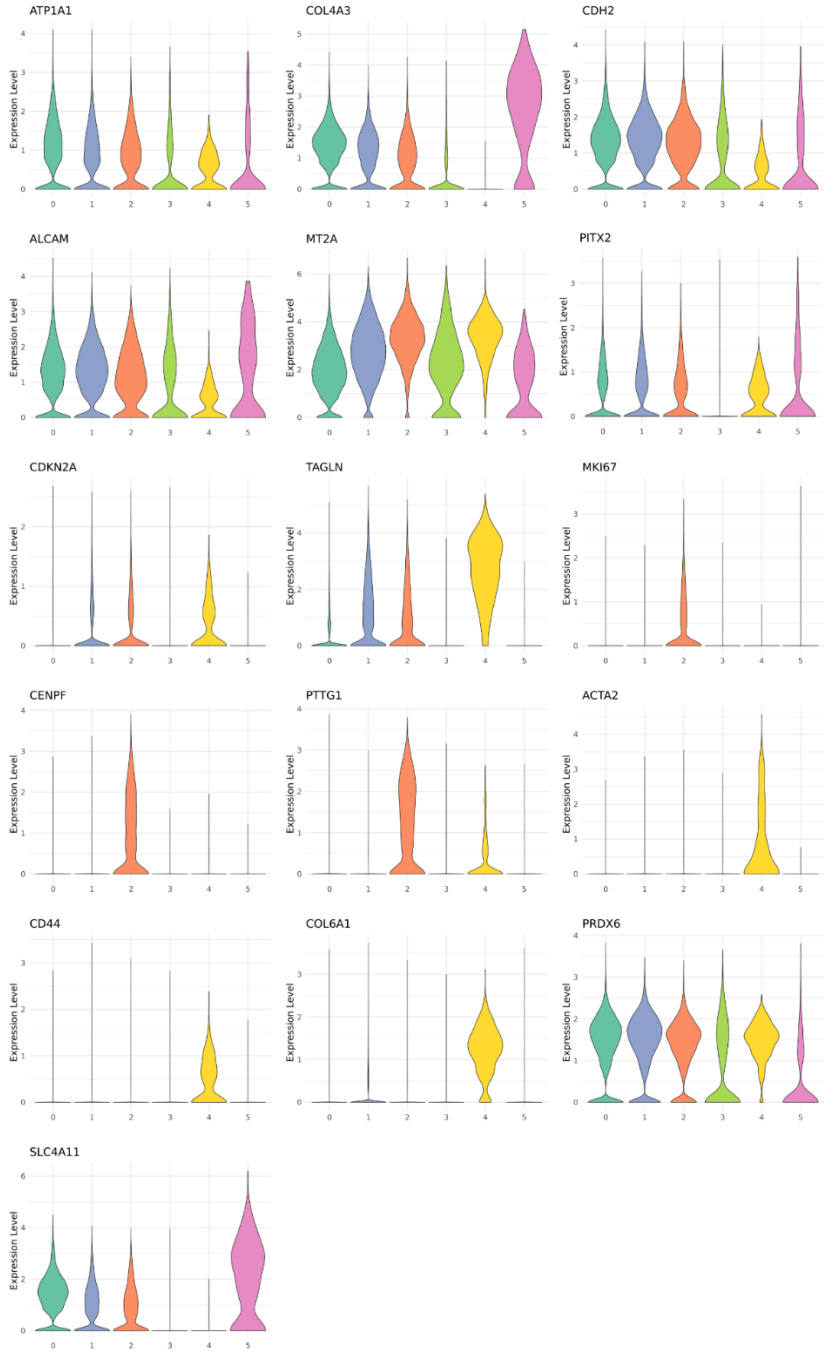

(Figure legend on next page)

Figure S4. Violin plots of differentially expressed genes for cluster identification, related to Figure 2. Violin plots of differentially expressed genes for cluster annotation. Corneal endothelium: *AP1A1*, *COL4A3*, *CHD2*, *ALCAM*, *SLC4A11*, *PITX2*. Senescence: *MT2A*, *CDKN2A*, *TAGLN*. Proliferation: *MKI67*, *CENPF*, *PTTG1*. Fibrosis and endothelial to mesenchymal transition: *ACTA2*, *CD44*, *COL6A1*.

Supplementary Figure S5

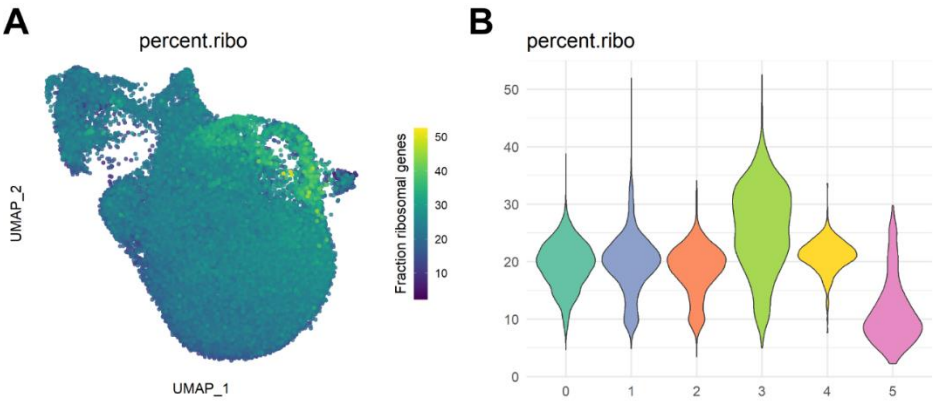

Figure S5. Cluster 3 is enriched in ribosomal gene expression. (A) UMAP representation of ribosomal gene fraction shows that cluster 3 expresses a high amount of ribosomal genes compared to other clusters. (B) Violin plot of ribosomal gene fraction shows further confirms a high expression of ribosomal genes in cluster 3 compared to the other detected clusters.

Supplementary Figure S6

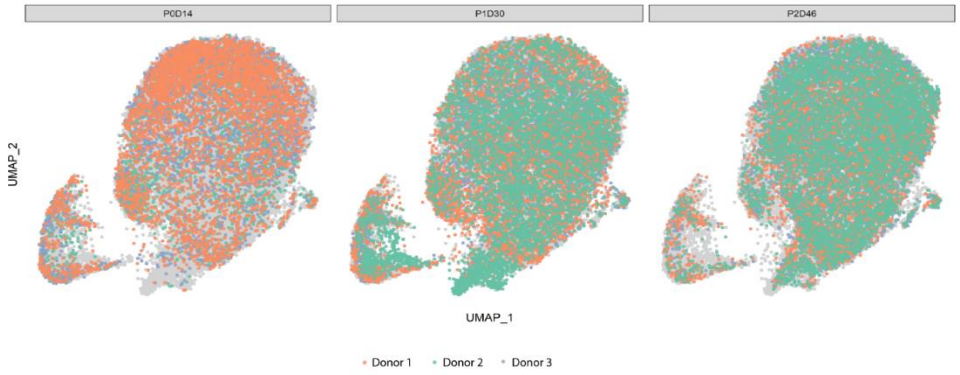

Figure S6. UMAP projection of cells per time point at confluency, related to Figure 3. Cell distribution UMAP per each time point at confluency level shows homogeneous distribution of donors across all cell clusters. P0D14: passage 0 maintenance media. P1D30: passage 1 maintenance media. P2D46: passage 2 maintenance media.

Supplementary Figure S7

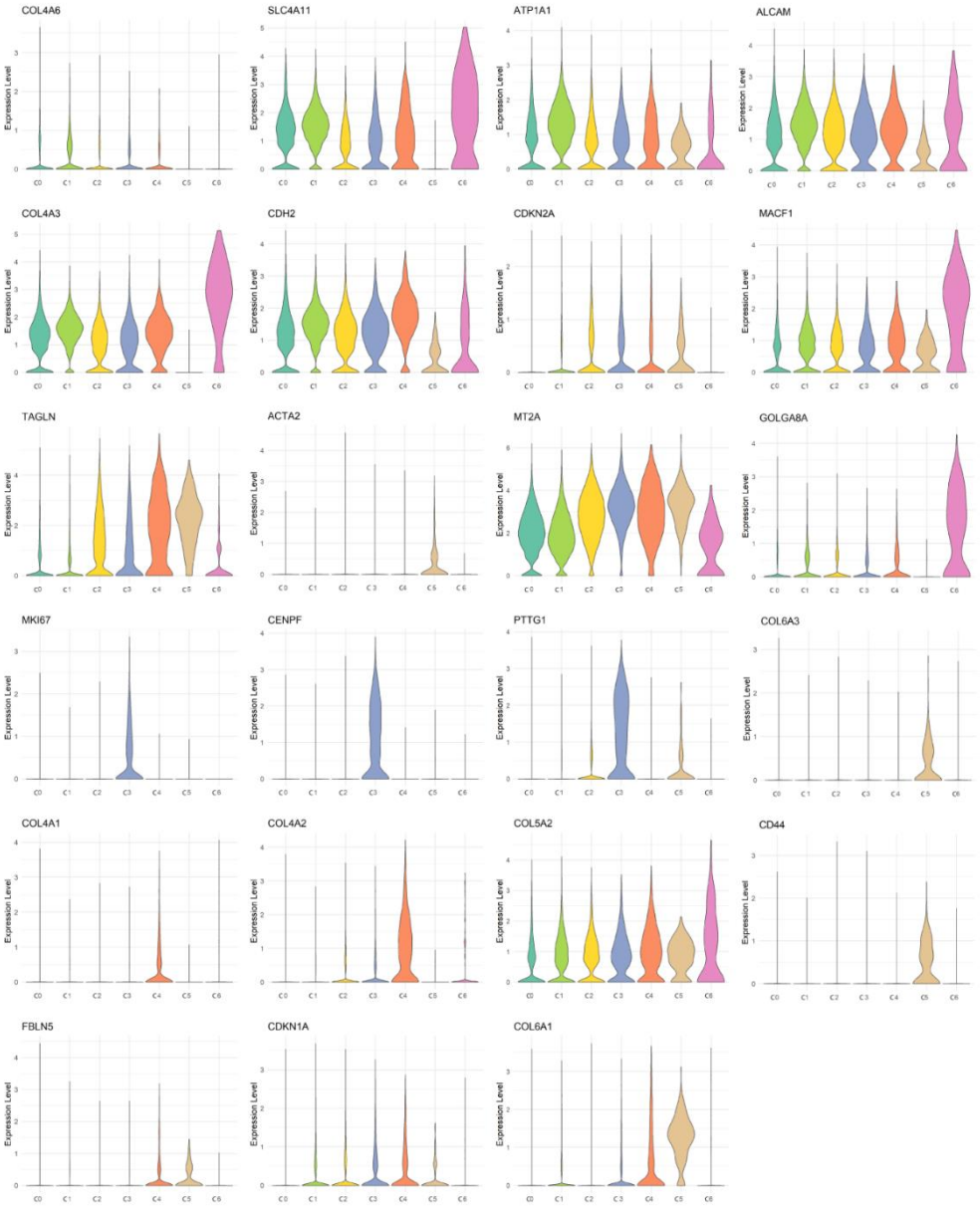

(Figure legend on next page)

Figure S7. Violin plots of differentially expressed genes for cluster identification, related to Figure 3. Violin plots of differentially expressed genes for cluster annotation at the confluency time points. Corneal endothelium: *SLC4A11*, *ATP1A1*, *ALCAM*, *CDH2*. Corneal endothelium extracellular matrix: *COL4A8*, *COL4A3*, *COL4A1*, *COL4A2*, *COL5A2*. Senescence: *CDKN2A*, *TAGLN*, *MT2A*, *CDKN1A*, *LGALS1*. Cell secretion: *GOLGA8A*. Proliferation: *MKI67*, *CENPF*, *PTTG1*. Fibrosis and endothelial to mesenchymal transition: *COL6A3*, *CD44*, *FBLN5*, *COL6A1*, *ACTA2*

Supplementary Figure S8

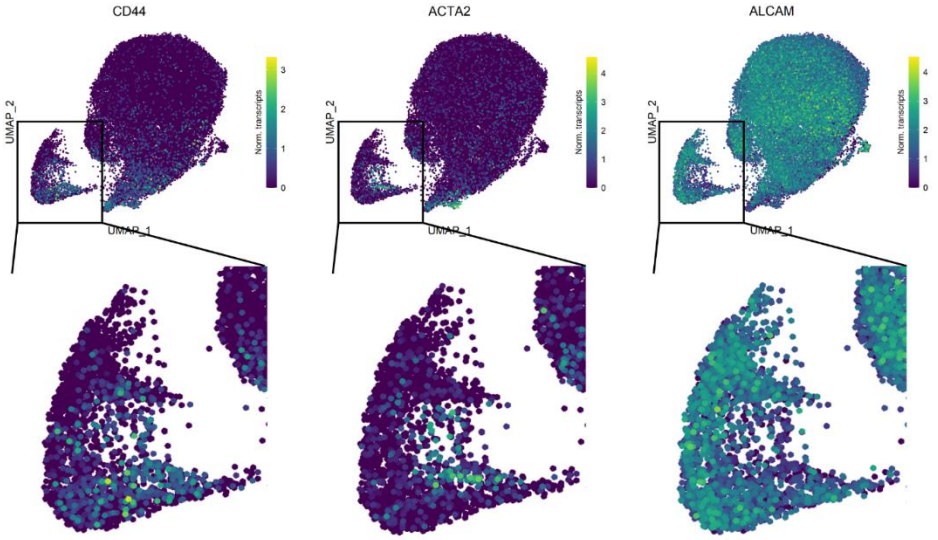

Figure S8. Gene expression UMAP of *ALCAM* (CD166), *CD44* and *ACTA2*, related to Figure 3. Gene expression UMAP shows heterogeneous expression of *ALCAM*, *CD44* and *ACTA2* across cell cluster C3.

Supplementary Figure S9

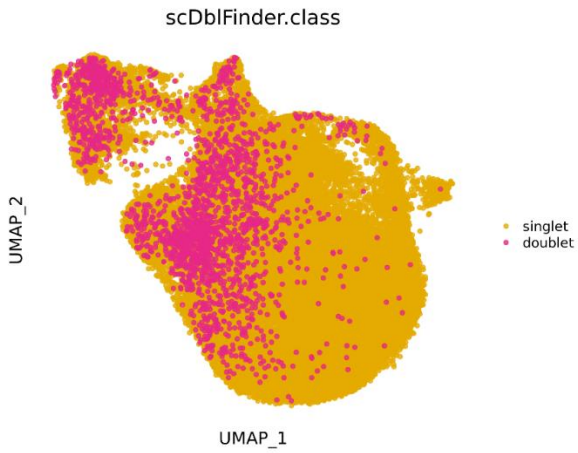

Figure S9. Identification of putative doublets. Putative doublets were identified with scDblFinder. The identified putative doublets were dispersed across all cell clusters and did not bias scRNAseq clustering therefore were not removed.

6

Elucidating the corneal endothelial cell proliferation capacity through an interspecies transcriptome comparison

This chapter has been published as:

Català, P., Vivensang, F., van Beek, D., Adriaens, M.E., Dickman, M.M., Kutmon, M., LaPointe, V.L.S., Elucidating the corneal endothelial cell proliferation capacity through an interspecies transcriptome comparison. *Adv Biol*. 2023; [2300065]

Abstract

The regenerative capacity of corneal endothelial cells (CECs) differs between species; in bigger mammals such as humans and sheep, CECs are arrested in a non-proliferative state. Damage to these cells can compromise their function leading to corneal opacity and impaired vision. Corneal transplantation is the current treatment for the recovery of clear eyesight, but the donor tissue demand is higher than the availability and there is a need to develop novel treatment modalities. In contrast, rabbit CECs retain a high proliferative profile and have the capacity to repopulate the endothelium upon injury. There is a lack of fundamental knowledge to explain the difference across species in the proliferation capacity of CECs. Gaining information on their transcriptomic differences could allow the identification of crucial drivers of CEC proliferation to enable the development of novel regenerative medicine therapies. In this study, we analyzed human, sheep, and rabbit CECs at the transcriptomic level. To understand the differences across each species, we generated an automated pipeline for the analysis of pathways with different activity. Our results revealed that 52 pathways had commonly different activity when comparing species with non-proliferative CECs (human and sheep) to species with proliferative CECs (rabbit). Our results showed that both Notch and TGF-β pathways had increased activity in species with non-proliferative CECs, which might be associated with their low proliferation capacity. Overall, this study illustrates transcriptomic pathway-level differences between sheep, human, and rabbit CECs, which might be used as a reference for the development of novel therapies to regenerate the corneal endothelium.

Introduction

The cornea is an avascular and transparent tissue located in the anterior segment of the eye that allows light to enter it. It is composed of five layers: epithelium, Bowman's layer, stroma, Descemet's membrane, and endothelium. The corneal endothelium is the innermost layer of the cornea and is composed of a monolayer of corneal endothelial cells (CECs) that reside in contact with the stroma on the Descemet's membrane.[1] The corneal endothelium function is to actively pump ions and metabolites from the stroma into the aqueous humor of the eye, thereby maintaining the cornea slightly dehydrated and transparent.[2]

The regenerative capacity of CECs differs between species. In humans[3] and sheep,[4] CECs are arrested in a quiescent state, lacking regenerative capacity through cell division. Iatrogenic damage after surgery, genetic diseases such as Fuchs' endothelial cell dystrophy, or infections in species with non-proliferative CECs can cause a decrease in their number, compromising the tissue function and leading to corneal opacity and impaired vision, also referred as corneal endothelial dysfunction. In contrast, rabbit CECs possess a high proliferative capacity and can repopulate the endothelium in response to damage.[5,6]

The standard treatment for corneal endothelial dysfunction is endothelial Keratoplasty,[3,7] but the increasing number of transplantations are causing a global donor cornea shortage leaving 12.7 million patients waiting for treatment.[8] There is a need to find alternative treatments to address corneal endothelial dysfunction. Promoting the proliferation of CECs could be an elegant approach to stimulate tissue regeneration and recovery of corneal transparency, but the mechanisms governing the differences between proliferative and non-proliferative CECs remain unknown. Therefore, to study the possible regulators of CEC proliferation, we performed an RNA sequencing (RNAseq) comparison between human, sheep, and rabbit CECs.

This study presents an interspecies transcriptome comparison of CECs originating from species with proliferative and quiescent endothelium. We identified pathways with different activity, which could be the driving force for CEC proliferation and regeneration. These findings can be used to improve current CEC expansion protocols and identify novel drug targets to promote corneal endothelial proliferation and regeneration.

Materials and methods

Research-grade tissue and ethical statement

This study was performed in compliance with the tenets of the Declaration of Helsinki. All human research-grade corneal tissue (*n=5*) was obtained from the ETB-BISLIFE Multi-Tissue Center (Beverwijk, the Netherlands), with informed consent from the next of kin. All human corneas were stored up to 22 days in organ culture media at 31 °C and had a minimum endothelial cell density of 2300 cells/mm^2. Organ culture media comprised the following: minimum essential medium supplemented with 20 mM HEPES, 26 mM sodium bicarbonate, 2% (v/v) newborn calf serum (Thermo Fisher Scientific), 10 IU/mL penicillin, 0.1 mg/mL streptomycin and 0.25 µg/mL amphotericin. All eyes from rabbits (*n=5*) and sheep (*n=5*) were enucleated from the animals used for other experimental procedures approved by the ethics committees of Maastricht University (Maastricht, the Netherlands), Utrecht University (Utrecht, the Netherlands), and Merck Sharp & Dome (MSD) animal testing facility (Boxmeer, the Netherlands) and were performed in accordance with Dutch national and European guidelines. All animal ocular tissue was used within 4 h after sacrifice. All donor and animal tissue information is specified in Table 1.

Isolation of human corneal endothelium

Of the five human corneal endothelial samples, four were discarded peripheral endothelial rims (1.5 mm wide) resulting from tissue preparation for Descemet's membrane endothelial keratoplasty (DMEK) according to clinical practice[9] and one (Human 5) was a whole endothelium stripped from a cornea deemed unsuitable for transplant (Table 1).

The four endothelial rims were lysed in 300 µL TRIzol within 48 h after tissue preparation. From the whole cornea, the complete endothelium was manually stripped following lysis in 300 µL TRIzol. Briefly, the cornea was vacuum-fixed in

a punch base (e.janach) endothelial-cell side up and trephined with a 10 mm Ø corneal punch at a fixed depth of 100 μm (e.janach). To delimit the endothelial trephined line, the cornea was stained with a trypan blue solution (0.4%) for 30 s, and washed with balanced salt solution ophthalmic irrigation solution. The corneal endothelium was then gently lifted using a DMEK cleavage hook (e.janach), fully stripped using angled McPherson tying forceps, and immediately transferred to TRIzol. All sample lysates were stored at -80°C until further use.

Table 1. Donor and animal tissue information. COD = cause of death. N/A = not applicable.

Sample name	Age	Gender	Experimental procedure	Strain	COD (only humans)
Human 1	66 years	Male	N/A	N/A	Other acute ischemic heart disease
Human 2	68 years	Male	N/A	N/A	Paralytic ileus and intestinal obstruction
Human 3	73 years	Female	N/A	N/A	Acute cerebrovascular accident
Human 4	57 years	Male	N/A	N/A	Malignant neoplasm bronchus and lung
Human 5	67 years	Female	N/A	N/A	Acute heart failure
Sheep 1	1–2 years	Female	Dorsal titanium implant	Texel	N/A
Sheep 2	1–2 years	Female	Dorsal titanium implant	Texel	N/A
Sheep 3	1–2 years	Female	Dorsal titanium implant	Texel	N/A
Sheep 4	1–2 years	Female	Dorsal titanium implant	Texel	N/A
Sheep 5	1–2 years	Female	Dorsal titanium implant	Texel	N/A
Rabbit 1	9 months	Male	Aorta stent implant	NZ White	N/A
Rabbit 2	9 months	Male	Aorta stent implant	NZ White	N/A
Rabbit 3	9 months	Male	Aorta stent implant	NZ White	N/A
Rabbit 4	3–4 months	Female	MSD vaccine testing	NZ White	N/A
Rabbit 5	3–4 months	Female	MSD vaccine testing	NZ White	N/A

Isolation of sheep corneal endothelium

All samples (*n=5*) were obtained from Texel sheep used for a dorsal titanium implant study from the animal facility at Maastricht University (Table 1). Five eyes were enucleated from 1 to 2-year-old female sheep within 4 h of sacrifice, and corneoscleral disks were excised from whole ocular gloves. Corneal endothelial cells were enzymatically treated and scraped from the corneoscleral disks because

stripping of the endothelium proved unsuccessful due to the tissue characteristics. For this purpose, corneoscleral disks were rinsed with Dulbecco's phosphate buffered saline, vacuum-fixed in a punch base (e.janach) endothelial-side up and treated with approximately 150 µL of StemPro Accutase (Thermo Fisher Scientific) for 20 min at ambient temperature. Corneal endothelial cells were then gently scraped using a DMEK cleavage hook (e.janach) and rinsed off the corneoscleral disk with approximately 2 mL of minimum essential medium (Thermo Fisher Scientific). The cell suspension was then transferred to a 15 mL tube, centrifuged at 800 × *g* for 5 min, and lysed in 300 µL TRIzol. All sample lysates were stored at -80°C until further use.

Isolation of rabbit corneal endothelium

Eyes were obtained from New Zealand White rabbits used for other experimental purposes from the Utrecht University animal facility (*n=3*) and MSD animal testing facility (*n=2*) (Table 1). The eyes were enucleated 30 min to 4 h after sacrifice, corneoscleral disks were excised from whole ocular globes, and the corneal endothelium stripped. In brief, corneoscleral disks were rinsed with PBS, vacuum-fixed in a punch base endothelial-cell side up and trephined with a 10 mm Ø corneal punch at a fixed depth of 100 µm. To delimit the endothelial trephined line, the cornea was stained with a trypan blue solution (0.4%) for 30 s, and washed with balanced salt solution ophthalmic irrigation solution. The corneal endothelium was then gently lifted using a DMEK cleavage hook, fully stripped using angled McPherson tying forceps, and immediately transferred to 300 µL TRIzol. All sample lysates were stored at -80 °C until further use.

RNA isolation and bulk RNA sequencing

RNA isolation was performed following TRIzol isolation procedure, and RNA integrity was assessed on a 2100 Bioanalyzer (Agilent). RNA sequencing was performed at Single Cell Discoveries (Utrecht, the Netherlands). Libraries were prepared following the CEL-seq2 protocol[10] to enable sample multiplexing. Paired-

end sequencing was performed on Illumina Nextseq500, high output 2 × 75 bp run mode, at a sequencing depth of 20 million reads/sample.

Data analysis and pre-processing

BCL files resulting from sequencing were transformed to FASTQ and read 1 was used to identify the Illumina library index and CEL-seq sample barcode. Read 2 was aligned to the specific RefSeq reference genome of each species, namely: hg38 for human, OryCun2.0 for rabbit, and ARS-UI_Ramb_v2.0 for sheep using the STAR genome aligner.[11]

The data from all samples were loaded in R (version 4.1.2)[12] for analysis. Gene homology mapping from rabbit and sheep to human was performed using the orthogene R-package (version 1.1.0) with the g:profiler method.[13] The three datasets were combined and only genes with homologs in all three species were included in the downstream analyses. Once the data were combined, quantile normalization was performed using the limma package (version 3.52.2).[14]

Pathway analysis

The human pathway collection from WikiPathways (release 10-07-2022) was used for assessing pathway activities in the three species.[15] A non-parametric Wilcoxon rank-sum test in R was used for identifying pathways with different pathway activities between the species ($p < 0.05$, $|\text{effect size}| > 1$). Pathway effect size was calculated as the differences of the averaged gene counts for each species compared. Disease-related pathways and pathways comprising less than 10 genes were not considered for data analysis. Pathway visualization was performed using Cytoscape (version 3.9.1).[16]

Results

Homology mapping of endothelial samples detected 9,757 protein coding transcripts commonly expressed across species

Corneal endothelium was isolated from human, sheep, and rabbit corneas, following RNA isolation. RNA integrity numbers ranged from 6.2 to 9.3. All samples were sequenced following an adapted CEL-Seq2 protocol on Illumina Nextseq500, high output 2 × 75 bp run mode, at a sequencing depth of 20 million reads/sample. After mapping to the species reference genome, a comparable number of protein coding genes, 16,852, 17,624, and 15,258, were detected in human, sheep, and rabbit, respectively. Homology mapping detected 9,757 full homologue protein coding genes across species which were then used for further pathway-level analyses (Figure 1), homology gene reads were normalized across samples using quantile normalization.

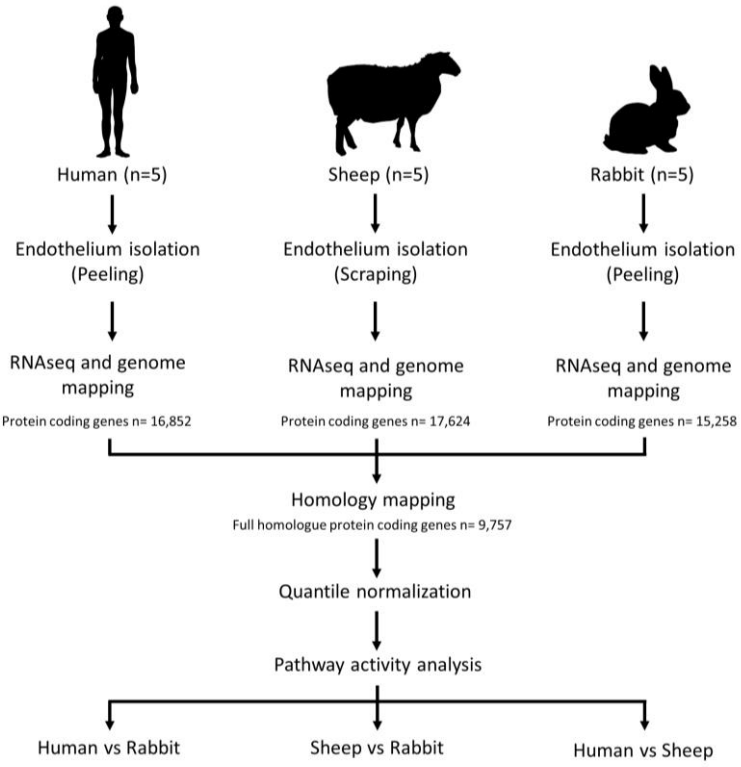

Figure 1. Schematic representation of the experimental pipeline and data analysis

Corneal endothelial cell transcriptomes differed highly across species

All endothelial samples showed a normal and comparable distribution of gene transcript counts after normalization (Figure 2A). Pearson's correlation analysis revealed that endothelial samples differed across species, with human and sheep having a higher correlation than rabbit (Figure 2B). Principal component analysis further confirmed these findings revealing that samples from the same species cluster together and rabbit samples cluster more distantly than sheep and human endothelial samples (Figure 2C). These findings are in line with the biological difference assessed in this study, being human and sheep species with non-proliferative CECs versus rabbit a species with proliferative CECs. The samples of all species showed expression of typical endothelial markers such as *ALCAM* (CD166), *TJP1* (ZO-1), *NCAM1*, *SLC4A4*, and *ATP1A1*[3,17,18] confirming the isolation of endothelium. Moreover, the absence of stromal markers *KERA*, *CD34*, and *LUM*,[17,19] absence of epithelial markers *WNT7A*, and *PAX6*,[17,20] and absence of immune markers *ITGAM*,[21] *CCR7*,[22] and *CD19*[23] confirmed the absence of contaminating cell types (Figure 2D).

Pathway level analysis revealed 52 pathways with different activity between proliferative and non-proliferative CECs

To elucidate possible drivers of CEC proliferation across the species studied, we performed a pathway level analysis benchmarking our data against WikiPathways. After filtering out disease-related pathways and pathways comprising less than 10 genes, we performed a non-parametric Wilcoxon rank-sum test to identify up- or down-regulated pathways between: (1) human and rabbit, (2) sheep and rabbit, and (3) sheep and human CECs. Only pathways with a p-value lower than 0.05 and an absolute effect size greater than |1| were retained for analysis in each of the comparisons.

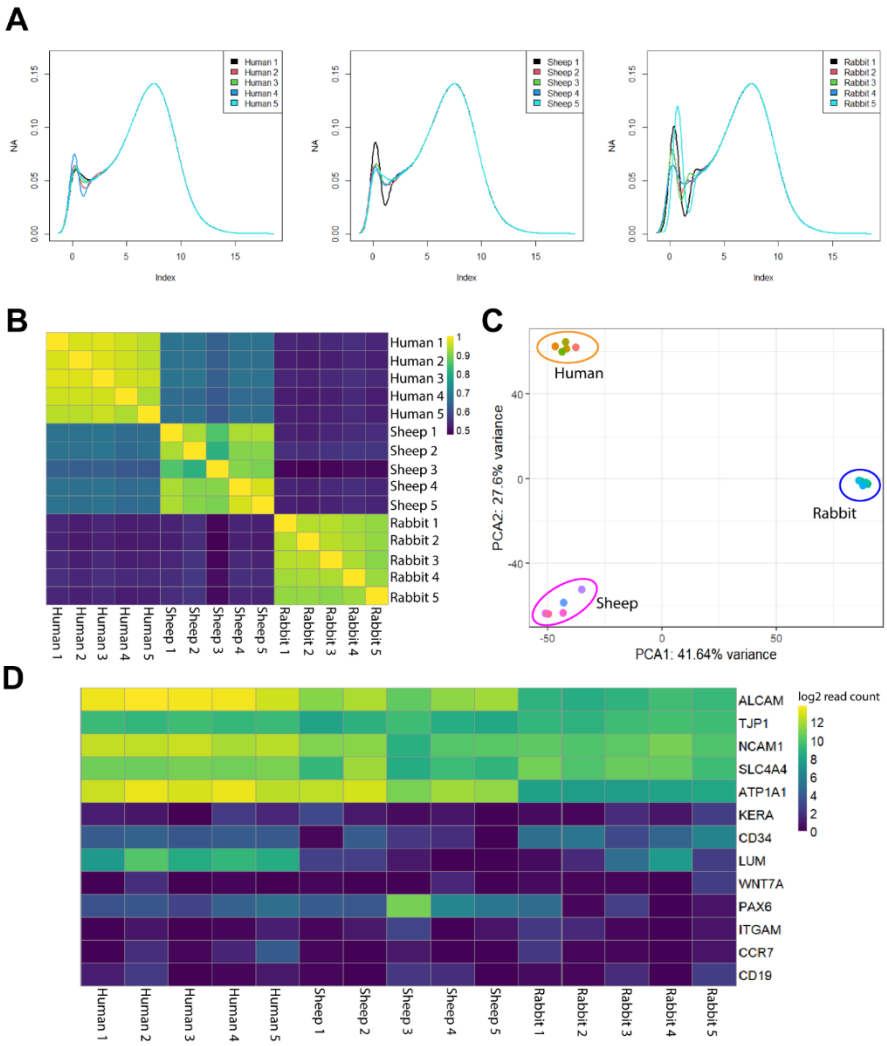

Figure 2. Human, sheep, and rabbit transcriptomic datasets shows comparable gene count distributions after data normalization (A). Correlation analysis shows that human and sheep samples have a higher correlation than rabbit corneal endothelium, confirming that rabbit corneal endothelial cells highly differed compared to human and sheep (B). Principal component analysis shows that samples originating from the same species cluster together, confirming the reproducibility of the sample isolation, and further confirms that rabbit corneal endothelial cells highly differed compared to human and sheep corneal endothelium (C). All samples had high expression of typical corneal endothelial cell markers, namely *ALCAM*, *TJP1*, *NCAM1*, *SLC4A11*, and *ATP1A1*; and absence of stromal markers (*KERA*, *CD34*, and *LUM*), epithelial markers (*WNT7A* and *PAX6*), and immune cell markers (*ITGAM*, *CCR7*, and *CD19*) confirming a successful isolation of the corneal endothelial cell transcriptome (D).

Our analysis revealed that sheep and rabbit CECs were most different, with different activity in 121 pathways (Figure 3A), followed by human and rabbit with 94 pathways with different activity (Figure 3A). Human and sheep corneal endothelium showed different activity in only 54 pathways. These results show that more pathways have a different activity when comparing species with non-proliferative and proliferative CEC (121 in sheep vs rabbit, and 94 in human vs rabbit), whereas species with non-proliferative CEC had fewer pathways with different activity, namely 54 in human vs sheep (Supplementary Figure 1).

To further understand the differences between species with proliferative (rabbit) and non-proliferative CECs (human and sheep), we selected the pathways that showed different activity when comparing both human vs rabbit as well as sheep vs rabbit, as these pathways might be related to their differing proliferative potential (Figure 3B). Our data analysis revealed a total of 52 pathways (Suppl Table 1) with different activity in both human vs rabbit and sheep vs rabbit. The detected pathways were diverse and included signaling, immune, and metabolic pathways. In all detected pathways the effect score correlated with the proliferation potential of the CECs, and pathways were more or less active in both human and sheep CECs when compared to rabbit CECs. Only 9 pathways were more active in rabbit CECs when compared to human and sheep, and 43 were more active in human and sheep when compared to rabbit (Figure 3C). These results might indicate that the possible drivers of CEC quiescence are pathways with increased activity in sheep and human.

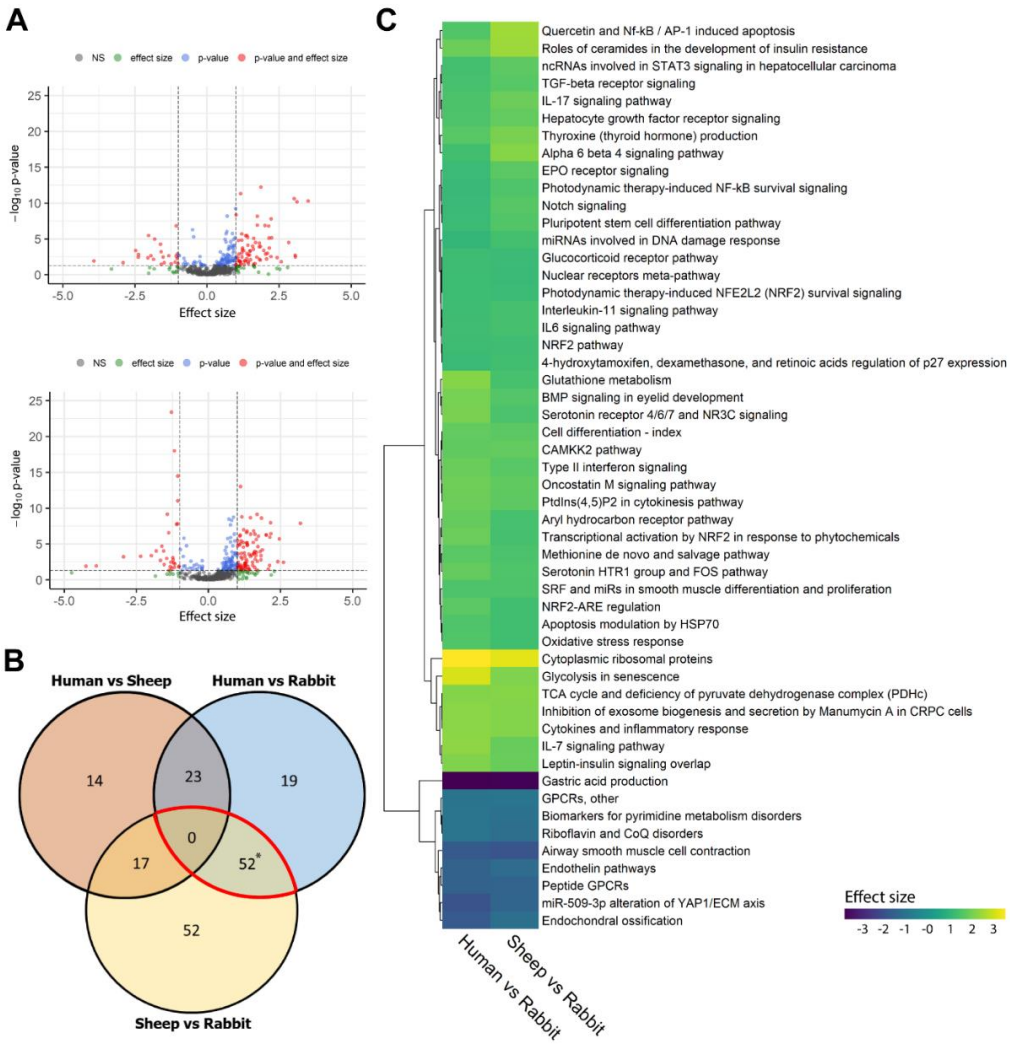

Figure 3. Volcano plots of the pathway analysis comparing species with non-proliferative corneal endothelial cells (human and sheep) with species with proliferative corneal endothelial cells (rabbit). Human vs rabbit (top) have 94 pathways with different activity and sheep vs rabbit (bottom) have 121 pathways with different activity (A). Venn diagram depicts common pathways with different activity level across species, the pathways that have a different activity in species with non-proliferative corneal endothelial cells vs species with proliferative corneal endothelial cells, namely human vs rabbit and sheep vs rabbit are highlighted with the red circle (B). Heatmap represents the effect size of pathways with different activity across human vs rabbit and sheep vs rabbit. Pathway effect size was calculated as the differences of the averaged gene counts for each species compared, e.g. human average - rabbit average (human vs rabbit). A positive effect size means higher pathway activity in sheep or human whereas a negative effect size means higher activity pathway in rabbit (C).

Notch and TGF-β signaling pathways are more active in species with non-proliferative CECs

For further analysis we did not consider pathways describing the effect of experimental procedures or external activities, such as 'photodynamic activation of NRF2'. Based on our research question, we selected pathways that could have implications on the CEC proliferative capacity. Our results revealed that Notch and TGF-β signaling pathways were more active in human and sheep CECs compared to rabbit CECs. These pathways have been demonstrated to induce senescence and endothelial to mesenchymal transition in CECs,[24–26] and could play a key role in the differences in CEC proliferative capacity between species. To better understand the implications of these pathways we performed a pathway visualization with Cytoscape (Figure 4).

Our analysis on the Notch signaling pathway showed that positive regulators of the pathway such as *DTX3*, *APH1A*, *PCAF*, and *MAML1* were more expressed in human and sheep, while Notch co-repressor genes, namely *HDAC1*, *HDAC2*, and *CTBP2* had a similar expression across species, indicating indeed an increased activity of this pathway in human and sheep CECs. We hypothesize that the downregulation of the Notch pathway could play a role in promoting the proliferative capacity of CECs in rabbits while inhibiting proliferation in human and sheep CECs.

Next, TGF-β pathway visualization showed that human and sheep CECs had increased expression of TGF-β receptors, *TGFBR1* and *TGFBR2*, and TGF-β ligand *TGFB1* when compared to rabbit CECs. In addition to this, rabbit CECs had increased expression of *LTBP1*, a *TGFB1* inhibitor, and a reduced expression of *THBS1*, an *LTBP1* inhibitor. These results together with an increased expression of downstream genes *FOS* and *SERPINE1* in human and sheep CECs compared to rabbit show an increased TGF-β signaling in species with non-proliferative CECs. We hypothesize that the increased activity in the TGF-β signaling pathway in sheep and humans may contribute to the growth arrest of CECs.

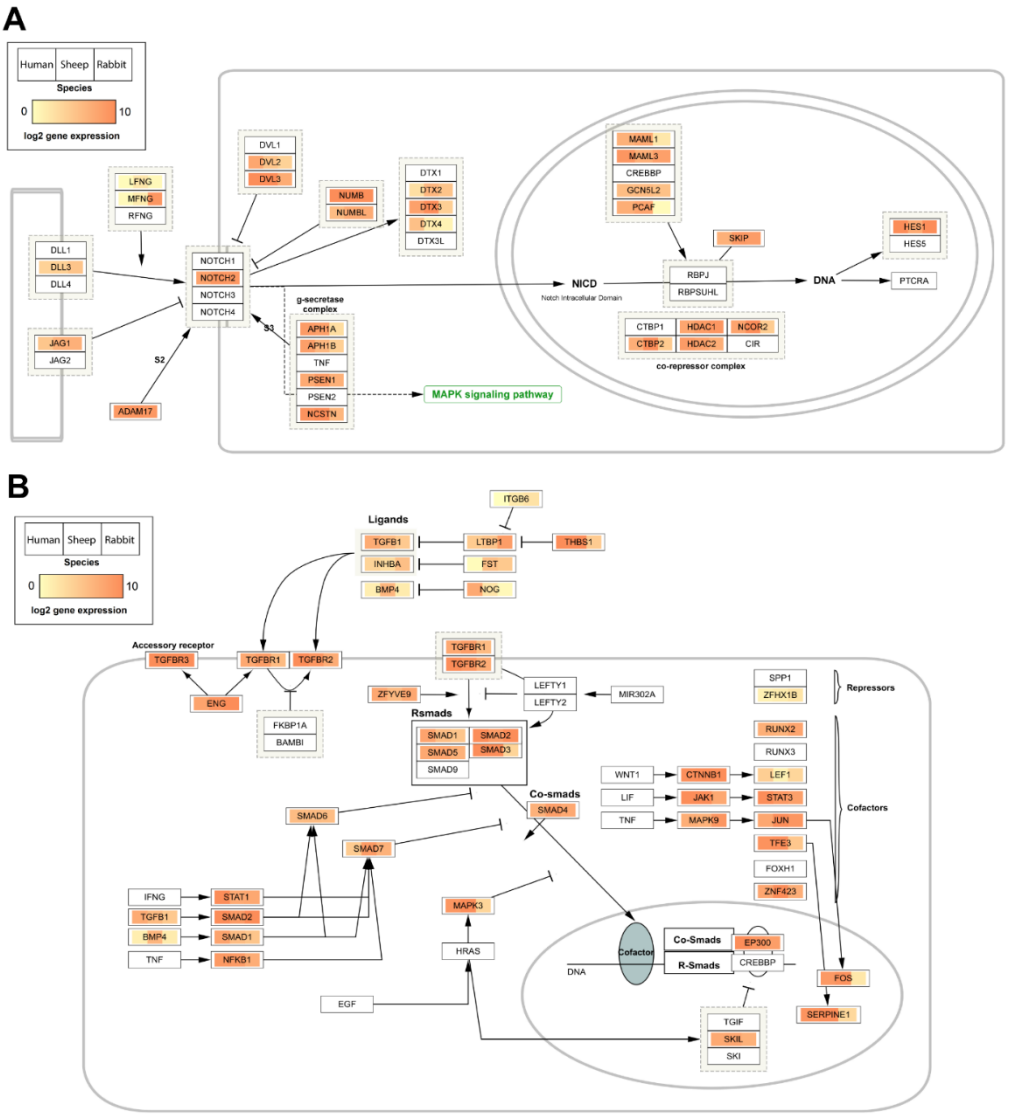

Figure 4. Visual representation of averaged read counts of human, sheep, and rabbit (left to right) of the Notch (A) and TGF-β (B) signaling pathways shows an increased activity in species with non-proliferative CECs, namely human and sheep, and a lower activity in the samples with proliferative CECs, namely rabbit.

Discussion

The proliferative capacity of CECs differs between species. While in larger mammals such as humans and sheep, CECs are arrested in a quiescent state, rabbit CECs retain a high proliferative capacity and can repopulate the endothelium upon injury. Nevertheless, there is a lack of fundamental knowledge to explain why CECs can proliferate in some species and remain quiescent in others. Gaining information on the transcriptomic differences between species with proliferative and non-proliferative CECs could allow the identification of crucial drivers of CEC proliferation to develop novel approaches to regenerate the human corneal endothelium. In this study we performed a cross-species RNA sequencing analysis between animals with non-proliferative CECs, namely human and sheep, and animals with proliferative CECs, namely rabbit. Our data present a reference transcriptomic dataset of CECs for human, sheep, and rabbit samples. Our analysis proposes a pipeline for transcriptomic homology mapping across species and subsequent pathway analysis, which could be applicable for other species comparisons. Furthermore, our analysis revealed that 52 pathways are more active when comparing two species with quiescent CECs (sheep and human) with a species with proliferative CECs (rabbit), which could play a potential role in the regulation of CEC proliferation.

We found that the decreased activity of Notch and TGF-β signaling in rabbit CECs could play a key role in their proliferation capacity. Based on previous findings, increased TGF-β has been shown to suppress proliferation in CECs *in vitro* [26] and to induce senescence in CECs.[25] Furthermore, the use of the TGF-β inhibitor SB431542 has been shown to induce human CEC proliferation *in vitro*.[27,28] Based on our results and previous findings, we suggest that TGF-β inhibition can play a crucial role in regulating CEC proliferation and could be a target to develop novel regenerative medicine therapies. Furthermore, our data shows that Notch signaling is more active in human and sheep CECs and could have biological implications in their non-

proliferative profile. This finding is similar to research performed in the corneal epithelial layer. Previous studies on cornea epithelial cells have shown that a downregulation of Notch and inhibition of the signaling pathway can cause an increase in their proliferative capacity and can contribute to epithelial regeneration [29,30]. Further research is required to understand if Notch signaling can have a similar effect on CECs and could be a suitable pathway target to promote corneal endothelium regeneration.

While our analysis reveals interesting findings at the transcriptomic level there are inherent limitations which require further attention and discussion. First, it is crucial to secure public access to updated reference genomes. While human and sheep reference genomes have been recently updated with new release versions in 2022 and 2021 respectively, improving their coverage compared to previous versions, the rabbit reference genome (OryCun2.0) has not been updated since 2009, which might limit the coverage compared to other reference genomes. It is crucial to promote the development of updated reference genomes to ensure a similar coverage of the compared species. Secondly, the gene homology mapping across species relies on publically available datasets. Our analysis could only identify 9,757 homologue genes across species, 63% of the total identified protein coding genes for rabbit and approximately 55% of the protein coding genes in sheep and human. It is possible that genes without a homologue might play a role on the proliferation capacity of CEC, which would then not be portrayed in our results. Further research in identifying gene homologues across species can directly impact this research by providing platforms for more extensive data analysis.

One of the main caveats in the field, which we also encountered in our study, is how to perform data normalization across each species' transcriptomic data. Each species' gene transcript length may vary, and should be taken into account when performing data normalization. Nevertheless, there is currently no existing method to perform such correction on transcriptomic datasets of three different species [31,32].

Taking into consideration such limitations, we performed a quantile normalization which took into account library size and distribution, and performed a non-parametric Wilcoxon rank-sum test to identify more or less active pathways across species. Analyzing the data with typical packages such as DESeq2 which performs a parametric test on gene expression would lead to the appearance of many false positive and negative results, which might impair the conclusions taken from such a study. Several studies are focusing on correcting such differences by mapping to a single reference genome, in the case of close species, with the risk of enriching for genes in the sample from the same species reference genome.[31,33] Future studies will shed light on this problem.

Besides analyzing the intrinsic interspecies transcriptome differences, a highly interesting follow-up study to our findings would be to compare the transcriptomic pathway changes in each species' CECs upon injury. After a scratch test of the cornea endothelium, the human, rabbit, and sheep CECs can be analyzed and compared to the transcriptome profiles presented in this study followed by an interspecies comparison of the differentially expressed genes upon injury within each species. This follow-up study would be a more targeted approach to identify differentially expressed genes upon injury and could provide additional information on the CEC post-injury CEC proliferation and healing capacity across species.

Overall, our study provides an automated pipeline for cross-species transcriptome comparisons and pathway activity analysis, which can be applied to any interspecies study. Our data suggests that species with non-proliferative corneal endothelium are more similar than those species with a proliferative corneal endothelium. Furthermore, our data analysis reveals that 52 pathways have different activity when comparing species with proliferative CECs (rabbit) to species with quiescent CECs (human and sheep).

Funding

The EyeSciTe consortium under the Chemelot InSciTe framework funded this research.

Acknowledgements

The authors thank Rachelle Peeters (Central Animal Laboratory (CPV), Maastricht University, Maastricht, the Netherlands) for providing us with sheep ocular globes. The authors also thank Dr Koen R.D. Vaessen (General Animal Laboratory (GDL), Utrecht University, Utrecht, the Netherlands) for providing us with the ocular tissue of three rabbits, and Dr Darragh Crosbie (MERLN Institute, Maastricht, the Netherlands) and Marloes Witte (Animal Welfare Body, MSD Animal Health, Boxmeer, the Netherlands) for providing us with the ocular globes of two rabbits. The authors finally thank the ETB-BISLIFE (Beverwijk, the Netherlands) for providing us research-grade human corneal tissue.

Data availability

The mapping of the transcriptomic data of each species was performed using the following reference genomes available in NCBI: OryCun2.0 (Rabbit) GCF_000003625.3, ARS-UI_Ramb_v2.0 (Sheep) GCF_016772045.1, and Hg38 (Human) GCF_000001405.26. The transcriptomic data regarding this study has been deposited to the Gene Expression Omnibus with accession number GSE222458. All data and figures have been deposited and made publically available in DataVerseNL and are accessible via the following link: https://doi.org/10.34894/9HK3GT. The R script pipeline for the data processing of this study has been made publically available in GitHub and is accessible using the following link: https://github.com/PereCatQ/Cross-species-pathway-analysis.

References

1. DelMonte, D. W. & Kim, T. Anatomy and physiology of the cornea. *J. Cataract Refract. Surg.* **37**, 588–598 (2011).
2. Bonanno, J. A. Molecular mechanisms underlying the corneal endothelial pump. *Exp. Eye Res.* **95**, 2–7 (2012).
3. Català, P. *et al.* Approaches for corneal endothelium regenerative medicine. *Prog. Retin. Eye Res.* **87**, 100987 (2022).
4. Al Abdulsalam, N. K., Barnett, N. L., Harkin, D. G. & Walshe, J. Cultivation of corneal endothelial cells from sheep. *Exp. Eye Res.* **173**, 24–31 (2018).
5. Valdez-Garcia, J. E., Lozano-Ramirez, J. F. & Zavala, J. Adult white New Zealand rabbit as suitable model for corneal endothelial engineering. *BMC Res. Notes* **8**, 4–7 (2015).
6. Park, S. *et al.* Animal models of corneal endothelial dysfunction to facilitate development of novel therapies. *Ann. Transl. Med.* **9**, 1271 (2021).
7. Price, M. O., Mehta, J. S., Jurkunas, U. V. & Price, F. W. Corneal endothelial dysfunction: Evolving understanding and treatment options. *Prog. Retin. Eye Res.* **82**, 100904 (2021).
8. Gain, P. *et al.* Global survey of corneal transplantation and eye banking. *JAMA Ophthalmol.* **134**, 167–173 (2016).
9. Català, P. *et al.* Transport and preservation comparison of preloaded and prestripped-only DMEK grafts. *Cornea* **39**, 1407–1414 (2020).
10. Hashimshony, T. *et al.* CEL-Seq2: Sensitive highly-multiplexed single-cell RNA-Seq. *Genome Biol.* **17**, 1–7 (2016).
11. Dobin, A. *et al.* STAR: Ultrafast universal RNA-seq aligner. *Bioinformatics* **29**, 15–21 (2013).
12. R Core Team. R: A language and environment for statistical computing. (2013).
13. Raudvere, U. *et al.* g:Profiler: A web server for functional enrichment analysis and conversions of gene lists (2019 update). *Nucleic Acids Res.* **47**, 191–198 (2019).
14. Ritchie, M. E. *et al.* Limma powers differential expression analyses for RNA-sequencing and microarray studies. *Nucleic Acids Res.* **43**, e47 (2015).
15. Martens, M. *et al.* WikiPathways: Connecting communities. *Nucleic Acids Res.* **49**, 613–621 (2021).
16. Shannon, P. *et al.* Cytoscape: A software environment for integrated models of biomolecular interaction networks. *Genome Res.* **13**, 2498–2504 (2003).
17. Català, P. *et al.* Single cell transcriptomics reveals the heterogeneity of the human cornea to identify novel markers of the limbus and stroma. *Sci. Rep.* **11**, 21727 (2021).
18. He, Z. *et al.* 3D map of the human corneal endothelial cell. *Sci Rep* **6**, 29047 (2016).

19. Fernández-Pérez, J. & Ahearne, M. Influence of biochemical cues in human corneal stromal cell phenotype. *Curr. Eye Res.* **44**, 135–146 (2019).

20. Hayashi, R. *et al.* Co-ordinated ocular development from human iPS cells and recovery of corneal function. *Nature* **531**, 376–380 (2016).

21. Zheng, P. F. *et al.* Identifying patterns of immune related cells and genes in the peripheral blood of acute myocardial infarction patients using a small cohort. *J. Transl. Med.* **20**, 1–18 (2022).

22. Förster, R., Davalos-Misslitz, A. C. & Rot, A. CCR7 and its ligands: Balancing immunity and tolerance. *Nat. Rev. Immunol.* **8**, 362–371 (2008).

23. Globerson Levin, A., Rivière, I., Eshhar, Z. & Sadelain, M. CAR T cells: Building on the CD19 paradigm. *Eur. J. Immunol.* **51**, 2151–2163 (2021).

24. Li, C. *et al.* Notch signal regulates corneal endothelial-to-mesenchymal transition. *Am. J. Pathol.* **183**, 786–795 (2013).

25. Li, Z. *et al.* TGF-b induces corneal endothelial senescence via increase of mitochondrial reactive oxygen species in chronic corneal allograft failure. *Aging (Albany. NY).* **10**, 3474–3485 (2018).

26. Harris, D. L. & Joyce, N. C. Transforming growth factor-β suppresses proliferation of rabbit corneal endothelial cells in vitro. *J. Interf. Cytokine Res.* **19**, 327–334 (1999).

27. Okumura, N. *et al.* Inhibition of TGF-β Signaling Enables Human Corneal Endothelial Cell Expansion In Vitro for Use in Regenerative Medicine. *PLoS One* **8**, (2013).

28. Kinoshita, S. *et al.* Injection of cultured cells with a ROCK inhibitor for bullous keratopathy. *N. Engl. J. Med.* **378**, 995–1003 (2018).

29. Djalilian, A. R. *et al.* Down-regulation of Notch signaling during corneal epithelial proliferation. *Mol. Vis.* **14**, 1041–1049 (2008).

30. Movahedan, A. *et al.* Notch inhibition during corneal epithelial wound healing promotes migration. *Investig. Ophthalmol. Vis. Sci.* **53**, 7476–7483 (2012).

31. Chung, M. *et al.* Best practices on the differential expression analysis of multi-species RNA-seq. *Genome Biol.* **22**, 121 (2021).

32. Zhou, Y. *et al.* A statistical normalization method and differential expression analysis for RNA-seq data between different species. *BMC Bioinformatics* **20**, 163 (2019).

33. Akkose, U. *et al.* Comparative analyses of two primate species diverged by more than 60 million years show different rates but similar distribution of genome-wide UV repair events. *BMC Genomics* **22**, 600 (2021).

Supplementary information

Supplementary Figure 1

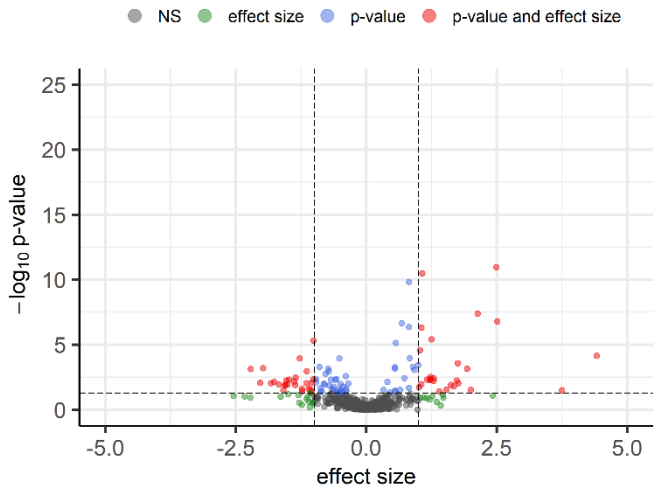

Supplementary Figure 1. Volcano plots of the pathway analysis in human vs sheep depicts different activity level in 54 pathways.

SUPPLEMENTARY TABLE 1. 52 Pathways with a common different activity when comparing Human vs Rabbit and Sheep vs Rabbit.

Pathway name	Pathway ID	Effect Size Human vs Rabbit	Pvalue Human vs Rabbit	Effect Size Sheep vs Rabbit	Pvalue Sheep vs Rabbit	Effect size Human vs Sheep	Pvalue Human vs Sheep
Glutathione metabolism	WP100	2,151381723	7,83E-06	1,333763109	0,00263735	0,817618613	0,021187285
GPCRs, other	WP117	-1,069610544	0,002469105	-1,012212914	0,012609825	-0,05739763	0,638751852
miRNAs involved in DNA damage response	WP1545	1,009731265	0,003279574	1,275640393	0,004458933	-0,265909128	0,855044223
Thyroxine (thyroid hormone) production	WP1981	1,58249933	0,000104373	2,003681276	5,44E-07	-0,421181946	0,434063804
SRF and miRs in smooth muscle differentiation and proliferation	WP1991	1,42556584	0,01551432	1,426359984	0,038102819	-0,000794143	0,52536065
Cell differentiation - index	WP2029	1,727202409	0,00353378	1,646132127	0,000400265	0,081070282	0,477913589
IL-7 signaling pathway	WP205	2,240694999	7,13E-06	1,794221517	0,000114961	0,446473483	0,780897923
IL-17 signaling pathway	WP2112	1,411267892	6,06E-06	1,841492929	2,47E-09	-0,430225037	0,362401208
Endothelin pathways	WP2197	-1,589904486	0,000622455	-1,318659024	0,014439021	-0,271245462	0,473616828
Interleukin-11 signaling pathway	WP2332	1,204687808	2,02E-06	1,323401723	2,45E-07	-0,118713915	0,488670106
Oncostatin M signaling pathway	WP2374	1,869383543	5,82E-13	1,686964335	7,25E-10	0,182419208	0,272328498
Peptide GPCRs	WP24	-1,610199064	5,59E-05	-1,552603364	9,30E-05	-0,0575957	0,981279133
Quercetin and Nf-kB / AP-1 induced apoptosis	WP2435	1,490931659	0,000447495	2,460513764	1,85E-06	-0,969582105	0,004390985
Alpha 6 beta 4 signaling pathway	WP244	1,271718006	0,000442489	2,154490961	1,06E-08	-0,882772955	0,021657844
TCA cycle and deficiency of pyruvate dehydrogenase complex (PDHc)	WP2453	2,140279267	1,53E-07	2,164972335	3,63E-07	-0,024693068	0,178598554
Aryl hydrocarbon receptor pathway	WP2586	1,745120672	1,23E-07	1,348726468	1,49E-05	0,396394205	0,384723671
Gastric acid production	WP2596	-3,920484099	0,011925234	-3,88822432	0,011159425	-0,032259779	0,823664389
Notch signaling	WP268	1,105651137	0,001304792	1,556776912	6,08E-06	-0,451125775	0,075830938
Pluripotent stem cell differentiation pathway	WP2848	1,142106558	0,012177929	1,503729429	0,000335791	-0,361622871	0,605618402
Glucocorticoid receptor pathway	WP2880	1,208883478	0,000865354	1,133947048	0,00068614	0,074936429	0,751234682

Nuclear receptors meta-pathway	WP2882	1,166666173	4,76E-12	1,118518038	9,61E-14	0,048148135	0,82583145
NRF2 pathway	WP2884	1,201457236	1,49E-05	1,22499089	1,06E-07	-0,023533654	0,983459042
Transcriptional activation by NRF2 in response to phytochemicals	WP3	1,851190202	0,000116624	1,306644221	0,001335604	0,544545981	0,200373577
Hepatocyte growth factor receptor signaling	WP313	1,4188864	7,52E-05	1,733751548	8,28E-07	-0,314865148	0,128373295
Methionine de novo and salvage pathway	WP3580	1,614354549	0,032870271	1,412016382	0,030168693	0,202338167	0,905991582
Photodynamic therapy-induced NFE2L2 (NRF2) survival signaling	WP3612	1,1707695	0,024299261	1,142848429	0,025621918	0,027921071	0,927941405
Photodynamic therapy-induced NF-kB survival signaling	WP3617	1,077397758	0,004717535	1,457086032	0,000525742	-0,379688274	0,37675763
IL6 signaling pathway	WP364	1,221570512	0,000319259	1,324601328	6,84E-06	-0,103030816	0,635597855
Apoptosis modulation by HSP70	WP384	1,475418028	0,001747636	1,272055773	0,007980561	0,203362255	0,935226283
4-hydroxytamoxifen, dexamethasone, and retinoic acids regulation of p27 expression	WP3879	1,116190834	0,012843455	1,265185218	0,010948671	-0,148994385	0,25872364
BMP signaling in eyelid development	WP3927	1,972201498	0,000399133	1,534076742	0,003392092	0,438124756	0,217962128
Leptin-insulin signaling overlap	WP3935	2,09528424	0,001035407	1,82344973	0,00042081	0,27183451	0,591510552
miR-509-3p alteration of YAP1/ECM axis	WP3967	-2,025707357	3,31E-06	-1,532208109	0,007549813	-0,493499248	0,237621004
Oxidative stress response	WP408	1,494165374	0,000517231	1,264096192	0,005320095	0,230069182	0,635806368
Inhibition of exosome biogenesis and secretion by Manumycin A in CRPC cells	WP4301	2,225258356	1,61E-08	2,130830506	1,15E-06	0,09442785	0,456706657
ncRNAs involved in STAT3 signaling in hepatocellular carcinoma	WP4337	1,285612363	0,036608456	1,66383334	0,000139561	-0,378220977	0,474483486
NRF2-ARE regulation	WP4357	1,622792244	8,52E-06	1,246502239	0,000168359	0,376290006	0,276631142
Biomarkers for pyrimidine metabolism disorders	WP4584	-1,004871049	0,028128626	-1,16222892	0,005635948	0,157357871	0,515974651
Endochondral ossification	WP474	-1,812888859	1,07E-05	-1,221297387	0,001663837	-0,591591472	0,143387899
Cytoplasmic ribosomal proteins	WP477	3,507109619	5,33E-11	3,192785027	1,31E-08	0,314324592	0,31210837
CAMKK2 pathway	WP4874	1,684009636	3,15E-05	1,718992188	2,35E-05	-0,034982552	0,877436604

Airway smooth muscle cell contraction	WP4962	-1,855532092	0,006979143	-1,97698521	0,000415968	0,121453118	0,943510886
Riboflavin and CoQ disorders	WP5037	-1,021460095	0,001258408	-1,231102923	0,000789328	0,209642828	0,908072237
Glycolysis in senescence	WP5049	3,067505998	0,003177612	2,075195905	0,031254308	0,992310093	0,193486375
Roles of ceramides in the development of insulin resistance	WP5181	1,845186768	0,009243993	2,407609337	0,002935555	-0,562422569	0,752969634
PtdIns(4,5)P2 in cytokinesis pathway	WP5199	1,82593528	0,007116697	1,67571373	0,040383449	0,15022155	0,964598395
Cytokines and inflammatory response	WP530	2,215688007	0,002890035	2,11970998	0,009373095	0,095978028	0,915789529
TGF-beta receptor signaling	WP560	1,339036975	3,48E-06	1,57030001	1,49E-07	-0,231263035	0,530314829
EPO receptor signaling	WP581	1,155729346	0,04308632	1,623190139	0,001231006	-0,467460793	0,348768998
Type II interferon signaling	WP619	1,814399682	0,000127894	1,584759989	0,000175036	0,229639693	0,477311973
Serotonin HTR1 group and FOS pathway	WP722	1,744295436	6,82E-09	1,46298378	4,14E-07	0,281311657	0,381625123
Serotonin receptor 4/6/7 and NR3C signaling	WP734	2,010104678	1,35E-07	1,407281882	0,000248749	0,602822796	0,067374541

7

Discussion

Discussion

Regenerative medicine (RM) aims to repair, replace, or regenerate cells, tissues or organs that have been damaged in order to reestablish physiological function. One of the main challenges RM aims to tackle is the donor tissue or organ shortage, which is still not solved even with national rules of opt-out organ donation. The cornea is no exception to that and the current human donor cornea imbalance requires an urgent need to develop novel therapies to treat corneal endothelial disease. The work reported in this thesis is aimed towards the development of clinically relevant regenerative medicine and cell therapies that could provide treatment to those patients without access to donor corneas.

More is needed to maximize donor tissue use

In addition to developing complex therapeutic approaches there is the need to maximize the use of each donor cornea available for transplant. With the advances in corneal transplantation techniques, surgeons can selectively replace a damaged corneal layer. For example, Descemet's membrane endothelial keratoplasty (DMEK) is used to selectively replace the corneal endothelium affected by corneal endothelial disease,[1–3] and deep anterior lamellar keratoplasty (DALK) is used to selectively replace the epithelium and stroma layers from corneas with stromal scarring or dystrophies such as keratoconus.[4,5] It is possible to obtain a graft for DMEK and a graft for DALK from the same donor cornea, an approach known as split-cornea,[6,7] optimizing the use of donor tissue. Nonetheless, given the low volume of DALKs, this approach is still insufficient to all the patients awaiting for donor tissue. Other approaches such as hemi[8] and even quarter[9] DMEK have been studied as approaches to maximize donor tissue use. Nevertheless, these techniques have been associated with significant cell loss and can only serve patients with mild disease.

A crucial aspect to be able to successfully maximize donor tissue use is to be able to transport DMEK tissue from areas with donor tissue surplus to areas with donor tissue shortage, meeting tissue supply and demand globally. Preloaded DMEK transport systems have been recently developed to allow the cornea bank to send an already prestripped endothelial graft for DMEK[10–12] and have shown that DMEK tissue can be transported cross-countries without affecting tissue quality.[13] Furthermore, the use of preloaded DMEK systems can enable the application the split-cornea approach into the clinics, and reduce the risk of iatrogenic tissue damage when stripping the corneal endothelium from pre-cut corneas on the operation theater, allowing novice surgeons to rapidly adapt to the DMEK procedure and making sure no donor tissue is lost. In Chapter 3, we performed a validation study confirming that stripped corneal endothelial grafts transported using the novel DMEK RAPID preloaded transport system reach the operation room with the same viability and quality as conventional prestripped endothelial grafts transported on a whole cornea. The validation of preloaded DMEK systems is a key aspect for their implementation into the clinics, which consequently allows optimization of donor tissue.

While preloading devices for DMEK can aid to optimize the use of donor corneas, there are aspects which require attention. Before performing the keratoplasty, it is necessary to wash with ophthalmic irrigation solution the preloaded endothelium in order to remove excess of cornea preservation media. The shear stress generated during this procedure could damage the tissue. Moreover, there is often the need to re-stain the endothelial graft in order to aid the tissue grafting in its correct position, which is laborious and can potentially damage the tissue. Developing preloaded DMEK systems that allow for an optimized wash could improve the adoption of these devices. Furthermore, the development of a ready-to-inject cornea transport media or the use of endothelium staining methods which ensured tissue staining over long periods of time without affecting tissue viability could facilitate the adoption of these systems.

Finally, it is worth to mention that many surgeons are used to transplanting pre-stripped corneas, as this is currently the default procedure. Changing practice patterns to adapt to a novel device might be challenging if this is not directly linked to an improvement in the therapeutic outcome, such as for this procedure. The early training of novice surgeons with preloaded DMEK devices could change the practice patterns enabling a maximization of tissue use. Furthermore, the high costs associated to these devices can also prevent its adoption.

How can we obtain sufficient understanding to develop translational regenerative medicine therapies?

Maximizing the use of donor corneas is an elegant approach to provide treatment to some patients in need, but it does not solve the current corneal donor tissue shortage. There is an imperative need to develop novel approaches to treat corneal endothelial disease.

The improvement of protocols to generate and expand corneal cells in the lab opens the possibility to treat patients with a cell therapy, drastically reducing the need for donor tissue.[14–16] Nevertheless, the cornea is a highly heterogeneous tissue, and to develop successful cell therapies it is critical to know its characteristics and how the cells populating it regulate tissue homeostasis. Without a good reference of cell types, generating therapeutically relevant cells is unlikely. Traditionally, the human corneal layers have been analyzed as bulk entities because of the lack of readily available tools to accurately account for their cellular heterogeneity. With the development of single cell RNA sequencing (scRNAseq) techniques, it is possible to critically evaluate the cornea at the single cell level to unravel the different transcriptomic blueprints of corneal cell types.

While many single-cell transcriptomic studies in different tissues have been published over the last 5–7 years,[17–20] scRNAseq has been only recently translated in the field of corneal research, with the first studies published in 2021.[21–24] In Chapter 4 we performed a high-quality scRNAseq analysis of the healthy human cornea to generate one of the first transcriptomic cell census of this tissue. This study allows us to further understand the cellular complexity of the human cornea, providing transcriptomic information of 19,472 corneal cells isolated from four female and four male donors. The deep characterization of corneal tissue we provide is of great importance for the development of novel cell therapies and regenerative medicine approaches as it provides a baseline and a reference on each corneal cell type in regards of phenotype, transcriptome and functionality. These studies are likely to have a major impact for future profiling of corneal disease states, to help guide pluripotent stem cells into different corneal lineages, and to understand how engineered substrates affect corneal cells to improve regenerative therapies. Furthermore, this dataset identified markers exclusively expressed in cells comprising the limbal epithelial stem cell niche, highly proliferating epithelial cells, and stromal keratocytes which could be used as reference to improve current corneal cell replacement therapies. Future research might allow to translate these findings into the clinic, for example using the novel markers to enrich for proliferative corneal epithelial cells.

Besides providing a reference for the development of regenerative medicine therapies, scRNAseq can be used as a platform for a targeted improvement of existing cell therapies. For example, the primary expansion of human corneal epithelial cells (CECs) appears as an alternative to treat multiple patients from a single donor. This cell therapy is currently being tested with clinical trials taking place mainly in Singapore and Japan, which will give powerful information regarding surgical procedure to deliver the cells, graft survival over time, and therapeutic outcome. Nevertheless, this technique is far from ideal and has some limitations, preventing its worldwide adoption: Primary CEC cultures are only

successful if derived from donors younger than 45 years; cell yields are limited; the cultures become heterogeneous over extended culture time; cell undergo major alterations after passage 2, affecting both cell phenotype and functionality; and there is a lack of clear markers to identify cells which will lead to therapy success. In the past five to seven years, no major advances on the protocols for the expansion of primary human CECs have been made.

In Chapter 5 of this thesis, we report using scRNA as a platform to improve the primary expansion protocols and primary CEC-based therapy using single cell transcriptomics. We provided the first scRNAseq dataset from 42,220 primary cultured human CECs. Our study is a step forward in the field and presents the changes in the transcriptome in human CECs over culture time. First, we could identify high-quality CECs that are the ideal target for a cell therapy, CECs transitioning towards an undesirable senescent phenotype, and CECs that had undergone an endothelial-to-mesenchymal transition and presented a fibrotic transcriptome profile. Besides the confirmation of the heterogeneity of primary cultured CECs, our study allowed us to track changes in genetic pathways activated over the detected populations of cells, suggesting possible genetic pathways that could be targeted with small molecules for the improvement of primary culture protocols. Follow-up studies are required to apply this findings in the attempt to improve primary culture protocols. Finally, this study allowed us to identify novel markers for the characterization of therapy-grade CECs and those of lower quality, which hopefully will have a major impact on the quality assessment of primary cultured CEC for its clinical use.

While the recent scRNAseq studies of the native human cornea present novel and powerful datasets to understand corneal cell heterogeneity there are aspects requiring attention. First, the published studies present datasets of 16,000 to 47,000 corneal cells originating from several donors, [21–24] this is a small fraction of cells if we take into account that the human cornea is composed of a few million cells. It is very

likely that these studies are missing minor corneal cell populations that were not detected by scRNAseq. A major relevant study that could be done as a follow-up to this thesis would be the integration of the different corneal scRNAseq datasets, to generate a cross-study scRNAseq cornea atlas. The integration of the scRNAseq data of different studies is not a trivial process, as sequencing technology and depth should be accounted for, but this could allow the identification of novel cell populations otherwise disregarded.

Overall, the work described in this thesis as well as the recent studies demonstrate the power of scRNAseq, we should point out one of its major pitfalls: its elevated operational costs. These costs often compromise researchers into performing a deep sequencing of a few cells or a shallow sequencing of many cells, when the ideal situation would be sequencing many cells at a high sequencing depth such as 50,000-80,000 reads per cell. Further developments and advances in single-cell transcriptomics will likely simplify the protocols and reduce costs, considerably increasing its accessibility and having a major impact on regenerative medicine and cell therapies. Furthermore, with the emerging of high-throughput multiomics, single-cell transcriptomic information will be combined with single-cell metabolomics and proteomics, unraveling novel biological processes previously unknown.

How can the diversity of the animal kingdom aid to guide the development of regenerative medicine therapies?

In addition to scRNAseq, we deployed bulk RNA sequencing (RNAseq) to investigate the mechanisms underlying CEC proliferation, an important goal for regenerative corneal therapies. To do so, we investigated the transcriptomic differences between human, sheep, and rabbit CECs because their regenerative capacity differs.

One of the main research focus on corneal endothelial regenerative medicine is to force CECs to exit their G1 phase to proliferate and repopulate the damaged tissue. Small molecules and recombinant proteins such as Y-27632,[25] K-115,[26] SB431542,[27] and FGF-1[28] have been identified to promote endothelial proliferation and regeneration. Nevertheless these drugs are far from optimal as they only promote regeneration on a low percentage of patients,[26,29–32] and could potentially cause a loss of cell phenotype and function. There is the need to further understand the mechanisms behind the promotion of CEC proliferation to design successful regenerative medicine therapies.

In Chapter 6 we followed an interesting approach to elucidate the mechanisms behind CEC proliferation by investigating the transcriptomic differences of CECs of different animals. The regenerative capacity of CECs differs between species: in bigger mammals such as humans and sheep, CECs are arrested at a quiescent state, lacking regenerative capacity of this tissue through cell division. In contrast, rabbit CECs retain a high proliferative capacity and can repopulate the endothelium in response to damage. With this interspecies transcriptome comparison we identified genetic pathways up and down regulated in each of the species, which could allow the identification of new drug candidates to promote CEC division and tissue repair.

This Chapter portrays how the diversity of the animal kingdom can be understood to develop regenerative therapies for treating corneal endothelial disease. The comparison across the transcriptome of different species is not a straightforward process and requires attention. First, it is crucial to secure public access to reference genomes, while human or mouse reference genomes have been recently updated, we found that the coverage of the rabbit reference genome (OryCun2.0) was not as deep as the ones found for other species and had not been updated since 2009. Moreover, the most updated sheep reference genome (ARS-UI_Ramb_v2.0) recently published in 2021 did not contain all the gene ENSEMBL identifiers for the newly included genes, hindering the downstream analysis of the data. It is of high importance to

promote research on improving the publically available reference genomes in order to perform more meaningful and complete analysis. Secondly, the homology mapping across species also relies on publically available datasets. In our analysis we could not include genes for which a homologue had not been described, further research in finding gene homologues across species can directly impact this research. Finally, the differences in transcript length across species hinders the parametric comparison of gene counts across species, and typical packages used for RNAseq analysis such as DESeq2[33] do not account for such differences and should not be used in such analysis. For this reason in our analysis we performed a Wilcoxon rank-sum test, non-parametric test, at the pathway level to detect for differences across species. To date, there is no solution this problem. Researchers are focusing in correcting such differences by mapping to a single reference genome, in the case of close species, with the risk of enriching for genes in the sample from the same species.[34–36] Alternatively, some studies are trying to correct for each transcript length in regards to each species, obtaining promising results.[36,37] Future studies will shed light into this problem likely solving it.

The research pipeline we developed is not only specific for CEC, but could be applicable to other regenerative medicine approaches comparing other species and organs. Different animals have shown regeneration of full limbs such as the starfish,[38] or more recently, a sea slug was proven to fully regenerate the whole body from its head.[39] Gaining insight into those exceptional cases could unravel novel ways to promote tissue regeneration. Besides analyzing the intrinsic interspecies transcriptome differences, a highly interesting follow-up study to this thesis would be to compare the transcriptomic pathway changes in each species CECs upon injury. After a scratch test of the corneas, the human, rabbit, and sheep corneal endothelium can be sequenced, then compared to its reference transcriptome presented in this thesis following an interspecies comparison of the differentially expressed genes upon CEC injury. This follow-up study could give additional crucial information on CEC proliferation capacity and healing post-injury across species.

Future perspectives on this thesis and corneal endothelial cell therapy

The results presented in this thesis focus on improving therapeutic options for corneal diseases, from pragmatic devices to maximize donor tissue use that can be immediately implemented to improve overall corneal surgeries and ease the donor burden to fundamental knowledge about native corneal cells and understanding the changes arising from the primary culture of CECs with the main aim to design successful cell therapies. Follow-up studies are required to translate the findings of this thesis to improve regenerative medicine approaches. Future research should focus on further characterizing the novel limbal and endothelial markers we identified to conclude if they indeed lead to more successful therapies. Furthermore, with the genetic pathway-level information we gained, it is highly likely to modify primary culture protocols to obtain more cells without loss of phenotype, but also to identify novel target drugs to promote corneal endothelial proliferation and healing *in vivo*. It is very likely that research based on the findings in this thesis will aid to develop protocols to successfully improve primary culture protocols of CECs and successfully culture older donor corneas. The presented the pseudotemporal transcriptomic changes arising from individual CECs over different culture passages could open the possibility to select for small molecules to tackle the alterations deriving from the primary culture.

Complementary research to this thesis will also be required to further develop cell delivery methods, as the success of such therapies hinges on a suitable method to deliver them into the cornea. Therapy-grade cells have to be delivered alive and with sufficient potential integrate in the cornea. The main two methods currently studied for delivery of CECs are cell injection into the anterior chamber of the eye, which its main appeal is its simplicity but uses 1 million cells per eye,[14] and the use of different substrates in the effort of bioengineering corneal endothelial grafts. CEC scaffolds allow to directly position the cells in contact with the cornea, reducing the

number of cells needed for therapy to approximately 200,000 per cornea, but requires a more technically challenging procedure.[40] The clinical trials in Japan and Singapore will soon provide novel insight on the delivery methods, but further research is required on trying to reduce the amount of CEC needed to treat a cornea with a cell injection and developing new scaffolds for bioengineering corneal endothelial grafts. A promising approach is the generation of a fully synthetic CEC scaffold which could integrate in the recipient cornea. Despite extensive research there is not yet a successful synthetic scaffold which can maintain endothelial thickness, transparency, resistance, and can integrate to the recipient cornea. Synthetic scaffolds would reduce both cost and requirement of donor tissue compared to the current stroma-derived scaffolds,[40] but also provide standardization on bioengineered corneal endothelial grafts.

Finally, due to the immune privileged nature of the corneal endothelium and its tolerogenicity, therapy-grade CECs could be successfully generated from both embryonic and induced pluripotent stem cells.[16] Differentiating human pluripotent stem cells to CECs presents several advantages, such as the faster *in vitro* expansion of pluripotent stem cells compared to primary cultured CECs and independence from donor corneas. However, protocols for deriving CECs from pluripotent stem cells are still at an early developmental stage.[41–44] The critical transcriptomic pathways and the identification of novel CEC markers described in this thesis, could improve pluripotent stem cell differentiation, which offers an unlimited cell source and breaks the reliance on donor corneas.

Research and Medicine are advancing towards a personalized approach for treating corneal endothelial disease

Nowadays, endothelial keratoplasty is the default intervention to treat corneal endothelial disease. Research on regenerative medicine therapies is increasing the therapeutic arsenal to treat corneal endothelial disease. With the increase in the therapeutic repertoire, it is the surgeons' responsibility to critically select the best

treatment option for each patient, advancing towards personalized corneal endothelium regenerative medicine. In the coming years, research will allow deeper understanding of what spectrums of corneal endothelial disease could be successfully treated with each approach. For example, it is possible that Fuchs' endothelial cell dystrophy (FECD), with a mildly affected Descemet's membrane and an intact peripheral endothelium, could be treated with a pharmacological approach, to promote cell proliferation, alone or in combination with Descemet's stripping only of the central damaged area. On the other hand, advanced FECD could be treated by lamellar keratoplasty or cell therapy delivered using a carrier. Patients suffering from bullous keratopathy could be treated with a cell injection of hCECs. A personalized medicine approach will allow greater access for more people to therapy and the cornerstone to tackle global donor shortage.

References

1. Dunker, S. L. *et al.* Real-world outcomes of DMEK: A prospective Dutch registry study. *Am. J. Ophthalmol.* **222**, 218–225 (2021).

2. Dickman, M. M. *et al.* Changing practice patterns and long-term outcomes of endothelial versus penetrating keratoplasty: A prospective Dutch registry study. *Am. J. Ophthalmol.* **170**, 133–142 (2016).

3. Birbal, R. S. *et al.* Five-year graft survival and clinical outcomes of 500 consecutive cases after Descemet Membrane Endothelial Keratoplasty. *Cornea* **39**, 290–297 (2020).

4. Bahar, I. *et al.* Comparison of three different techniques of corneal transplantation for keratoconus. *Am. J. Ophthalmol.* **146**, 905–912 (2008).

5. Awan, M. A., Roberts, F., Hegarty, B. & Ramaesh, K. The outcome of deep anterior lamellar keratoplasty in herpes simplex virus-related corneal scarring, complications and graft survival. *Br. J. Ophthalmol.* **94**, 1300–1303 (2010).

6. Gadhvi, K. A. *et al.* Eye banking: One cornea for multiple recipients. *Cornea* **39**, 1599–1603 (2020).

7. Heindl, L. M. *et al.* Split cornea transplantation for 2 recipients: A new strategy to reduce corneal tissue cost and shortage. *Ophthalmology* **118**, 294–301 (2011).

8. Lie, J. T., Lam, F. C., Groeneveld-Van Beek, E. A., Van Der Wees, J. & Melles, G. R. J. Graft preparation for hemi-Descemet membrane endothelial keratoplasty (hemi-DMEK). *Br. J. Ophthalmol.* **100**, 420–424 (2016).

9. Zygoura, V. *et al.* Quarter-descemet membrane endothelial keratoplasty (quarter-dmek) for fuchs endothelial corneal dystrophy: 6 months clinical outcome. *Br. J. Ophthalmol.* **102**, 1425–1430 (2018).

10. Parekh, M., Ruzza, A., Ferrari, S., Busin, M. & Ponzin, D. Preloaded tissues for Descemet Membrane Endothelial Keratoplasty. *Am. J. Ophthalmol.* **166**, 120–125 (2016).

11. Romano, V. *et al.* Comparison of preservation and transportation protocols for preloaded Descemet membrane endothelial keratoplasty. *Br. J. Ophthalmol.* **102**, 549–555 (2018).

12. Català, P. *et al.* Transport and preservation comparison of preloaded and prestripped-only DMEK grafts. *Cornea* **39**, 1407–1414 (2020).

13. Wojcik, G. *et al.* Preloaded descemet membrane endothelial keratoplasty grafts with endothelium outward: A cross-country validation study of the DMEK rapid device. *Cornea* **40**, 484–490 (2021).

14. Kinoshita, S. *et al.* Injection of cultured cells with a ROCK inhibitor for bullous keratopathy. *N. Engl. J. Med.* **378**, 995–1003 (2018).

15. Peh, G. S. L. *et al.* Propagation of human corneal endothelial cells: A novel dual media approach. *Cell Transpl.* **24**, 287–304 (2015).

16. Català, P. *et al.* Approaches for corneal endothelium regenerative medicine. *Prog. Retin. Eye Res.* **87**, 100987 (2022).

17. Muraro, M. J. *et al.* A Single-Cell Transcriptome Atlas of the Human Pancreas. *Cell Syst.* **3**, 385-394.e3 (2016).

18. Plasschaert, L. W. *et al.* A single-cell atlas of the airway epithelium reveals the CFTR-rich pulmonary ionocyte. *Nature* **560**, 377–381 (2018).

19. Darmanis, S. *et al.* A survey of human brain transcriptome diversity at the single cell level. *Proc. Natl. Acad. Sci. U. S. A.* **112**, 7285–7290 (2015).

20. Guo, J. *et al.* The adult human testis transcriptional cell atlas. *Cell Res.* **28**, 1141–1157 (2018).

21. Català, P. *et al.* Single cell transcriptomics reveals the heterogeneity of the human cornea to identify novel markers of the limbus and stroma. *Sci. Rep.* **11**, 21727 (2021).

22. Collin, J. *et al.* A single cell atlas of human cornea that defines its development, limbal progenitor cells and their interactions with the immune cells. *Ocul. Surf.* **21**, 279-298 (2021).

23. Li, D. Q. *et al.* Single-cell transcriptomics identifies limbal stem cell population and cell types mapping its differentiation trajectory in limbal basal epithelium of human cornea. *Ocul. Surf.* **20**, 20–32 (2021).

24. Dou, S. *et al.* Molecular identity of human limbal heterogeneity involved in corneal homeostasis and privilege: Single-cell RNA sequencing of human limbus. *Ocul. Surf.* **21**, 206–220 (2021).

25. Okumura, N. *et al.* The ROCK inhibitor eye drop accelerates corneal endothelium wound healing. *Investig. Ophthalmol. Vis. Sci.* **54**, 2439–2502 (2013).

26. Okumura, N. *et al.* Effect of the rho-associated kinase inhibitor eye drop (Ripasudil) on corneal endothelial wound healing. *Investig. Ophthalmol. Vis. Sci.* **57**, 1284–1292 (2016).

27. Okumura, N. *et al.* Inhibition of TGF-β Signaling Enables Human Corneal Endothelial Cell Expansion In Vitro for Use in Regenerative Medicine. *PLoS One* **8**, (2013).

28. Xia, X., Babcock, J. P., Blaber, S. I., Harper, K. M. & Blaber, M. Pharmacokinetic Properties of 2nd-Generation Fibroblast Growth Factor-1 Mutants for Therapeutic Application. *PLoS One* **7**, e48210 (2012).

29. Moloney, G. *et al.* Descemetorhexis without grafting for fuchs endothelial dystrophy-supplementation with topical ripasudil. *Cornea* **36**, 642–648 (2017).

30. Okumura, N. *et al.* Rho kinase inhibitor enables cell-based therapy for corneal endothelial dysfunction. *Sci. Rep.* **6**, 26113 (2016).

31. Koizumi, N. *et al.* Rho-associated kinase inhibitor eye drop treatment as a possible medical treatment for fuchs corneal dystrophy. *Cornea* **32**, 1167–1170 (2013).

32. Okumura, N. *et al.* Effect of the Rho Kinase inhibitor Y-27632 on corneal endothelial wound healing. *Investig. Ophthalmol. Vis. Sci.* **56**, 6067–6074 (2015).

33. Love, M. I., Huber, W. & Anders, S. Moderated estimation of fold change and dispersion for RNA-seq data with DESeq2. *Genome Biol.* **15**, 1–21 (2014).

34. Akkose, U. *et al.* Comparative analyses of two primate species diverged by more than 60 million years show different rates but similar distribution of genome-wide UV repair events. *BMC Genomics* **22**, 600 (2021).

35. Parekh, S., Vieth, B., Ziegenhain, C., Enard, W. & Hellmann, I. Strategies for quantitative RNA-seq analyses among closely related species. *bioRxiv* 297408 (2018).

36. Chung, M. *et al.* Best practices on the differential expression analysis of multi-species RNA-seq. *Genome Biol.* **22**, 121 (2021).

37. Zhou, Y. *et al.* A statistical normalization method and differential expression analysis for RNA-seq data between different species. *BMC Bioinformatics* **20**, 163 (2019).

38. Ben Khadra, Y. *et al.* Re-growth, morphogenesis, and differentiation during starfish arm regeneration. *Wound Repair Regen.* **23**, 623–634 (2015).

39. Mitoh, S. & Yusa, Y. Extreme autotomy and whole-body regeneration in photosynthetic sea slugs. *Curr. Biol.* **31**, R233–R234 (2021).

40. Peh, G. S. L. *et al.* Functional evaluation of two corneal endothelial cell-based therapies: tissue-engineered construct and cell injection. *Sci. Rep.* **9**, 6087 (2019).

41. Grönroos, P., Ilmarinen, T. & Skottman, H. Directed differentiation of human pluripotent stem cells towards corneal endothelial-like cells under defined conditions. *Cells* **10**, 331 (2021).

42. Wagoner, M. D. *et al.* Feeder-free differentiation of cells exhibiting characteristics of corneal endothelium from human induced pluripotent stem cells. *Biol. Open* **7**, 1–10 (2018).

43. Zhao, J. J. & Afshari, N. A. Generation of human corneal endothelial cells via in vitro ocular lineage restriction of pluripotent stem cells. *Invest Ophthalmol Vis Sci* **57**, 6878–6884 (2016).

44. McCabe, K. L. *et al.* Efficient generation of human embryonic stem cell-derived corneal endothelial cells by directed differentiation. *PLoS One* **10**, e0145266 (2015).

8

Impact statement

Introduction

It has been estimated that at least 12.7 million people worldwide require a corneal transplantation but have no access to donor tissue.[1] This estimation is based on 2012–2013 data and probably undervalues the current figures, as it does not include individuals that require keratoplasty but are not yet registered for transplantation and does not account for the future projection of corneal-related blindness.

The loss of vision associated to endothelial dysfunction has a major effect on the quality of life and causes difficulty in mobility, increased risk of falls and fractures, higher risk of depression and anxiety, and a greater likelihood to entering nursing homes, among other impacts.[2] Furthermore, vision impairment poses a major financial burden associated with a loss of productivity.[2] Developing novel therapeutic approaches is therefore crucial to provide swift and safe treatment to those in need. This thesis aims to assist the development of novel cell and regenerative medicine therapies, with the ultimate mission of granting better eyesight. In this section, we aim to provide insight into the scientific, economic, and societal implications related to the findings presented in this thesis.

Scientific impact

The research in this thesis has generated novel knowledge and crucial reference datasets that can impact the development of novel therapies (Chapters 4, 5, and 6), which have been made publicly available in the Gene Expression Omnibus (GSE186433) and DataVerseNL (doi:10.34894/X7ZSDZ).

Firstly, the human cornea was traditionally considered to be a tissue composed of three main cell types, namely epithelial cells, stromal keratocytes, and endothelial cells, a view that does not account for the true cellular heterogeneity. The results reported in this thesis portray the human cornea as a highly heterogeneous tissue at the single cell level, with each corneal layer comprising several cell populations

(Chapter 4). Secondly, our findings revealed the heterogeneity of primary cultured corneal endothelial cells (Chapter 5), providing insights into the alterations that occur through their primary expansion and identifying markers to enrich for clinical-grade cells.

Overall, the single cell transcriptomic (scRNAseq) datasets presented in Chapters 4 and 5 identified subpopulations with different roles in the maintenance of corneal homeostasis. These readily available and accessible datasets can provide a reference baseline to impact future research. The information gained in Chapter 4 can be used for better disease profiling when comparing these data to scRNAseq studies on specific corneal diseases. This could allow the identification of disease-specific genetic mechanisms in the aim to improve therapies. Secondly, the identification of novel cell-specific markers described in Chapter 4 and 5 can play a crucial role in the selection of cell types that are suitable for therapy, potentially improving therapeutic outcomes of cell-based therapies. These markers can also be used to improve stem cell differentiation to specific corneal cell types by targeting the enrichment of the specific markers. Besides the cellular markers highlighted in Chapters 4 and 5, the transcriptomic pathway-level information provided in Chapter 5 provides pivotal background to understand the alterations that occur in CECs upon their *in vitro* culture. These findings open the possibility to improve the current primary culture protocols by targeting specific pathways with small molecules, which could enable sourcing more cells from a single donor or to expand CECs from older donors.

In Chapter 6 we used an interesting approach to gain insights on the proliferation capacity of CECs. By isolating and comparing endothelial tissue of species with non-proliferative CECs, namely sheep and human, with rabbit proliferative CECs at the transcriptomic level, we were able to highlight pathways that could drive the proliferation potential (and thereby regenerative potential) of human CECs. These findings open novel paths for the improvement of regenerative therapies for treating

corneal endothelial dysfunction by specifically targeting the highlighted pathways, but also provide the scientific community with reference datasets of corneal endothelial samples of human, sheep, and rabbit, which are readily usable in other studies. Besides generating a central reference dataset, we have developed an automated pipeline for a cross-species comparison, which has been made publicly available in GitHub (Chapter 6). This pipeline is not specific to corneal endothelial research and can be applied to any tissue and cross-species comparison, enabling a fast and reproducible data analysis in other fields and species comparison.

Impact on clinical translation

Besides the generation of scientific knowledge associated to this thesis, the findings reported in Chapter 6 on the specific markers to select or assess the quality of primary cultured corneal endothelial cells have opened the possibility to file for intellectual property protection. The patentability of our findings has two major repercussions. Firstly, it opens the option to license the markers for the assessment of the therapeutic potential of corneal endothelial cells, which might have a direct financial impact in case of licensing out the technology to a third party. Secondly and most importantly, it opens the possibility for the development and commercialization of a corneal endothelial cell–based therapy without some of the barriers currently faced. Namely, markers associated with the therapeutic quality of primary expanded corneal endothelial cells such as CD166 or CD44 have already been patent-registered in the European Union, and can only be used in the therapeutic setting with a license. As the success of a cell-based therapy heavily relies on the quality assessment of the generated cells, the existing patents might limit the development and application of a corneal endothelial cell–based therapy if there is no licensing agreement. The discovery and patent protection of the markers reported in Chapter 6 opens an alternative possibility for assessing the quality of the corneal endothelial cells intended as a cell-based therapy.

Societal and ethical impact

Corneal endothelial regenerative medicine aims to treat those without access to a donor cornea. But there is a major worldwide imbalance in corneal-related blindness and access to donor corneas in different areas of the world. Most European and North American countries can meet the donor tissue demand, and in some specific cases such as in the United States of America or the Netherlands, can even export surplus corneas to other regions in need. It is in fact in African, Asian and some Middle Eastern countries where donor tissue shortage is a major burden, and patients lack access to treatment in the short-term.

It is essential to understand the worldwide imbalance when developing regenerative medicine approaches for treating corneal endothelial dysfunction. Corneal endothelial cell therapies will probably be more expensive than corneal transplantation. We can use Holoclar as a reference, an autologous transplantation of corneal epithelial stem cells to treat unilateral limbal stem cell deficiency, which has a price of EUR 105,000 per eye in Europe.[3] Taking this in mind, cell therapies to treat corneal endothelial dysfunction are only conceivable in countries with a self-sufficient donor system, with the exception of Japan or Singapore, countries that suffer from donor cornea shortage but have the financial means and facilities for a cell transplantation program. The work reported in this thesis can potentially help to reduce the costs of a cell therapy. Specifically, improvements to the primary cell culture protocols based on our findings could increase the cell pool derived from a single donor, reducing the therapeutic cost. Furthermore, the cost effectiveness of corneal endothelial cell–based therapies can be dramatically reduced by using cell scaffolds, as reported in a recent study.[4]

From the perspective of a global and communal attitude, the use of a corneal endothelial cell therapy in a self-sufficient country could generate a surplus of donor corneas, which in turn could be exported to countries without the infrastructure to

develop and implement a cell therapy. However, there is the need to justify the development and use of a cell-based therapy when there is a treatment and donor tissue readily available for those in need. For the approval of a corneal endothelial cell–based therapy, which is considered an advanced therapeutic medicinal product in the European Union, the therapy must either provide a very strong rationale for a return on investment to elicit commercial interest or provide an improvement compared to the current lamellar therapy; therefore, a corneal endothelial cell–based therapy should be measured against the outcomes of the current DMEK. Considering this, primary cultured corneal endothelial cells could be engineered in a "super-DMEK" graft with a high cell density (≥3,000 cells/mm^2), potentially increasing graft survival. Finally, logistic solutions to transport bioengineered endothelial grafts and frozen cells could also allow countries lacking the necessary infrastructure to benefit from a cell-based therapy.

In the short term, developing and applying a corneal endothelial cell–based therapy in the countries with major cornea shortages is not feasible. For this reason, we might consider the use of other cost-effective therapeutic modalities, such as the Descemet's stripping only combined with the use of Rho associated protein kinase inhibitors or the use of the revolutionary endothelial keratoprosthesis with the capacity to regulate corneal deturgescence, such as EndoArt. Their relatively low cost and the minimal infrastructure needed could allow their implementation, reducing the need for transplantation.

In our view, regenerative therapies should be combined with the international development of efficient eye bank infrastructures and clinical facilities, as well as with promoting organ donation. The present global shortage of donor corneas, expected to increase as the world population ages, can only be tackled with an international effort and a communal attitude.

References

1. Gain, P. *et al.* Global survey of corneal transplantation and eye banking. *JAMA Ophthalmol* **134**, 167–173 (2016).

2. World Health Organization. World report on vision. World Health Organization (2019).

3. Shukla, V., Seoane-Vazquez, E., Fawaz, S., Brown, L. & Rodriguez-Monguio, R. The landscape of cellular and gene therapy products: Authorization, discontinuations, and cost. *Hum. Gene Ther. Clin. Dev.* **30**, 102–113 (2019).

4. Tan, T. E. *et al.* A cost-minimization analysis of tissue-engineered constructs for corneal endothelial transplantation. *PLoS One* **9**, e100563 (2014).

Addendum

Summary

The cornea is the clear window that lets light into the eye. Its inner surface is lined by a monolayer of corneal endothelial cells (CECs) that selectively pump ions and other metabolites, regulating the corneal hydration and maintaining the transparency of this avascular tissue. Human CECs are arrested in a non-dividing state, and their density slowly decreases over the years to an average of 2600 cells/mm^2 in healthy adults aged 60–79 years. Iatrogenic damage, ageing or genetic diseases can cause an accelerated loss of CECs, weakening the endothelial function, and thus affecting corneal hydration and causing corneal endothelial disease, which is characterized by corneal edema and opacity impairing sight.

Endothelial keratoplasty is the current therapy for corneal endothelial disease. Advances in surgical procedures are improving reproducibility and accessibility to corneal transplantation, causing an increase in the number of corneal transplantations globally. Unfortunately, there is currently a worldwide donor cornea shortage, aggravated by the increasing number of transplantations. It has been estimated that only one out of seventy patients in need has access to a donor cornea, and 12.7 million people in the world are awaiting treatment. The development of regenerative medicine approaches to treat corneal endothelial disease is necessary to tackle the increasing demand for donor corneal tissue and to provide treatment to those in need. Understanding the fundamental processes happening *in vitro* and *in vivo* are crucial aspects for developing such therapies and for their implementation from bench to bedside. The work described in this thesis addresses this need, with our main goal to contribute to the development of such innovative therapies.

We review the current and developing approaches for the regeneration of the corneal endothelium, presenting its pros and cons, but also providing a social perspective and a regulatory guide for the approval of such treatments in the European Union. We show experimentally that corneal endothelial tissue could be delivered to the operation theater preloaded in an injection cannula, without affecting its quality. This

system reduces iatrogenic tissue damage in the operation theater and can allow eye banks to send only the tissue necessary for the selective replacement of the corneal endothelium, optimizing donor availability for other procedures. We went on to use single cell RNA sequencing to elucidate the different cell populations composing the healthy cornea and to understand the transcriptomic changes and the emergence of side populations that occur during the primary expansion of CECs for therapeutic purposes. To understand why rabbits have proliferative CECs and the CECs from larger mammals such as humans and sheep are arrested and cannot divide, we studied the transcriptomic differences across these species. Finally, we summarize the main findings of this thesis, and present a perspective of how this research has impacted the field and discussed on how it is likely to develop.

Samenvatting

Het hoornvlies is het doorzichtige venster dat licht het oog inlaat. De binnenzijde van het hoornvlies is bekleed met een monolaag van corneale endotheelcellen (CEC's) die selectief ionen en andere metabolieten pompen, waarmee ze de hydratatie van de cornea reguleren en de transparantie van dit avasculaire weefsel waarborgen. Menselijke CEC's verouderen en komen in een niet-delende toestand, waardoor de dichtheid in de loop der jaren langzaam afneemt tot gemiddeld 2600 cellen/mm^2 bij gezonde volwassenen van 60-79 jaar. Iatrogene schade, veroudering of genetische ziekten kunnen een versneld verlies van CEC's veroorzaken en de endotheel functie verzwakken. Dit tast de hydratatie van het hoornvlies aan en leidt tot endotheel ziekte van het hoornvlies, dat wordt gekenmerkt door hoornvlies oedeem en vertroebeling wat het gezichtsvermogen aantast.

Endotheliale keratoplastiek is de huidige therapie voor cornea endotheel ziekte. Vooruitgang in chirurgische procedures heeft de reproduceerbaarheid en toegankelijkheid van hoornvliestransplantatie verbeterd, waardoor het aantal hoornvliestransplantaties wereldwijd is toegenomen. Helaas is er momenteel wereldwijd een tekort aan donorhoornvlies, gestegen door het toenemende aantal transplantaties. Er wordt geschat dat slechts één op de zeventig behoeftige patiënten toegang heeft tot een donorhoornvlies, en 12,7 miljoen mensen in de wereld wachten op behandeling. De ontwikkeling van regeneratieve geneeswijzen voor de behandeling van endotheel ziekte van het hoornvlies is noodzakelijk om de toenemende vraag naar hoornvliesweefsel van donoren aan te pakken en om behandeling te bieden aan mensen in nood. Kennis over fundamentele processen die *in vitro* en *in vivo* plaatsvinden, zijn cruciaal voor het ontwikkelen van dergelijke therapieën en voor translationele implementatie. Het werk beschreven in dit proefschrift richt zich op deze behoefte, met ons belangrijkste doel bij te dragen aan de ontwikkeling van dergelijke innovatieve therapieën.

We bespreken de huidige en ontwikkelende technieken voor de regeneratie van het cornea-endotheel, presenteren de voor- en nadelen, maar bieden ook een sociaal perspectief en een regelgevende gids voor de goedkeuring van dergelijke behandelingen in de Europese Unie. We laten experimenteel zien dat cornea endotheel weefsel geladen in een injectiecanule kan worden getransporteerd naar de operatiekamer zonder de kwaliteit ervan aan te tasten. Dit systeem vermindert iatrogene weefselbeschadiging in de operatiekamer en kan oogbanken in staat stellen alleen het weefsel te sturen dat nodig is voor de selectieve vervanging van het cornea-endotheel, waardoor de donorbeschikbaarheid voor andere procedures wordt geoptimaliseerd. Vervolgens hebben we met het gebruik van single-cell RNA-sequencing de verschillende cel-populaties waaruit het gezonde hoornvlies bestaat opgehelderd om de transcriptomische veranderingen en de opkomst van nevenpopulaties die optreden tijdens de primaire expansie van CEC's voor therapeutische doeleinden te begrijpen. Om te begrijpen waarom konijnen proliferatieve CEC's hebben en de CEC's van grotere zoogdieren zoals mensen en schapen overgaan in groeiarrest, hebben we de transcriptomische verschillen tussen deze soorten bestudeerd. Ten slotte vatten we de belangrijkste bevindingen van dit proefschrift samen en presenteren we een perspectief over de invloed van dit onderzoek op het veld en speculeren we over toekomstige ontwikkelingen.

List of Publications

Català, P., Groen, N., LaPointe, V.L.S., Dickman, M.M., A single-cell RNA-seq analysis unravels the heterogeneity of primary cultured corneal endothelial cells. *Sci Rep*. 13: 9361 (2023).

Català, P., Vivensang, F., van Beek, D., Adriaens, M.E., Dickman, M.M., LaPointe, V.L.S., Kutmon, M. Elucidating the corneal endothelial cell proliferation capacity through an interspecies transcriptome comparison. *Adv Biol*. [2300065] (2023).

Català, P., Thuret, G., Skottman, H., Mehta, J.S., Parekh, M., Ni Dhubhghaill, S., Collin, R.W.J., Nuijts, R.M.M.A., Ferrari, S., LaPointe, V.L.S., Dickman, M.M. Approaches for corneal endothelium regenerative medicine. *Prog Retin Eye Res*. 87: 100987 (2022).

Català, P., Groen, N., Dehnen, J.A., Soares, E., van Velthoven, A.J.H., Nuijts, R.M.M.A., Dickman, M.M., LaPointe, V.L.S. Single cell transcriptomics reveals the heterogeneity of the human cornea to identify novel markers of the limbus and stroma. *Sci Rep*. 11: 21727 (2021).

Formisano, N., Sahin, G., **Català, P.,** Truckenmuller, R., Nuijts, R.M.M.A., Dickman, M.M., LaPointe, V.L.S., Giselbrecht, S. Nanoscale topographies for corneal endothelial regeneration. *Appl Sci*. 11: 827 (2021).

Català, P., Vermeulen, W., Rademakers, T., van den Bogaerdt, A., Kruijt, P.J., Nuijts, R.M.M.A., LaPointe, V.L.S., Dickman, M.M. Transport and preservation comparison of preloaded and prestripped-only DMEK grafts. *Cornea*. 39 (11): 1407-1414 (2020).

Awards and grants

Bayer Ophthalmology Research Awards (BORA) 2021 first prize for the project titled: “Understanding the corneal endothelium, one cell at a time”. Prize: 24,000.00 EUR.

Methods and Protocols – MDPI travel award 2022 to attend and present in ARVO 2022 annual meeting in Denver, CO, USA. Prize: 800.00 CHF.

ARVO EyeFind Research Grant 2022 – For the project titled: “Determining the quality of primary cultured corneal endothelial cells through a single cell RNA-sequencing analysis”. Prize: 5,000.00 USD.

Scientific communications

Oral presentation in conferences:

Català, P., Formisano, N., Soares, E., Truckenmüller, R., Giselbrecht, S., LaPointe, V.L.S., Nuijts, R.M.M.A., Dickman, M.M. Generation of functional human corneal endothelial cells for regenerative medicine of the cornea [Conference presentation]. 28th International Congress of European Association of Tissue and Cell Banks (EATCB), Leiden, the Netherlands (2019, October 16–18).

Català, P., Grant, R., Zagorodko, O., Vrehen, A., Dankers, P., Giselbrecht, S., Nuijts, R.M.M.A., Dickman, M.M., LaPointe, V.L.S. Bioengineering the corneal endothelium: A corneal endothelial graft using biomimetic substrates [Conference presentation]. 6th World Congress of Tissue Engineering and Regenerative Medicine International Society (TERMIS), Maastricht [Online], the Netherlands (2021, November 15–19).

Català, P., Groen, N., Nuijts, R.M.M.A., LaPointe, V.L.S., Dickman, M.M. A single cell transcriptome analysis unravels the heterogeneity of primary cultured human corneal endothelial cells [Conference presentation]. The Association for Research in Vision and Ophthalmology (ARVO) 2022 annual meeting, Denver, CO, USA (2022, May 1–4).

Català, P., Groen, N., Dehnen, J.A., Soares, E., van Velthoven, A.J.H., Nuijts, R.M.M.A., Dickman, M.M., LaPointe, V.L.S. A single cell transcriptome atlas reveals the cellular heterogeneity of the healthy human cornea [Conference presentation]. Nederlands Oogheelkundig Gezelschap (NOG) Congres 2022, Groningen, the Netherlands (2022, June 29–July 1).

Posters in conferences:

Català, P., Soares, E., van Blitterswijk, C.A., Nuijts, R.M.M.A., Dickman, M.M., LaPointe, V.L.S., Generation of functional corneal endothelial-like cells from pluripotent stem cells for regenerative therapy of the human cornea [Poster presentation]. International Society for Stem Cell Research (ISSCR) 2019 annual meeting, Los Angeles, CA, USA (2019, June 26–29).

Català, P., Formisano, N., Soares, E., van Blitterswijk, C.A., Trückenmuller, R., Giselbrecht, S., Dickman, M.M., LaPointe, V.L.S., Nuijts, R.M.M.A. Generation of functional corneal endothelial-like cells from pluripotent stem cells for regenerative therapy of the human cornea [Poster presentation]. 4th InSciTe Annual Meeting, Horst, the Netherlands (2019, October 8–9).

Acknowledgements

This is one of the parts I was most looking forward to write, I just hope not to forget anyone. To my parents and my family, for the constant support they gave me all these years, and the education they provided me. *Pares, avis, Eli, Gerard, gràcies per ser-hi sempre*.

To Vanessa, and Mor, my supervisors, thank you for trusting me and giving me the opportunity to pursue this PhD. These years have been a constant learning experience, and without you, I would not be the same person I have become. You transmitted me the passion you both have for science and with our discussions and meetings you constantly challenged me to reach higher goals and perform better. You also showed me the importance of planning and defining realistic goals for the projects we worked with, something which before my PhD I did not realize how important was. I have always admired your vocation and perseverance, I am sure you will bring great impact on the years to come in the field of ophthalmology and regenerative medicine. To my promotor, Rudy, thank you for welcoming me in the Ophthalmology department, and supporting me during this endeavor.

Mariona, you were the person who was right by my side for most of my PhD. You gave me all the support when it was most needed, even had to patiently cope with my sleep-talking about my projects. You were there in both my ups and downs and without your constant support this journey would have been a very different one. I am very happy to have done it along your side. *Gràcies per ser la meva companya de viatje, pel teu suport incondicional i la pau mental que sempre em saps transmetre, al teu costat tot sembla més fàcil.*

In Maastricht I was able to meet some of the nicest human beings I have ever come across. To the guys, Daniel, Nello, Tristan, Shivesh, and Afonso with whom I could always count and trust. I will miss our dinners, FIFA nights, and parties in Maastricht

(not so much the nights we went to watch Champions league, every time I saw a game with you Barça lost). I have to also include here Claudia, Einav, and Frances, thank you for accompanying and coping with us, and of course to our new addition to the group, Leo!

To Mar, you were one of the first people I met when I arrived in MERLN, you made my integration in this working environment and city smooth and easy, and made me feel as if I was home.

The work on this thesis would have not been possible with the bioinformaticians that helped me with the analysis. Nathalie, thanks a lot for all your help over these years, you are a machine of single cell RNAseq analysis, and you helped me a lot to better understand the technique and its potential. Tina, you had the courage and patience to introduce and teach me coding with R for RNA sequencing data analysis, one of the most valuable skills I acquired during my PhD time, I will be always grateful for this. Though we expected an easier project, we could handle all the drawback we faced and the manuscript we wrote is a proof of it. With your patience, skills and mindset I am sure you will become a successful principal investigator in the field of bioinformatics.

I was lucky to belong to a place like MERLN, where I could work along very friendly people. To my friends Giota, Joanna, Francesca, Ane, Carlos, Brenda, Gabriele, Adrian, Monize, Paula, Julia thank you for making this endeavor more enjoyable. To my colleagues at the LaPointe group: Virginie, Arianne, Annika, Thomas, Paula, Fiona, Mireille, Fredrik, Darragh, Demi, Elisa, Marco, Eduardo, Timo, and Nadia thank you for all your help. And to the PIs, Elizabeth, Aurélie, Stefan, Lorenzo, Matt, Paul, Carlos, that even with a very full agenda were able to maintain nice chats and give you some tips and tricks.

Martijn, I just want to thank you for being there when I most needed it. You are a great person, scientist, and department head. You showed me what honesty and fairness are, for which I will always be grateful.

Outside of MERLN I have to thank many people, to the friends I met in the Netherlands, Winant, Roc, Nil, Jannik, Sonia, Dennis, Boning, Pablo, Lisa, Fati, thank you for allowing me to disconnect from work every time I met you. To my Scharn IV team-mates, though I had to prematurely leave the team due to my recurrent injuries, one of the things that made me happy during my stay in Maastricht was to get my weekly dose of football while still being in a very friendly atmosphere. To my high school friends, who after so many years are still one of the greatest support, Pau, Jose, Miquel, Sergio, Bosch, Ferran, Marti, Claudia, Marta, Maria, Rosa, Ana P., Ana I.. And to my friends from my bachelor's, Esther, Kiko, Guille, Jordi, Guerra, Boix.

Thank you all for being there for me.

Biography

Pere Català Quilis was born in Sant Cugat del Vallès, Barcelona (Spain) on January 13th 1994, where he grew up. In 2012, he enrolled in the Bachelor of Biotechnology at the Universitat Autònoma de Barcelona. During his bachelor studies he performed his thesis in the Institute for Bioengineering of Barcelona (Department of Nanoprobes and Nanoswitches) under supervision of Prof. Pau Gorostiza, working on imaging tools for optopharmacological approaches. In 2016, after graduating from his bachelor studies, Pere enrolled in the MSc program of BioPharmaceutical Sciences at Leiden University. During this program, Pere performed two main research internships: The first in the Leiden Academic Centre for Drug Research (Department of BioTherapeutics) under supervision of Prof. Wim Jiskoot working on the development of a liposome-based vaccine for the treatment of birch pollen allergy. The second at Utrecht University (Department of Pharmaceutics) under supervision of Dr. Massimiliano Caiazzo researching the generation of reprogramming astrocytes from human embryonic and human mesenchymal stem cells in 2D and 3D culture. In 2018 Pere graduated *cum laude* from his MSc in BioPharmaceutical Sciences from Leiden University and moved to Maastricht to perform a PhD under the supervision of Dr. Vanessa LaPointe, Dr. Mor Dickman, and Prof. Rudy Nuijts in the University Eye Clinic Maastricht (Maastricht UMC+) and the MERLN Institute for Technology-Inspired Regenerative Medicine. The results of such PhD are described in this book.